Methods in
Molecular Biology 2144

Springer Protocols

Sean P. Curran *Editor*

Aging

Methods and Protocols

Humana Press

METHODS IN MOLECULAR BIOLOGY

Series Editor
John M. Walker
School of Life and Medical Sciences
University of Hertfordshire
Hatfield, Hertfordshire, UK

For further volumes:
http://www.springer.com/series/7651

For over 35 years, biological scientists have come to rely on the research protocols and methodologies in the critically acclaimed *Methods in Molecular Biology* series. The series was the first to introduce the step-by-step protocols approach that has become the standard in all biomedical protocol publishing. Each protocol is provided in readily-reproducible step-by-step fashion, opening with an introductory overview, a list of the materials and reagents needed to complete the experiment, and followed by a detailed procedure that is supported with a helpful notes section offering tips and tricks of the trade as well as troubleshooting advice. These hallmark features were introduced by series editor Dr. John Walker and constitute the key ingredient in each and every volume of the *Methods in Molecular Biology* series. Tested and trusted, comprehensive and reliable, all protocols from the series are indexed in PubMed.

Aging

Methods and Protocols

Edited by

Sean P. Curran

Leonard Davis School of Gerontology, University of Southern California, Los Angeles, CA, USA

Humana Press

Editor
Sean P. Curran
Leonard Davis School of Gerontology
University of Southern California
Los Angeles, CA, USA

ISSN 1064-3745 ISSN 1940-6029 (electronic)
Methods in Molecular Biology
ISBN 978-1-0716-0591-2 ISBN 978-1-0716-0592-9 (eBook)
https://doi.org/10.1007/978-1-0716-0592-9

This Humana imprint is published by the registered company Springer Science+Business Media, LLC, part of Springer Nature.
The registered company address is: 1 New York Plaza, New York, NY 10004, U.S.A.

Preface

Understanding the impact of aging on biological system is critical for defining strategies to improve health across the life span. The inherent lack of uniformity of the aging process across individuals has sparked interest to understand the basis of this diversity with the goal of elucidating mechanisms to optimize health. Several animal models have emerged to study the aging process. The geroscience field has developed sophisticated methodologies to examine aging at the organism, tissue, cellular, and molecular levels across the life span.

Los Angeles, CA, USA *Sean P. Curran*

Contents

Contributors

Jennifer Ailshire • *Leonard Davis School of Gerontology, University of Southern California, Los Angeles, CA, USA*

T. Em Arpawong • *Leonard Davis School of Gerontology, University of Southern California, Los Angeles, CA, USA*

Adrien Assié • *Alkek Center for Metagenomics and Microbiome Research, Baylor College of Medicine, Houston, TX, USA*

Bérénice A. Benayoun • *Leonard Davis School of Gerontology, University of Southern California, Los Angeles, CA, USA; USC Norris Comprehensive Cancer Center, Epigenetics and Gene Regulation, Los Angeles, CA, USA; USC Stem Cell Initiative, Los Angeles, CA, USA*

Sebastian Brandhorst • *Longevity Institute, Leonard Davis School of Gerontology, University of Southern California, Los Angeles, CA, USA*

Roberta Buono • *Department of Molecular Biology and Biochemistry, University of California, Irvine, Irvine, CA, USA*

Maria Calvillo • *Ethel Percy Andrus Gerontology Center, Leonard Davis School of Gerontology, University of Southern California, Los Angeles, CA, USA*

Jessica T. Chang • *Development, Aging and Regeneration Program, Sanford Burnham Prebys Medical Discovery Institute, La Jolla, CA, USA*

Amy Christensen • *Leonard Davis School of Gerontology, University of Southern California, Los Angeles, CA, USA*

Khalyd J. Clay • *Department of Molecular Medicine, Chemistry, and Neuroscience, The Scripps Research Institute, La Jolla, CA, USA*

Lucio Comai • *Department of Molecular Microbiology and Immunology, Keck School of Medicine, University of Southern California, Los Angeles, CA, USA*

Adam B. Cornwell • *Department of Biomedical Genetics, University of Rochester Medical Center, Rochester, NY, USA*

Sean P. Curran • *Leonard Davis School of Gerontology, University of Southern California, Los Angeles, CA, USA; Department of Molecular and Computational Biology, Dornsife College of Letters, Arts, and Sciences, University of Southern California, Los Angeles, CA, USA; Norris Comprehensive Cancer Center, Keck School of Medicine, University of Southern California, Los Angeles, CA, USA*

Weiwei Dang • *Department of Molecular and Human Genetics, Baylor College of Medicine, Houston, TX, USA; Huffington Center on Aging, Baylor College of Medicine, Houston, TX, USA*

Devon Doherty • *Molecular and Computational Biology Program, Department of Biological Sciences, University of Southern California, Los Angeles, CA, USA*

Di Fan • *Ethel Percy Andrus Gerontology Center, Leonard Davis School of Gerontology, University of Southern California, Los Angeles, CA, USA*

Henry Jay Forman • *Leonard Davis School of Gerontology, University of Southern California, Los Angeles, CA, USA*

Kyle J. Foster • *Program in Innate Immunity, Division of Infectious Diseases and Immunology, University of Massachusetts Medical School, Worcester, MA, USA*

Amin Haghani • *Leonard Davis School of Gerontology, University of Southern California, Los Angeles, CA, USA*
Malene Hansen • *Development, Aging and Regeneration Program, Sanford Burnham Prebys Medical Discovery Institute, La Jolla, CA, USA*
Julia Hong • *Department of Developmental Biology and Department of Genetics, Washington University in St. Louis, St. Louis, MO, USA*
Juan Manuel Iglesias-Pedraz • *Laboratorio de Genética Molecular y Bioquímica, Departamento de Investigación, Desarrollo e Innovación, Universidad Científica del Sur, Lima, Peru*
Andrei Irimia • *Ethel Percy Andrus Gerontology Center, Leonard Davis School of Gerontology, University of Southern California, Los Angeles, CA, USA*
Myeong Chan Jo • *Innovative Biochips LLC, Houston, TX, USA*
Rachel Kaletsky • *Department of Molecular Biology, Princeton University, Princeton, NJ, USA; Lewis-Sigler Institute for Integrative Genomics, Princeton University, Princeton, NJ, USA*
Anastasia S. Khodakova • *Alkek Center for Metagenomics and Microbiome Research, Baylor College of Medicine, Houston, TX, USA*
Holly E. Kinser • *Department of Developmental Biology and Department of Genetics, Washington University in St. Louis, St. Louis, MO, USA; Department of Biomedical Engineering, Washington University in St. Louis, St. Louis, MO, USA*
Caroline Kumsta • *Development, Aging and Regeneration Program, Sanford Burnham Prebys Medical Discovery Institute, La Jolla, CA, USA*
Gary N. Landis • *Molecular and Computational Biology Program, Department of Biological Sciences, University of Southern California, Los Angeles, CA, USA*
Changhan Lee • *Leonard Davis School of Gerontology, University of Southern California, Los Angeles, CA, USA; USC Norris Comprehensive Cancer Center, Los Angeles, CA, USA; Biomedical Science, Graduate School, Ajou University, Suwon, South Korea*
Siu Sylvia Lee • *Department of Molecular Biology and Genetics, Cornell University, Ithaca, NY, USA*
Mario Loeza-Cabrera • *Alkek Center for Metagenomics and Microbiome Research, Baylor College of Medicine, Houston, TX, USA*
Ryan Lu • *Leonard Davis School of Gerontology, University of Southern California, Los Angeles, CA, USA; Graduate Program in the Biology of Aging, University of Southern California, Los Angeles, CA, USA*
Natalie Lyn • *Leonard Davis School of Gerontology, University of Southern California, Los Angeles, CA, USA*
Deborah L. McEwan • *Department of Molecular Biology, Massachusetts General Hospital, Boston, MA, USA*
Brendan Miller • *Leonard Davis School of Gerontology, University of Southern California, Los Angeles, CA, USA*
Coleen T. Murphy • *Department of Molecular Biology, Princeton University, Princeton, NJ, USA; Lewis-Sigler Institute for Integrative Genomics, Princeton University, Princeton, NJ, USA*
James D. Nhan • *Leonard Davis School of Gerontology, University of Southern California, Los Angeles, CA, USA; Department of Molecular and Computation Biology, Dornsife College of Letters, Arts, and Sciences, University of Southern California, Los Angeles, CA, USA*

Nisha S. Patil • *Department of Developmental Biology and Department of Genetics, Washington University in St. Louis, St. Louis, MO, USA*
Michael Petrascheck • *Department of Molecular Medicine, Chemistry, and Neuroscience, The Scripps Research Institute, La Jolla, CA, USA*
Christian J. Pike • *Leonard Davis School of Gerontology, University of Southern California, Los Angeles, CA, USA*
Zachary Pincus • *Department of Developmental Biology and Department of Genetics, Washington University in St. Louis, St. Louis, MO, USA*
Elizabeth C. Pino • *Center for Translational Epidemiology and Comparative Effectiveness Research, Boston University School of Medicine, Boston, MA, USA*
William E. Pittman • *Department of Developmental Biology and Department of Genetics, Washington University in St. Louis, St. Louis, MO, USA; Department of Biomedical Engineering, Washington University in St. Louis, St. Louis, MO, USA*
Isaac B. Plutzer • *Department of Developmental Biology and Department of Genetics, Washington University in St. Louis, St. Louis, MO, USA*
Mintie Pu • *Center for Life Sciences, School of Life Sciences, Yunnan University, Kunming, YN, China*
Read Pukkila-Worley • *Program in Innate Immunity, Division of Infectious Diseases and Immunology, University of Massachusetts Medical School, Worcester, MA, USA*
Joseph C. Reynolds • *Leonard Davis School of Gerontology, University of Southern California, Los Angeles, CA, USA*
Nirmal K. Sampathkumar • *Leonard Davis School of Gerontology, University of Southern California, Los Angeles, CA, USA*
Buck S. Samuel • *Alkek Center for Metagenomics and Microbiome Research, Baylor College of Medicine, Houston, TX, USA*
Andrew V. Samuelson • *Department of Biomedical Genetics, University of Rochester Medical Center, Rochester, NY, USA*
Drew B. Sinha • *Department of Developmental Biology and Department of Genetics, Washington University in St. Louis, St. Louis, MO, USA; Department of Biomedical Engineering, Washington University in St. Louis, St. Louis, MO, USA*
Alexander A. Soukas • *Department of Medicine, Endocrine Division, and Diabetes Unit, Massachusetts General Hospital and Harvard Medical School, Boston, MA, USA*
Eric S. Terry • *Department of Developmental Biology and Department of Genetics, Washington University in St. Louis, St. Louis, MO, USA*
John Tower • *Molecular and Computational Biology Program, Department of Biological Sciences, University of Southern California, Los Angeles, CA, USA*
Daniela Vidal • *Alkek Center for Metagenomics and Microbiome Research, Baylor College of Medicine, Houston, TX, USA*
Junxiang Wan • *Leonard Davis School of Gerontology, University of Southern California, Los Angeles, CA, USA*
Jessica L. Weckhorst • *Alkek Center for Metagenomics and Microbiome Research, Baylor College of Medicine, Houston, TX, USA*
Chia-An Yen • *Leonard Davis School of Gerontology, University of Southern California, Los Angeles, CA, USA; Department of Molecular and Computational Biology, Dornsife College of Letters, Arts, and Sciences, University of Southern California, Los Angeles, CA, USA*

Ruofan Yu • *Department of Molecular and Human Genetics, Baylor College of Medicine, Houston, TX, USA; Huffington Center on Aging, Baylor College of Medicine, Houston, TX, USA*

Fan Zhang • *Alkek Center for Metagenomics and Microbiome Research, Baylor College of Medicine, Houston, TX, USA*

Hongqiao Zhang • *Leonard Davis School of Gerontology, University of Southern California, Los Angeles, CA, USA*

Chapter 1

Measuring the Replicative Lifespan of *Saccharomyces cerevisiae* Using the HYAA Microfluidic Platform

Ruofan Yu, Myeong Chan Jo, and Weiwei Dang

Abstract

The replicative aging of the budding yeast, *Saccharomyces cerevisiae*, has been a useful model for dissecting the molecular mechanisms of the aging process. Traditionally, the replicative lifespan (RLS) is measured by manually dissecting mother cells from daughter cells, which is a very tedious process. Since 2012, several microfluidic systems have been developed to automate the dissection process, significantly accelerating RLS determination. Here, we describe a detailed protocol of RLS measurement using a ommercially available microfluidic system based on the HYAA chip design, which enables data collection of up to 8000 cells in a single experiment.

Key words Budding yeast, Replicative aging, Replicative lifespan, Microfluidics

1 Introduction

The budding yeast, *Saccharomyces cerevisiae*, is one of the most genetically tractable eukaryotic models in aging studies. Yeast cells undergo asymmetric cell division, producing a smaller daughter cell from a larger mother cell. The smaller daughter cell can be physically dissected away from mother cell, hence the cell division events for a particular mother cell can be counted. A yeast cell can only produce a limited number of daughter cells, that is a finite replicativelifespan (RLS), before entering a permanently arrested state followed by cell lysis. Studies in yeast replicative aging have led to the discovery of several conserved molecular pathways that regulate aging in diverse eukaryotic species.

Traditionally, RLS is measured by physically separating daughter cells from mother cells using fiber-optic needles under microscope [1], by which a round of RLS measurement typically takes 4–6 weeks. An experienced dissector usually handles no more than 300 cells in an experiment, making this procedure very labor-intensive and time-consuming.

Sean P. Curran (ed.), *Aging: Methods and Protocols*, Methods in Molecular Biology, vol. 2144,
https://doi.org/10.1007/978-1-0716-0592-9_1,

Since 2012, several microfluidic designs have been developed to enable fast and reliable measurement yeast RLS. In all these systems, yeast cells are fixed in microfluidic channels via different mechanisms and daughter–mother cell separation is driven by medium flow. When coupled with time-lapse imaging, cell division events for the entire replicativelifespan of hundreds of single yeast cells can be tracked, recorded, and counted. These methods have drastically reduced the time required for RLS measurement and increased experimental throughput. Specifically, the high-throughput yeast aging analysis (HYAA)-chip developed by our group enables simultaneous RLS measurement for 16 different strains, generating data containing up to 520 cells per strain or 8000 cells in total, in a short period of 72 h. The HYAA-chip design has been used in several published yeast aging studies [2–5] and proved to be robust and consistent.

2 Materials, Reagents, and Equipment

2.1 Sample Preparation

1. Yeast extract–peptone–dextrose (YPD) medium: 1% yeast extract, 2% peptone, 2% dextrose, filter sterilized.
2. Yeast strains.

2.2 Setting Up Microfluidic Experiment

1. 50 ml syringes (Air-Tite™ HSW Soft-Ject™ Luer Lock Disposable Syringe).
2. Luer-stub adapters (BD Intramedic™ PE Tubing Adapters).
3. Non-DEHP medical grade tubing (Saint-Gobain Tygon™ ND 100-80 Tubing).
4. Computer-controlled dual syringe pump (Innovative Biochips).
5. HYAA microfluidic chip (Innovative Biochips).
6. Microscope (fluorescence) with autofocus, time-lapse abilities and preferably an automated X–Y control stage (e.g., A1 Cell Imaging System; Innovative Biochips).
7. Hollow pins (Type 304 stainless steel pins; Innovative Biochips).
8. Solid pins (Type 316 stainless steel pins; Innovative Biochips).

2.3 Loading Yeast Cells into HYAA-Chip

1. 1 ml syringes (BD Luer Lock Disposable Syringes).
2. Computer-controlled multisyringe pump (Innovative Biochips).

2.4 Time-Lapse Imaging

1. Microscope temperature control system (e.g., Onstage Incubator; Innovative Biochips).

3 Methods

All procedures are performed under room temperature. A typical microfluidic system is depicted in Fig. 1.

3.1 Sample Preparation

1. Culture yeast cells overnight (*see***Note 1**). On next morning, transfer 50 μl of cultured cells to 1 ml of filtered YPD medium (*see***Note 2**). Keep on ice until you start the experiment.

3.2 Setting Up Microfluidic Experiments

1. Fill 50 ml syringe with liquid YPD medium or other medium of choice (*see***Note 3**). Dispose of any air bubbles in the syringe. Connect syringe with luer-stub adapters and non-DEHP medical grade tubing with hollow pin, then fix onto a computer-controlled dual syringe pump for supplying media. Turn on the media supply syringe pump and make sure liquid flow is not obstructed (*see***Note 4**). The flow rate is set at 20 μl/min (*see***Note 5**).
2. Connect syringe with the medium inlet of HYAA-Chip once medium flow is stable (*see***Note 6**). Wait until medium comes out from cell loading inlets (Fig. 2), then insert solid pin

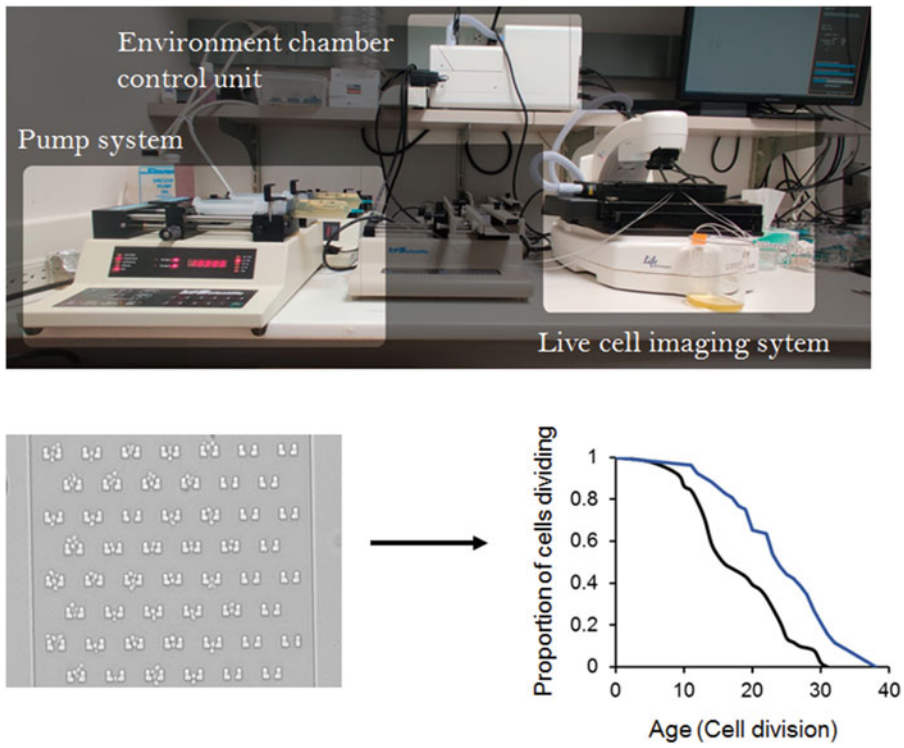

Fig. 1 Microfluidic platform for yeast RLS measurement. Top: The platform consists of a pump system and live cell imaging system connected with an environmental chamber control unit

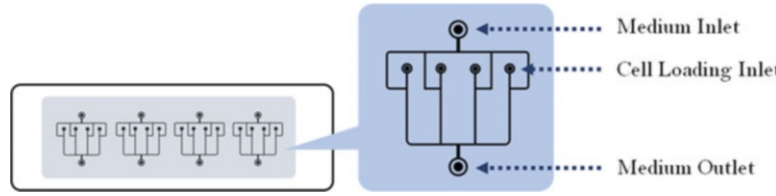

Fig. 2 Schematic design of HYAA microfluidic chip

(*see***Note 7**) into cell loading inlets to block the flow. Connect tubing to outlets for disposal (*see***Note 8**).

3. Check the HYAA-Chip under microscope and wait until all channels are filled with medium.

3.3 Loading Yeast Cells into HYAA-Chip

1. Thoroughly vortex diluted yeast media prepared in A and fill 1 ml syringe (*see***Note 9**). Dispose of any air bubbles and connect with luer-stub adapters and non-DEHP medical grade tubing. Install syringe on the syringe pump for loading cells, turn on the cells loading syringe pump and wait for medium flow to stabilize. Multiple syringes can be installed at same time if using a computer-controlled multisyringe pump.
2. Remove solid pin blocking loading inlets, connect syringe with loading inlet on HYAA-chip, set initial flow rate of the cells loading syringe pump at 1 μl/min (*see***Note 10**).
3. Closely monitor channel loading status under microscope to ensure no cross-contamination is happening (*see***Note 11**).
4. When cells are loaded at desired rate, remove connected tubing and insert solid pin back to stop the flow (*see***Note 12**).
5. Turn off the cells loading syringe pump.
6. Set the medium flow rate of the media supply syringe pump to 10 μl/min.

3.4 Time-Lapse Imaging

1. Set up beacons for imaging, ensure that at least 100 cells are captured. The magnitudes should not be less than 20×.
2. After setting up beacons, turn on automatic focusing and set chamber temperature to 30 °C and humidity to off. Set experimental time as desired.
3. For determination of replicative lifespan, image cells every 10 min. When using fluorescence microscopy, it is preferred to image the cells less frequently (e.g., every 20 min) to avoid phototoxic effects. It is recommended to regularly check the focus of the images during the experiment and, if necessary, adjust it.

4 Notes

1. The regular HYAA chip is designed to be used on budding yeast cells with normal morphology. Since the cup-shaped trap has an opening of 3 μm, some mutant cells of large size cannot be captured. The chip also does not work well with strains whose mother and daughter cells do not separate after division, as inability to remove daughter cells through medium flow will cause blockage.
2. The actual amount of overnight culture added can vary according to cell growth rate and other properties but is best kept between OD600 0.1 and 0.4. The lanes may be hard to fill at a desired proportion if too little cells are added, and too much cells may lead to blockage.
3. Any liquid medium used in experiments should be filter-sterilized instead of autoclaving, as unfiltered medium may contain crystals and other insoluble components which could block the channels. The medium should be at least room temperature, using cold medium will interfere with cell growth and cause complications on experiments.
4. Diameter of syringe is a factor when setting up automatic pumping. Special attention should be kept especially when using same pumping system to operate syringes of different sizes.
5. Pump should be oiled if experiencing difficulty to move around.
6. All components of experimental system should be connected in an airtight fashion and be void of any air bubbles. If stalling of liquid flow is observed, disassemble the system and make sure no air bubble is present.
7. The solid metal pin should only be inserted after medium comes out from cell loading inlets to ensure all air is pushed out from the channels.
8. The tubing connected to outlet should be fixed to disposal container in order to avoid dislocation caused by motion of microfluidic platform.
9. Vortex culture thoroughly before filling. The experiment steps after filling up the syringe should not take too long, or cells will start to settle on the bottom of the syringe, making them hard to come out.
10. The cell filling rate is determined empirically and may vary drastically for different pumping systems, chip designs, or cell concentrations. We suggest performing pilot experiments to determine appropriate speed. Start with a lower filling rate and increase if not enough.

11. When filling rate is too high, the cells will flow backward and increase the possibility of cross-contamination; thus, all channels should be monitored closely during the cell filling process when using the multisyringe pumping system.
12. Be as slow as possible when inserting back the blocking pin as the acute pressure applied may flush fixed cells out.

Acknowledgments

This work was supported by NIH grant R42AG058368 to M.C.J. and W.D.

References

1. Steffen KK, Kennedy BK, Kaeberlein M (2009) Measuring replicative life span in the budding yeast. J Vis Exp (28). https://doi.org/10.3791/1209
2. Schlissel G, Krzyzanowski M, Caudron F et al (2017) Aggregation of the Whi3 protein, not loss of heterochromatin, causes sterility in old yeast cells. Science 355:1184–1187. https://doi.org/10.1126/science.aaj2103
3. Orner EP, Zhang P, Jo MC et al (2019) High-throughput yeast aging analysis for Cryptococcus (HYAAC) microfluidic device streamlines aging studies in Cryptococcus neoformans. Commun Biol 2:256. https://doi.org/10.1038/s42003-019-0504-5
4. Singh P, Ramachandran SK, Zhu J et al (2017) Sphingolipids facilitate age asymmetry of membrane proteins in dividing yeast cells. Mol Biol Cell 28:2712–2722. https://doi.org/10.1091/mbc.E17-05-0335
5. Yu R, Sun L, Sun Y et al (2019) Cellular response to moderate chromatin architectural defects promotes longevity. Sci Adv 5: eaav1165. https://doi.org/10.1126/sciadv.aav1165

Chapter 2

Analysis of Lifespan in *C. elegans*: Low- and High-Throughput Approaches

Adam B. Cornwell and Andrew V. Samuelson

Abstract

Lifespan is the most straightforward surrogate measure of aging, as it is easily quantifiable. A common approach to measure *Caenorhabditis elegans* lifespan is to follow a population of animals over time and score viability based on movement. We previously developed an alternative approach, called the Replica Set method, to quantitatively measure lifespan of *C. elegans* in a high-throughput manner. The replica set method allows a single investigator to screen more treatments or conditions in the same amount of time without loss of data quality. The method requires common equipment found in most laboratories working with *C. elegans* and is thus simple to adopt. Unlike traditional approaches, the Replica Set method centers on assaying independent samples of a population at each observation point, rather than a single sample over time as with "traditional" longitudinal methods. The protocols provided here describe both the traditional experimental approach and the Replica Set method, as well as practical considerations for each.

Key words Aging, Lifespan, Survival analysis, *C. elegans*, High-throughput, Statistical analysis of quantitative phenotypes, Kaplan–Meier, Logistic regression

1 Introduction

Aging research was transformed by two major discoveries in *Caenorhabditis elegans*. The first was the discovery that single genetic changes could drastically alter *C. elegans*lifespan [1, 2]. However, lifespan is not a phenotype that is amenable to analysis by classic forward genetic approaches. Thus, the technological breakthrough of feeding-based RNAi, and subsequent development of comprehensive RNAi libraries, heralded a period of genetic discovery in aging research; to date over 900 genes are known to alter *C. elegans* lifespan after genetic perturbation (WormBase release WS270). Briefly, gene knockdown is achieved through the targeted degradation of endogenous mRNA via complementary dsRNA production within *E. coli* [3].

The most common method for assessing *C. elegans* lifespan is to follow relatively small populations of individual animals over

Sean P. Curran (ed.), *Aging: Methods and Protocols*, Methods in Molecular Biology, vol. 2144,
https://doi.org/10.1007/978-1-0716-0592-9_2,

time, scoring viability based on age-associated decrease in coordinated movement [4, 5]. This method has been widely used, as it provides straightforward, direct measurements of median and maximum lifespan. In this approach—here referred to as the traditional longitudinal method (TLM)—the same population of animals are scored at each observation, and the resulting data is analyzed with standard survival analysis tools such as the Kaplan–Meier estimator and the log-rank test [6, 7]. While this approach can scale to include more conditions by adding additional plates, throughput is limited. Furthermore, as the animals age they demonstrate progressively lower rates of spontaneous movement, necessitating mechanical stimulation with a light touch in order to accurately ascertain viability. In addition to requiring more time on the part of the investigator, manipulations involving touch can damage increasingly frail animals, which may lead to accidental mis-scoring or death of the animal.

The replica set method (RSM) is a high-throughput approach for measuring *C. elegans* lifespan [8–10]. Briefly, a population of isogenic, age-synchronized animals is divided into subpopulations (or "replicas"). Each replica covers a time point in the planned experiment. At each time point, one replica is scored, after which that replicate is discarded. Thus, over the expected lifespan for a given genetic background, a series of isogenic but independent populations are sampled and each individual animal is only ever scored once (*see* **Note 1**). Thus, there is no repeated handling of animals and minimal exposure to the outside environment, which minimizes environmental error. Finally, viability observed at one time point is completely independent of other observations, which minimizes the effect of experimental scoring error and increases throughput by an order of magnitude. This has allowed us to quantitate changes in lifespan over treatment with hundreds of RNAi clones simultaneously [8, 9].

Here, we describe methods for both the TLM (*see* Subheading 3.5) and RSM (*see* Subheading 3.6) approaches to assaying lifespan in *C. elegans*. Figure 1 shows a schematic overview of some of the key differences in setup and scoring between TLM (1a) and RSM (1b).

1.1 General Considerations

There are six major considerations when setting up a lifespan experiment using either approach. Attention to these points will improve rigor and reproducibility both within and across experiments.

1. **Strain**. Genetic background can substantially impact lifespan. Because self-fertilizing hermaphrodites tend to drive alleles to homozygosity, it is critical that strains obtained from different laboratories, knockout consortiums, or the Caenorhabditis Genetics Center (CGC, https://cgc.umn.edu/) be extensively backcrossed (6–10×) to internal wild-type control strains used within one's laboratory. The ideal wild-type (N2) strain to use in *C. elegans* lifespan studies varies, and not all N2 stocks have the same lifespan [11] (*see* **Note 2**).

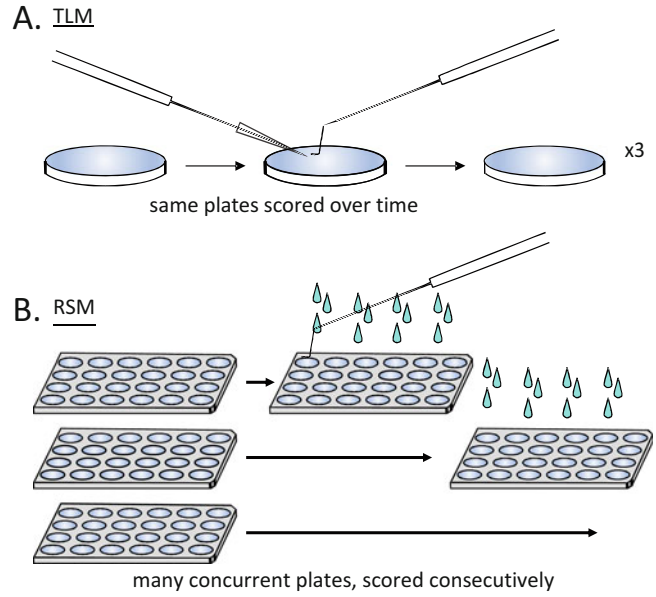

Fig. 1 Traditional Longitudinal (TLM) and Replica Set (RSM) methods of assaying lifespan in *C. elegans*. TLM involves scoring the same animals at multiple observation points during the course of an experiment, while with RSM an independent subpopulation of animals is scored at each time point. RSM improves throughput, enabling many more conditions to be tested by a single investigator in one experimental trial. (**a**) In scoring TLM plates, lethargic animals are touched to check vital status, dead animals are picked off, and cases such as low food or fungal growth on plates may require careful transfer of all the animals to new plates. (**b**) For RSM, each plate is only observed once—a plate is scored by flooding each well with M9 buffer, which stimulates movement of lethargic animals and frees them from sticky bacteria. Animals that do not move on their own are touched with a pick to determine their status. The plate is discarded after scoring at each time point (i.e., a replica is all of the conditions tested at one time point). The minimum number of replicate sets is equal to the total number of time points

2. **Population genetics**. Despite the tendency of self-fertilizing hermaphrodites to drive alleles to homozygosity, *C. elegans* maintained under laboratory conditions are subject to the same population genetic forces as all living creatures (e.g., selective pressure). This is not a theoretical concern for *C. elegans* lifespan analysis, but can be minimized by keeping reference stock strains for all genotypes at −80 °C or in liquid nitrogen, and thawing a new stock every 3–6 months. *An additional control we recommend every laboratory adopt to improve reproducibility and rigor is to freeze back leftover animals used in every lifespan experiment as a resource, which is stored at −80 °C or in liquid nitrogen* (*see* **Note 3**).

3. **Temperature**. Generally, the lower the temperature, the longer *C. elegans* will live (between a range of approximately 16–25 °C) [4]. Notable exceptions are strains with temperature sensitive alleles, such as *daf-2(e1370)*, which are maintained at the 16 °C permissive temperature during development but shifted to higher temperatures for genetic analysis. We have previously shown that animals at 25 °C are under mild heat stress [12] and have found genetic perturbations with differential effects on longevity at different temperatures (unpublished observations).
4. **Amount of food and food choice**. Animals that exhaust their food supply become dietarily restricted and long lived. Plates where the food supply has been exhausted can be distinguished by the loss of a bacterial lawn and burrowed animals, and such cases must be censored (*see* **Note 4**). One must also consider bacterial food source, as *C. elegans* lifespan varies dependent upon the bacteria being consumed as a food source due to varying nutrient content, pathogenicity, and other factors [13]. Genetic background may also increase sensitivity to diet with respect to lifespan; for example, lifespan of *rict-1* mutants is shorter than N2 when fed OP50 but feeding HB101 bacteria substantially extends *rict-1* lifespan while having only marginal impact on wild-type [14].
5. **Reproduction**. A single hermaphrodite can produce 300 self-progeny over the first few days of adulthood. Thus, it is essential to either prevent progeny production or separate parental animals from offspring. Several choices exist to deal with the production of progeny: (1) periodically move animals to new plates, (2) test lifespan in a "feminized" genetic background, or (3) add 5-fluoro-2′-deoxyuridine (FUdR) to late L4/young adult animals (i.e., after the completion of larval development but prior to the formation of internally fertilized progeny). The advantages and disadvantages of each are discussed in **Notes 5**–**7** respectively.
6. **Start with "clean" strains and reagents**. Populations of *C. elegans* can pick up bacterial and fungal contaminants, which can be transferred between plates and even survive freezing and thawing. Contaminated reagents may necessitate early termination of an experiment. The RSM approach reduces exposure to airborne fungal contamination during the course of an experiment. However, there is no substitute for clean workspaces/incubators, use of sterile technique, and keeping stocks of *C. elegans* free of contamination. Alkaline hypochlorite treatment for synchronization prior to a lifespan trial kills many contaminants (*see* Subheading 3.4 and **Note 24**). However, some contaminants colonize the intestinal lumen and survive the procedure outlined in these methods. An alternative method to remove luminal contaminants is described in **Note 8**.

2 Materials

Use ultrapure water (filtered and UV sterilized) for preparing reagents. Practice sterile technique to prevent contamination of both *C. elegans* culture plates and bacterial growth media (*see* **Note 9**). Reagent solutions that cannot be autoclaved (e.g., FUdR and IPTG stocks) should be filter-sterilized with a 0.2-μm filter using a syringe or bottle-top filter system.

2.1 Agarose Growth Media for C. elegans

1. Round petri plates, 60 mm × 15 mm (used in the TLM).
2. Rectangular 24-well plate (used in the RSM, Fig. 2f).
3. Peristaltic dispensing pump, tubing.
4. Hot plate, stir bars.
5. 55 °C large sterile water bath (*see* **Note 10**).
6. Parafilm.

2.1.1 Nematode Growth Media (NGM) for Culture of C. elegans on OP50 E. coli

1. Per 1 L: Combine 17 g bacteriological grade agar, 3 g NaCl (crystal), and 2.5 g Bacto peptone in a 2 L Erlenmeyer flask with stir bar. Add 1 L ultrapure water, stir. Cover and autoclave on a liquid program (~90 min).
2. Transfer to stir plate, add 1 mL 5 mg/mL cholesterol, 1 mL 1 M $CaCl_2$, 1 mL 1 M $MgSO_4$, and 25 mL 1 M KPO_4.
3. Allow to cool to 55 °C, then optionally add 250 μL 40 mg/mL nystatin and 8 mL 25 mg/L streptomycin (*see* **Note 11**).
4. Use standard plate pouring procedures to dispense 12 mL media per 60 mm petri plate.

2.1.2 RNAi Growth Media for Culture of C. elegans on HT115 E. coli

1. Follow **items 1** and **2** of Subheading 2.1.1.
2. Allow to cool to 55 °C. Add 1 mL 25 mg/mL carbenicillin and 6 mL 0.2 g/mL isopropyl β-D-1-thiogalactopyranoside (IPTG) (*see* **Note 12**).
3. Use standard plate pouring procedures to dispense 12 mL media per 60 mm petri plate, or 1.5 mL per well for 24-well plates.

2.2 E. coli and RNAi for Feeding-Based RNAi

1. OP50 *E. coli* (*see* **Note 13**).
2. HT115 *E. coli*, the typical strain used for feeding-based RNAi (*see* **Note 13**).
3. RNAi clones in HT115 can be ordered individually pretransformed into HT115 or as collections of pretransformed clones in frozen glycerol stocks in microtiter plates (*see* **Note 14**).

2.3 Bacterial Cultures (Handling)

1. Luria broth (LB), with an appropriate antibiotic (*see* **Note 15**).
2. Bleach.

Fig. 2 Equipment and consumables for Replica Set experiments. Equipment necessary for RSM experiments is commonly available in laboratories that work with *C. elegans*, especially those which regularly utilize feeding-based RNAi. (**a**) 96-Well culture plate for storage of frozen libraries of bacterial RNAi clones as glycerol stocks. (**b**) Rectangular single-well plate for LB amp + tet agar slabs for creating intermediate-term working cultures of RNAi libraries on solid media. (**c**) Reagent reservoir for bulk reagent pipetting tasks with multichannel pipettes, such as adding fresh LB to a new 96-well plate. (**d**) Gas-permeable adhesive membrane for sealing deep-well plates during incubation while allowing gas exchange. Note that in the image a corner of the backing has been peeled back to reveal the membrane. (**e**) 2 mL deep-well culture plate for seeding replica plates. (**f**) 24-Well culture plate for use as replica plates. In a typical experiment, wells would be filled with solid RNAi growth media before seeding with bacteria and then *C. elegans*. (**g**) Electronic 1250 μL six-channel repeat pipette with adjustable tip spacing (sometimes referred to as an "equalizer" pipette). (**h**) Electronic 300 μL 12-channel repeat pipette (fixed spacing). (**i**) Pin plate replicator for 96-well plates with stainless-steel pins. Allows easy transfer of bacteria from glycerol stocks to liquid culture, or from liquid culture to solid media, while also being easy to sterilize. (**j**) Adhesive foil cover for frozen RNAi library glycerol stock plates. (**k**) Rubber roller for securing adhesive foil plate covers

3. Ethanol, pure.
4. 96-Well cultureplates, 340 μL wells (for glycerol stocks of RNAi collections, Fig. 2a).
5. Rectangular plate (Fig. 2b) (for colonies of RNAi clones, Fig. 3).
6. 50 mL media reservoir (Fig. 2c).

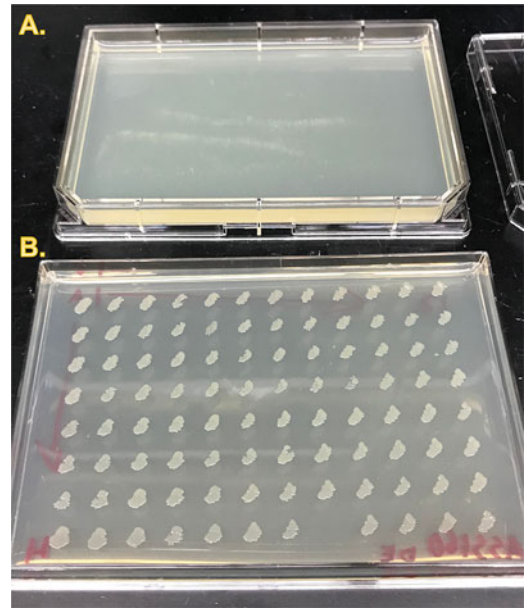

Fig. 3 Typical working stock of an RNAi library. To minimize handling of frozen glycerol stocks, the frozen stocks are "stamped" to agar plates using a pin replicator (Fig. 2i) to create a "working plate" that will be good for 2–8 weeks when stored at 4 °C (*see* **Note 18**). The pin replicator or a multichannel pipette can then be used to inoculate liquid cultures. (**a**) Single-well rectangular plate with uninoculated LB amp + tet agar, lid removed. (**b**) An RNAi library plate after overnight incubation at 37 °C. Note that the spacing between spots is such that it is possible to pick from any spot without risk of cross-contamination

7. Permeable membrane (e.g., Breathe-Easy microplate seals, Fig. 2d).
8. 96-Well plates, deep well, 2 mL capacity wells (Fig. 2e).
9. 96-Well plates, deep well, 600 μL capacity wells.
10. 24-Well plates (RSM only) (Fig. 2f).
11. 6-Well multichannel repeat pipette with adjustable tip spacing (Fig. 2g).
12. 12-Well multichannel repeat pipette (Fig. 2h).
13. 96-Pin plate replicator (Fig. 2i).
14. Adhesive aluminum foil cover (Fig. 2j).
15. Rubber roller to seal foil to plates (Fig. 2k).

2.4 LB + Ampicillin + Tetracycline Agar Plate Recipe for HT115 Culture

1. Per 1 L: Add 32 g LB agar to 1 L of ultrapure water with a sterile stir bar in a 2 L flask. Stir on a stir plate. Once well-mixed, add 1.5 mL 2 N NaOH. Autoclave on a liquid program. Allow to cool with stirring until reaching 55 °C. Add 3 mL of 5 mg/mL tetracycline, and 1 mL of 50 mg/mL ampicillin. Allow to mix.

2. Use standard plate pouring procedures to dispense about 45 mL sterilized liquid LB agar mix per rectangular single-well plate.

2.5 Caenorhabditis elegans

1. *C. elegans* strains; typically obtained from the Caenorhabditis Genetics Center (CGC) (*see* **Note 16**).
2. Motorized tube rotator.
3. Plastic lidded storage boxes (to hold plates).
4. Plastic bags (to hold boxes).
5. *C. elegans* M9 buffer (3 g KH_2PO_4, 6 g Na_2HPO_4, 5 g NaCl. Add H_2O to 1 L. Autoclave. Allow to cool; add 1 mL sterile 1 M $MgSO_4$).
6. Hypochlorite egg prep solution (6 mL bleach, 3.2 mL 5 M NaOH, 800 μL H_2O), store for a maximum of 2 weeks.
7. 5-Fluoro-2′-deoxyuridine (FUdR), 1000× stock: dissolve 1 g FUdR into 10 mL ultrapure water, filter-sterilize with a 0.2-μm filter. Aliquot into sterile 1.5 mL tubes. Store at −20 °C.

3 Methods

Here we describe the necessary preparatory steps and both the TLM and RSM in detail. Examples of actual lifespan data generated by each approach using similar conditions are shown in Fig. 4. For each approach, *C. elegans* populations and experiment plates with animals should always be stored in a dark temperature-controlled incubator at a temperature appropriate to the strain(s) under study when not being prepared, inspected, or scored.

3.1 RNAi Library Preparation for RSM

1. Remove adhesive foil cover (Fig. 2j) from previously prepared frozen 96-well glycerol sock library plate containing RNAi clones (*see* **Note 14**).
2. Sterilize plate replicator (Fig. 2i) by immersing the pins in 50% bleach, ultrapure H_2O, and ethanol (sequentially). Immerse pins for 30 s when in bleach and ethanol. Flame the tips briefly after ethanol immersion. Repeat (*see* **Note 17**).
3. Gently—but firmly—grind plate replicator into the wells of the still-frozen glycerol stocks. Inoculate 200 μL LB + Amp cultures and seal the inoculated plate with a permeable membrane (such as Breathe-Easy microplate seals, Fig. 2d). Allow cultures to grow overnight at 37 °C with optional shaking. Reseal the glycerol stock plate with an adhesive foil cover.
4. Sterilize plate replicator as in **step 1** and immerse tips into the overnight culture. Apply the tips with even pressure to a rectangular LB amp + tet agar plate, and transfer bacteria to the plate gently with a small circular motion without allowing the

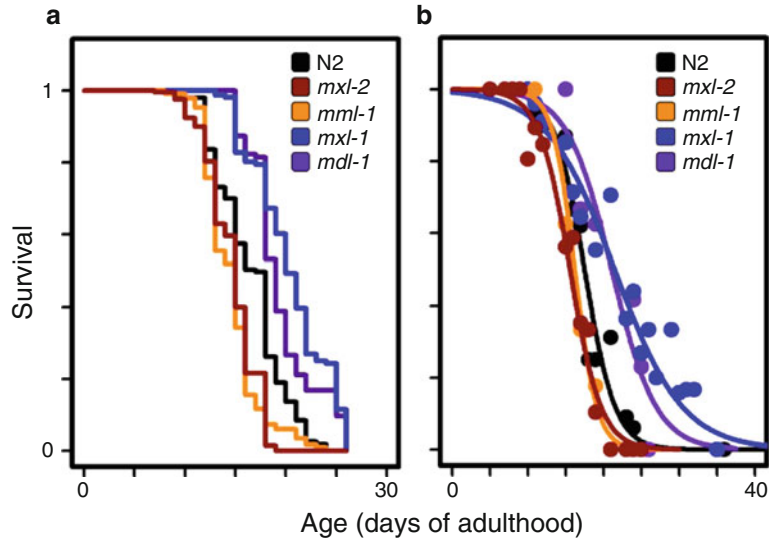

Fig. 4 Results from the Replica Set method are similar to those of the traditional approach. An example of lifespan results from both the RSM and TLM for the same set of experimental conditions: perturbation of either gene of the MML-1::MXL-2 heterodimeric complex shortens lifespan compared to N2 (WT), while perturbation of either component of the opposing MDL-1::MXL-1 complex extends lifespan. While the approach to plotting the data between the RSM and TLM is different, the conclusions reached are the same. (**a**) Traditional lifespan assay, Kaplan–Meier plot. (**b**) Replica set data, fit to a logit curve. (This figure is reprinted from [31] with permission via a Creative Commons Attribution (CC BY) license)

pins to dig into the agar. Ensure adequate space is left between adjacent spots. Allow colonies to grow overnight at 37 °C (Fig. 3).

5. Store agar plate at 4 °C inverted (lid side down), wrapped in Parafilm. Plates can be stored for 2–8 weeks (*see* **Note 18**).

3.2 Preparation and Seeding of Agar Nematode Plates: 60 mm Plates for TLM

1. Prepare enough liquid LB media to grow cultures for seeding at least three to six 60 mm plates per test condition (*see* **Note 19**). Each plate requires 3 mL of culture which will be 10× concentrated before seeding (*see* **Note 20**). Include the appropriate antibiotics, if applicable (*see* **Note 15**).
2. Grow cultures of *E. coli* overnight (16–20 h at 37 °C in a shaking incubator at 220 rpm).
3. Concentrate bacteria to 10× by centrifugation at 3000 × *g* for 15–20 min in a benchtop centrifuge, aspirate the supernatant, and resuspend the pellet at 1/tenth starting volume of LB.
4. Aliquot 200–300 μL of bacteria to each 60 mm plate. To increase experimental rigor, label plates so the experimenter will be blind to the test conditions.

5. Allow open plates to dry in a clean environment, such as a laminar flow hood/bench, until all liquid has been absorbed or allow covered plates to dry on the bench overnight. Drying may take several hours. Monitor plates while drying to ensure that the agar is dry without overdrying (*see* **Note 21**). For seeded RNAiplates dried in a hood, store dried plates within a plastic worm box overnight (up to 24 h) at room temperature to allow the induction of dsRNA production.
6. Store unused seeded plates at 4 °C (*see* **Note 22**).

3.3 Preparation of Bacterial Cultures and Seeding of Agar Nematode Plates: Multiwell Replicate RNAi Plates for RSM

1. Determine the necessary number of 24-well replicate plate sets, and the number of plates per replicate set to calculate the total number of necessary plates (*see* **Note 23** for considerations). Figure 5 illustrates how the liquid culture grown in a 96-well plate is allocated to the 24-well replicate plates. Replicate plates in each 24-well block should be distinguished by a colored stripe or other label.
2. For every ten replicate sets, inoculate 1.5 mL LB + Amp cultures in 96-well deep-well plates (Fig. 2e) using the plate replicator (Fig. 2i) and the bacterial colonies previously prepared on an LB amp + tet agar slab plate (Fig. 3b). Cover with breathable membrane seal (Fig. 2d) and grow 16–20 h at 37 °C with shaking.
3. Using a 6-well multichannel repeat pipette with adjustable tip spacing (Fig. 2g), seed 120 µL of an overnight culture to each well. Allow plates to dry uncovered in laminar flow hood until all liquid has been absorbed. Do not over-dry plates (*see*

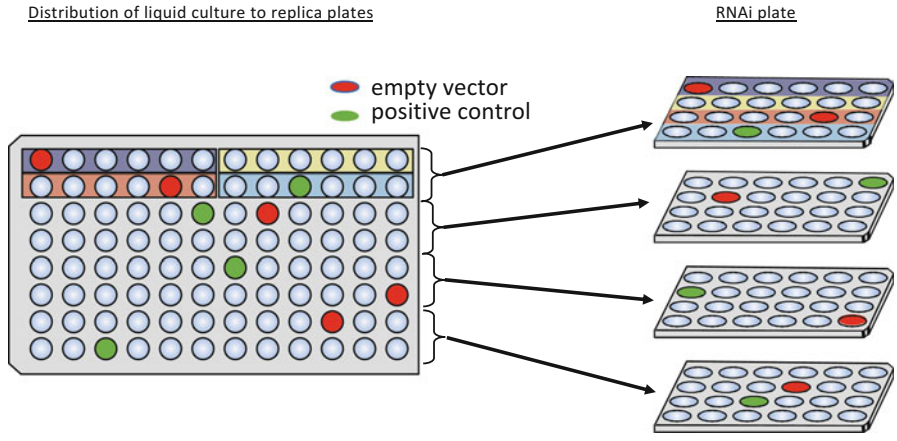

Fig. 5 Creating a "replicate set" from a 96-well RNAi library plate. A 96-well RNAi library plate is divided into four blocks of 24 wells, where the four unique 24-well plates make up part of one "replicate set." The library should be set up such that each block of 24 wells has at least one randomly placed empty-vector control (L4440 RNAi) and positive control. Well A1 of the 96-well library is usually reserved for an empty vector control

Note 21). To allow for induction of dsRNA in HT115 *E. coli*, store dried plates overnight at room temperature (*see* **Note 12**).

4. Store unused seeded plates at 4 °C (*see* **Note 22**).

3.4 Obtaining a Synchronized Population of Animals

1. A synchronized population of *C. elegans* may be obtained from gravid adults by methods including (A) an "egg lay," or (B) alkaline hypochlorite treatment ("egg prep") (*see* **Note 24**). Use hypochlorite treatment for RSM experiments. Either technique will provide enough animals for most TLM experiments (*see* **Note 25**).

(A) For an egg lay:

1. Move 5–10 gravid adult animals to new plates (with food) that will be used for the lifespan experiment. Use only animals that have not starved for at least three generations (*see* **Note 24**).
2. Allow the adults to lay eggs for 4 h or until there are about 50 eggs on each plate.
3. Remove the adults, and move the plates to incubator.

(B) For hypochlorite treatment:

1. Using M9, collect animals into 15 mL centrifuge tube using a glass Pasteur pipette with a plug. A strain may be pooled from multiple plates.
2. Centrifuge tubes for 15 s at approximately ~650 × *g*. Aspirate supernatant.
3. Wash with M9: add 10 mL fresh M9, centrifuge 30 s, aspirate supernatant. Repeat.
4. Resuspend in 4 mL M9 and add 2 mL hypochlorite egg prep solution. After adding the hypochlorite solution, the timing of the remaining steps is critical to optimize yield.
5. Vortex for 3 min, with occasional shaking (every 30–60 s). After the 3 min have elapsed, check the tube under a dissecting microscope—eggs should be visible and depending on the density may appear as a "cloud." If no eggs are yet visible and adults are still intact, vortex for an additional 10–20 s and check again.
6. Centrifuge for 30 s, aspirate the supernatant, and wash twice with M9 as in **step 3**. The first wash in particular should be performed as quickly as possible, to minimize the additional exposure of embryos to bleach.
7. Resuspend the eggs in 3 mL M9, and transfer to a new tube. Allow hatching overnight with rotation at 20 °C (or other temperature, if necessary). The embryos with hatch and arrest at L1, yielding a synchronized population.

8. Determine the density of L1 animals per μL: pipette 10 μL of resuspended L1s onto a 60 mm plate and count (3×) to determine the average number of L1s per μL. Calculating the density of animals is necessary for the distribution of the appropriate number of animals. The "L1 solution" may need to be diluted.

3.5 Traditional Longitudinal Method (TLM; Low-Throughput)

1. Identify necessary *C. elegans* strains and RNAi clones. OP50 *E. coli* can be used if feeding-based RNAi is not needed. Transformed HT115 *E. coli* is used for feeding-based RNAi. Prepare 3–6 60 mm plates per condition using RNAi growth media for RNAi experiments, or NGM media for OP50 (*see* Subheading 2.1). If not immediately preparing bacteria, unseeded plates can be stored at 4 °C. Choice of approach in handling progeny may influence the selection of *C. elegans* strains for the experiment (*see* **Notes 5**–**7** for considerations).
2. Prepare and seed bacterial cultures as described in Subheading 3.2.
3. Prepare *C. elegans* as described in Subheading 3.4. For the TLM use at least 50 animals per plate (i.e., each technical replicate).
4. If using FUdR to control progeny production, when animals reach the L4 stage dilute filter-sterile 1000× FUdR stock to 160× with ultrapure water and add 50 μL of 160× FUdR to the center of each 60 mm plate.
5. Inspect plates and remove males. Males can be distinguished on a dissecting stereomicroscope from hermaphrodites at the L4 stage. When studying hermaphrodites, it is important that males be removed before the adult stage, *see* **Note 26**.
6. Score viability daily. Animals that are not moving spontaneously can be touched gently on the head with a platinum wire (or alternatively with an eyelash). Animals that fail to move are scored as dead and removed from the plate. Record the number of dead animals observed for each plate/condition for each time point observed. As animals age they become increasingly lethargic and are eventually paralyzed, such that older live animals may only be able to be distinguished by a subtle movement of the head in response to touch.
7. Animals that die for reasons unrelated to aging should be censored, examples include: overt developmental defects, desiccation on the side of the dish, and intestinal rupturing through the vulva.
8. Any males observed during the course of the experiment should be removed and the number recorded.

9. If a plate appears likely to starve before the end of the experiment, or if fungal contamination is observed, move all remaining animals to a backup plate with the relevant bacteria (and FUdR, if appropriate).
10. Repeat from **step 6** until no live animals remain.
11. Additional experiment trials should be conducted independently and recorded separately.
12. *See* Subheading 3.7 for data analysis.

3.6 Replica Set Method (RSM; High-Throughput)

1. Prepare RNAi library plates and create LB amp + tet agar plates for inoculating the bacterial cultures that will be used for seeding the replicate plates. *See* Subheading 3.1.
2. Determine the necessary number of 24-well agar *C. elegans* plates for the replicate sets (*see* **Note 23**) and prepare as outlined in Subheading 2.1.
3. Seed bacterial cultures to prepared 24-well replica plates according to Subheading 3.3.
4. Determine the minimum number of animals needed and expand parental populations accordingly. The number needed can be calculated based on 15–20 animals per well, 24 wells per plate, for the number of plates determined in **step 2**. Depending on the density of the starting population, one 100 mm plate with many gravid adults can provide 20,000–50,000 L1s from a hypochlorite treatment egg prep (*see* **Note 25**).
5. Prepare populations of synchronized L1s by hypochlorite treatment as described in Subheading 3.4.
6. Add 15–20 L1 animals to each well of the 24-well replica plates. This can be done efficiently with a reagent reservoir and a 6-well electronic pipette, with the volume based on the previously calculated density of the L1 solution. Be sure to gently mix the L1s in the reservoir occasionally, to prevent settling.
7. When the animals have reached L4, add 25 μL of 50× FUdR (dilute filter-sterile 1000× FUdR stock with ultrapure water) to each well using a 6-channel electronic pipette or repeat pipettor (*see* **Note 7**).
8. For each observation timepoint, take one complete set of plates (i.e., 1 replicate) from the incubator and flood each well with M9. Record the total number of animals, and then touch any nonmoving animals on the head with a platinum wire. Animals that do not move are counted as dead; at later time points movement may be limited to subtle head motion. Animals that die for reasons unrelated to aging should be censored, examples include: overt developmental defects, desiccation on the side of the dish, and intestinal rupturing through the vulva.

9. Do not score wells that have been starved or are contaminated—make a note of the event but do not record the total.
10. Discard plates after scoring. For each well, repeat from **step 8** daily until no live animals have been observed for two consecutive time points.
11. Additional experimental trials should be conducted independently.
12. *See* Subheading 3.7 for data analysis.

3.7 Plotting and Analysis of Lifespan Data

1. TLM data can be plotted and analyzed with any one of the many software tools that support survival analysis with the nonparametric Kaplan–Meier estimator [6] and the log-rank test [7] (*see* **Note 27**), Different software tools vary in their requirements for data formats. Be sure to consider censored animals appropriately—in this case as right-censored—as including this information avoids bias [15].
2. For RSM experiment analysis, data is fit to a logit curve to estimate median and maximum lifespan, as logit curves are most appropriate for modelling *C. elegans* mortality data [16]. As most tools for survival analysis do not support logit curve modeling, we developed a tool, WormLife, that handles both logit (for Replica Set) and Kaplan–Meier (for traditional lifespan) survival analyses. *See*https://github.com/samuelsonlab-urmc/wormlife for documentation and to find the latest version (*see* also **Note 28**).

4 Notes

1. For the RSM, one must determine how long a strain on a control RNAi will survive prior to any experiment, then plan the number of time points to best measure how an RNAi clone will impact lifespan (i.e., 15 time points requires a minimum of 15 sets).
2. N2 is the wild-type strain, and the Caenorhabditis Genetics Center (CGC, https://cgc.umn.edu/) has three different stocks available: "N2" (often referred to as "N2H," https://cgc.umn.edu/strain/N2), "N2 Male" (referred to as "N2M," https://cgc.umn.edu/strain/N2%20Male), and "N2 (ancestral)" (https://cgc.umn.edu/strain/N2%20(ancestral)). Variations in lifespan have been found between these three stocks, with "N2 (ancestral)" being the shortest lived and "N2M" the longest lived under standard laboratory conditions [11]. For years the "N2M" stock was recommended as the ideal reference wild-type stock [11]. However, recently a mutation in *fln-2* has been found that alters longevity of N2M, suggesting

"N2H" may be a more appropriate wild-type reference strain (*see* "'N2 male' is a long-lived fln-2 mutant," http://wbg.wormbook.org/2018/12/11/n2-male-is-a-long-lived-fln-2-mutant/).

3. Leftover arrested L1 animals can be readily frozen back to create a "snap shot" of the specific genetic profile of the strain used in each lifespan experiment. Carefully annotating frozen stocks that were actually used in specific experiments provides a critical resource: at a later date it could be compared to other strains that are at least superficially of an identical genetic background (either within or between laboratories). This greatly improves experimental reproducibility and rigor, as direct comparison allows assessment of the effect of genetic background.
4. It is possible to reseed with concentrated bacteria or move animals to a new plate with food, but this must occur prior to exhaustion of food. Note, RNAi clones require induction of dsRNA production via IPTG prior to reseeded (i.e., directly adding to the bacterial culture).
5. Picking animals to new plates every other day or so during the reproductive period is an option only applicable to traditional lifespan analysis (TLM). However, there are also some strain-specific considerations. Some strains (e.g., *daf-2(e1370)*) have much longer "reproductive spans," necessitating additional days on which parents would have to be picked to new plates. Strains with an *egl* phenotype (egg-laying defect) cannot be analyzed by this method and require FUdR, as they undergo high rates of premature death due to internal hatching. For example, the link between TGF-β signaling and lifespan was not initially appreciated due to such defects, and was only realized when FUdR was used [17].
6. Feminized genetic mutants fail to produce sperm and therefore cannot produce progeny in the absence of males. One must inspect plates for males and remove them to prevent mating. *Fem* mutations, such as *fer-15(b26);fem-1(hc17)* which is a temperature-dependent sterile strain, have been utilized used in aging studies and do not appear to cause any overt aging-phenotypes [18, 19]. However, the use of *fem* alleles requires the creation of double mutant animals for every genetic background to be examined. Note that strains with mutations that ablate the germ line are long-lived (e.g., *glp-1*) and are not equivalent to *fem* backgrounds.
7. FUdR (5-fluoro-2′-deoxyuridine) is a nucleotide base analog that blocks DNA synthesis. Since adult *C. elegans* somatic cells are postmitotic, treatment with FUdR does not affect the soma, but prevents germline proliferation. FUdR is commonly

added directly to plates, but care must be taken with timing, as addition must occur at the L4 stage, after somatic development but before egg production. Addition of FUdR after animals have become gravid adults will result in progeny that will arrest at the L1 stage but will feed, thereby exhausting the food from the plates. Addition of FUdR prior to L4 will disrupt development, especially at the vulva, which will eventually cause animals to rupture between day 7 and 14 of adulthood. Higher concentrations of FUdR can also lead to rupturing. It is worth noting that FUdR treatment influences lifespan in some genetic backgrounds [20, 21].

8. Here is a brief method for cleaning up strains with luminal contamination: (1) Pick 5–10 gravid animals to an NGM plate with no food and let them crawl around a few minutes. (2) Pipet 10–15 μL of hypochlorite egg prep solution close to the edge of a different NGM plate (away from the bacterial lawn). (3) Pick up the animals from the unseeded intermediate plate by sliding the pick under them ("spatula style") and transfer them directly into the spot of hypochlorite solution. Adults will die; internally fertilized eggs will hatch overnight and crawl to the bacteria. (4) Transfer L1 animals farthest from the hypochlorite spot to a new plate.
9. Sterile technique is essential when preparing for lifespan experiments. Sterilize work areas with a 10% bleach solution followed with an ultrapure water rinse, then 70% ethanol. This includes lab benches and other surfaces such as hoods. Work over a flame when possible, and wear gloves, a surgical mask, and a clean lab coat. Minimize the time plates are left open to the air and outside of the incubator. Never store boxes, plates, lab coats, and so on on the floor. Anything that touches the floor should be considered as contaminated.
10. As it is often difficult to maintain sterility of a water bath, we use Laboratory Armor Beads (e.g., Fisher Scientific #A1254301) instead of water in the bath. We have found the "bead bath" to be both cleaner and lower maintenance.
11. Streptomycin and nystatin can optionally be added to prevent undesired growth of contaminating organisms on plates, which is important for long experiments, such as for lifespan assays. However, not all laboratories typically work with an OP50 stock that is streptomycin-resistant. The CGC has both variants available, OP50 (*not* streptomycin resistant) and OP50-1 (resistant).
12. Unseeded RNAi agar plates can be stored at 4 °C for several months before seeding with bacteria. Some laboratories add fresh IPTG (concentration) at the same time as bacterial seeding, to ensure adequate dsRNA production in case of

degradation of the IPTG in the agar over time. Do not add IPTG to bacterial cultures too early, as this can severely reduce the bacterial growth rate.

13. For experiments using RNAi, dsRNA production is induced in transformed HT115 *E. coli* [22] on RNAi plates, and for lifespan studies without RNAi, OP50 *E. coli* on standard NGM plates can be used. HT115 is derived from K12 *E. coli* and is used for feeding based RNAi, as it lacks RNase III, the enzyme normally responsible for degradation of double-stranded RNA in *E. coli* [23]. In contrast, the typical food source to maintain *C. elegans* is OP50 which is *E. coli* B.

14. Collections of RNAi clones are commonly maintained as glycerol stocks in a 96-well format and stored at −80 °C. Always keep frozen—work on dry ice when at the bench—and minimize exposure to even slight warming, as this greatly reduces *E. coli* viability. Custom RNAi sublibraries (i.e., a group of RNAi clones selected from a larger library) can be easily assembled for convenience. Within a collection, each RNAi clone is represented at least once. In principle, this approach could be similarly applied for different chemical treatments, different animal strains, and so on. When assembling sublibraries in a 96-well format, typically, an empty vector negative control is included in the first well of a collection of 96. Specifically, for RSM assays, as the clones from each 96-well plate are split into blocks of 24 wells on different plates, an additional empty vector is inserted randomly within every 24 wells of the library, so that every resulting 24-well plate has an empty vector well as a negative control (Fig. 5). Similarly, a positive control should be randomly inserted within every group of 24-wells (Fig. 5). For example, when looking at a collection of RNAi clones expected to increase lifespan, *daf-2(RNAi)* is frequently included. *Daf-2* encodes the *C. elegans* insulin/IGF-1 receptor, and *daf-2* inactivation via feeding-based RNAi robustly increases lifespan at least two-fold in wild-type animals [1]. As of the time of writing, both the Ahringer [24] and Vidal (ORFeome) [25] RNAi libraries or individual clones are available from two commercial vendors, Source Bioscience (https://www.sourcebioscience.com/products/life-sciences-research/clones/rnai-resources/) and Horizon Dharmacon (https://dharmacon.horizondiscovery.com/cdnas-and-orfs/non-mammalian-cdnas-and-orfs/c-elegans/). Note that the former provides library plates in a 384-well format, whereas the latter utilizes 96-well plates.

15. HT115 *E. coli* is grown in LB with ampicillin (50 μg/mL). Standard OP50 *E. coli* is not ampicillin resistant.

16. Strain selection may influence the design of the assay, and is necessary to consider prior to preparing other reagents, as different strains may have substantial differences in lifespan even without additional treatment. Additionally, larger populations of animals are required for RSM than TLM experiments, which may be difficult to obtain for very slow-growing strains, or for those with extrachromosomal transgenes or balanced mutations. Some strains may also have temperature-sensitive alleles, requiring growth development at a temperature different from the typical 20 °C; as temperature can have a dramatic effect on *C. elegans* lifespan, it is necessary to treat all strains in an experiment similarly in order to achieve comparable results.
17. Be sure to remove all bleach from the pins of the plate replicator, as it could inadvertently kill bacteria. Do not leave the pins in bleach for extended periods, it will corrode the stainless-steel pins. Avoid overly long exposure of the pin replicator to the flame after ethanol immersion so that the pins cool fast enough before transferring bacteria without affecting viability.
18. Bacterial colonies on the stamped agar plate are now ready for subsequent use. Always store plates lid side down; lid side up will allow condensation to cross-contaminate RNAi clones! Colonies of *E. coli* can be stored for 2–8 weeks at 4 °C, depending on particular RNAi clones, as RNAi clones retain efficacy in dsRNA production after IPTG induction for variable lengths of time. For small collections of RNAi clones, RNAi efficiency should be empirically determined by qRT-PCR to confirm gene expression knockdown.
19. At least three technical replicate plates should be set up per condition. When using FUdR, set up two extra backup plates in case animals need to be moved off of contaminated plates to a backup plate. When not using FUdR, three additional plates will be needed per condition to transfer parental animals away from progeny every 2 days, until the cessation of progeny production—additional plates may be handy in case of contamination issues.
20. Concentration of bacteria is optional but recommended to decrease incidence of starvation during the course of the experiment. If not concentrating, adjust starting volumes of culture appropriately.
21. Cracking of the agar is a symptom of overdry plates/wells. Dry agar and cracking can lead to *C. elegans* burrowing. Wet plates or wells can also lead to burrowing behavior. As burrowed animals should be censored when scoring lifespan experiments, monitoring of plates during drying is important.

22. Do not leave dried plates at room temperature for more than 24 h. After 1 day at RT, plates can be stored at 4 °C for up to 2 weeks in a sealed zip-lock bag (to prevent plates from drying out). Before use, return plates stored at 4 °C to room temperature within the zip-lock bag to prevent condensation from introducing airborne fungal contaminants.
23. As RSM requires one set of replicate plates per observation, it is necessary to estimate the number of necessary observations at the beginning of the experiment. This is usually based on preliminary knowledge of the lifespan for a given set of experimental conditions of interest (strain, RNAi, etc.). Observation frequency is also important to consider; we will usually score a set for a given strain every other day until deaths are observed, at which point we change to daily scoring. Thus, the number of plates necessary for one strain in an RSM trial can be calculated as $R * (O + E)$, where R is the number of plates in each replicate set (usually four if using 24-well replicate plates and a full 96-well library), O is the estimated number of observations, and E is a number of extra replicate sets allocated for cases such as contamination.
24. The "egg lay" method is a relatively quick way to obtain small synchronized populations, which does not necessarily involve synchronization by larval arrest, which is worth considering in the context of possible synthetic interactions with larval arrest. Alternatively, alkaline hypochlorite treatment could be used to isolate eggs, which are directly seeded for subsequent lifespan analysis. However, some eggs will not survive (leading to a smaller number of animals than anticipated) and synchronizing L1 animals via arrest yields a population with a tighter developmental window between animals. As many more L1s are often obtained than are needed for the experiment, the remaining animals can be frozen (*see* **Note 3**).
25. Starvation leads to transgenerational changes in gene expression that can influence lifespan [26, 27]. When preparing for an experiment, ensure that the parent population has not starved for at least three generations.
26. Even with FUdR treatment, hermaphrodites that have mated live shorter than those that have not which can skew the results of a TLM experiment [28–30]. As such, it is critical to check plates and remove any males at the L4 stage.
27. The Kaplan–Meier estimator and associated plots, as well as the log-rank test are supported by many software tools, available both online and as part of statistical packages. A popular free option is the web-based OASIS2 (https://sbi.postech.ac.kr/oasis2/). Other tools supporting such analysis that might already be available to investigators include Graphpad Prism

(https://www.graphpad.com/scientific-software/prism/) and JMP (https://www.jmp.com/). Be sure to use tools which support right-censored data and enter your recorded information on censored animals. Check for data quality issues such as missing observations and unexpected results for control conditions before running statistical analysis.

28. We developed WormLife for analysis of Replica Set experiments; support is also included for Kaplan–Meier-style plots. The primary user interface includes features for plotting survival curves from both methods, comparing curves between trials, and obtaining the estimated median survival values. Features are included for automating plotting for large-scale experiments with many different conditions. An R script is also included for permutation-based statistical testing between conditions. As detailed discussion is beyond the scope of this chapter, *see* https://github.com/samuelsonlab-urmc/wormlife for current documentation, and our previously published protocol for getting started with the software in [10].

Acknowledgments

This work was supported by NIH grants R01AG043421 and R01AG62593.
Some strains were provided by the CGC, which is funded by NIH Office of Research Infrastructure Programs (P40 OD010440).

References

1. Kenyon C, Chang J, Gensch E et al (1993) A *C. elegans* mutant that lives twice as long as wild type. Nature 366:461–464. https://doi.org/10.1038/366461a0
2. Johnson T (1990) Increased life-span of age-1 mutants in *Caenorhabditis elegans* and lower Gompertz rate of aging. Science 249:908–912. https://doi.org/10.1126/science.2392681
3. Timmons L, Fire A (1998) Specific interference by ingested dsRNA [10]. Nature 395:854. https://doi.org/10.1038/27579
4. Klass MR (1977) Aging in the nematode *Caenorhabditis elegans*: major biological and environmental factors influencing life span. Mech Ageing Dev 6:413–429. https://doi.org/10.1016/0047-6374(77)90043-4
5. Raj F, Amrit G, Ratnappan R et al (2014) The *C. elegans* lifespan assay toolkit. Methods 68:465–475. https://doi.org/10.1016/j.ymeth.2014.04.002
6. Kaplan EL, Meier P (1958) Nonparametric estimation from incomplete observations. J Am Stat Assoc 5318910:457–481. https://doi.org/10.2307/2281868
7. Mantel N (1966) Evaluation of survival data and two new rank order statistics arising in its consideration. Cancer Chemother Rep 50:163–170
8. Samuelson AV, Carr CE, Ruvkun G (2007) Gene activities that mediate increased life span of *C. elegans* insulin-like signaling mutants. Genes Dev 21:2976–2994. https://doi.org/10.1101/gad.1588907
9. Samuelson AV, Klimczak RR, Thompson DB et al (2007) Identification of *Caenorhabditis elegans* genes regulating longevity using enhanced RNAi-sensitive strains. Cold Spring Harb Symp Quant Biol 72:489–497. https://doi.org/10.1101/sqb.2007.72.068
10. Cornwell AB, Llop JR, Salzman P et al (2018) The replica set method: a high-throughput

approach to quantitatively measure *Caenorhabditis elegans* lifespan. J Vis Exp (136):e57819

11. Gems D, Riddle DL (2000) Defining wild-type life span in *Caenorhabditis elegans*. J Gerontol A Biol Sci Med Sci 55:215–219
12. Das R, Melo JA, Thondamal M et al (2017) The homeodomain-interacting protein kinase HPK-1 preserves protein homeostasis and longevity through master regulatory control of the HSF-1 chaperone network and TORC1-restricted autophagy in *Caenorhabditis elegans*. PLoS Genet 1:1–46
13. Kim DH (2013) Bacteria and the aging and longevity of *Caenorhabditis elegans*. Annu Rev Genet 47:233–246. https://doi.org/10.1146/annurev-genet-111212-133352
14. Soukas AA, Kane EA, Carr CE et al (2009) Rictor/TORC2 regulates fat metabolism, feeding, growth, and life span in *Caenorhabditis elegans*. Genes Dev 23:496–511. https://doi.org/10.1101/gad.1775409.2004
15. Clark TG, Bradburn MJ, Love SB, Altman DG (2003) Survival analysis part I: basic concepts and first analyses. Br J Cancer 89(2):232–238
16. Vanfleteren JR, De Vreese A, Braeckman BP (1998) Two-parameter logistic and Weibull equations provide better fits to survival data from isogenic populations of *Caenorhabditis elegans* in axenic culture than does the Gompertz model. J Gerontol Ser A Biol Med Sci 53A:B393–B403. https://doi.org/10.1093/gerona/53A.6.B393
17. Shaw WM, Luo S, Landis J et al (2007) The *C. elegans* TGF-B Dauer pathway regulates longevity via insulin signaling. Curr Biol 17:1635–1645. https://doi.org/10.1016/j.cub.2007.08.058
18. Hansen M, Hsu AL, Dillin A, Kenyon C (2005) New genes tied to endocrine, metabolic, and dietary regulation of lifespan from a *Caenorhabditis elegans* genomic RNAi screen. PLoS Genet 1:0119–0128. https://doi.org/10.1371/journal.pgen.0010017
19. Hansen M, Chandra A, Mitic LL et al (2008) A role for autophagy in the extension of lifespan by dietary restriction in *C. elegans*. PLoS Genet 4:e24. https://doi.org/10.1371/journal.pgen.0040024
20. Anderson EN, Corkins ME, Li J-C et al (2016) *C. elegans* lifespan extension by osmotic stress requires FUdR, base excision repair, FOXO, and sirtuins. Mech Ageing Dev 154:30–42
21. Lucanic M, Plummer WT, Chen E et al (2017) Impact of genetic background and experimental reproducibility on identifying chemical compounds with robust longevity effects. Nat Commun 8:14256. https://doi.org/10.1038/ncomms14256
22. Kamath RS, Martinez-Campos M, Zipperlen P et al (2000) Effectiveness of specific RNA-mediated interference through ingested double-stranded RNA in *Caenorhabditis elegans*. Genome Biol 2:research0002.1-10. https://doi.org/10.1186/gb-2000-2-1-research0002
23. Timmons L, Court DL, Fire A (2001) Ingestion of bacterially expressed dsRNAs can produce specific and potent genetic interference in *Caenorhabditis elegans*. Gene 263:103–112
24. Kamath RS, Fraser AG, Dong Y et al (2003) Systematic functional analysis of the *Caenorhabditis elegans* genome using RNAi. Nature 421:231–237. https://doi.org/10.1038/nature01278
25. Ceron J, Koreth J, Hao T et al (2004) Toward improving *Caenorhabditis elegans* phenome mapping with an ORFeome-based RNAi library. Genome Res 14:2162–2168. https://doi.org/10.1101/gr.2505604.7
26. Rechavi O, Houri-Ze'Evi L, Anava S et al (2014) Starvation-induced transgenerational inheritance of small RNAs in *C. elegans*. Cell 158(2):277–287. https://doi.org/10.1016/j.cell.2014.06.020
27. Larance M, Pourkarimi E, Wang B et al (2015) Global proteomics analysis of the response to starvation in *C. elegans*. Mol Cell Proteomics 14:1989–2001. https://doi.org/10.1074/mcp.M114.044289
28. Shi C, Murphy CT (2014) Mating induces shrinking and death in Caenorhabditis mothers. Science 343:536–540. https://doi.org/10.1126/science.1242958
29. Maures TJ, Booth LN, Benayoun BA et al (2014) Males shorten the life span of *C. elegans* hermaphrodites via secreted compounds. Science 343:541–544
30. Gems D, Riddle DL (1996) Longevity in *Caenorhabditis elegans* reduced by mating but not gamete production. Nature 379:723
31. Johnson DW, Llop JR, Farrell SF et al (2014) The *Caenorhabditis elegans* Myc-Mondo/Mad complexes integrate diverse longevity signals. PLoS Genet 10:e1004278. https://doi.org/10.1371/journal.pgen.1004278

Chapter 3

A Simple Apparatus for Individual *C. elegans* Culture

William E. Pittman, Drew B. Sinha, Holly E. Kinser, Nisha S. Patil, Eric S. Terry, Isaac B. Plutzer, Julia Hong, and Zachary Pincus

Abstract

We miniaturized standard, solid-phase *C. elegans* culture conditions to produce a system in which many isolated, individual *C. elegans* can be housed throughout their lives. This system, the "worm corral," is compatible with high-resolution brightfield and fluorescent microscopy, allowing imaging of fluorescent transgenes and morphological phenotypes from hatch until death. These culture devices can be constructed on the benchtop with commercially available reagents and standard laboratory equipment, making this an attainable solution for most labs.

Key words *C. elegans*, Longitudinal imaging, Culture system, Lifespan

1 Introduction

We have developed a culture system capable of housing hundreds of isolated, individual *C. elegans* on a single microscope slide [1]. Animals in this system, which we refer to as a "worm corral," are reared in conditions very similar to standard solid-media culture: atop a hydrogel surface to which food bacteria is adsorbed (Fig. 1a). This avoids many of the technical and biological difficulties inherent in liquid media and microfluidic systems, including the need for fluid flow or exchange and the profound alterations to *C. elegans* physiology caused by liquid media. This system is compatible with whole-body imaging on a standard upright microscope with 5× and 10× objectives.

We have previously validated this culture system and provided a brief protocol for its use [1]. Here we expand on and update our initial protocol with several additional years' experience and refinement. The full protocol, including all optional steps, is somewhat complex and requires access to specialized tooling and materials. However, we and others have had excellent results with even the simplest variant, which requires no special hardware, microscopes, or software and should be accessible to any *C. elegans* lab.

Sean P. Curran (ed.), *Aging: Methods and Protocols*, Methods in Molecular Biology, vol. 2144,
https://doi.org/10.1007/978-1-0716-0592-9_3,

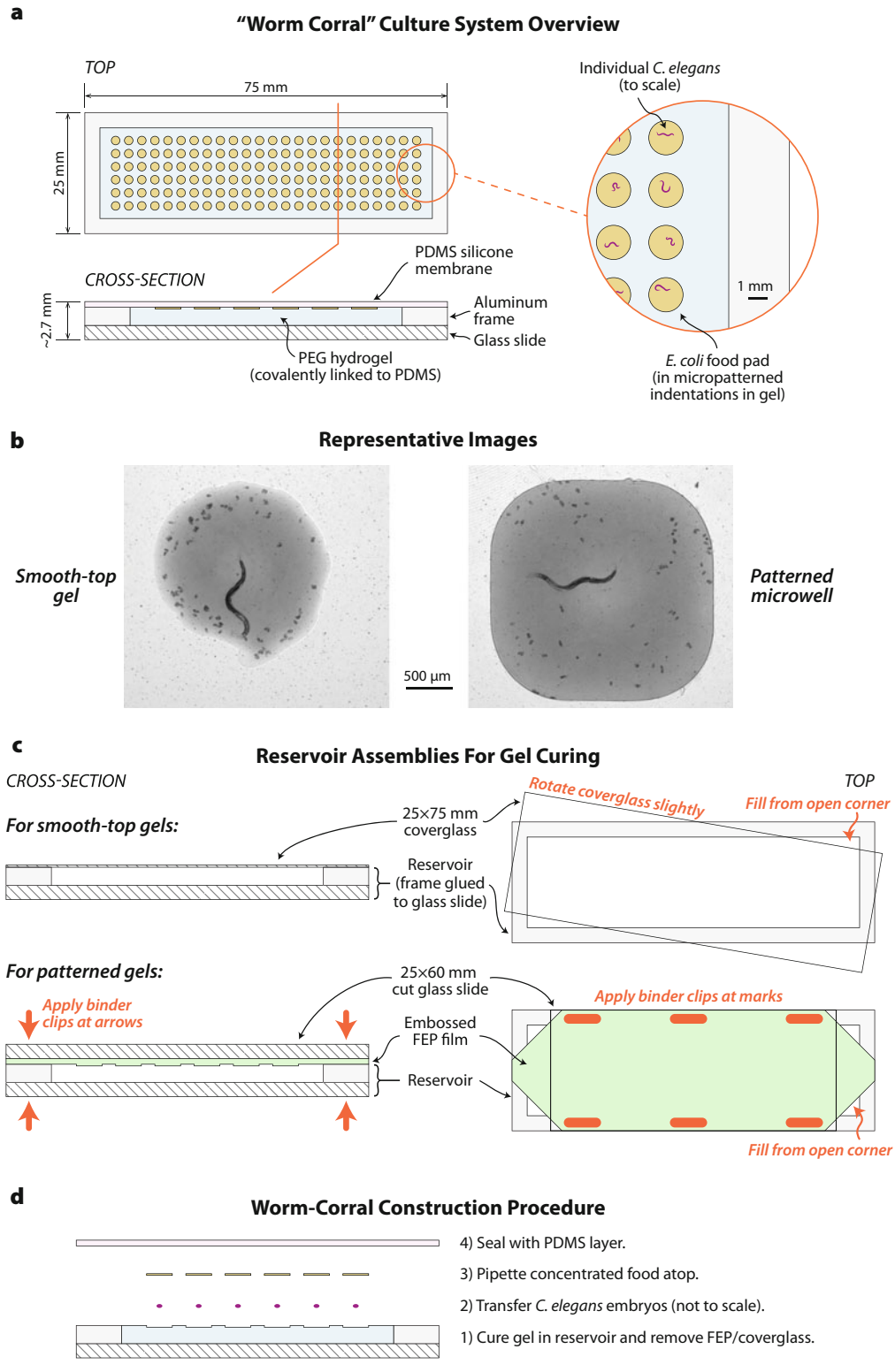

Fig. 1 (**a**) Schematic of "worm corral" culture apparatus. (**b**) Representative image of a single young adult in a standard bacterial food pad (left) vs. in a food pad in a micropatterned well (right). In this case, the

Figure 1d schematizes the protocol. In brief, we first polymerize multifunctional polyethylene glycol (PEG) monomers to form a hydrogel in a reservoir affixed to a glass slide. *C. elegans* eggs and individual droplets of concentrated bacterial food are added atop. Finally, a layer of polydimethylsiloxane (PDMS) is dispensed and allowed to cross-link with itself and the gel surface below, producing a tough, transparent, and gas-permeable membrane that entraps each individual *C. elegans* on its own food pad. We also describe a variant protocol where embossed sheets of fluorinated ethylene propylene (FEP; a relative of Teflon) are used to pattern microwells into the gel surface for increased uniformity and density of culture.

2 Materials

This section begins with a comprehensive list of all materials and equipment used in the construction of the culture system. Optional parts will be listed in a separate section. The subsequent sections provide an in-depth guide to the preparation of reagents required prior to constructing an actual culture device.

2.1 General

1. Sylgard 184 (PDMS; Dow Corning).
2. Parafilm.
3. Plastic inoculating loop (for stirring).
4. Pasteur pipettes.
5. M9 salt solution (per standard *C. elegans* recipe [2]).
6. Two-part epoxy.
7. Sterile 1, 5, and 60 mL syringes.
8. Sterile water.
9. 1.5, 5, and 50 mL conical tubes.

2.2 Frame and Chamber Construction

1. 75 × 25 mm glass slides.
2. 75 × 25 mm glass coverslip.
3. 100 × 20 mm glass petri dish with cover.
4. Kimwipes.

Fig. 1 (continued) micropatterned geometry is a rounded rectangle to best fill the whole the field of view of the microscope camera. (**c**) Cross-sectional and top views of reservoir and top-surface assemblies into which a PEG solution is introduced and allowed to gel. Assemblies are shown for standard smooth-top gels (top) and micropatterned gels (bottom). (**d**) Outline of steps to construct a worm corral

5. Rectangular frame; 75 × 25 mm outside with ~70 × 20 mm interior hole (Fig. 1), in any material that can be adhered to a glass microscope slide. Autoclavable materials available from McMaster-Carr that are known to work include:
6. Adhesive-backed polyethylene sheet; 1/32″ (0.79 mm) thick or 3/64″ (1.19 mm) thick.

   This material can be cut by hand with a sharp blade into frames of the appropriate dimension.
7. Rectangular 1 × 3″ (25.4 × 76.2 mm) extruded aluminum tubing; 1/8″ (3.18 mm) wall thickness.

   This material can be easily and inexpensively cut in a machine shop to produce slide-sized frames of any desired thickness. We prefer 1.3 mm thickness, producing a reservoir volume of ~1.7 mL.

2.3 Surface Patterning (Optional)

1. 10-ton/300 °C Heated Hydraulic Press.
2. 0.25 mm FEP film (American Durafilm, cat. 1000A).
3. Large Binder Clips (2″).
4. Small Binder Clips (0.5″).
5. Glass Cutting Tool.

2.3.1 Bacterial Culture

1. LB broth.
2. 10 cm LB agar plates.
3. 600 nm spectrophotometer.
4. Sterile 5 μm syringe filter.
5. 10 mg/mL ampicillin in H_2O (if using RNAi).
6. 1 M IPTG in H_2O (if using RNAi).

2.3.2 Hydrogel Reagents

1. 1 M KH_2PO_4.
2. 1 M K_2HPO_4.
3. Bacto Peptone.
4. 5 M NaCl.
5. 1 M $MgSO_4$.
6. 5 mg/mL cholesterol in ethanol.
7. Sterile 0.22 μm vacuum filter.
8. Sterile 0.22 μm syringe filter.
9. 1 M sodium hydroxide.
10. PEG-Thiol (JenKem USA; Item code: A10022-10; item number: 8ARM(TP)-SH-10 K).
11. PEG-Diacrylate (Sigma-Aldrich; cat. 437441).

2.3.3 Embryo/Bacteria Transfer (Optional, But Recommended)

1. 5 μL eLINE Electronic Repeater (Sartorius; cat. 730011).
2. 10 μL Low Retention Tips (Vertex; cat. 4117NS0).

2.4 Device Frame and Humid Chamber

The metal or plastic frame, when attached to a standard glass slide with an adhesive, serves as the reservoir for liquid phase NGM-PEG solution while it gels and protects the gel throughout the subsequent experiment. The thickness of the frame determines the thickness of the gel. Thicker gels are more resistant to desiccation during long experiments but require more PEG monomer (and are thus more expensive). A gel thickness of 1–2 mm is typical. Many materials can be used for the frame, provided only that the material chosen (1) must be able to be glued/adhered to a glass slide, (2) must not contain sulfur or tin (which poison the PDMS curing process), and (3) ideally will be autoclave-safe. For long-lasting frames that can be repeatedly autoclaved, we use aluminum adhered to glass with PDMS. During gel curing, the slide and frame are kept in a humid chamber; we use petri dishes with moistened Kimwipes.

1. *Construct a gel reservoir by adhering a frame to a glass slide*. In all cases, start with a glass slide cleaned with ethanol and dried with compressed air or Kimwipes. If using PDMS, follow this protocol: first, preheat a hot plate or oven to 100–120 °C. Make approximately 200 μL PDMS (*see* **Note 1**). Using a 1 mL syringe, apply 60–120 μL PDMS to the bottom side of a frame and invert the frame onto a glass slide. Excess PDMS can be carefully removed with Kimwipes. Bake the slide at 100–125 °C for 30–45 min. Once cooled, cover the surface of exposed glass within the reservoir using scotch tape to limit dust accumulation.
2. *Construct blocks to elevate the reservoir assembly*. It is recommended to place the reservoir on PDMS strips to prevent the assembly from sliding in the humidity chambers and to prevent liquid from wicking underneath the slide. Using a large flat-bottomed container, cure a 2–3 mm thick mat of PDMS by baking at 100–120 °C for 30–45 min. Remove the silicone from the container and cut into 25 × 5 mm strips.
3. *Prepare a humidity chamber for corral storage during curing and animal transfer*. We recommend glass petri dishes to allow all device components to be autoclaved together. Place the reservoir assembly in the middle of a 10 cm petri dish, supported by two PDMS strips at either end. Prepare two Kimwipes strips from regular Kimwipes by folding into 1 × 3 cm strips. Press the strips to the edge of the dish, roughly parallel to the long edge of the reservoir (so the strips are maximally distant from the slide).

4. *Place the mold top on the reservoir assembly.* The smoothest and most uniform gel surface can be obtained by placing glass or Teflon on top of the reservoir. When the reservoir is filled with gel, the gel cures completely surrounded by flat surfaces of the desired geometry. (If a slight meniscus is acceptable, the gel can be cured without a lid on the reservoir and this step can be skipped.) For a smooth, unpatterned surface (Fig. 1c, top), place a clean 75 × 25 mm glass coverslip on top of the slide–frame assembly in the humid chamber. For a patterned gel surface (Fig. 1c, bottom), sandwich the embossed FEP strip (*see* Subheading 3.5) between the assembly and a glass slide cut down to 60 × 25 mm. This second glass slide placed on top of the FEP strip is used to keep the strip flat during autoclaving and the curing process. Clamp the 60 mm slide, the FEP strip, and the frame–slide assembly together using six small binder clips, three on each side of the device. Autoclave the entire chamber for approximately 1 h on a dry cycle. Store indefinitely.

2.5 Concentrated Bacterial Food Source

C. elegans are generally cultured on the slow growing *E. coli* strain OP50 as a food source. Bacteria are grown overnight in LB broth and dispensed onto solid-phase media days prior to use for experiments. This allows the bacteria to proliferate and form a thick lawn capable of sustaining a large population of worms. In contrast, for our culture system, it is not practical to seed bacteria onto the gel surface in advance. (In particular, this runs the risk of gel desiccation.) Instead, we concentrate a bacterial culture prior to depositing it onto the gel. We have developed protocols for using either standard OP50 as the food source, or an OP50 derivative (strain *xu363* [3]) capable of producing dsRNA for feeding RNAi (*see* **Notes 2** and **3**).

We suspect that variation in bacterial growth or storage contributes to variability in *C. elegans*phenotypes. For this reason, the investigator should establish expectations for growth (i.e., expected optical density of cultures after overnight incubation and at each step of RNAi induction) and discard cultures that significantly deviate from expectations. We find it is good practice to determine both the effective OD and percent weight/volume of concentrated bacterial food. Variation in the state of the bacteria and the dryness of the bacterial pellet may cause overestimations of food concentrate if using the weight percentage alone. Comparing weight percentage to OD allows for bacterial cultures in such states to be discarded. The following OD values are based on our experience with these strains, but baseline OD expectations should be established by each lab based on their specific culture techniques, timelines, and spectrophotometer model. For similar reasons, we strongly recommend using freshly prepared concentrated bacteria, stored at most 2–3 days at 4 °C before use.

1. *Grow desired bacteria*. Streak bacteria from a frozen stock onto a 10 cm LB plate (with appropriate antibiotic for selection). Incubate overnight at 37 °C. Because *xu363*-derived strains are slower growing, we incubate them at 37 °C for 24 h on LB + 100 μg/mL ampicillin and then leave the cultures overnight (17 h) at room temperature to proliferate further. Plates can be stored at 4 °C for up to 2 weeks. Prepare an overnight culture by inoculating a single colony into a 250 mL Erlenmeyer flask containing 80 mL of LB broth and shaking the culture at 37 °C for 17 h; for RNAi strains, include ampicillin in the broth at 100 μg/mL.
2. *Check OD*. After 17 h, dilute a sample of the culture 1:10 in LB broth. Evaluate the OD of the diluted sample at 600 nm (OD600) on a spectrophotometer. For OP50, if the OD of the dilute sample is not 0.4–0.45 (corresponding to an OD of 4–4.5 of the undiluted sample), discard the culture. Otherwise, continue to **item 3**. For *xu363*, the overnight culture should have an OD of 2.5–3.0. Dilute this culture into 250 mL LB such that the final OD is 0.25. Shake at 37 °C for ~1 h, growing to an OD of 0.5. Add IPTG to the culture to a final concentration of 1 mM to induce RNA production and shake for an additional 3 h to obtain a final OD of 1.2–1.3.
3. *Concentrate bacteria*. Aliquot the culture into multiple 50 mL conical tubes as needed, and centrifuge at 5000 rpm for 5 min to pellet (Thermo HighConic III rotor, 3354 rcf at tip of tube). Decant the supernatant and resuspend each pellet in 5 mL of M9. Filter with a sterile 5 μm syringe filter and 60 mL syringe to remove large particulates from the LB broth (which can interfere with imaging); place the filtrate into a single, preweighed 50 mL conical tube. Store overnight if necessary.
4. *Resuspend to a known concentration*. Centrifuge the bacteria at 5000 rpm (3354 rcf) for 10 min and decant the supernatant. Invert tubes over a clean paper towel and allow the bacteria pellet to dry for ~30 min. Weigh the tube to determine the weight of the pellet. Resuspend the bacteria in M9 to obtain a solution that is 75% w/v bacteria. Generally it suffices to add a volume of M9 equal to 1/3 of the pellet weight (e.g., if the pellet weighs 240 mg, add 80 μL). Determine the OD of the concentrate by performing a 1:500 dilution of this sample in M9 in two steps: dilute 10 μL of the concentrate in 990 μL of M9, and then dilute 1:5 in the cuvette. (This method minimizes waste of concentrated bacteria and also minimizes technical variation in OD measurements.) The OD of the 1:500 dilution should be between 0.75 and 1. Add additional M9 to the resuspended pellet such that the OD of the 1:500 dilution is 0.75 and confirm that the weight percentage of the bacteria is remains roughly 65–75%. Aliquot and store at 4 °C no more than 3 days.

2.6 Corral-Variant Nematode Growth Media

Nematode Growth Media (NGM) is traditionally made in combination with agar and poured into petri dishes to produce standard cultureplates. Because of the potential for hydrolysis of the PEG monomers, we avoid autoclaving and instead filter-sterilize after mixing all components. We have also made several other changes compared to standard NGM. To facilitate PEG cross-linking chemistry, we increased the pH to 6.3 from the standard 6.0. We also omit $CaCl_2$ (previously reported to be unnecessary [4]) because it is prone to forming crystals in the media and interferes with imaging. As we do not add cholesterol until after the PEGs have been incorporated, the filter-sterilized media is shelf-stable. We refer to this formulation as "Corral NGM" to distinguish from regular NGM for agar plates.

Preparation of Corral NGM. Weigh 250 mg of peptone and add to 965 mL of DI water. Add 2.5 mL of pH 6.3 KPO_4 buffer. (The KPO_4 buffer is made by mixing 1 M KH_2PO_4 and 1 M K_2HPO_4 at approximately a 5:1 ratio. Using a pH meter, carefully track the changes in pH as you gradually add additional KH_2PO_4.) Add 1 mL 5 M NaCl and 100 μL of 1 M $MgSO_4$ to the solution. Measure pH and adjust to 6.3 with 1 M NaOH as needed. Sterilize with a 0.22 μm vacuum filter. Store indefinitely at room temperature.

2.7 PEG Monomers

The PEG hydrogel is made of two components: an 8-arm PEG with thiol groups at the terminus of each arm (PEG-8SH), and a linear PEG diacrylate (PEG-DA). The PEG-8SH slowly hydrolyzes, so it is shipped sealed under argon and should be stored at −20 °C upon receipt. It is best to minimize handling the PEG-8SH; if ordering larger quantities, the manufacturer will package then into smaller aliquots on request. (We find that 600 mg aliquots are a good size.) The PEG-DA should be stored at 4 °C. At this temperature, it is a waxy solid and difficult to handle, so ~1 mL working aliquots can be removed and kept as a liquid at room temperature in 1.5 mL tubes for up to 2 months.

2.8 C. elegans Embryos and Pick for Embryo Transfer

Individual *C. elegans* are transferred from traditional agar plates into our device as late embryos (threefold stage) to ensure they hatch at a high rate. Larvae can also be transferred into the system, but this increases the risk that they will depart the food pad prior to the PDMS crosslinking with the PEG gel. To transfer embryos, we use an eyebrow hair fastened to the tip of a Pasteur pipette. The eyebrow is used to gently coax individual embryos off a plate without damage.

Construction ofembryopick. Mix general-purpose two-part epoxy in a weigh-boat and push the small end of a glass Pasteur pipette into the epoxy. Wipe off the outside, leaving 2–4 mm of epoxy inside the barrel of the pipette. Obtain an eyebrow or eyelash hair and use tweezers to insert the follicle end of the hair into the pipette. Allow the epoxy to cure.

3 Methods

3.1 Preliminaries

At least 1 day prior to producing the corral gel, construct and autoclave the reservoir–humid chamber assembly as per Subheading 2.1. Three days prior to transferring embryos to the corral, begin the process of growing concentrated OP50 from a single colony on a petri dish, as per Subheading 2.2. (Five days prior for RNAi with xu363.) 48 h prior to transferring embryos to the corral, pick 30–50 L4 stage larvae onto a standard NGM plate and incubate at 20 °C; each plate will provide sufficient late-stage eggs to transfer onto a single corral (>200).

(Note that embryos are transferred to the corral the same day that the gel is polymerized when using a standard glass coverslip as the mold top. However, when using embossed FEP, embryos are transferred the following day.)

3.2 Hydrogel

We have found that a gel consisting of 8.5% PEG w/v in corral-NGM provides a substrate similar in elastic properties to standard NGM-agar plates. The PEG- 8SH and PEG-DA react in a 4:1 molar ratio; thus, based on their molecular weights, we require 6.64% w/v PEG-8SH and 1.86% w/v PEG-DA. To achieve this, separate 2× solutions are made for each PEG, which are then mixed at a 1:1 ratio. The following steps produce 2–3 mL of gel, which is an appropriate amount to make for our standard frame size: a 1.3 mm-thick frame with inner dimensions of 19 × 70 mm, yielding a 1.73 mL reservoir. Adjust as necessary based on the interior volume of the reservoir used.

If surface patterning the gel with FEP (Subheading 2.1), **steps 1–5** below should be performed the day before transferring embryos onto the corral. Otherwise, complete all steps on the day of the experiment.

1. *Make ~1.5 mL of 13.28% NGM-PEG-8SH*. Weigh ~210 mg PEG-8SH into a preweighed 5 mL tube and note the final weight of the material dispensed. Divide the weight of the PEG in mg by 0.1328 to find the final volume needed in mL. (e.g., if exactly 210 mg were weighed out, this would be 1581 mL) We observe negligible volume expansion when PEG-8SH is dissolved, so simply add the desired volume of corral-NGM without accounting for the powdered PEG. Dissolve with vigorous vortexing and tapping, which can take 5–10 min.
2. *Make ~1.5 mL of 3.72% NGM-PEG-DA*. Aim to make at least the same volume of NGM-PEG-DA as NGM-PEG-8SH, as the PEG-DA is a very inexpensive reagent compared to PEG-8SH. Multiply the final volume of the PEG-8SH solution from **step 1** by 0.0372 to obtain the desired weight of

PEG-DA to add. Room-temperature PEG-DA has a density of approximately 1.1 g/mL, so transfer approximately the same number of μL as mg desired to obtain a slight excess of PEG-DA. As PEG-DA is difficult to pipet, round up the desired volume 10–20%. (If 1600 μL of PEG-8SH were produced, aim to transfer 60–70 μL of PEG-DA.) Transfer the PEG-DA to a preweighed 5 mL tube and note the final weight of the material dispensed. Divide the weight of the PEG-DA in mg by 0.0372 to obtain the final volume needed. Add an amount of corral-NGM equal to the final volume required, less the volume of PEG-DA dispensed, and vortex vigorously.

3. *Filter-sterilize PEG solutions.* Filter each PEG solution separately via an 0.22 μm syringe filter. (The PEG can either be added to the back of the syringe or drawn up via a needle or a pipette tip screwed into the Luer connector.) Dispense into sterile 5 mL tubes. PEG solutions can be stored for up to a week at 4 °C, but we prefer to make the solutions fresh or at most 2 days prior to the experiment.
4. *Produce final NGM-PEG solution.* Mix the 13.28% NGM-PEG-8SH and 3.72% NGM-PEG-DA solutions in a 1:1 ratio to produce the desired amount of gel solution. Add 4 μL of 5 mg/mL cholesterol in EtOH for each mL of solution produced. (This is 4× the usual concentration of cholesterol, as we find that cholesterol is poorly soluble and/or bioavailable in the NGM-PEG compared to standard NGM-agar. *See***Note 4**.) Vortex immediately after transfer to minimize cholesterol precipitation.
5. *Prepare a surface-patterned gel.* If using a glass coverslip to as the mold top, skip to **step 7**. If using embossed FEP to surface pattern the gel, centrifuge the PEG mixture for 30 s to remove air bubbles from the solution. Retrieve the humidity chamber from Subheading 2 and add 3 mL of DI water to each Kimwipes strip. Gently pipet the NGM-PEG solution into one of the cut-out corners until the reservoir is filled. Occasionally the liquid will not flow evenly and air pockets will form. Smalls voids can be ignored; large ones can be removed by carefully tilting the device. Once filled, place the lid back on the petri dish and seal well with Parafilm. Place in a flat box and allow to cure at 20 °C overnight.
6. *Remove FEP.* The next day, remove the chamber from the incubator. Remove the binder clips and glass slide from the top of the device. With an ethanol-cleaned razor blade, carefully pry up the FEP mold and set aside. Mix ~1 mL of PDMS (*see***Note 1**) and dispense it in small increments (~ 5 μL at a time) on any air bubbles in the gel surface and along the short edge of the device. This protects the areas that are most prone to desiccation during the following steps. Be careful not to

dispense too much PDMS, or it will spread over a large region of the hydrogel before individuals can be deposited. This is most easily achieved by using a plunger-driven repeater pipette such as an Eppendorf E3 with an 0.2 mL Combitip, set to dispense in 5 μL increments. Alternatively, dip a 1000 μL pipette tip into the PDMS and gently daub it onto the device, taking care not to poke the gel surface. Skip to **step 8**.

7. *Prepare a smooth-surface gel.* Open the humidity chamber and carefully rotate the coverslip on top of the reservoir to leave small gaps at opposite corners of the frame (Fig. 1c, top). Gently pipet the gel solution into the reservoir via one gap, allowing air to be displaced via the other gap. Once no/few bubbles remain, realign the coverslip to the frame and allow to cure for ~2 h. Assay gelation by keeping leftover gel mix in a 5 mL tube and flicking/probing gently. When the leftover solution has solidified, it will be safe to remove the top glass slide. With an ethanol-cleaned razor blade, gently pry up the coverslip and discard. Do not allow the coverslip to stay on top too long after curing is finished, otherwise it will be hard to remove.

3.3 Transfer Embryos and Bacterial Food

The easiest and fastest method of transferring embryos is to pipet small drops of M9 onto the corral surface and then use an eyelash pick to deposit the embryos in the drops. Concentrated food is then dispensed atop the embryos once the M9 has absorbed into the gel. (It is also possible to pick embryos directly into the concentrated food, but the embryos are difficult to see.) An automated repeater pipette capable of dispensing in increments of 0.1 μL is ideal to produce M9 droplets. This allows for many droplets to be dispensed at once, and the small volume ensures the M9 absorbs quickly. An automated repeater pipette is also extremely useful dispensing the food droplets; if picking directly into the food, the repeater pipette needs only to be able to dispense in increments of 0.2 or 0.4 μL. If a repeater is not available, these steps can be performed with a manual 0.2–2 μL pipette.

1. *Transfer embryos.* Pipet 10–20 0.1 μL droplets of M9 at a time. If using the patterned surface, place droplets in each microwell. Otherwise, pipet droplets in rows of 5. Using the eyelash pick, carefully transfer a single threefold stage egg into each droplet. Use the eyelash to pick up a small amount of bacteria from the plate with embryos, which helps the embryos adhere. (Too much bacteria, however, makes it difficult to wash embryos off in the M9 droplets; if necessary, remove excess bacteria by jabbing the tip of the eyelash into the agar surface of the embryo plate.) Using a gentle flicking motion, sweep a single embryo up with the eyelash. Detach the embryo in the M9 droplet by gently brushing against the PEG gel surface or the top of the M9 droplet.

Keep the slide in the humid chamber the entire time, only uncovering when transferring each embryo. This is most easily accomplished using two dissection microscopes: one focused on the embryo plate, and one focused on the gel within the humid chamber (*see***Note 5**). An intermediate level of magnification makes it easiest to see the egg detach into the M9 droplet. Repeat until the desired number of embryos are transferred, but do not spend more than 1.5 h: any longer risks hydrogel desiccation. An experienced user can transfer 100–120 embryos within 1–1.5 h.

2. *Add bacterial food*. Allow M9 droplets to absorb and then add the desired amount of food (0.4 μL will ensure an excess of food throughout life) atop each embryo. Be careful not to pipet the droplets too close together, so that they do not merge. Allow the bacteria to adsorb onto the plates in the humid chambers (~15 min).

3.4 Seal the Device with PDMS

1. *PreparePDMSwhile the bacterial slurry adsorbs to the gel*. Coating a 25 × 75 mm slide with a 0.4–0.5 mm layer of PDMS (the thinnest easily achievable) requires ~1 mL of PDMS; so prepare ~2 mL PDMS per slide in 5 mL centrifuge tubes to allow sufficient margin for error (*see* **Note 1**).
2. *DispensePDMS*. After the pads of food bacteria are dry, gently dispense ~1 mL PDMS atop the slide with a 1 mL syringe. Using a serpentine pattern, try to cover most of the surface of the slide in PDMS without creating bubbles. As PDMS is very viscous but has low surface tension, it will slowly spread to cover the entire slide after about 15 min. With careful handling, it will not spill over the edges, however. It may be necessary to pop a few bubbles with a syringe needle or pipette tip, but these usually disappear on their own within ~15 min.
3. *AllowPDMSto cure*. Seal the humid chamber with Parafilm and let the PDMS cure overnight at the desired experimental temperature (15–25 °C). Make sure that the slide and chamber are level, otherwise the PDMS will flow unevenly. Alternatively, place the slide in the desired (humidified) experimental apparatus directly. After 12–24 h, the PDMS will be tacky but cured. (This can be gently assayed by touching the PDMS surface with the same type of inoculator or sealed-end Pasteur pipette used to stir the PDMS.) After 24–48 h, the PDMS will be fully cured. (*See* **Note 6**.) Retaining the residual PDMS in the centrifuge tubes can also help assay when it has completely cured.
4. *Conduct desired experiments*. Long-term imaging is possible with automated, temperature-controlled microscopes (*see* **Note 7**), though experiments can easily be conducted by

manual imaging at fixed intervals, or simple manual inspection under a dissection microscope. It is possible to retrieve individuals from worm corral devices, with some planning and effort (*see* **Note 8**).

3.5 Optional Protocol: Emboss FEP for Microwell Patterning

We have found it is advantageous to pattern small indentations into the surface of the PEG hydrogel. This produces small wells with precise geometry that allow the production of very uniform food pads which use the maximum available field of view for any given objective–camera combination (Fig. 1b). (Indeed, it is not generally possible to manually pipette droplets small enough to easily fit in a 10× field of view without micropatterned wells.)

To produce such a patterned mold top, we "hot-emboss" a thin sheet of FEP by heating and pressing it against a block of aluminum with an array of wells cut into it [5]. Any academic or commercial machine shop, using a general-purpose CNC vertical milling machine and a high-quality miniature end mill (~0.5–1 mm diameter), can easily cut an array of smooth, flat-bottomed wells (or "pockets" in machining terminology) into an aluminum block. It is critical that an end mill smaller than the diameter of the desired pocket be used to sweep out the bottom face of the pocket: a single vertical down-and-up "plunge cut" will produce a bowed bottom surface that will interfere with keeping animals in focus in the finished device.

While FEP requires a higher embossing temperature and pressure compared to many other materials, it appears to be the only material sufficiently inert to easily peel away from the cured hydrogel without tearing the wells. Because this step requires additional resources and hardware that may not be available to all labs, it is strictly optional.

1. Obtain use of a heated hydraulic press capable of reaching 250–300 °C and producing 10 US tons of force (~90 kN). Many academic machine shops or materials science facilities have this capability. We have found that some commercial, low-cost (sub-$1000) presses can be coaxed into this range of temperature and pressure with additional insulation, high-temperature–rated hydraulic fluid, and consulting with the manufacturer to increase the temperature limit of the controller (which may void the warranty).
2. Machine a pair of aluminum master plates. One plate should be smooth, and the other should contain the desired grid of wells milled into it. For ease of embossing, well depth should not exceed 100–120 μm. These plates should be sufficiently large to extend approximately 2–4 cm beyond one edge of the heated platens of the hydraulic press. This allows the master plates to be clamped together lightly, independent of the force of the press, and thus removed from the press as a unit.

3. Cut a strip of 0.25 mm thick FEP into a roughly 8 × 4 cm rectangle and sandwich it between the aluminum master plates, such that the patterned features are centered on the FEP strip. Attach the plates together using two large binder clips along each of the edges of the plates that are intended to extend past the press platens. Then transfer to a press that has been pre-heated to 250 °C. Adjust to ~5000 PSI/35 MPa (measured at the hydraulic piston; this is approximately 2 US tons of force applied to a standard 1″ diameter piston) and heat for 15 min. Turn off the heating element and allow the materials to cool under pressure for another 15 min. At this point the plates will still be hot but can be safely removed from the press and allowed to cool elsewhere. Do not remove the binder clips until the aluminum plates are at room temperature; otherwise the embossed features may be marred. Using fans (such as a pair of standard computer case fans), the plates can be cooled to room temperature in about 10 min; without fans it takes approximately 30 min.
4. Remove the binder clips and peel the FEP from the aluminum master. Check the FEP features under a dissection scope to verify complete and even patterning. (Successful patterning will transfer onto the FEP the minute tool marks left by the end-mill at the bottom of the aluminum wells.) Cut the FEP strip to 75 × 25 mm and clip off the four corners to create fill ports for the hydrogel (*see* Fig. 1c). Store with scotch tape on the patterned side to prevent particulate buildup. FEP can be autoclaved without affecting the patterning, but it may warp if not held under pressure (e.g., sandwiched between glass slides clamped together by small binder clips).

4 Notes

1. Polydimethylsiloxane (PDMS) is a silicone-based polymer often used as a resin for microfluidic and other lab-on-a-chip applications. We use Sylgard 184, which is packaged in two parts: a base and a curing agent. These components are mixed 10:1 to form a soft silicone rubber. (The ratio can be altered from 5:1 to 20:1, which influences both the reaction rate and the firmness of the rubber. We have found that increasing the amount of curing agent from one part in ten weakens the interaction between the PDMS and PEG hydrogel, resulting in a low rate of escape from the food pads. With standard 10:1 PDMS, there is essentially zero escape.)

   To preparePDMS: using a 1 or 2 mL syringe (without a needle) transfer the PDMS base reagent to a centrifuge tube of at least twice the volume of the PDMS desired. Using a 1 mL

pipette tip, transfer 1/10th of that volume of the cure reagent to the same tube. Vigorously stir the base and cure together using a sterile plastic inoculator or Pasteur pipette with the small end melted closed. The PDMS should be homogeneously mixed and frothy throughout. Degas the PDMS mixture with a 1-min spin at maximum speed in a clinical centrifuge (5 mL tubes and larger) or microcentrifuge (2 mL tubes and smaller).

2. There are various means of preventing reproduction in the corrals. RNAi against *pos-1* or *mex-3* produces maternal-effect embryonic lethality with few other obvious phenotypes. Alternately, the temperature-sensitive *spe-9(hc88)* mutation impairs fertilization at 25 °C, resulting in animals that produce unfertilized oocytes. Though this technique is reliable, 25 °C is thought to be a mild stressor and the *hc88* allele must be cross-bred with other genotypes of interest. Culturing strains with an auxin-degradable *spe-44* transgene [6] in Corral NGM supplemented with 0.5 mg/mL indole-3-acetic acid (auxin) is also effective and does not require an elevated temperature.

   Certain sterilization techniques are incompatible with the system, however. FUDR, commonly used to block DNA synthesis and thus prevent oocyte production, must be delivered only after the L4 stage. This is difficult after sealing a worm corral device in PDMS. C22 is a commercially available compound (via ChemBridge/Hit2Lead) that produces maternal-effect lethality [7]. Unfortunately, C22 appears to be insufficiently soluble or bioavailable in the PEG hydrogel to have consistent effects throughout the reproductive span.

3. Because OP50 and *xu363* appear to be mildly pathogenic, we often treat bacteria with the bactericidal antibiotic gentamicin prior to concentration. Gentamicin irreversibly inhibits bacterial ribosomes, halting protein production and thus proliferation while retaining other metabolic activity for some time. The gentamicin protocol was recently described in Podshivalova et al. [8].

4. If standard concentrations of cholesterol are used in the corral system, we observe that many individuals have classic cholesterol-deprivation phenotypes: shorter, slightly clear, and low fecundity, and producing offspring that arrest as larvae. Increasing the amount of cholesterol fourfold returns individuals to normal. However, we observe that certain corral devices still retain a low fraction (10–15%) of small, sickly appearing individuals with these phenotypes, perhaps due to the cholesterol occasionally precipitating out of solution when it is added to the PEG mixture. In such cases, that particular corral may be excluded from analysis.

5. Contamination with mold spores is also a concern while transferring embryos. Use of two dissection microscopes (which limits the need to move the corral) and ensuring that the humid chamber and embryo plate are covered when not in use helps greatly. If an open-front (horizontal), laminar-flow clean bench/PCR workstation is available, the microscopes can be placed inside for additional protection. Running the airflow while transferring embryos risks desiccating the gel, however the microscopes and transfer setup can be purged via flow of filtered air prior to transfer (and during breaks) to minimize contamination risk. This is strictly optional, however: an operator experienced in sterile technique can transfer embryos at an open lab bench with tolerably low contamination rates.
6. *C. elegans* can be imaged in the corrals before the PDMS cures, but make sure to not accidentally get uncured PDMS on microscope objectives. If this happens, it is best to immediately suspend the end of the objective in a shallow dish of PDMS to a depth of ~5 mm and allow to cure overnight. Unlike a thin smear of PDMS, the larger quantity of PDMS will peel off easily from the lens without residue, and may well leave the objective cleaner than before!
7. For more complex longitudinal studies, an automated imaging system may be advantageous. We perform our experiments in a computer-controlled microscope with a custom enclosure to control temperature and humidity. Unlike enclosures for 37 °C cell culture, maintaining temperatures in the 15–25 °C range requires insulated walls and a temperature controller capable of both heating and cooling. We use a water heater/chiller (Polysciences) with remote temperature probe and remote circulation capabilities to pump water through a small radiator inside the enclosure. We use a USB humidifier in a water bath, controlled by an industrial humidistat (Omega Engineering) to maintain 85+% humidity within the enclosure. At specified intervals, the microscope moves the stage to the coordinates of each food pad (prespecified at the start of the experimental run), executes an autofocus routine to account for any warping of the gel, and then acquires desired brightfield and fluorescence images. sCMOS cameras with large sensor dimensions aid in capturing an entire food pad and *C. elegans* in one 5× or 10× field of view.
8. To retrieve individual *C. elegans* from specific locations on a worm corral, two approaches can be taken. The PDMS can be carefully peeled back, which (usually) leaves the animals on the hydrogel side of the interface. Using PDMS with a 5:1 base–cure ratio (which is stiffer and less well-linked with the PEG gel) can facilitate this, at the cost of a potentially higher rate of escape of individuals during the experiment. Alternately, the

PDMS and PEG layers can both be cut from the reservoir with a thin blade and inverted (PEG side up), then individuals can be retrieved using a standard biopsy punch to take a core through the gel and PDMS.

References

1. Pittman WE, Sinha DB, Zhang WB, Kinser HE, Pincus Z (2017) A simple culture system for long-term imaging of individual *C. elegans*. Lab Chip 77:71. https://doi.org/10.1039/c7lc00916j
2. Stiernagle T (2006) Maintenance of C. elegans. WormBook:1–11. https://doi.org/10.1895/wormbook.1.101.1
3. Xiao R, Chun L, Ronan EA, Friedman DI, Liu J, Xu XZS (2015) RNAi interrogation of dietary modulation of development, metabolism, behavior, and aging in C. elegans. Cell Rep 11:1123–1133. https://doi.org/10.1016/j.celrep.2015.04.024
4. Stroustrup N, Ulmschneider BE, Nash ZM, López-Moyado IF, Apfeld J, Fontana W (2013) The Caenorhabditis elegans lifespan machine. Nat Methods 10:665. https://doi.org/10.1038/nmeth.2475
5. Ren K, Dai W, Zhou J, Su J, Wu H (2011) Whole-Teflon microfluidic chips. Proc Natl Acad Sci U S A 108:8162–8166. https://doi.org/10.1073/pnas.1100356108
6. Kasimatis KR, Moerdyk-Schauwecker MJ, Phillips PC (2018) Auxin-mediated sterility induction system for longevity and mating studies in Caenorhabditis elegans. G3 (Bethesda) 8:2655–2662. https://doi.org/10.1534/g3.118.200278
7. Weicksel SE, Mahadav A, Moyle M, Cipriani PG, Kudron M, Pincus Z, Bahmanyar S, Abriola L, Merkel J, Gutwein M, Fernandez AG, Piano F, Gunsalus KC, Reinke V (2016) A novel small molecule that disrupts a key event during the oocyte-to-embryo transition in *C. elegans*. Development 143:3540–3548. https://doi.org/10.1242/dev.140046
8. Podshivalova K, Kerr RA, Kenyon C (2017) How a mutation that slows aging can also disproportionately extend end-of-life decrepitude. Cell Rep 19:441–450. https://doi.org/10.1016/j.celrep.2017.03.062

Chapter 4

Analysis of *Drosophila melanogaster* Lifespan

Gary N. Landis, Devon Doherty, and John Tower

Abstract

The laboratory fruit fly *Drosophila melanogaster* is one of the leading models for the study of aging. Whereas several behavioral and physiological biomarkers of aging have been identified for Drosophila, lifespan remains the most robust measure of aging rate. Aging and lifespan can be modulated by genetic alterations, as well as by drugs and dietary components, to reveal basic and conserved mechanisms of aging. Here methods are presented for Drosophila lifespan assay, including media preparation, supplementation of media with various drugs, culturing of the flies, passaging flies and recording deaths, and the analysis of lifespan data.

Key words Drosophila, Lifespan, Aging, Mortality rate, Drosophila media, Gompertz

1 Introduction

Drosophila has a long and storied history of contributions to research in biology and aging [1, 2]. In recent years, several biomarkers of aging and remaining lifespan have been identified for Drosophila, including locomotor activity, decreased egg laying, and expression of transgenic reporters for immune genes and heat shock protein genes [3–7]. Despite these successes, lifespan remains the most robust measure of aging rate for Drosophila. Lifespan data can be fitted to the Gompertz–Makeham equation to reveal if an intervention alters lifespan by altering aging rate (mortality rate acceleration with age, Gompertz parameter b) or if it does so by altering animal health (initial mortality rate, Gompertz parameter a) [8]. In our hands, the most critical component of the lifespan assay is the quality of the media, especially the surface of the media in the food vials. The food surface must be moist enough to support optimal feeding/drinking by the fly but not too wet as to be sticky and create a trap for the flies and/or promote growth of sticky bacterial species. Here we describe methods for making Drosophila media, including pumping hot media into vials and bottles, cooling, and storage. Many experiments on aging in Drosophila utilize

Sean P. Curran (ed.), *Aging: Methods and Protocols*, Methods in Molecular Biology, vol. 2144,
https://doi.org/10.1007/978-1-0716-0592-9_4,

conditional transgene expression systems, where transgene expression is triggered by feeding the flies a drug, such as doxycycline or mifepristone [9, 10]. The most precise way to administer a defined concentration of drug to the fly in the media is to add concentrated drug stock solution to the hot liquid media and mix thoroughly before the media cools and hardens. However, this approach has the limitation that some drugs might be sensitive to the heat of the liquid media. Another limitation is that the preparation of media with titrations of drug, and/or various combinations of two or more drugs, becomes prohibitive in terms of time and effort. We describe our simplified method for supplementation of media with various drugs and drug combinations, by applying concentrated drug stock solutions directly to the surface of cooled and solidified media vials [11–13]; this approach has since been adopted by numerous labs.

2 Materials

1. Drosophila fly vials (Narrow, polystyrene, Genesee Scientific).
2. Drosophila fly bottles (6 ounce, Genesee Scientific).
3. Fly food pump (Automatic pipetting machine, Brewer).
4. 5-Headed nozzle (Brass, custom-made by machine shop).
5. Steam-jacketed kettle.
6. Dextrose (LabScientific).
7. Agar (Gelidium 700, MoorAgar Inc.)
8. Yeast (miniflakes, Red Star).
9. Cornmeal (ground yellow, MP Biomedical).
10. Tegosept stock solution of 194 g/L in ethanol (Genesee Scientific).
11. Propionic acid (99%, Mallinckrodt Baker).
12. 95% ethanol.
13. Large Rayon balls (Genesee Scientific).
14. Flugs for plastic fly bottles (Genesee Scientific).
15. 40 × 46 × 1.1 Mil Clear Plastic bags.
16. Cheesecloth.
17. Gas dispersion tube (Chemglass).
18. Side-arm flask.
19. 4 mg/ml mifepristone stock solution in ethanol.

Fig. 1 Equipment. (**a**) Steam-jacketed kettle. (**b**) Pump. (**c**) 5-headed nozzle. (**d**) Bubbler

3 Methods

Use personal protective equipment including lab coat, gloves, and splash goggles.

3.1 Making Fly Food

1. Prepare each of the components of the fly food ahead of time according to the recipe as follows. Per liter of H_2O: 105 g dextrose, 7.5 g agar, 26 g yeast, 50 g cornmeal, 8.5 ml Tegosept stock solution, and 1.9 ml propionic acid. Depending on the setting of the pump (Fig. 1b), vials contain ~6 ml media and bottles contain ~30 ml media.
2. Add 4/5 of the required amount of water to the kettle (Fig. 1a), keep 1/5 amount nearby in a 20 L bucket for use later. Start to stir the water and start the steam to heat.

3. Add each of dextrose, yeast, cornmeal, and agar slowly to the water.
4. When the mixture starts to boil, reduce the steam to maintain a very low boil, and cook for 30 min.
5. In case of overboil, add some water from the 1/5 amount of water in the bucket and turn down the steam.
6. After boiling for 30 min, turn off the steam. Add the remaining water to the kettle (this helps cool the media), and then add the Tegosept solution and propionic acid. Keep stirring.
7. Pump the hot mixture into bottles using plastic tubing.
8. Pump the hot mixture in vials, 5 at a time, using the 5-headed nozzle (Fig. 1c).
9. Move the boxes of hot food onto benchtops or racks. Do not stack any box on top of another—this helps prevent condensation from collecting in the vials and bottles. Cover the food with cheesecloth to prevent any stray flies from accessing the food and laying eggs on the food. Let cool for 24–48 h.
10. Stuff the vials with Rayon balls. Stuff bottles with bottle Flugs. Stack five boxes of food into a plastic bag and seal the bag with a rubber band. Store the food in 4 °C cold room.

3.2 Making Drug Vials

Here we present methods for making vials supplemented with mifepristone (RU486) to a final concentration of ~200 μg/ml ("+drug" vials), and control vials supplemented with ethanol vehicle alone ("−drug" vials). Similar procedures can be used to make vials supplemented with other drugs, including drugs dissolved in water (*see* **Note 1**).

1. Prepare 4 mg/ml mifepristone stock solution. Place 200 mg of RU486 in a 50 ml centrifuge tube, add 50 ml 100% ethyl alcohol. Mix to dissolve all RU486. Store at −20 °C.
2. Pipet 50 μl of the 4 mg/ml RU486 stock solution onto the surface of each "+drug" vial needed. Pipet 50 μl of 100% ethyl alcohol onto the surface of each "−drug" vial needed. Shake the box of vials to distribute the solutions evenly over the top of the food in each vial. Stripe the "+drug" vials with a red marker, and stripe the "−drug" vials with a blue marker.

   Let dry on benchtop under cheesecloth for 2 days. The 50 μl of ethanol solution absorbs into the top ~1 ml of media (Fig. 2b), yielding a 1:200 dilution of the stock solution and a final concentration of ~200 μg/ml mifepristone.

3.3 Lifespan Assay

1. The GAL4/UAS binary transgenic system typically involves crossing a GAL4 "driver" strain to a UAS "target" strain to generate overexpression or RNAi flies, and crossing the "driver" to a control strain (often the *w[1118]* strain) to

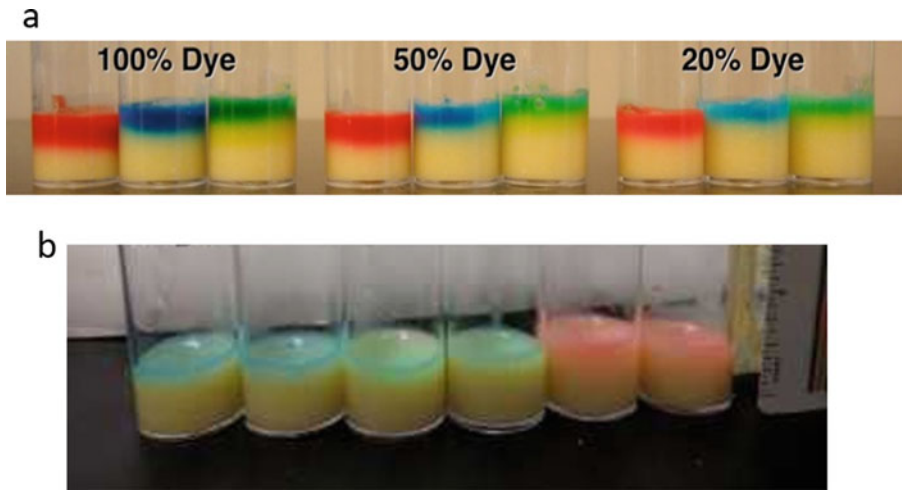

Fig. 2 Estimating drug dilution in media using dyes. (**a**) Each of red, blue, and green commercial food colorings was used, directly (100% dye) or was diluted with water to 50% concentration or 20% concentration. 100 μl of each solution was added to the surface of a vial with fly food media, and allowed to absorb overnight. (**b**) Blue, green, and red commercial food colorings were diluted into ethanol at 20% dye concentration, and 50 μl of each solution was added to the surface of a vial with fly food media (two vials for each color of dye), and allowed to absorb overnight. (**a**, **b**) Measurement of the colored area of the food indicates that the solutions absorb into the top ~1 ml of media

generate control flies [14]. The conditional systems, for example the Gene-Switch system [10, 15, 16], are activated by feeding the flies a drug. These experiments typically involve crossing a Gene-Switch "driver" strain to a UAS "target" strain and assay of the flies in the presence/absence of drug, plus crossing the "driver" to a control strain (often the *w[1118]* strain) to generate control flies, which are assayed in the presence/absence of drug to identify any potential background effects of the drug [16].

2. Set up bottles of the driver and target strains. Put 20 females and at least 10 males of each strain into fly food bottles. Using more than 20 females may make the bottles overcrowded. To determine the number of bottles required, calculate that you should get ~100 virgins or males from each bottle from a healthy stock.
3. Collect virgins and males for the lifespan cross. From the bottles set up above in **step 1**, collect virgins into fresh vials at 20 virgins/vial, and males into fresh vials at 20 males/vial. Label the vials with the date and genotype. If virgins are suspect, wait 4 days before using to see if there are larvae present. If so, discard that vial.
4. Calculate the number of flies and bottles of each cross required for the experiment. Each sample will require at least 100 flies.

Assume you will get ~100 virgins and ~100 males from each cross bottle. For example, if your experiment has six treatments, say males ±drug, virgin females ±drug and mated females ±drug, then you would need a total of 600 flies from six bottles. However, to ensure all flies come out of the bottles on the same day, set up three times that number of bottles. If the target or driver strains are over a balancer, then further double the number of bottles.

5. Set up the crosses to generate progeny for the lifespan assay. Use 40 virgins and 20 males per bottle (*see* **Notes 2** and **3**).
6. After 2 days, toss the flies in the bottles into new bottles, these will be used for the second cohort. After 2 days, discard the flies from the second cohort bottles (*see* **Note 4**).
7. Collect progeny for lifespan assay. When pupae turn dark the flies will come out the next day (*see* **Note 5**). Collect 20 virgin females per vial, and collect 20 virgin males per vial (*see* **Note 6**).
8. Generate mated females. Some experiments will involve analysis of mated females.

   To generate mated females, add 20 3–5-day-old *w[1118]* males to each vial of 20 virgin females, allow to mate for 48 h, and then remove the males.
9. Collect flies onto ±drug vials for the lifespan assay. If mating is not needed, collect flies directly into ±drug vials. Make sure to alternate putting flies into −drug and +drug vials: that is, transfer the first vial of flies you collect into a −drug vial, then transfer next vial of flies you collect into a +drug vial, repeat this alternation for all the flies. This way any potential differences in flies due to handling during collection (time on gas, etc.), will be evenly distributed between the ±drug groups. For mated flies, also be sure to alternate putting flies into −drug and +drug vials: that is, transfer first vial of mated flies into a −drug vial, then transfer next vial of mated flies into a +drug vial, repeat this alternation for all the flies. For purposes of lifespan calculation, the day of collection is considered day 0 of the lifespan assay.
10. Labeling and handling the lifespan vials. To make tags for the lifespan vials, take a piece of colored tape about 3″ long, and fold over halfway. This will make a sticky tag that can be transferred from one vial to another every other day. Use blue tape for −drug treatment and red tape for +drug treatment; in this way, the tape tags are color-coordinated with the marker stripes on the vials. Write the vial number on the tape tag with a marker. Make sure tags are placed low on the vials to prevent them from sticking to the rayon. Transfer the flies every other day into fresh ±drug vials, and transfer the tape tag to the new vial as you toss each vial (*see* **Notes 7–9**).

a

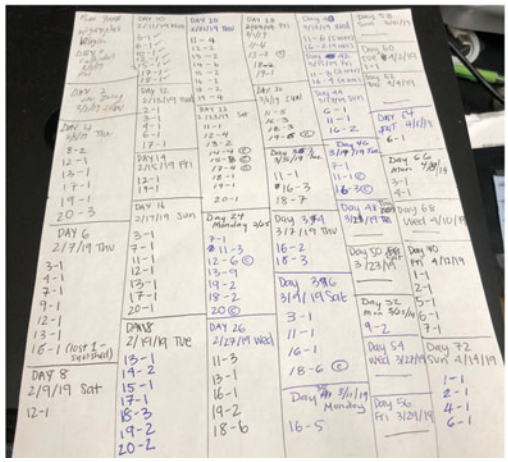

b

	Line	Virgin females WIG X y;Elav										Mated females WIG X y;Elav									
	Sample Size	100					100					100					100				
	Treatment	-RU486					+RU486					-RU486					+RU486				
	Date	1	2	3	4	5	6	7	8	9	10	11	12	13	14	15	16	17	18	19	20
2	2/3/19																				
4	2/5/19								2				1	1				1		1	3
6	2/7/19			1	1			1		1			1	1			1				
8	2/9/19												1								
10	2/11/19			1			1				1		1			1		1	1		
12	2/13/19	1	1	1			1											1			
14	2/15/19												1							1	
16	2/17/19			1				1				1	1	1				1			1
18	2/19/19													1	2	1		1	3	2	2
20	2/21/19											4	2	2	6	2	1		2	4	
22	2/23/19											1	4	2	4	8		4	1	1	1
24	2/25/19							1				3	6	9					2	2	
26	2/27/19											3		1			1		6	2	
28	3/1/19											4		3					2	1	
30	3/3/19											5					3		3	6	
32	3/5/19											1					3		7		
34	3/7/19																2		3		
36	3/9/19			1								1					1		6		
38	3/11/19																5				
40	3/13/19											6					2				
42	3/15/19											3					4				
44	3/17/19						1					1					2				
46	3/19/19							1				1					3				
48	3/21/19																				
50	3/23/19																				

Fig. 3 Data recording. (**a**) Raw data sheet. (**b**) Excel spreadsheet

11. How to score and record deaths. At each transfer record the number of dead flies in each of the numbered vials. Record the data on the raw data sheet (Fig. 3a), which is kept in the box with the cohort. If a fly sticks to the food or the wall of the vial and will not shake off, even with a vigorous bang of the old vial onto the top of the new vial, then count that fly as dead, even if it is still moving (*see* **Note 10**). If there is one or more dead flies in a vial, record the vial number and the number of dead flies, separated by a dash, on the raw data sheet (Fig. 3a). If a fly is dead but transfers into the new vial, put the number 1 followed by an asterisk on the data sheet (if two dead flies transfer, then put the number 2 with an asterisk, etc.). On the next toss, subtract the number of dead with asterisks on the previous toss from the total number dead in that vial for the current toss (*see* **Note 11**). Once all flies in a vial have died, record "C" for "complete" on the raw data sheet next to the last number dead. Example:

    Day 46.

    7/26/10 Tue.

    4-2.

    14-1.

    6-2, 1∗.

    85-4 C.

12. On Day 46, 7/26/10, Tuesday, two flies died in vial 4, one fly died in vial 14, two flies died in vial 6 and one dead fly was transferred from vial 6 into a new vial, four flies died in vial 85 and that was completed the flies in vial 85.

13. How to organize and handle the data. After all the flies in a cohort have died, all the data should be recorded on the raw data sheet (Fig. 3a). Transfer the data to an Excel spread sheet (Fig. 3b), and retain the raw data sheets for reference. Organize the data in the Excel spread sheet in the order −drug first, +drug second. Do not enter 0's. We use a custom script written in *R* to calculate median lifespan for each group, to compare groups using log-rank test, and to plot the survival curves. The total number of deaths recorded for the experiment is used as the starting number of flies; this omits any flies lost due to escape. Finally, fitting the lifespan data to the Gompertz–Makeham equation [8] reveals if an intervention alters lifespan by altering aging rate (mortality rate acceleration with age, Gompertz parameter *b*) or if it does so by altering animal health (initial mortality rate, Gompertz parameter *a*).

4 Notes

1. For drugs dissolved in ethanol, use 50 μl per vial. For drugs dissolved in water, use 100 μl per vial. In each case the solution will absorb into the top ~1 ml of media (Fig. 2).
2. If possible, use virgins for the driver strain, and males for the target strains; this way virgins only need be collected from one strain, and this facilitates crosses to multiple target strains. This will not work if the target is on the *X* chromosome, and in that case use target strain virgins and driver strain males to set up the cross.
3. Using a relatively large number of parent flies for only 2 days results in a more synchronous eclosion of the progeny. This in turn facilitates collection of the virgins over the span of 1 day, resulting in a more age-synchronous cohort.
4. If the bottles start to dry out, add water. Dry bottles will have many small spaces between the food and the side of the vial. Add water slowly using a water squirt bottle carefully inserted between the bottle opening and the Flugs closure, so that no flies escape. Add only enough water to fill the spaces, do not leave any water on the surface of the food, or flies will become trapped. If you add too much water, invert the bottle and the excess water will flow into the Flugs closure and be absorbed.
5. When pupae start to turn dark in the bottles, put a single layer of Kimwipes on top of the food in the bottles. This provides a dry place for the emerging flies to land without getting trapped in the sticky food surface, or on the sticky side of the bottle. This increases the yield of flies, especially with wet or sticky bottles.

6. Make sure to use a bubbler (Fig. 1d), in which the CO_2 gas moves through a sintered glass tube (gas dispersion tube), under the water level, inside a stoppered beaker. In this way, the CO_2 is humidified before it reaches the flies. Without a bubbler, the dry CO_2 gas will dehydrate the flies, and this can result in male infertility and shortened lifespan in both males and females. Reduce CO_2 flow to lowest amount possible (before the flies start to walk) to limit total CO_2 stress on the flies.
7. It is recommended that tossing is practiced several times before the experiment is started, to prevent unnecessary loss of flies during transfers.
8. Make sure that when you toss, the rayon ball is placed securely in the new vial. Do not leave "holes" or gaps for flies to escape through. Do not toss flies into a foodless vial—this quickly kills the flies.
9. Do not toss flies into vials where the food is separated from the wall of the vial, as the flies will tend to become trapped in that space. Also, in vials where the food is separated from the wall of the vial, the food will tend to come loose during the toss, fall onto the flies in the new vial, and kill the flies. Do not use vials which have cracks in the plastic as these will tend to dry out.
10. In our experience flies trapped in this way will be dead within ~12 h.
11. Usually, the dead flies will stick to the surface of the food and will not transfer to the new vial.

Acknowledgments

This work was supported by a grant to J.T. from the Department of Health and Human Services, National Institute on Aging (AG057741). Conflicts of interest: none.

References

1. Tower J (2019) Drosophila flies in the face of aging. J Gerontol A Biol Sci Med Sci 74 (10):1539–1541
2. Partridge L, Tower J (2008) Yeast, a feast: the fruit fly Drosophila as a model organism for research into aging. In: Guarente LP, Partridge L, Wallace DC (eds) Molecular biology of aging. Cold Spring Harbor Laboratory Press, Cold Spring Harbor, pp 267–308
3. Carey JR, Papadopoulos N, Kouloussis N, Katsoyannos B, Muller HG, Wang JL, Tseng YK (2006) Age-specific and lifetime behavior patterns in Drosophila melanogaster and the Mediterranean fruit fly, Ceratitis capitata. Exp Gerontol 41(1):93–97
4. Mueller LD, Shahrestani P, Rauser CL (2009) Predicting death in female Drosophila. Exp Gerontol 44(12):766–772
5. Rogina B, Wolverton T, Bross TG, Chen K, Muller HG, Carey JR (2007) Distinct biological epochs in the reproductive life of female Drosophila melanogaster. Mech Ageing Dev 128(9):477–485. https://doi.org/10.1016/j.mad.2007.06.004

6. Landis GN, Abdueva D, Skvortsov D, Yang J, Rabin BE, Carrick J, Tavare S, Tower J (2004) Similar gene expression patterns characterize aging and oxidative stress in Drosophila melanogaster. Proc Natl Acad Sci U S A 101 (20):7663–7668. https://doi.org/10.1073/pnas.0307605101
7. Yang J, Tower J (2009) Expression of hsp22 and hsp70 transgenes is partially predictive of drosophila survival under normal and stress conditions. J Gerontol A Biol Sci Med Sci 64 (8):828–838
8. Shen J, Landis GN, Tower J (2017) Multiple metazoan life-span interventions exhibit a sex-specific Strehler-Mildvan inverse relationship between initial mortality rate and age-dependent mortality rate acceleration. J Gerontol A Biol Sci Med Sci 72(1):44–53. https://doi.org/10.1093/gerona/glw005
9. Bieschke ET, Wheeler JC, Tower J (1998) Doxycycline-induced transgene expression during Drosophila development and aging. Mol Gen Genet 258(6):571–579
10. Ford D, Hoe N, Landis GN, Tozer K, Luu A, Bhole D, Badrinath A, Tower J (2007) Alteration of Drosophila life span using conditional, tissue-specific expression of transgenes triggered by doxycyline or RU486/Mifepristone. Exp Gerontol 42(6):483–497
11. Ren C, Webster P, Finkel SE, Tower J (2007) Increased internal and external bacterial load during Drosophila aging without life-span trade-off. Cell Metab 6(2):144–152
12. Ren C, Finkel SE, Tower J (2009) Conditional inhibition of autophagy genes in adult Drosophila impairs immunity without compromising longevity. Exp Gerontol 44(3):228–235
13. Shen J, Curtis C, Tavare S, Tower J (2009) A screen of apoptosis and senescence regulatory genes for life span effects when over-expressed in Drosophila. Aging (Albany NY) 1 (2):191–211
14. Brand AH, Perrimon N (1993) Targeted gene expression as a means of altering cell fates and generating dominant phenotypes. Development 118(2):401–415
15. Roman G, Davis RL (2002) Conditional expression of UAS-transgenes in the adult eye with a new gene-switch vector system. Genesis 34(1–2):127–131
16. Landis GN, Salomon MP, Keroles D, Brookes N, Sekimura T, Tower J (2015) The progesterone antagonist mifepristone/RU486 blocks the negative effect on life span caused by mating in female Drosophila. Aging (Albany NY) 7(1):53–69

Chapter 5

Mouse Fitness as Determined Through Treadmill Running and Walking

Joseph C. Reynolds and Changhan Lee

Abstract

Endurance testing simultaneously assesses a wide variety of physiological systems including the cardiovascular, respiratory, metabolic, and neuromuscular systems (Gabriel and Zierath, Cell Metab 25:1000–1011, 2017). Treadmill running is a noninvasive method to evaluate fitness capacity in a longitudinal or cross-sectional manner. High-intensity exercise tests can be used to determine peak physical capacity in mice. However, because aging is associated with a progressive loss of physical capacity the running protocols can be adapted and optimized for aged mice.

Key words Mice, Fitness, Running, Treadmill, Aging

1 Introduction

Treadmill running in mice provides a functional measure of exercise tolerance. While voluntary wheel running is a useful indicator of overall activity level, forced treadmill running utilizes different physiological realms, and has been extensively tested in both mice and humans [1, 2]. Mice are placed on a motorized treadmill and encouraged to run to reach the dark covered end of the treadmill, which they prefer to the bright exposed area. Manual stimulation, such as gently prodding with a stick, encourages mice to reengage with the treadmill after they fall back on the resting platform. While some protocols utilize a shock plate to encourage running, this has been shown to potentially lead to a decrease in running performance or increased escape behavior [3, 4]. One major benefit of motorized treadmill running is that the procedures are easily adjustable. Exercise intensity can be varied by increasing or decreasing the running speed and incline. Increasing the incline of the treadmill places more strain on the mouse muscle and is more energy intensive. Running on a decline, meanwhile, can be used to measure eccentric muscle contraction [5, 6]. This degree of sensitivity has benefits over swimming tests, or wheel running analysis [7].

Sean P. Curran (ed.), *Aging: Methods and Protocols*, Methods in Molecular Biology, vol. 2144,
https://doi.org/10.1007/978-1-0716-0592-9_5,

Another key benefit of using treadmill running as a way to measure exercise performance is the ability to test mice over time. This noninvasive measure allows flexibility in experimental design, and the ability to follow mice longitudinally. Several studies utilize repeated treadmill training to study a wide variety of biological benefits associated with long-term running protocols [8–11]. Conversely, treadmill running can also be used for short-term assessment of single bouts of exercise, or comparison between groups [12, 13]. Forced treadmill running is frequently used as a method to test alterations in skeletal muscle, as adaptive stress response to exercise occurs quickly in this tissue [2, 14–16]. However, while skeletal muscle certainly plays an important role in exercise capacity, treadmill running combines performance of several different biological systems [2]. For this reason, other assays, such as grip strength or rotarod performance, should be used in combination with exercise capacity to determine skeletal muscle specific contributions to physical capacity [17, 18].

Here, we developed a treadmill running protocol which allows for testing the running capacity of mice at a variety of ages. Young and middle-aged mice (up to 22 months) have been tested using a high-intensity running protocol [19]. Older mice (30 months) are generally incapable of running to the same degree as their younger counterparts, so a 60 s walking test can be sufficient to determine their physical capacity. This protocol has been used for mice of the C57BL/6 and CD-1 (ICR) background. Additional optimization for other mouse strains is recommended.

2 Materials

While minimal materials are required, it is crucial to keep the treadmill and all supplies well maintained (*see* **Notes 1–3**).

1. Mouse Treadmill Apparatus: 4-lane treadmill systems are available from TSE Systems, USA. Treadmills connect to the manufacturer's software via USB ports, so multiple treadmill systems may be used simultaneously. Treadmill setup is shown in Fig. 1.
2. Paintbrush (or similar): A long tool with a soft end is used to gently encourage mice to reengage with the treadmill.
3. Ethanol: 70% solution in water.

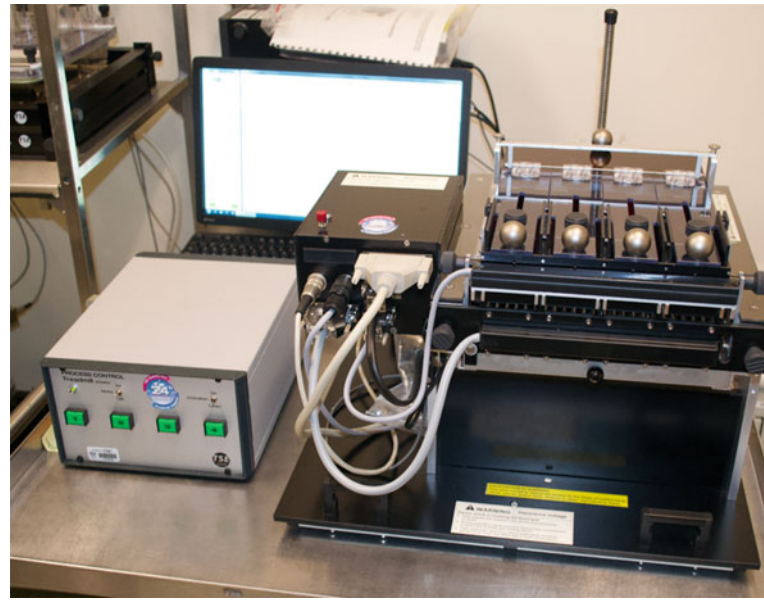

Fig. 1 Treadmill equipment overview: This is the complete treadmill setup. The box on the left is the power source, as well as the indicator of mouse resting. The light for each lane illuminates if the mouse is on the resting platform. Mice should be encouraged to reengage with the treadmill when this occurs. This treadmill has four lanes, with the vertical pole in the back controlling the angle of the treadmill. Treadmills are connected to the computer software via USB, and multiple treadmills can be operated at once

3 Methods

3.1 Acclimating Mice

Before any physical exercise testing can begin, mice must be properly and thoroughly acclimated to the treadmill. This will help to minimize escape behavior and allow for proper assessment of physical capacity. It will also help the mice familiarize themselves with tactics to encourage reengagement with the treadmill.

1. Day 1: Place the mice on the stationary treadmill without any belt movement. If possible, place the mice on the same single track, and with the same neighboring mice that they will experience during the physical test. Allow the mice to freely explore the stationary treadmill for 10 min. Do not interact with the mice and allow them to move (or remain stationary) without any involvement (*see* **Note 4**).
2. Place the mice back in their home cage. If the study design allows, positive reinforcement can be given at this point. If the mice are on a fasting, or caloric restriction diet, feeding the mice after returning to their home cage may help improve their interaction with the treadmill in future tests (*see* **Note 5**).

3. Day 2: Repeat the 10-min stationary exposure to the treadmill. Return the mice to their home cage.
4. Day 3: Allow the mice to rest with no exposure to the treadmill for one full day (*see* **Note 6**).
5. Day 4: Place the mice on the treadmill. Using the TSE Systems software, program the treadmill to run at 10 m/min for 20 min (*see* **Note 7**). This is a relatively low intensity speed and is intended to get the mice acclimated to moving on the treadmill. Adjust the treadmill to be level (or the appropriate incline/decline as desired).
6. Start the 20-min running protocol. Mice are allowed to momentarily fall back onto the resting platform; however, we find that less time between the mice resting, and intervening to encourage reengagement usually has the most success in sustained time on the treadmill (*see* **Note 8**).
7. As mice use the resting platform, use the paintbrush or other tools to encourage reengagement with the treadmill. There are three methods that we found most effective. First, open the lid to the lane of the treadmill with the resting mouse. Using a paintbrush or a similar tool, gently poke the mouse near the hind legs to nudge the mouse toward the treadmill belt. Alternatively, if the tail of the mouse is sticking out from the back of the treadmill, a gentle tail squeeze often works to the same effect. Finally, tapping the wooden end of the paintbrush on the lid of the treadmill, followed by nudging the mouse to run creates a learned behavior. Eventually, simply tapping the end of the brush of the lid becomes sufficient to get the mouse to reengage. A combination of these techniques will likely be required to achieve sustained running from all mice.
8. After the 20-min run, return the mice to their home cages.
9. Day 5: Allow the mice to rest with no exposure to the treadmill.
10. Day 6: Repeat the 20-min run at a fixed speed of 10 m/min. The mice should now be fully acclimatized, and ready for the high-intensity running test following a day of rest.

3.2 High-Intensity Running Test

This test allows the assessment of physical capacity of the mice to be tested.

1. Using the TSE Systems software, prepare the running protocol. There are four stages of the protocol as described in Fig. 2, Stage (A) 13 m/min for 5 min. Stage (B) Increase the speed from 13 to 18 m/min over 5 min. Stage (C) mice run at the fixed speed of 18 m/min for 30 min. Stage (D) Increase the treadmill speed to a fixed speed of 23 m/min until mice reach exhaustion.

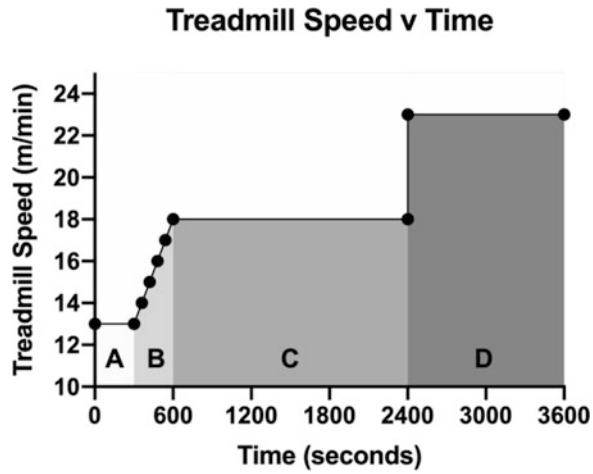

Fig. 2 High-intensity running test protocol. Time and speed of the four stages of forced treadmillrunning. Mice run through all four stages and are considered exhausted after 30 s of refusing to reengage with the treadmill. Running stages A–D are labeled and described in Subheading 3.2

2. As mice rest on the stationary platform, encourage reengagement as previously described.
3. Any mouse that refuses to reengage with the treadmill after 30 s of encouragement should be considered to have reached exhaustion. Record this time and move this mouse from the treadmill lane to its home cage (*see* **Notes 9–12**).

3.3 Low Intensity Walking Test

Aged mice will reach a point where performing the same high-intensity running test becomes impossible. Therefore, we have developed a simple test to measure the physical capabilities of mice no longer able to run on a treadmill.

1. Acclimate the mice to the treadmill by exposing them to the stationary apparatus (Subheading 3.1, **steps 1–4**).
2. Program the TSE System software to run for 1 min at 13 m/min.
3. Start the treadmill and encourage the mice to stay on the treadmill for the full 60 s. This is a binary test and is recorded simply as "pass" or "fail." This test is not intended to measure physical performance but rather to determine if a mouse has reached a point of frailty where they can no longer run.
4. After the test, return the mice to their home cages. This test should not be repeated without adequate recovery times for the mice. This time period should be determined by close observation of the mice, and with input from the veterinary staff.

4 Notes

1. Make sure all equipment is well cleaned. Use 70% ethanol to sterilize the treadmill and any tools used. Additionally, allow ample time for the scent of alcohol to vanish. Lingering odors may impair performance and increase escape behavior by the mice.
2. We use a dedicated room to do the treadmill tests to avoid disruptions. Excessive noise such as the opening and closing of doors may distract the mice and cause them to retreat to the resting platform.
3. It works best to sterilize the treadmill immediately after a round of tests. This allows the treadmill to fully dry and rid of residual odors prior to the next round of running tests or acclimation periods.
4. Some treadmill models come equipped with a barrier that runs perpendicular to the treadmill track Fig. 3. We find that this barrier, intended to keep the mouse on the treadmill, increases escape behavior. Proper training allows for this barrier to be removed. Acclimate the mice in the same condition as the anticipated test.

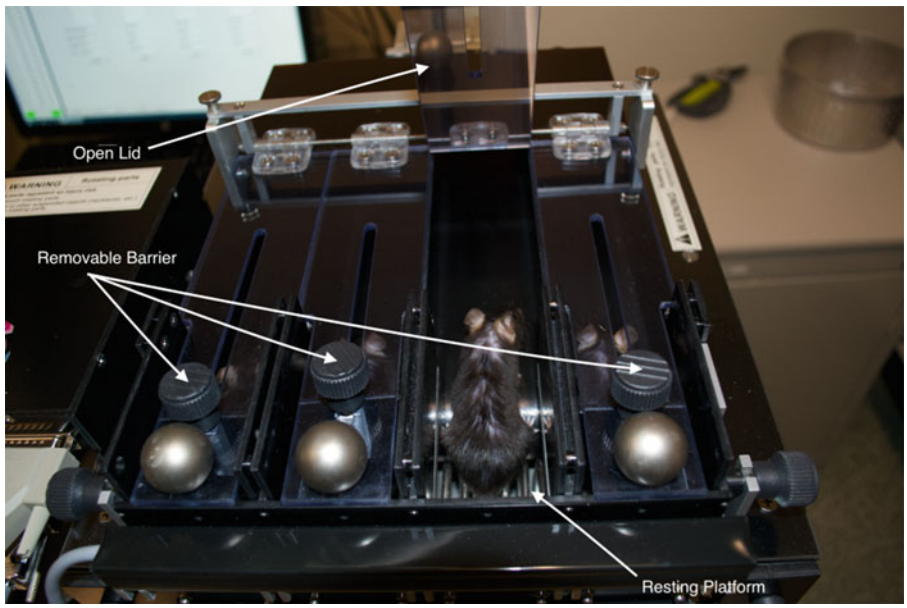

Fig. 3 Setup of treadmill and mice. This is the view of the treadmill with all four lanes occupied. Note the position of the resting platform. Since the mouse in Lane 3 has its hind limbs on the platform, that mouse is considered resting. Also note the removable barriers. Removing these during acclimation and running help limit escape behavior

5. In some cases, we gave the mice food that is 60% calories by fat, which the mice show preference for when given as a reward.
6. While the treadmill training bouts are not designed to train the mice physically, it is designed to get them comfortable with the experimental procedures. Other protocols give detail on how to train mice physically [20]. Regardless, the days in between training are important for acclimation. If desired, the mice can be placed on the treadmill that is not moving to further expose them to the apparatus itself.
7. The TSE Software system can be used to control multiple treadmills simultaneously. To do this, plug in one treadmill via USB, and open the software. Enter the experiment details and continue to get to the page to start the treadmill. Next, plug in the next treadmill and repeat this process. Repeat for any additional treadmills. Finally, start each running window separately so that there is one experimental timer per treadmill.
8. Often times, the mouse will sit on the resting platform and "run" using only its front limbs. This does not count as running and should be considered resting.
9. Some mice will simply refuse to ever engage with the treadmill to begin the run. If this occurs, do not apply too much force to the mouse. Rather, return the mouse to its home cage and try again after 30 min. If the mouse still refuses, try again later in the day, or the next day. For the High-Intensity Running Test, if a mouse refuses to begin running, it should not be counted as a sample for that experiment. This should count as a fail for the Low Intensity Walking Test.
10. Mice may continue to display escape behavior during the treadmill run. While using the paintbrush to encourage running, mice may use this opportunity to escape out the top of the treadmill, now that the plastic barrier is lifted. If a mouse continues to do this, use the tapping method or gentle tail squeeze to encourage running. A mouse that spends considerable time attempting to escape should be omitted from the results and tested again at a later time.
11. It is helpful to do all treadmill training and tests at the same time of day for each trial. Circadian effects can influence both the willingness and abilities of the mice running on the treadmill [21]. Keep in mind that the High-Intensity Running Test can take over 40 min for high-performing mice. If multiple rounds of tests are needed, take this timing into account during the training stages.
12. Mice are most likely to fall back onto the resting platform during certain stages of the High-Intensity Running Test. Stage B has the speed increasing over a 5-min period. When the treadmill speed increases, even by small amounts, the mice

are more likely to rest. This is particularly true when entering Stage D, where the speed goes from 18 to 23 m/min. Extra attention must be paid during these times to ensure the mice remain engaged with the treadmill.

References

1. Gabriel BM, Zierath JR (2017) The limits of exercise physiology: from performance to health. Cell Metab 25(5):1000–1011. https://doi.org/10.1016/j.cmet.2017.04.018
2. Richardson A, Fischer KE, Speakman JR, de Cabo R, Mitchell SJ, Peterson CA, Rabinovitch P, Chiao YA, Taffet G, Miller RA, Renteria RC, Bower J, Ingram DK, Ladiges WC, Ikeno Y, Sierra F, Austad SN (2016) Measures of healthspan as indices of aging in mice—a recommendation. J Gerontol A Biol Sci Med Sci 71(4):427–430. https://doi.org/10.1093/gerona/glv080
3. Dougherty JP, Springer DA, Gershengorn MC (2016) The treadmill fatigue test: a simple, high-throughput assay of fatigue-like behavior for the mouse. J Vis Exp (111). https://doi.org/10.3791/54052
4. Conner JD, Wolden-Hanson T, Quinn LS (2014) Assessment of murine exercise endurance without the use of a shock grid: an alternative to forced exercise. J Vis Exp (90): e51846. https://doi.org/10.3791/51846
5. Castro B, Kuang S (2017) Evaluation of muscle performance in mice by treadmill exhaustion test and whole-limb grip strength assay. Bio Protoc 7(8). https://doi.org/10.21769/BioProtoc.2237
6. Batra A, Vohra RS, Chrzanowski SM, Hammers DW, Lott DJ, Vandenborne K, Walter GA, Forbes SC (2019) Effects of PDE5 inhibition on dystrophic muscle following an acute bout of downhill running and endurance training. J Appl Physiol (1985) 126(6):1737–1745. https://doi.org/10.1152/japplphysiol.00664.2018
7. Feng R, Wang L, Li Z, Yang R, Liang Y, Sun Y, Yu Q, Ghartey-Kwansah G, Sun Y, Wu Y, Zhang W, Zhou X, Xu M, Bryant J, Yan G, Isaacs W, Ma J, Xu X (2019) A systematic comparison of exercise training protocols on animal models of cardiovascular capacity. Life Sci 217:128–140. https://doi.org/10.1016/j.lfs.2018.12.001
8. Hollinski R, Osterberg A, Polei S, Lindner T, Cantre D, Mittlmeier T, Vollmar B, Bruhn S, Muller-Hilke B (2018) Young and healthy C57BL/6 J mice performing sprint interval training reveal gender- and site-specific changes to the cortical bone. Sci Rep 8 (1):1529. https://doi.org/10.1038/s41598-018-19547-z
9. Mees LM, Coulter MM, Chrenek MA, Motz CT, Landis EG, Boatright JH, Pardue MT (2019) Low-intensity exercise in mice is sufficient to protect retinal function during light-induced retinal degeneration. Invest Ophthalmol Vis Sci 60(5):1328–1335. https://doi.org/10.1167/iovs.18-25883
10. Walton RD, Jones SA, Rostron KA, Kayani AC, Close GL, McArdle A, Lancaster MK (2016) Interactions of short-term and chronic treadmill training with aging of the left ventricle of the heart. J Gerontol A Biol Sci Med Sci 71 (8):1005–1013. https://doi.org/10.1093/gerona/glv093
11. Nguemeni C, McDonald MW, Jeffers MS, Livingston-Thomas J, Lagace D, Corbett D (2018) Short- and long-term exposure to low and high dose running produce differential effects on hippocampal neurogenesis. Neuroscience 369:202–211. https://doi.org/10.1016/j.neuroscience.2017.11.026
12. Hoene M, Li J, Li Y, Runge H, Zhao X, Haring HU, Lehmann R, Xu G, Weigert C (2016) Muscle and liver-specific alterations in lipid and acylcarnitine metabolism after a single bout of exercise in mice. Sci Rep 6:22218. https://doi.org/10.1038/srep22218
13. Shi Y, Shi H, Nieman DC, Hu Q, Yang L, Liu T, Zhu X, Wei H, Wu D, Li F, Cui Y, Chen P (2019) Lactic acid accumulation during exhaustive exercise impairs release of neutrophil extracellular traps in mice. Front Physiol 10:709. https://doi.org/10.3389/fphys.2019.00709
14. Ikeda SI, Tamura Y, Kakehi S, Sanada H, Kawamori R, Watada H (2016) Exercise-induced increase in IL-6 level enhances GLUT4 expression and insulin sensitivity in mouse skeletal muscle. Biochem Biophys Res Commun 473(4):947–952. https://doi.org/10.1016/j.bbrc.2016.03.159
15. Brandt N, Dethlefsen MM, Bangsbo J, Pilegaard H (2017) PGC-1alpha and exercise intensity dependent adaptations in mouse skeletal muscle. PLoS One 12(10):e0185993.

https://doi.org/10.1371/journal.pone.0185993

16. Sako H, Yada K, Suzuki K (2016) Genome-wide analysis of acute endurance exercise-induced translational regulation in mouse skeletal muscle. PLoS One 11(2):e0148311. https://doi.org/10.1371/journal.pone.0148311
17. Jin Q, Qiao C, Li J, Xiao B, Li J, Xiao X (2019) A GDF11/myostatin inhibitor, GDF11 propeptide-Fc, increases skeletal muscle mass and improves muscle strength in dystrophic mdx mice. Skelet Muscle 9(1):16. https://doi.org/10.1186/s13395-019-0197-y
18. Gill JF, Santos G, Schnyder S, Handschin C (2018) PGC-1alpha affects aging-related changes in muscle and motor function by modulating specific exercise-mediated changes in old mice. Aging Cell 17(1):e12697. https://doi.org/10.1111/acel.12697
19. Das A, Huang GX, Bonkowski MS, Longchamp A, Li C, Schultz MB, Kim LJ, Osborne B, Joshi S, Lu Y, Trevino-Villarreal JH, Kang MJ, Hung TT, Lee B, Williams EO, Igarashi M, Mitchell JR, Wu LE, Turner N, Arany Z, Guarente L, Sinclair DA (2018) Impairment of an endothelial NAD(+)-H2S signaling network is a reversible cause of vascular aging. Cell 173(1):74–89. e20. https://doi.org/10.1016/j.cell.2018.02.008
20. Moore KM, Girens RE, Larson SK, Jones MR, Restivo JL, Holtzman DM, Cirrito JR, Yuede CM, Zimmerman SD, Timson BF (2016) A spectrum of exercise training reduces soluble Abeta in a dose-dependent manner in a mouse model of Alzheimer's disease. Neurobiol Dis 85:218–224. https://doi.org/10.1016/j.nbd.2015.11.004
21. Tahara Y, Shibata S (2018) Entrainment of the mouse circadian clock: effects of stress, exercise, and nutrition. Free Radic Biol Med 119:129–138. https://doi.org/10.1016/j.freeradbiomed.2017.12.026

Chapter 6

Human Population Genetics in Aging Studies for Molecular Biologists

Brendan Miller, Amin Haghani, Jennifer Ailshire, and T. Em Arpawong

Abstract

Testing hypotheses in human populations, then translating such findings into an experimental paradigm to test for causality can accelerate the rate of therapeutic discovery for many aging-related diseases. Integration of human genomics data has become much more accessible to molecular biologists in recent years due to the explosion of data availability and wealth of bioinformatic resources, tools, and methods that work together to minimize barriers related to its use. There are specific skill sets that can promote integration of human data into the work of molecular biologists, which include the ability to download, organize, store, and analyze human genomics data. In this chapter, key considerations and resources are presented, focusing on approaches that might be unfamiliar to molecular biologists, with regard to human subjects protection guidelines, heterogeneity in human genetics, data security and storage, programming languages, and training for data analysis.

Key words Human subject research, Population substructure, Gene homologs, Unix, Comparative genomics, Principal components, Statistical genetics

1 Introduction

Big data can lead to important discoveries for identifying etiologies and therapeutics for age-related diseases that currently levy an enormous burden of morbidity and cost on individuals and the healthcare system. Genomics data are often referred to as big data because the components are derived from large scale samples and subsume multiple types of data pieces, often collected according to the interests of researchers across multiple fields (e.g., population-geneticists, social scientists, clinical medicine).

Complex age-related diseases (e.g., Alzheimer's disease, osteoarthritis, osteopenia and sarcopenia, Parkinson's disease) involve gene main effects and/or gene-by-environment interactions that have been detected using genomics from human populations. These findings, however, are only observational and not causal. Molecular biologists attempt to translate human population

Sean P. Curran (ed.), *Aging: Methods and Protocols*, Methods in Molecular Biology, vol. 2144,
https://doi.org/10.1007/978-1-0716-0592-9_6,

findings into an experimental paradigm to test for causality. This has promoted unique collaborations between social scientists and molecular biologists. Nevertheless, molecular biologists are realizing the power of these tools and are rapidly translating large human population data into experimental paradigms to discover and develop therapeutic targets.

An incredible amount of biological, environmental, and clinical data have been made accessible to molecular biologists over the past decade due to widespread genotyping and DNAsequencing studies in large cohorts. For example, resources and databases such as The Cancer Genome Atlas [1] (TCGA; https://portal.gdc.cancer.gov), the Encyclopedia of DNA Elements [2] (ENCODE; https://www.encodeproject.org), and the Genotype-Tissue Expression [3] (GTEx; https://www.gtexportal.org/home/) portal have changed the way molecular biologists approach experimental design. The effects of ethnicity on gene expression signatures or the effect of aging on epigenome remodeling has been largely attributed to the utilization of these large databases. TCGA alone has sequenced nearly 7000 tumors; ENCODE has made available over 2500 genomic datasets; GTEx provides tissue-specific gene expression from over 1000 individuals. Additionally, large population-representative panel surveys, such as the U.S. Health and Retirement Study [4] (HRS; http://hrsonline.isr.umich.edu) and associated sister studies around the globe, have provided a wealth of phenotypes and genetic data with which to test hypotheses. The HRS alone has genomewide data on 15,000 individuals and RNA-Seq data on almost 4000 individuals of multiple ethnicities, with more samples being added in on-going data collections. It is no surprise that molecular biologists want to utilize these rich resources.

Molecular biologists often do not have the technical expertise to handle big data, nor the training with which to study aging parameters in human populations (refer to the Chapter on Integrating Longitudinal Population Studies of Aging in Biological Research for important considerations when translating research from model systems to humans). As a consequence, it is easy to become discouraged by the seemingly overwhelming differences in approach to and amount of genomic data. The following topics are tailored specifically to molecular biologists who seek to form experimental hypotheses based on mining human genetic data. The focus is to present key considerations and methods that are not typically within the training repertoire of molecular biologists.

2 Human Subject Research and Protection

Because human genomics data is typically derived from individuals still living, who consent to participation in a study, and do not want to be individually identified, there are multiple safeguards for data confidentiality and security that require processes that differ from those molecular biologists might be used to. These involve additional trainings, certifications, and steps for data access and assurance of confidentiality through the researcher's respective Institutional Review Board and data use agreements.

2.1 Training and Certificates

Regardless of funding source, researchers affiliated with universities and research institutes are required to complete some form of approved responsible conduct of research training, as delineated by the "Common Rule", put forth by the U.S. Department of Health and Human Safety [5]. Typically, in the USA, this includes training for human subjects protection and a certification of completion offered through the Collaborative Institutional Training Initiative [6] (CITI; https://www.citiprogram.org/).

Other programs are available as long as they meet all criteria detailed by the National Institutes of Health's (NIH) Human Subjects research guidelines [7] found here:

http://grants.nih.gov/grants/policy/hs_educ_faq.htm#228

2.2 Institutional Review Board (IRB) for Human Subjects Research

The above trainings need to be completed and certificates supplied during the application process to the researcher's IRB. Additional considerations involving human data need to be delineated in the IRB application such as those that involve data security measures specifically for genetic data or using personal identifiers, procedures in the case of data breeches, and methods for maintaining confidentiality (e.g., no attempts to identify participants). These considerations will be covered in approved human subjects research trainings.

2.3 Data Use Agreements

Data Use Agreements are documents that specify how data can be shared and used by researchers requesting access. These are typically created and required from the entity supplying the data, and govern how data can be shared, stored, analyzed, as well as how the results should be reported. Molecular biologists will want to understand how these agreements differ for human data as many include important restrictions due to Health Insurance Portability and Accountability Act of 1996 (HIPAA) privacy rules [8].

3 Computing

The greatest issues molecular biologists face downloading data of such magnitude include operating in command line computing environments, learning new programs and coding languages, and finding storage necessary to house this high-dimensional data.

3.1 Hardware for Storage and Security

The typical computer hard drive or flash drive does not have the capacity to house raw genotyped data, imputed data files, intermediary data files, and output. In many cases, researchers will have to procure external storage, either in the form of an external hard drive or space purchased on secure clouds (e.g., Google, Amazon, OneDrive, Dropbox) if they meet the requirements according to data use and/or consent agreements.

When downloading data, the size of data files can vary widely from several megabytes to terabytes, and is contingent upon the depth of genotyping or sequencing, the stage of processing (e.g., directly genotyped, imputed dosage files), and number of samples included. Some data that requires high computational power will require use of high-performance computing clusters for both storage and efficient use of analytical resources. Often these high-performance clusters are offered through university systems or third-party organizations. Their use can minimize the computational costs to researchers in terms of procuring hardware, maintaining backups, and speed of analyses.

A critical component for human genomics data storage and use is adhering to security parameters agreed upon by data use agreements or consent forms referred to in Subheading 2. Thus, hardware for storage and data transfer processes need to comply with specified procedures, such as maintaining restricted access to only approved users, password protection, physical lock-and-key barriers for hard drives, and/or encryption processes.

3.2 Software for Data Download, Management, and Analysis

For molecular biologists unfamiliar with using a command line, it is imperative to understand basic unix commands, such as "cd," "ls," and "rm," and pathway structures that are necessary to download data according to the protocol in this chapter, Subheading 4.1. Numerous resources for unix commands can be found online (e.g., https://www.unixtutorial.org/basic-unix-commands).

For data management and analysis, multiple software and coding programs exist. For data formatting, preparation, merging, analysis and visualization of any omics data, *R* [9] has increasingly become the program of choice for researchers (https://www.r-project.org). Reasons for this include that it is open-source, efficient for handling of big data without current limitations for file sizes plaguing other programs, and has a growing pool of preprogrammed packages that can be easily downloaded and incorporated

into a user's set of analytical tools. To get started with R, individuals can navigate to the homepage and follow the instructions for download, installation, and link to tutorials.

For management of genotyped data, and conducting statistical analysis, including gene association and genomewide association scans (GWAS), using PLINK [10] software (https://www.cog-genomics.org/plink/2.0/) has become a standard in the field. A tutorial and guidance can be found through the webpage. One can navigate to the link below, and in the left-hand menu, click on "Getting started" under General usage.

Additional software and tools are available for specific types of analysis. Readers are referred to external sources for listings, such as at the Broad Institute (https://www.broadinstitute.org/data-software-and-tools). For example, navigate to the link below, select "Software" from the second drop-down filter, and click the SEARCH button.

Other useful resources for software or analysis packages are hosted by the University of Michigan (https://sph.umich.edu/csg/software.html) and Bioconductor (https://bioconductor.org).

4 Genomics Data in Human AgingCohorts

There are multiple databases available that provide researchers with access to genotype and phenotype data for human samples.

4.1 Finding Genomics Data in AgingCohorts

One main repository from which human genomics data can be accessed is through the database of Genotypes and Phenotypes [11] (dbGaP) housed by The National Center for Biotechnology: https://www.ncbi.nlm.nih.gov/gap/

The following lists a few examples of human population genetic data with Alzheimer's disease phenotypes that, with approval, can be downloaded from dbGaP:

1. Alzheimer's DiseaseSequencing Project (ADSP), dbGaP Study Accession: phs000572.v1.p1.
2. NIA Alzheimer's Disease Centers Cohort (ADC), dbGaP Study Accession: phs000372.v2.p1.
3. Late Onset Alzheimer's Disease (LOAD) Family Study, dbGaP Study Accession: phs000168.v2.p2.

Another repository where users can search data sources for variables of interest and include the search term of genetics is the National Archive of Computerized Data on Aging [12] (NACDA; https://www.icpsr.umich.edu/icpsrweb/NACDA//).

Another common repository for genomics data specific to Alzheimer's Disease includes the National Institute on AgingGenetics of Alzheimer's Disease Data Storage Site [13] (NIAGADS; https://www.niagads.org).

4.2 Downloading Data

The following is an example of downloading HRS GWAS data from dbGaP (dbGaP Study Accession: phs000428.v1.p1) using a unix-based command line approach.

1. Download Aspera software. This is a high-speed file transfer system that permits direct downloads from dbGaP.
2. Download the NCBI SRA Toolkit.
3. Download the dbGaP repository key. This key is necessary to download data that is restricted and only accessible through approval for the listed Principal Investigator and his/her approved associates.
   - After logging into your dbGaP account, locate "My Projects" to find the project to which the data fits.
   - Click "get dbGaP repository key" in the "Actions column."
   - Save the key file (in .ngc format).
4. Download PLINK2.0. PLINK is among the most widely used GWAS software cited and includes several tools for GWAS data processing and analysis. Refer to Subheading 3.2 above for more information on PLINK.
5. Import the dbGaP repository key during the SRA toolkit configuration process. This process is streamlined in easy-to-understand detail by NCBI.
6. After successfully configuring the SRA toolkit and PLINK2.0, add configured tools to your computer pathway. This will allow you to initiate a procedure from your command line program.
   - Type the following into your command line: "export PATH='path/to/your/SRAtoolkit:$PATH".
   - Type the following into your command line: "export PATH='path/to/your/PLINK2.0:$PATH".
7. Use the "prefetch" command to download the data based on its SRA ID.
   - Type the following into your command line: "prefetch -a / path/to/aspera/ SRR#.
   - The size of datasets is often in TBs and will likely need to be stored on an external hard drive, high-capacity computing cluster, or cloud.
   - Data will begin to download. Be patient, as this will take several hours and perhaps even days.
8. Navigate to the directory in which all HRS data is stored.
9. Extract out SNPs of interest using PLINK2.0. Note quality-assured SNPs and refer to documentation on quality control checking for the SNPs included. These SNPs are included in a separate text file.

- Create a .txt file that contains your SNPs of interest. For example, we can extract mitochondrial SNPs from HRS:
  - MitoT217 MitoC458T ....
- Type the following into your command line: "plink2 --bfile /path/to/hrs/HRSGeneticData/PhenoGenotypeFiles/RootStudyConsentSet_phs000428.CIDR_Aging_Omni1.v2.p2.c1.NPR/GenotypeFiles/phg000842.v1.CIDR_HRS_phase123.genotype-calls-matrixfmt.c1/subject_level_-PLINK_sets/HRS_MIWAS/HRS_phase123_TOP --extract /path/to/snps.txt --make-bed 'name_of_your_choice'.

10. You now have PLINK2.0 files in binary format (referred to as .bed, .bim, and .fam) files that contain subject-specific mitochondrial genotypes. You can convert these files to a VCF file that is more suitable for programs such as R, STATA, and Excel.
    - Type the following into your command line: "plink2 --bfile 'name_of_your_choice' --recode VCF --out 'name_of_your_choice'.
11. Open the VCF file that contains subject-specific SNPs in your downstreamsoftware of choice. If, for example, you use Excel, then you may want to transpose the file in order to have subject IDs as rows and SNPs as columns.

4.3 Managing and Analyzing Data

Merging data sets is another significant challenge for molecular biologists. There are several ways to merge data sets by using a variety of different downstream programs. In general, though, a common subject identifier is all that is needed to successfully merge data sets using computing programs or data management software discussed in Subheading 3.2.

For data analysis, it is advisable that researchers take statistics or programming courses to facilitate testing hypothesis. There are also popular multiday workshops offered by reputable institutes. The following are links to some of these organizations:

Workshop on Statistical Genetic Methods for Human Complex Traits, Institute for Behavioral Genetics, University of Colorado, Boulder: https://www.colorado.edu/ibg/

Summer Institute in Statistical Genetics, University of Washington: https://www.biostat.washington.edu/suminst/sisg

Statistical Genetics, Broad Institute: https://www.broadinstitute.org/broade/broade-statistical-genetics

Courses in Genetics Analysis, The Rockefeller University: http://lab.rockefeller.edu/ott/shortcourses

Genetic Analysis of Population-based Association Studies, Wellcome Trust Genome Campus: https://coursesandconferences.wellcomegenomecampus.org/event-type/courses/

Workshops for Working with Genomes: https://www.sanger.ac.uk/about/open-door-workshops

Alternatively, taking online courses such as through *Coursera* or *EdX* has been useful when those courses include data analysis with big data, genomic data science, and statistical methods. Some online programs offer Data Science certificates or degrees for completing a series of courses on biostatistics and bioinformatics.

4.4 Application of Experimental Biology in Designing the Analytic Plan

Experimental biology could guide the approach for analysis and facilitate the statistical design when working with human genetic data. For instance, rather than conducting a GWAS of common variants across the genome to find associations in human data—an approach often fraught with challenges of sample size and power—findings from biological experiments could justify analyzing several candidates genes or a set of rare variants in a human cohort. Using experimental biology as a guide for the analytic design is advantageous particularly for rare variants because they are typically filtered out of a typical GWAS. By identifying a set of candidates or rare variants experimentally, researchers would be able to conduct hypothesis-driven analyses that is not only improved in statistical power but also can reveal important genetic targets that would have otherwise been ignored in an agnostic GWAS [14].

5 Data Translation

5.1 How to Find SNPs of Interest in Human Data

Molecular biologists might be interested in studying the effect of genetic variation of one particular gene. A single gene is typically represented by numerous SNPs, or a haplotype of more than one SNP, and thus, a molecular biologist might want to extract all SNPs believed to be a marker of that gene. This is particularly relevant if not all SNPs marking that gene are the same across species. We can utilize the UCSC Genome Browser to find all SNPs marking one gene. The following example extracts all SNPs from the mitochondrial genome.

1. Go to https://genome.ucsc.edu/index.html. Click on the "Tools" tab and then on "Table Browser."
2. Input the following settings:
   (a) Clade: Mammal.
   (b) Genome: Human.
   (c) Assembly: Dec. 2013 (GRCh38/hg38).
   (d) Group: Variation.
   (e) Table: snp151Common.
   (f) Position: chrM:1-16569.
   (g) Output format: GTF.
   (h) Output file: Mito_snps.txt.
3. Click "get output." A file will be automatically downloaded in GTF format that contains the genomic locus of all SNPs and associated RS numbers.

Now that all SNPs of one genomic region of interest have been extracted, we can check to see if particular array chips from which human samples were genotyped contain the same SNPs. To do so, one can identify the chip used by the cohort, go to the manufacturer's website, and locate the file that contains all captured SNPs. This file often contains millions of SNPs, which is computationally intensive. Common text editing programs, however, can handle this data size. Simply utilizing the "find" (e.g., cntl + f) feature and searching for the RS number will suffice. In addition, you may seek customer service from the chip manufacturer and ask if a group of SNPs, based on RS identification number, are on the chip.

5.2 How to Compare Genes Across Species

To find genes that are in common across species, or to translate findings from model systems to humans and vice versa, readers are referred to public resources for guidance and tutorials on comparative genomics. The following are two public references:

National Center for Biotechnology Information [15]:
https://www.ncbi.nlm.nih.gov/guide/howto/find-homolog-gene/

Ensembl Genome Browser for Vertebrates [16]:
https://uswest.ensembl.org/info/website/tutorials/compara.html

5.3 Population Substructure and Heterogeneity in Human Genetics

An important consideration for human population genetics research surrounds heterogeneity in genome structure. Human genetic variation is highly dependent upon ancestry, which dictates differences in allele frequencies and linkage disequilibrium [17]. Additionally, genetic associations found in a single race/ethnic population may not transfer to groups of other ancestries and highly admixed groups [18]. Often analyses requires stratification by race/ethnic groups as well as correction for ancestral variation through use of principal components *within* stratified groups [19, 20]. Not accounting for such heterogeneity could result in spurious associations [21]. These issues have been well-documented, and readers are advised to refer to articles cited in this section for an in depth discussion. Issues related to population substructure are critical when planning and conducting analysis with human genetic data.

6 Other Resources

6.1 Genes and Human Health

For molecular biologists investigating genes and wanting to translate any findings into work with human populations, links between genes and human diseases or conditions can be explored using the *GeneticsHome Reference* [22]:

https://ghr.nlm.nih.gov/gene/ALDH4A1#resources

Acknowledgments

Contributions to this work were partially supported by funding from the National Institutes of Health, with support from the National Institute on Aging (NIA) training grant to B. Miller (T32 AG00037; PI: Eileen Crimmins), from an NIA training grant to A. Haghani (T32 AG052374: PI: Kelvin Davies), and from the NIA through a pilot award to T.E. Arpawong (parent award P30 AG017265; PI: Eileen Crimmins).

References

1. Tomczak K, Czerwińska P, Wiznerowicz M (2015) The Cancer Genome Atlas (TCGA): an immeasurable source of knowledge. Contemp Oncol 19(1A):A68
2. Consortium EP (2004) The ENCODE (ENCyclopedia of DNA elements) project. Science 306(5696):636–640
3. Lonsdale J et al (2013) The genotype-tissue expression (GTEx) project. Nat Genet 45 (6):580
4. Sonnega A et al (2014) Cohort profile: the health and retirement study (HRS). Int J Epidemiol 43(2):576–585
5. Health UDo, Services H (2009) Basic HHS policy for protection of human research subjects. Title 45 Code of Federal Regulations
6. Braunschweiger P, Hansen K (2010) Collaborative institutional training initiative (CITI). J Clin Res Best Pract 6:1–6
7. Regulations COF (2009) Protection of human subjects. National Institutes of Health Office for Protection from Research Risks. 45
8. Congress U, Health Insurance Portability and Accountability Act of 1996, Privacy Rule. 45 CFR 164, Aug 2002
9. R Core Team (2017) R: a language and environment for statistical computing. R Found. Stat. Comput. Vienna, Austria. URL: http://www.R-project.org/. page R Foundation for Statistical Computing
10. Purcell S et al (2007) PLINK: a tool set for whole-genome association and population-based linkage analyses. Am J Hum Genet 81 (3):559–575
11. Mailman MD et al (2007) The NCBI dbGaP database of genotypes and phenotypes. Nat Genet 39(10):1181
12. Arbour U (2006) National Archive of Computerized Data on Aging
13. Wang L-S et al (2014) Nia genetics of Alzheimer's disease data storage site (NIAGADS): 2014 update. Alzheimer's Dement 10(4): P634–P635
14. Visscher PM et al (2017) 10 years of GWAS discovery: biology, function, and translation. Am J Hum Genet 101(1):5–22
15. Coordinators NR (2016) Database resources of the national center for biotechnology information. Nucleic Acids Res 44(Database issue): D7
16. Yates AD et al (2020) Ensembl 2020. Nucleic Acids Res 48(D1):D682–D688
17. Hellenthal G et al (2014) A genetic atlas of human admixture history. Science 343 (6172):747–751
18. Martin AR et al (2017) Human demographic history impacts genetic risk prediction across diverse populations. Am J Hum Genet 100 (4):635–649
19. Miller B et al (2019) Comparing the utility of mitochondrial and nuclear DNA to adjust for genetic ancestry in association studies. Cell 8 (4):306
20. Reich D, Price AL, Patterson N (2008) Principal component analysis of genetic data. Nat Genet 40(5):491
21. Novembre J, Stephens M (2008) Interpreting principal component analyses of spatial population genetic variation. Nat Genet 40(5):646
22. Medicine NLo (2018) Genetics home reference

Chapter 7

Design and Analysis of Pharmacological Studies in Aging

Khalyd J. Clay and Michael Petrascheck

Abstract

Measuring lifespan of the model organism, *Caenorhabditis elegans*, in a 96-well format enables the screening of large chemical libraries to identify biologically active molecules. Furthermore, the wide availability of these animals with specific genetic mutations allows the identification of genes that influence lifespan, and by extension, age-related biological pathways. Here, we present a method for measuring the lifespan of *C. elegans* in 96-well microtiter plates to identify and study pharmacologically active molecules that extend lifespan. The format of this assay is readily adapted for automated liquid handling systems and imaging of phenotypes.

Key words High-throughput screening, Aging, Lifespan, Drug discovery, *C. elegans*

1 Introduction

Aging is the greatest risk factor for several age-related diseases including cancer, neurological disorders, and cardiovascular disease [1, 2]. As the global population increases the total number of diseased individuals will undoubtedly increase, taxing global healthcare systems [3]. One way to address this problem is to study the physiological effects of lifespan extension to learn the mechanisms that underlie the cellular dysfunction associated with aging, a branch of science called geroscience. This approach allows for the discovery of novel therapeutics targeting newly discovered molecular pathways that delay the onset of age-associated disease.

Chemical genetics offers one strategy to study the biology of aging, in which small molecules are used to modulate the lifespan of an organism [4]. The Interventions Testing Program (ITP) by the National Institute on Aging identified an array of compounds known to extend lifespan in mice [5]. While impressive, the vast amount of unexplored chemical matter made available through natural products research, as well as fragment and combinatorial libraries uncharacterized for aging research clearly suggest that this list is incomplete [6, 7].

Sean P. Curran (ed.), *Aging: Methods and Protocols*, Methods in Molecular Biology, vol. 2144,
https://doi.org/10.1007/978-1-0716-0592-9_7,

This protocol outlines a high-throughput assay, based on 96-well microtiter plates, to study the pharmacological effects of lifespan extension in the invertebrate *Caenorhabditis elegans*. It involves the treatment of adult animals with a chemical of interest then observing the change in lifespan compared to untreated *C. elegans*. Then, rational changes can be made to the molecular architecture to study structure–activity relationships (SAR) or the molecule may be counter screened against various worm mutants to elucidate the genetic mechanism of action (MOA). Furthermore, we provide a detailed practical procedure with special attention to any potential problems encountered, and specific notes to address them, based on our past experience optimizing this protocol [8, 9]. This platform was successfully used to screen over 90,000 molecules for lifespan extending compounds [10, 11] and uncovered new mechanisms involved in aging [12]—the surprising discovery of one such pathway would not have been possible in traditional genetic screens [13].

Existing assays to determine lifespan are distinguished by the maintenance of *C. elegans* on solid media (*see* NGM below) or liquid media (like this assay). There are key advantages to both assays. NGM-based assays are the de facto standard in the aging field; nearly all genetic studies on longevity have been done using the NGM assay, and various automated survival assays are now available [14–17].

While we would recommend the NGM assay for most other experiments, the advantages of the liquid microtiter-based assay described here are substantial for any longevity studies involving pharmacological compounds. First, we observe that the drug concentrations necessary for optimal effects are generally lower in the liquid microtiter plate assay than for NGM plates. In some cases, no drug uptake was observed on NGM plate, while no similar issue was encountered in the liquid microtiter plate assay. This is to be expected, as NGM is a highly complex mixture that contains two undefined components (Bacto peptone & agar) that will affect drug uptake, potentially activating the xenobiotic response, and reducing solubility. Bacto peptone is produced form scrap meat derived from beef and pork, and therefore contains many small molecule metabolites found in those tissues rendering many drugs poorly soluble in NGM plates. The results are often "crystal gardens" caused by precipitation of the drug affecting the applied dose. Conversely, the only undefined component in the liquid microtiter assay is the feeding bacteria. In addition, *C. elegans* cannot avoid the drug, forcing uptake, which reduces over-all variability and allows for the recording of in vivo dose–response curves.

DMSO is used as a solvent in this assay because it increases bioavailability by facilitating compound transport through membranes. This increased bioavailability, however, is true for any component in the culture medium. For example, we and others

observed that the addition of Bacto peptone can change the effect of cyproheptadine from a lifespan extending compound to one that is toxic, suggesting that an unknown component of Bacto peptone interacts with the biological action of cyproheptadine [18, 19]. The liquid microtiter assay is also compatible with liquid handling robots and a typical high-throughput screening infrastructure. For large screens with over 1000 compounds this is a considerable advantage that should not be underestimated. A final advantage of the liquid assay is that it requires approximately ten times less drug to test the same number of animals because of the miniaturized format. This can result in substantial cost savings as the prices for some compounds can be in the range of $100 per milligram.

2 Materials

All solutions are prepared using ultrapure deionized water (Millipore) and analytical grade reagents. All solutions can be stored at room temperature, unless otherwise indicated.

2.1 Materials for Feeding Bacteria

1. **Luria broth (LB)**: Dissolve one capsule Luria Broth from RPI Research Products (L24045-1000.0), dilute to 1000 mL, and autoclave.
2. **Solution of 0.17 M KH_2PO_4/0.72 M K_2HPO_4**: Dissolve 23.1 g of KH_2PO_4 and 125.4 g of K_2HPO_4 in 900 mL of deionized water. After the salts have dissolved, adjust the total volume of the solution to 1000 mL with deionized water and sterilize by autoclaving.
3. **Terrific Broth (TB)**: Dissolve 12 g of Terrific Broth Ultrapure and dissolve into a total volume of 250 mL deionized water, and then autoclave the solution. This solution can be stored long-term at RT. Prior to use, add 2 mL 50% glycerol dissolved in EtOH.
4. **100 mg/mL Ampicillin stock solution**: Dissolve 1 g of ampicillin in 10 mL of sterile deionized water. Sterile filter, aliquot into 200 μL portions, and store at −20 °C. Use at a final concentration of 50–100 μg/mL.
5. **250 μg/mL Amphotericin B (Fungizone) stock solution**: Dissolve 1 mg of amphotericin B in 4 mL of ethanol. Aliquot into 100 μL portions and store at −20 °C. Use at a final concentration of 0.1 μg/mL (*see* **Note 1**).
6. **100 mg/mL Carbenicillin stock solution**: Dissolve 1 g of carbenicillin in 10 mL of sterile deionized water. Sterile filter, aliquot into 200 μL portions, and store at −20 °C. Use at a final concentration of 50 μg/mL.

7. **1 M Potassium phosphate buffer, pH 6.0**: Dissolve 136 g of KH_2PO_4 in 900 mL of sterile deionized water. Adjust the pH to 6.0 with 5 M KOH and then add deionized water to 1000 mL and autoclave the solution.
8. **S-basal medium**: Weigh 5.9 g of NaCl and add 50 mL of 1 M potassium phosphate, pH 6.0. Add deionized water to 950 mL and then autoclave. After autoclave, let the solution cool to 55 °C. Before use add cholesterol 1 mL cholesterol stock (5 mg/mL in ethanol) per liter to a final concentration of 5 mg/L (*see* **Note 2**).
9. **1 M Potassium citrate, pH 6.0**: Dissolve 268.8 g of tripotassium citrate ($C_6H_5K_3O_7$) and 26.3 g of citric acid monohydrate ($C_6H_8O_7{\cdot}H_2O$) in 900 mL of deionized water. Adjust the pH to 6.0 with 5 M KOH. Add deionized water to 1000 mL and then autoclave.
10. **Trace metals solution**: Dissolve 1.86 g of Na_2EDTA, 0.69 g of $FeSO_4{\cdot}7H_2O$, 0.20 g of $MnCl_2{\cdot}4H_2O$, 0.29 g of $ZnSO_4{\cdot}7H_2O$, and 0.016 g of $CuSO_4$ in 1000 mL deionized water and autoclave. Store this solution in the dark or cover with aluminum foil.
11. **S-complete medium**: To a 950 mL solution of S-basal, add: 10 mL of 1 M potassium citrate pH 6.0 (sterile), 10 mL of trace metals solution (sterile), 3 mL of 1 M $CaCl_2$ (sterile), and 3 mL of 1 M $MgSO_4$ (sterile). Add cholesterol to a final concentration of 5 mg/L unless cholesterol was already added to the S-basal (*see* **item 8**).
12. **Amp resistant OP50**: Some compounds may require the presence of live bacteria in order to extend lifespan (e.g., metformin). If that is the case and if carbenicillin is still added to the culture to prevent contamination, Ampicillin/carbenicillin resistant OP50 will be required. These can be generated by transforming OP50 with an amp resistant plasmid [20].

2.2 *Materials for* C. elegans *Culture*

1. **Nematode growth medium (NGM) agar plates**: Dissolve 3.0 g of NaCl, 2.5 g of peptone (from casein, pancreatic digest), and 17 g of agar in 975 mL of deionized water with a stirring bar. Autoclave the solution, allow to cool down to 55 °C, and then add 0.5 mL of 1 M $CaCl_2$ (sterile), 1 mL of 5 mg/mL cholesterol stock in ethanol, 1 mL of 1 M $MgSO_4$ (sterile), 25 mL of potassium phosphate buffer, pH 6.0 (sterile), and 0.5 mL of 100 mg/mL carbenicillin stock to get a final concentration of 50 μg/mL. Once everything is dissolved while stirring, pour the still hot NGM into Petri dishes using sterile technique. Leave the plates at room temperature for 2 days to cool off and for moisture to evaporate (*see* **Note 3**).

2. **M9 buffer**: Dissolve 15 g of $Na_2HPO_4 \cdot 12H_2O$, 3 g of KH_2PO_4, 5 g of NaCl in 1000 mL of deionized water and autoclave. After the solution has cooled to RT add 0.25 g of $MgSO_4 \cdot 7H_2O$.
3. **0.6 mM 5-fluoro 2′-deoxyuridine (FUDR) stock solution**: Dissolve 100 mg of 5-fluoro 2′-deoxyuridine in 670 mL of sterile S-complete. Make 10 or 45 mL aliquots and store at −20 °C. Use at a final concentration of 100–120 μM (*see* **Note 4**).
4. **Bleach/NaOH solution** (prepared fresh before synchronization): Mix 7.7 mL of sterile deionized water, 1.8 mL of household bleach, and 0.5 mL of 10 M NaOH.

3 Methods

This protocol is designed to culture and measure the lifespan of *C. elegans* in 96-well microtiter plates. Use of the below method, in liquid format, allows an investigator to screen a large number of chemicals and their influence of wildtype or genetic mutant worms efficiently. A working knowledge regarding the maintenance of *C. elegans* is helpful but not required [21]. It is imperative to establish and maintain a synchronous population, so we include days, weeks, and important timepoints. These are organized into subsections to aid the investigator (*see* **Note 5** and Fig. 1). The first day of adulthood (Day 1) is defined as 1 day following the last larval stage (L4) of worm development (Day 0).

3.1 Preparing OP50 Feeding Bacteria

OP50 is the strain of *E. coli* used as a food source for *C. elegans* (available from the *Caenorhabditis* Genetics Center (CGC)). As noted above, the OP50 bacterial strain used in this protocol was previously made Carbenicillin/Ampicillin resistant to prevent cross-contamination of the worm culture with other bacteria [20]. Prepare OP50 under sterile conditions 4–5 days before it is used in the worm culture.

3.1.1 Day −7: Thursday (Week 1): Prepare OP50 Preinoculum

1. Preinoculate 5 mL of LB containing 100 μg/mL Ampicillin and 0.1 μg/mL Amphotericin B (*see* **Note 1**) with a single OP50 colony and incubate with shaking for at least 6 h in a bacterial shaker at 37 °C.
2. Add 125 μL of OP50 preinoculum to 250 mL TB containing 50 μg/mL ampicillin and 2 mL 50% glycerol. Incubate at 37 °C in a bacterial shaker until saturation is reached, typically 12–18 h. Do not let the culture grow longer than 19 h.

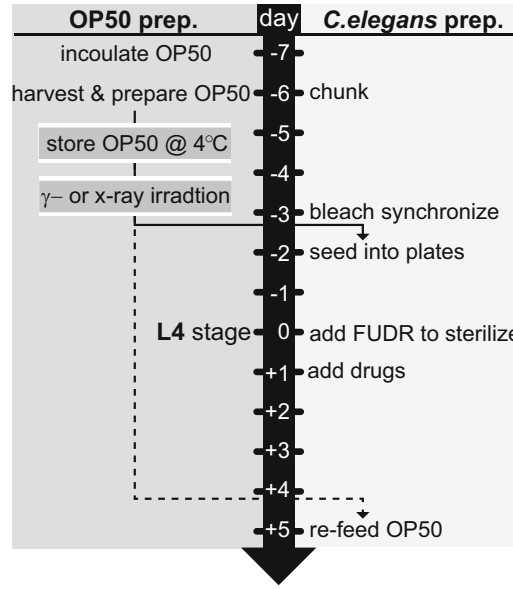

Fig. 1 A timeline of a typical lifespan experiment including important days with their respective steps. OP50 is prepared during Days −7 to −3 and seeded into plates at Day −2. *C. elegans* preparation begins at Day −6 with chunking starved L1 worms, synchronized and seeded at Days −3 to −2. FUDR is added at the L4 stage to prevent offspring (this timepoint is considered Day 0) and drugs are added at Day 1. Finally, on Day 5 OP50 is added to prevent starvation. Starting at Day 1, the animals are counted every 2–3 days until only 5% of the population remains

3.1.2 Day −6: Friday (Week 1): Prepare OP50

1. Transfer OP50 solution to 250 mL sterilized centrifuge tube. Centrifuge at 3800 rpm (2200 × *g*) for 15 min at 4 °C (*see* **Note 6**). Remove supernatant and resuspend bacteria in ~150 mL sterile DI water. Centrifuge at 3800 rpm (2400 × *g*) for 15 min at 4 °C. Complete this wash twice.
2. Following the second wash resuspend bacteria in 50 mL sterile DI water and transfer to a tared 50 mL centrifugation tube. Centrifuge at 3800 rpm (2400 × *g*) for 20 min at 4 °C.
3. Aspirate as much water as possible from the tube without disturbing the pellet. Weigh the tube with the pellet inside. Determine the mass of the pellet by subtracting the mass of the tared tube from the total mass of the tube and pellet.
4. Thoroughly resuspend the pellet in S-complete by pipetting up and down, or vigorously vortex, to a concentration of 100 mg/mL. This should correspond to approximately 2×10^{10} bacteria/mL. Use a spectrometer to determine the number of bacteria per mL if the relationship between the optical density and number of bacteria per mL is known. Adjust the concentration of OP50 feeding solution to 2×10^{10} bacteria/mL.

5. Spot a single 60 mm NGM plate with 50 μL OP50 then incubate overnight at 37 °C. Check for any growth of contaminants the following morning.
6. Store OP50 at 4 °C until ready for use. Immediately return to 4 °C when not in use (*see* **Note 7**).

3.2 Preparing a Synchronous Worm Culture

Below we outline how to generate a population of worms that are age synchronized. It is important to handle the animals under sterile conditions, next to a flame from a Bunsen burner, following bleach treatment in Subheading 3.2.2. We recommend to wipe down the workbench with 70% EtOH daily before working. Incubate plates at 20 °C unless otherwise noted, and do minimize time outside that temperature to ensure minimal environmental temperature fluctuations [22].

3.2.1 Day −6: Friday (Week 1): "Chunk" the Worms

1. Take a 5–10-day-old NGM plate on which much of the worm population is starved L1 larvae. With a flame-sterilized metal spatula cut out agar squares from the plate of starved worms. Transfer several of these chunks onto a fresh 100 mm NGM plate preseeded with 100 μL of OP50 prepared in Subheading 3.1 (*see* **Note 8**).

3.2.2 Day −3: Monday (Week 2): Synchronize the Worms

1. Collect gravid adults from 100 mm plate by washing NGM plate with 10 mL sterile water and transfer solution to 15 mL conical tube (*see* **Note 9**).
2. Wash the worms twice by centrifuging 2 min in a centrifuge at 1200 rpm (280 × *g*), removing the supernatant, then adding 10 mL water. Repeat.
3. Following the second water wash, remove as much water from the tube without disturbing the worm pellet. Then add 4 mL of freshly prepared alkaline bleach solution prepared in 2.2.5. Incubate worms until the worms break open, but no longer than 5 min. Vortex the solution every minute and monitor the reaction using a dissecting microscope (*see* **Note 10**).
4. When most adults break in half, add 6 mL M9 buffer to neutralize the reaction. Immediately wash the eggs three times with 10 mL M9 buffer by centrifuging 2 min at 2500 rpm (1100 × *g*) (*see* **Note 11**).
5. Wash eggs once with 10 mL S-complete by centrifuging 2 min at 2500 rpm (1100 × *g*).
6. Suspend eggs in 10 mL S-complete, and gently shake overnight at RT using a nutator or similar device.

3.2.3 Day −2: Tuesday (Week 2) 12:00 Noon: Seeding Worms

1. Under the dissecting scope, check to see if the worms hatched overnight. Determine the concentration of worms by counting the number present in a 10 μL drop. Count ten drops per sample (*see* **Note 12**).

2. Prepare in a 50 mL Falcon tube: Dilute the synchronized worms from **step 1** in S-complete at a concentration of 70–80 worms/mL. Add Carbenicillin (stock 100 mg/mL) to a final concentration of 50 μg/mL. Add Amphotericin B (stock 250 μg/mL) to a final concentration of 0.1 μg/mL. Shake on a nutator until ready to use.
3. At 2:30 P.M. add RT equilibrated OP50, prepared in Subheading 3.1, to a final concentration of 6 mg/mL ($= 1.2 \times 10^9$ bacteria/mL).
4. Transfer 120 μL of worm/OP50 solution into each well of a 96 well plate with a transparent bottom. Multichannel pipettes are helpful for this operation. Keep worms suspended with gentle shaking to ensure even distribution.
5. Seal the plate with a plate sealer. Incubate at 20 °C for 2 days until animals reach L4 stage (*see* **Note 13**).

3.2.4 Day 0: Thursday (Week 2) Before 12:00 a.m.: Sterilize Animals Using FUDR

1. To sterilize the animals add 33 μL of a 0.6 mM FUDR stock solution to each well. This step brings the final volume in each well to 150 μL and reduces the final concentration of OP50 from 6 mg/mL to 5 mg/mL (1×10^9 bacteria/mL). Seal the plate using plate sealers and shake it for 15–20 min on a microtiter plate shaker. If the OP50 was added at 2:30 p.m. on Day −2, it is important that the FUDR is added before the eggs are fertilized (*see* **Note 4**). Return plates to the 20 °C incubator.

3.2.5 Day 1: Friday (Week 2): Add Drugs to Plate Wells

1. By the morning of Day 1, the animals should have developed into adults containing visible eggs. Drugs whose effect on lifespan is to be tested are added at the desired concentration (*see* **Notes 14–16**). After adding compounds, seal the plates with plate sealer and shake for 2–3 min. Then return to 20 °C.
2. After incubating for 6 h, check for dead worms using an inverted microscope. Generally, there should be less than ten dead worms per plate. Note the presence of dead animals in a well that have died due to compound addition artifacts to censor them from the lifespan analysis.
3. Once a week, remove the tape sealer, wait 1 min, and reseal the plate with a fresh sealer to allow fresh oxygen into the wells. Shake for 2–3 min and return to 20 °C incubator or whatever temperature was chosen for the experiment.

3.2.6 Day 5: Tuesday (Week 3): Prevent Starvation by Adding OP50

1. Add 5 μL of the same previously prepared OP50 solution to each of the 96 wells to prevent starvation.

3.3 Scoring of Phenotypes

1. For this protocol we define the L4 stage as Day 0 of adulthood. On Day 1, account for animals that died from addition artifacts, count the total number of worms in each well. Censor wells that contain 16 or more worms in a well.
2. Shake the 96-well plate for 2 min on a microtiter plate shaker before counting the number of animals that are alive. Typically in strong light the animals will move (*see* **Note 17**).
3. Following a counting session return the plates to 20 °C incubator.
4. Repeat **steps 2–3** every 2–3 days until only 5% of the population remains.

4 Notes

1. Amphotericin B is poorly soluble in ethanol and will precipitate when stored at −20 °C. Warm to room temperature then vortex well before use.
2. If buffer is to be stored long term (weeks to months), do not add cholesterol, rather put a piece of tape over the cap preventing the bottle from being opened, and note that cholesterol must be added prior to use. This is because the cholesterol is somewhat unstable if stored long term in solution. We store the cholesterol dissolved in ethanol at −20 °C until use, in which we allow it to equilibrate to room temperature prior to addition.
3. Different sized petri dishes are used for different applications. To fill a 100 mm diameter dish, which we typically use to maintain larger populations of worms, use 20 mL NGM agar. To fill a 60 mm dish, which we typically use for smaller populations, use 10 mL NGM. The NGM plates are stored in plastic boxes with lids, upside down to prevent condensation, at 4 °C.
4. FUDR is added to L4 animals. FUDR intercalates into sperm DNA, preventing fertilization of the eggs. Addition before L4 will result in growth defects. Again, timing this dependent on the distinct morphological features of the animal, in this specific case, the presence of a moon-shaped vulva characteristic of L4 *C. elegans*. We only thaw the stock solution of FUDR prepared in **item 4** of Subheading 2.2 up to two times because in our experience repeated cycles of thawing reduces its effect. FUDR is very temperature sensitive and should be thawed at room temperature. Exposure to 37 °C will inactivate it.
5. The timing outlined here fits to a 5-day work week (Monday through Friday), and is with respect to N2 animals. Some mutant strains develop significantly different compared to N2. Optimize timing of chunking (Subheading 3.2.1),

synchronization (Subheading 3.2.2), and FUDR sterilization (Subheading 3.2.4) based on the unique morphological characteristics of each larval stage into adulthood (*see* Fig. 1).

6. To resuspend the bacteria, we find a 10 mL serological pipette and a Pipet-Aid to be most useful. Be sure not to directly touch the tip to the bacteria, as it will stick and be difficult to get off. In addition, it is useful to spray down the tubes with 70% EtOH prior to opening to help prevent contamination.
7. One important consideration for experiments is whether to feed the worms dead or alive bacteria. We do not observe any bacterial growth in our experiments since there are no nutrients available, however it is reasonable to assume the addition of compounds may affect the bacteria, thereby affecting the worm [23]. With this in mind, most of our lifespan experiments are conducted using gamma or X-ray irradiated OP50, which we preform after ensuring there is no contaminate growth, and before feeding to *C. elegans*.
8. Consider the number of worms transferred to a fresh food source, since seeding too many results in the animals consuming all of the OP50 before they fully develop into gravid adults. To help prevent starvation, we will seed dedicated plates with concentrated OP50 (centrifuge leftover OP50 like in **step 2** of Subheading 3.1.1 and aspirate some supernatant. For 60 mm use 50 μL and for 100 mm use 400 μL). Alternative to chunking, one may use approximately 100 μL of sterile water to wash a plate of starved L1 larvae, then transfer this solution to a plate with fresh food and allow the liquid to evaporate under sterile conditions.
9. We recommending checking the animals under a dissecting scope prior to bleaching to ensure the adults contain eggs since some types of worm mutations delay development.
10. The bleaching reaction dissolves the chitinous outer layer of the adults to harvest the eggs within, which are resistant to this solution. As with **Note 7**, it is important to monitor the worms under a dissecting scope during the reaction. While it takes some experience, one should ideally quench with M9 buffer in **step 4** of Subheading 3.2.2 just as the adults break open. Over-bleaching results in a reduced number of hatched larvae, and under bleaching will leave L1 and undissolved adults in the solution. Undissolved adults containing eggs will inadvertently be included in a well, over–saturating the number of worms in the specific well. In addition, the sodium hypochlorite in the bleach appreciably degrades over time, so we replace the bottle every 6 months.

11. Each wash with M9 will result in some egg loss, since the eggs will stick to the side of the tube and pipette tip. Wash three times if there is much debris, like unbroken adults, in the solution. If the solution is mostly clean or a greater number of eggs are needed, wash twice.
12. We find the lid of a clear 96-well plate ideal for holding a 10 μL drop to count the hatched larvae. Do not include unhatched eggs, as the viability of eggs varies from strain to strain. It is important to count ten drops to ensure an optimum number of worms are seeded into individual wells—too many worms in a well will quickly consume available OP50.
13. Do not use plate sealers with perforations for gas exchange because the liquid in the wells may evaporate and there is a possibility for contamination.
14. Many compounds are insoluble in water, and most compound libraries are predissolved in DMSO. In our hands, *C. elegans* will accept DMSO concentrations up to 0.5% will minimal effects, which is up to 0.75 μL of compound dissolved in DMSO. When handling small volumes, it is helpful to dilute the solution in buffer to ensure the proper amount is precisely dispensed. Note that at these DMSO concentrations we do not observe changes in lifespan as has been reported for different assays [24, 25].
15. The solubility of each compound in water or DMSO determines the maximal concentration at which the compound can be tested. In general, most compounds are soluble to 10 mM in DMSO, which results in a final concentration of 50 μM using the maximal 0.5% DMSO concentration.
16. We found that the age of the animal when the drug is added may or may not change the effect of the drug on lifespan dramatically [26].
17. We check for dead animals three times a week, Monday, Wednesday, and Friday. Observe the animals with a 2× or 4× objective. It is possible that 1 day an animal will not move and determined to be dead, then next measurement it is moving and counted alive; however, this is only an occasional occurrence. We account for "resurrected" worms only after all worms are dead, during post hoc analysis the miscount is clear. Very old worms may only slightly move, so using a higher magnification at the tip of the pharynx will help detect subtle movement.

Acknowledgments

This protocol was originally developed by Xiaolan Ye and Michael Petrascheck in the Laboratory of Linda Buck. It was then further optimized by Sunitha Rangaraju and Gregory M. Solis. The most current version presented here was prepared by K.J.C. and M.P. with the critical reading of Alan To and Anabel Perez. This work was supported by grant funding to M.P., provided by NINDS R21 NS107951.

References

1. Franceschi C, Garagnani P, Morsiani C, Conte M, Santoro A, Grignolio A, Monti D, Capri M, Salvioli S (2018) The continuum of aging and age-related diseases: common mechanisms but different rates. Front Med (Lausanne) 5:61. https://doi.org/10.3389/fmed.2018.00061
2. Niccoli T, Partridge L (2012) Ageing as a risk factor for disease. Curr Biol 22(17): R741–R752. https://doi.org/10.1016/j.cub.2012.07.024
3. Kennedy BK, Berger SL, Brunet A, Campisi J, Cuervo AM, Epel ES, Franceschi C, Lithgow GJ, Morimoto RI, Pessin JE, Rando TA, Richardson A, Schadt EE, Wyss-Coray T, Sierra F (2014) Geroscience: linking aging to chronic disease. Cell 159(4):709–713. https://doi.org/10.1016/j.cell.2014.10.039
4. Kennedy BK, Pennypacker JK (2014) Drugs that modulate aging: the promising yet difficult path ahead. Transl Res 163(5):456–465. https://doi.org/10.1016/j.trsl.2013.11.007
5. Nadon NL, Strong R, Miller RA, Nelson J, Javors M, Sharp ZD, Peralba JM, Harrison DE (2008) Design of aging intervention studies: the NIA interventions testing program. Age (Dordr) 30(4):187–199. https://doi.org/10.1007/s11357-008-9048-1
6. Bajorath J (2016) Extending accessible chemical space for the identification of novel leads. Expert Opin Drug Discov 11(9):825–829. https://doi.org/10.1080/17460441.2016.1210126
7. Newman DJ, Cragg GM (2016) Natural products as sources of new drugs from 1981 to 2014. J Nat Prod 79(3):629–661. https://doi.org/10.1021/acs.jnatprod.5b01055
8. Rangaraju S, Solis GM, Petrascheck M (2015) High-throughput small-molecule screening in Caenorhabditis elegans. In: Hempel JE, Williams CH, Hong CC (eds) Chemical biology: methods and protocols. Springer New York, New York, NY, pp 139–155. https://doi.org/10.1007/978-1-4939-2269-7_11
9. Solis GM, Petrascheck M (2011) Measuring Caenorhabditis elegans life span in 96 well microtiter plates. J Vis Exp (49). https://doi.org/10.3791/2496
10. Petrascheck M, Ye X, Buck LB (2007) An antidepressant that extends lifespan in adult Caenorhabditis elegans. Nature 450 (7169):553–556. https://doi.org/10.1038/nature05991
11. Ye X, Linton JM, Schork NJ, Buck LB, Petrascheck M (2014) A pharmacological network for lifespan extension in Caenorhabditis elegans. Aging Cell 13(2):206–215. https://doi.org/10.1111/acel.12163
12. Rangaraju S, Solis GM, Andersson SI, Gomez-Amaro RL, Kardakaris R, Broaddus CD, Niculescu AB 3rd, Petrascheck M (2015) Atypical antidepressants extend lifespan of Caenorhabditis elegans by activation of a non-cell-autonomous stress response. Aging Cell 14 (6):971–981. https://doi.org/10.1111/acel.12379
13. Chen AL, Lum KM, Lara-Gonzalez P, Ogasawara D, Cognetta AB 3rd, To A, Parsons WH, Simon GM, Desai A, Petrascheck M, Bar-Peled L, Cravatt BF (2019) Pharmacological convergence reveals a lipid pathway that regulates C. elegans lifespan. Nat Chem Biol 15(5):453–462. https://doi.org/10.1038/s41589-019-0243-4
14. Stroustrup N, Ulmschneider BE, Nash ZM, Lopez-Moyado IF, Apfeld J, Fontana W (2013) The Caenorhabditis elegans lifespan machine. Nat Methods 10(7):665–670. https://doi.org/10.1038/nmeth.2475
15. Churgin MA, Jung SK, Yu CC, Chen X, Raizen DM, Fang-Yen C (2017) Longitudinal imaging of Caenorhabditis elegans in a microfabricated device reveals variation in behavioral decline during aging, Elife 6. https://doi.org/10.7554/eLife.26652

16. Ching TT, Hsu AL (2011) Solid plate-based dietary restriction in Caenorhabditis elegans. J Vis Exp (51). https://doi.org/10.3791/2701
17. Sutphin GL, Kaeberlein M (2009) Measuring Caenorhabditis elegans life span on solid media. J Vis Exp (27). https://doi.org/10.3791/1152
18. Zarse K, Ristow M (2008) Antidepressants of the serotonin-antagonist type increase body fat and decrease lifespan of adult Caenorhabditis elegans. PLoS One 3(12):e4062. https://doi.org/10.1371/journal.pone.0004062
19. Petrascheck M, Ye X, Buck LB (2009) A high-throughput screen for chemicals that increase the lifespan of Caenorhabditis elegans. Ann N Y Acad Sci 1170:698–701. https://doi.org/10.1111/j.1749-6632.2009.04377.x
20. Chung CT, Niemela SL, Miller RH (1989) One-step preparation of competent Escherichia coli: transformation and storage of bacterial cells in the same solution. Proc Natl Acad Sci U S A 86:2172–2175. https://doi.org/10.1073/pnas.86.7.2172
21. Brenner S (1974) The genetics of Caenorhabditis elegans. Genetics 77(1):71–94
22. Galbadage T, Hartman PS (2008) Repeated temperature fluctuation extends the life span of Caenorhabditis elegans in a daf-16-dependent fashion. Mech Ageing Dev 129 (9):507–514. https://doi.org/10.1016/j.mad.2008.04.012
23. Cabreiro F, Au C, Leung KY, Vergara-Irigaray-N, Cocheme HM, Noori T, Weinkove D, Schuster E, Greene ND, Gems D (2013) Metformin retards aging in C. elegans by altering microbial folate and methionine metabolism. Cell 153(1):228–239. https://doi.org/10.1016/j.cell.2013.02.035
24. Guan XL, Wu PF, Wang S, Zhang JJ, Shen ZC, Luo H, Chen H, Long LH, Chen JG, Wang F (2017) Dimethyl sulfide protects against oxidative stress and extends lifespan via a methionine sulfoxide reductase A-dependent catalytic mechanism. Aging Cell 16(2):226–236. https://doi.org/10.1111/acel.12546
25. Frankowski H, Alavez S, Spilman P, Mark KA, Nelson JD, Mollahan P, Rao RV, Chen SF, Lithgow GJ, Ellerby HM (2013) Dimethyl sulfoxide and dimethyl formamide increase lifespan of C. elegans in liquid. Mech Ageing Dev 134(3–4):69–78. https://doi.org/10.1016/j.mad.2012.10.002
26. Solis GM, Kardakaris R, Valentine ER, Bar-Peled L, Chen AL, Blewett MM, McCormick MA, Williamson JR, Kennedy B, Cravatt BF, Petrascheck M (2018) Translation attenuation by minocycline enhances longevity and proteostasis in old post-stress-responsive organisms. Elife 7. https://doi.org/10.7554/eLife.40314

Chapter 8

Methods for Assessing Fertility in *C. elegans* from a Single Population

Chia-An Yen and Sean P. Curran

Abstract

Reproductive senescence occurs in a wide range of species with mechanistic aspects that are conserved from *Caenorhabditis elegans* to humans. Genetic and environmental factors can influence fertility and reproductive output can impact rates of aging. The *C. elegans* Bristol N2 strain commonly used in laboratories is hermaphroditic, producing a defined number of sperm during larval development before switching exclusively to oogenesis. Here we show a method of assaying both oocyte and sperm quality from a single population of animals.

Key words Fertility, Fecundity, Oocyte quality, Sperm quality, Reproductive senescence, *C. elegans*, Fertility assays, Spermatogenesis, Aging

1 Introduction

Fertility is a major life history trait that can be readily assayed to define the impact of specific experimental conditions (genetic or environmental). The disposable soma theory of aging states that organisms age due to the trade-off of resources to satisfy the energetic requirements of growth, reproduction, and maintenance [1–3]. Conditions that alter reproduction can impact lifespan and multiple lifespan altering manipulations can change reproductive output [2–7]. As such, environmental and genetic factors that alter the balance of these energetic requirements can have multiple effects on animal health and longevity. Therefore, the assessment of fertility of an animal under defined experimental conditions is essential for understanding the aging process.

Like humans, *C. elegans* experience a decline in fertility with age; at roughly one-third of their lifespan [8]. In addition, regulators of reproductive aging like insulin/IGF-1 and *sma*-2/TGF-β signaling have conserved roles from worms to human [9]. While the majority of studies in reproductive senescence have focused on maternal effects, male factors contribute to a large portion of

Sean P. Curran (ed.), *Aging: Methods and Protocols*, Methods in Molecular Biology, vol. 2144,
https://doi.org/10.1007/978-1-0716-0592-9_8,

fertility complications with increasing evidence of an inverse relationship between paternal age and sperm health [10]. Thus, fertility measurements in assessing the quality of gametes of both sexes are equally important.

C. elegans are androdioecious nematodes with both hermaphrodites and males. Hermaphrodites undergo spermatogenesis at larval stage 4 (L4) to produce around 300 spermatids. After spermatogenesis, hermaphrodites switch exclusively to oogenesis as they molt into adults [11].

As sex determination is regulated by copies of the X chromosome—hermaphrodites are XX and males are XO—males can be maintained at Mendelian ratios when mated to hermaphrodites. Since mated hermaphrodites can produce significantly more progeny compared to animals restricted to self-fertilization, a large number of F1 progeny containing both males and females can be easily maintained.

Fertility of hermaphrodites can be tested by singling individual animals and tracking the generation of live progeny, unfertilized oocytes, and dead eggs during their reproductive span. Quality of oocyte or sperm can be better understood by mating males to a hermaphrodite in a mated reproductive assay. Wild-type male spermatozoa are better poised for fertilization than wild-type hermaphrodite spermatozoa due to their larger size and faster mobility, giving them a competitive advantage in reaching an unfertilized oocyte [12, 13]. Male sperm quality can also be determined through isolation of L4-stage virgin males and dissecting 24 h after isolation for spermatid number, morphology, size, and ability to activate upon known in vitro activators [14, 15]. Once gender isolated, males can be maintained in the absence of hermaphrodites to assess the impact of aging on sperm function, which can be influenced by genetics, environment, and nutrition [18].

2 Materials

Prepare all solutions using ultrapure water (prepared by purifying deionized water, to attain a sensitivity of 18 MΩ-cm at 25 °C). Prepare and store all reagents at room temperature (unless indicated otherwise). Filter-sterilize with 0.22 μM filter or autoclave to sterilize (as indicated).

2.1 C. elegans Culture and Synchronization

1. *C. elegans* strains (e.g., wild type (WT) N2 Bristol) can be obtained from the CGC.
2. Bacterial diets (e.g., *Escherichia coli* B/OP50) can be obtained from the CGC.
3. Nematode Growth Medium (NGM): 3 g/L NaCl, 17 g/L agar, 2.5 g/L peptone, 1 mM $MgSO_4$, 5 mg/L cholesterol in ethanol, 25 mM KH_2PO_4, 1 mM $CaCl_2$, 0.01875% streptomycin.

4. 60 × 15 mm sterile petri dishes (small).
5. 100 × 15 mm sterile petri dishes (large).
6. Alkaline hypochlorite treatment: bleach, NaOH, H_2O.
7. M9: 30 g/L KH_2PO_4, 60 g/L Na_2HPO_4, 50 g NaCl, 1 mM $MgSO_4$.
8. Rotating mixer with rotisseries that fit 15 mL conical tubes.

2.2 Fertility and Mated Reproductive Assays

1. Stereomicroscope.
2. 70% ethanol.
3. Bunsen burner.
4. Worm pick (platinum wire).
5. Mating plates: 60 × 15 mm sterile petri dishes containing NGM and 10 μL OP50 spot seeded.

2.3 Sperm Morphology, Size, and Activation Assays

1. Stereomicroscope (for dissection).
2. Compound microscope with 100× objectives and DIC filter (for imaging).
3. 70% ethanol in H_2O (v/v).
4. Bunsen burner.
5. Worm pick (platinum wire).
6. 25 G needles or scalpel.
7. Unseeded plates: 60 × 15 mm sterile petri dishes containing just NGM (no OP50).
8. Microscope slide.
9. Grease pen.
10. Coverslips.
11. Vaseline.
12. 1 M HEPES (pH 7.8).
13. 5 M NaCl.
14. 2 M KCl.
15. 1 M $CaCl_2$.
16. 1 M $MgSO_4$.
17. pH meter.
18. Bovine serum albumin (BSA, Millipore Sigma) purified by heat shock fractionation. Store at 4 °C.
19. Sperm Medium Buffer (SM Buffer): 50 mM HEPES, 50 mM NaCl, 25 mM KCl, 5 mM $CaCl_2$, 1 mM $MgSO_4$, 1 mg/mL BSA, pH 7.8. Store at 4 °C.
20. Pronase (Millipore Sigma P8811). Lyophilized in powder form are typically stored at −20 °C.

21. SM Buffer + Pronase: SM Buffer with 200 μg/mL Pronase. Make fresh each time.
22. Plastic container that can be sealed.
23. Parafilm.
24. Paper towel.

2.4 DAPI Staining for Sperm Count

1. 10× phosphate buffered saline (PBS): In 500 mL of deionized water add 25.6 g $Na_2HPO_4 \cdot 7H_2O$, 80 g NaCl, 2 g KCl, and 2 g KH_2PO_4. Bring up to volume to 1 L with H_2O. Sterilize by autoclave.
2. 40% isopropanol in H_2O (v/v).
3. DAPI (4′,6-diamidino-2-phenylindole) staining solution (1 mg/mL stock).
4. Triton X-100.
5. Shaker/mixer for 1.5 mL tubes.
6. Centrifuge for 1.5 mL tubes.
7. Compound microscope with 40–63× objectives, DAPI and DIC filters, and camera for fluorescent image acquisition.
8. Microscope slide.
9. Coverslip.
10. Vectashield mounting medium.

3 Methods

C. elegans were cultured using standard techniques at 20 °C (*see* **Note 1**). Worm strains should adapt to diets for at least three generations without experiencing starvation prior to experiments. Age-matched hermaphrodites and males are used for all experiments.

3.1 Expanding a Single Population of Worms up for Assays (Prior to all Assays Below)

1. Mate 10 L4-stage hermaphrodites to 30 young adult males on small NGM plates with a small spot of OP50 seeded in center for 24 h.
2. On the next day, move mated hermaphrodites to a large seeded NGM plate and allow them to lay progeny for 1 day before removing them.

   Wait 5 days for F1 population with both males and hermaphrodites to become adults and have mated with each other (*see* **Note 2**).
3. Treat gravid adults with alkaline hypochlorite treatment to obtain eggs [16]. Allow eggs to hatch overnight in M9 buffer for synchronization (*see* **Note 3**).

4. On the next day, drop synchronized larval stage 1 (L1) larvae on a large seeded NGM plates (*see* **Note 4**).
5. Forty-eight hours later, L4-stage virgin hermaphrodites or males for each genotype or condition can be isolated for each of the assay below.

3.2 Fertility Assay

Make sure you have enough plates for moving hermaphrodites until the end of reproduction (egg laying ceases). This will require two moves per day (every 12 h) for 6 days.

1. Single 12 L4-stage hermaphrodites for each genotype/condition onto individual small seeded NGM plates.
2. Move individual hermaphrodite every 12 h until egg laying ceases. Average reproductive output over reproductive span of wild-type hermaphrodite fed standard OP50 (Fig. 1).
3. After moving each hermaphrodite to the next plate, score the previous plate or time point for number of unfertilized oocytes (*see* **Note 5**).
4. Twenty-four hours after moving the hermaphrodite to the next plate, count the original plate for number of unhatched or dead eggs.
5. Forty-eight hours after moving hermaphrodite to the next plate, count the original plate for number of progeny by picking off worms and burning them (*see* **Note 6**). Check plate again next day for any worms you might have missed.
6. Number of total oocytes can be calculated by summing up total progeny, unfertilized oocytes, and dead eggs. Average brood size of wild-type hermaphrodite (Fig. 2).

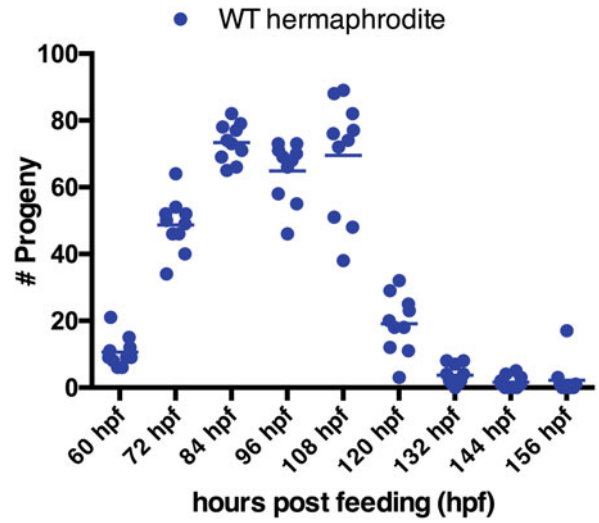

Fig. 1 Reproductive output time course for wild-type N2 hermaphrodites

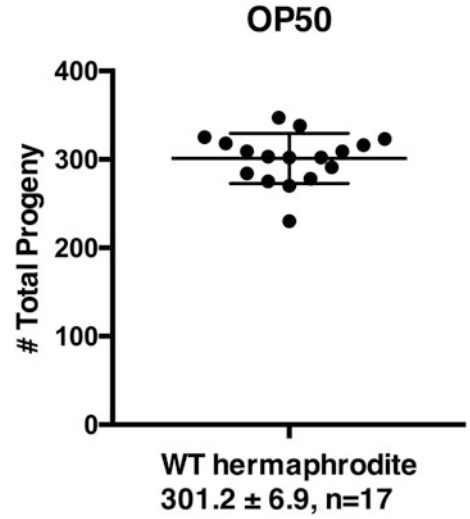

Fig. 2 Average brood size of wild-type N2 hermaphrodites

3.3 Mated Reproductive Assay

Make sure you have enough plates for moving hermaphrodites until the end of reproduction (egg laying ceases). This will be one move every 24 h for 9–10 days. Mating plates are made with NGM poured into small plates and seeded with 10 μL OP50 food spot in the center.

1. For just this experiment, a separate alkaline treatment of the plates containing gravid hermaphrodites and males need to be done a day earlier to have males that are day 1 adults for mating to L4-stage hermaphrodites that are from the other preparation (*see* **Note 7**).
2. The day prior to experiments, age-matched L4-stage virgin males from this separate treatment were moved to a small seeded NGM plate day without hermaphrodite (*see* **Note 8**).
3. Set up mating of 20 individual L4-stage hermaphrodite and young adult (or age of interest) male in a 1:1 ratio on NGM plate seeded with small 10 μL OP50 spot (*see* **Note 9**).
4. Move individual hermaphrodite every 24 h until egg laying ceases. Plot progeny number every 24 h to assess reproductive output over time.
5. Verify successful mating even by presence of male progeny on the plates (*see* **Note 10**). The progeny number from first two plates (48 h) may be excluded in order to account for difference in time when the hermaphrodite is mated.
6. After moving each hermaphrodite to the next plate, score the previous plate or time point for number of unfertilized oocytes (*see* **Note 5**).

7. Twenty-four hours after moving the hermaphrodite to the next plate, count the original plate for number of unhatched or dead eggs.
8. Forty-eight hours after moving hermaphrodite to the next plate, count the original plate for number of progeny by picking off worms and burning them (*see* **Note 6**). Check plate again next day for any worms you might have missed.
9. Number of total oocytes can be calculated by summing up the number of progeny, unfertilized oocytes, and dead eggs.

3.4 Sperm Morphology and Size

1. The day prior to experiments, put L4-stage virgin males onto a small seeded NGM plate day without hermaphrodite (need five worms for each replicate of an experimental condition) (*see* **Note 8**).
2. During the day of experiment, start by preparing slides for performing dissections. Using a grease pen, draw a small circle with its diameter about 1/3 the width of standard slide. This grease circle keeps the buffer and worms in place during dissection. Let the circle dry for at least 2 h (*see* **Note 11**).
3. Make SM buffer following recipe in materials and pH to 7.8. Filter-sterilize and store at 4 °C. Warm up to room temperature before use. Note that spermatids are sensitive to pH and temperature changes.
4. Move day 1 (or age of interest) adult males onto an unseeded plate. Allow worms to crawl on the plate to get rid of OP50 that are adhered to their body (*see* **Note 12**).
5. Pipette 35 μL of SM Buffer into the middle of grease circle on prepared slide.
6. Using a worm pick without any food, pick up one male at a time and move it into the drop of SM Buffer inside grease circle. Do this for five males.
7. Dissect males near the tail end (where the seminal vesicle is located) using sterile 25 G needles or scalpel to release spermatids (*see* **Note 13**).
8. Put Vaseline along the edges of a coverslip and place coverslip down gently (the side with Vaseline) to cover the area with grease circle. Image spermatids at 100× on a compound microscope with DIC filter for morphology and size (Fig. 3).

3.5 Sperm Activation

1. The day prior to experiments, put L4-stage virgin males onto a small seeded NGM plate day without hermaphrodite (need five worms for each replicate of an experimental condition) (*see* **Note 8**).
2. During the day of experiment, start by preparing slides for performing dissections. Using a grease pen, draw a small circle with its diameter about 1/3 the width of standard slide. This

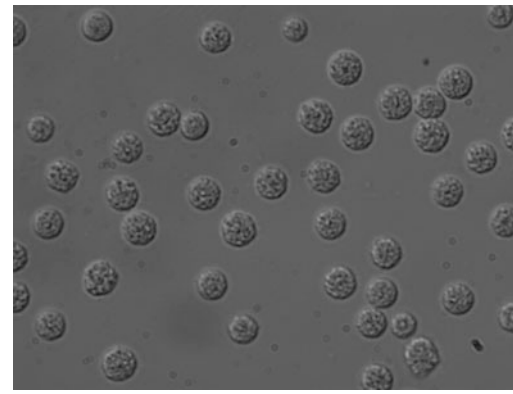

Fig. 3 Spermatids released from dissected wild-type N2 males

grease circle keeps the buffer and worms in place during dissection. Let the circle dry for at least 2 h (*see* **Note 11**).

3. Make SM buffer as in **step 3** of Subheading 3.4 (*see* **Note 14**). Pronase is a mixture of several nonspecific endo- and exoproteases that triggers the differentiation of round immobile spermatids into mobile spermatozoa in a process called spermiogenesis. Dissolve Pronase to a final concentration of 10 mg/mL in water. Dilute to 200 μg/mL in SM Buffer prior to experiment (*see* **Note 15**).
4. Make a humid chamber by placing a wet paper towel on the bottom of plastic container. Layer a piece of Parafilm on top of paper towel and close lid to retain moisture (*see* **Note 16**).
5. Move day 1 (or age of interest) adult males onto an unseeded plate. Allow worms to crawl on the plate to get rid of OP50 that are adhered to their body (*see* **Note 12**).
6. Pipette 35 μL of SM Buffer + Pronase into the middle of grease circle on prepared slide.
7. Using a worm pick without any food, pick up one male at a time and move it into the drop of SM Buffer inside grease circle. Do this for five males.
8. Dissect males near the tail end (where the seminal vesicle is located) using sterile 25 G needles or scalpel to release spermatids (*see* **Note 17**).
9. Add 25 μL more SM Buffer + Pronase onto slide (*see* **Note 18**) and incubate slide in the humid chamber assembled earlier in **step 4** for 30 min at room temperature.
10. Put Vaseline along the edges of a coverslip and place coverslip down gently (the side with Vaseline) to cover the area with grease circle. Image spermatids at 100× on a compound microscope with DIC filter. Take two images for each field:

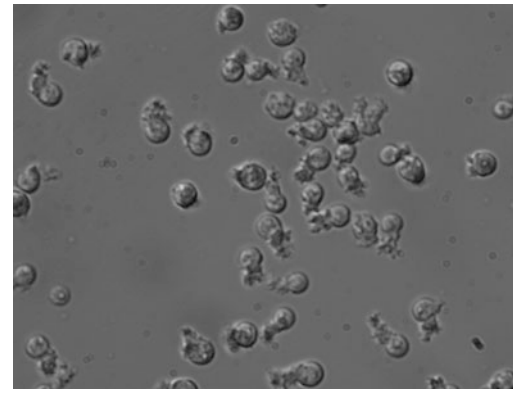

Fig. 4 Pseudopods are visible in Pronase-activated spermatozoa released from dissected wild-type N2 males

one focal plane in focus and the other a little higher (*see* **Note 19**). Differentiation of spermatids into spermatozoa upon Pronase treatment (Fig. 4).

3.6 Sperm Number

1. Make 1× PBST—Dilute to 10× PBS to 1× and add in Triton X-100 to final conc. of 0.01% (*see* **Note 20**).
2. The day prior to experiments, put about 30–40 L4-stage virgin males onto a small seeded NGM plate day without hermaphrodite (*see* **Note 8**). Need at least 10 for each sample/condition.
3. The day of experiment, wash day 1 (or age of interest) adult males into a 1.5 mL tube with 1×PBST.
4. Spin down at 560 × *g* for 1 min and remove supernatant to 100 μL mark on the tube.
5. Wash 1–3× with 1 mL 1×PBST (*see* **Note 21**).
6. Spin down at 560 × *g* for 1 min and remove supernatant to 100 μL mark on the tube.
7. Add in 600 μL of 40% isopropanol and incubate on shaker for 3 min to fix worms.
8. Spin down at 560 × *g* for 1 min and remove supernatant to 100 μL mark on the tube.
9. DAPI binds to DNA and allows visualization of nuclei in cells (*see* **Note 22**). Make DAPIstaining solution: Dilute 1 mg/mL DAPI stock solution to 10 μg/mL in 40% isopropanol.
10. Add in 600 μL of DAPIstaining solution and incubate in the dark for 2 h.
11. Remove supernatant to 100 μL mark.
12. Add in 600 μL of 1×PBST and incubate for 30 min in the dark to remove excess dye.
13. Mount samples on slide with Vectashield mounting medium.

14. Gently cover with coverslip and seal with nail polish.
15. Image at 40–63× with DIC and DAPI filter. Make sure you image all the spermatids in each animal (*see* **Note 23**).

4 Notes

1. NGM plates are made and seeded using standard techniques [17].
2. F1 population should be roughly 50% males due to mating.
3. Incubate at least 12 h to allow all animals to hatch. Do not exceed 24 h.
4. Drop synchronized L1 stage animals directly onto food to allow animals to resume development at the same rate. Animals dropped on side of food will be asynchronous.
5. Unfertilized oocytes are brown colored and circular. Eggs are shelled and oval.
6. Waiting 2 days allow progeny to develop to a size that is easy to be spotted and picked off for counting.
7. Young adult virgin males are needed to mate readily to L4-stage hermaphrodites as they molt into adults.
8. Allow hermaphrodites to crawl on OP50 lawn for 5–10 min and burn them off prior to moving males onto the plates. The scent of hermaphrodite encourages males to stay on OP50 lawn instead of crawling onto the side of plates and dying from dehydration.
9. Small area of food keeps worm in a small area to maximize chance of mating.
10. Male progeny usually can be spotted in the first two plates (first 48 h). For those plates with no male progeny, censor animals as not mated.
11. Can speed this up by drying slides in a fume hood. 2 h is the minimum time required for grease circle to dry completely. You can do this the day before experiment.
12. Prod worms gently or move to another unseeded plate as needed. Too much bacteria can cause sperm cells to lyse.
13. Dip needle or scalpel in 70% ethanol and flame needle/scalpel between each sample to sterilize. Allow to cool before use.
14. 10 mM dextrose can be used in place of BSA in SM Buffer. In our hands, sperm activation by Pronase does not work as well with dextrose supplemented SM Buffer compared to BSA.
15. Dissolve Pronase in solution fresh each time. Do not reuse the solution. For example of dilution in SM Buffer: 20 μL of 10 mg/mL Pronase should be added to 980 μL of SM Buffer.

The low volume of water added to SM Buffer is negligible in altering the concentration of contents of SM Buffer. If concerned, dilute 10 mg/mL stock Pronase in SM Buffer.

16. A sealed container with wet paper towel on the bottom and a Parafilm separating slide from paper towel is used for humid chamber.
17. Dip needle or scalpel in 70% ethanol and flame needle/scalpel between each sample to sterilize. Allow to cool before use.
18. This helps with evaporation of liquid and the sensitivity of spermatids to these changes. Evaporation makes spermatids appear irregular in shape instead of circular.
19. This helps with identifying activated versus nonactivated spermatids since pseudopods can be hard to see at only one plane field.
20. Spermatids are sensitive to pH levels. HEPES is used because of its buffering property.
21. Wash 1–2 more time depending on how cloudy the tubes look. Careful to not remove worms accidentally when taking out supernatant from washes.
22. DAPI is a blue fluorescent dye that binds to AT regions of DNA and is readily excited by violet (405 nm) laser line.
23. Spermatids have compact nuclei that are distinguishable from earlier stages of spermatogenesis.

Acknowledgments

This work was funded by the NIH R01GM109028 and R01AG058610 to S.P.C. and the American Federation of Aging Research (C.-A.Y. and S.P.C.).

References

1. Kirkwood TB (2002) Evolution of ageing. Mech Ageing Dev 123(7):737–745. https://doi.org/10.1016/s0047-6374(01)00419-5
2. Lynn DA, Dalton HM, Sowa JN, Wang MC, Soukas AA, Curran SP (2015) Omega-3 and -6 fatty acids allocate somatic and germline lipids to ensure fitness during nutrient and oxidative stress in Caenorhabditis elegans. Proc Natl Acad Sci U S A 112(50):15378–15383. https://doi.org/10.1073/pnas.1514012112
3. Khanna A, Johnson DL, Curran SP (2014) Physiological roles for mafr-1 in reproduction and lipid homeostasis. Cell Rep 9 (6):2180–2191. https://doi.org/10.1016/j.celrep.2014.11.035
4. Paek J, Lo JY, Narasimhan SD, Nguyen TN, Glover-Cutter K, Robida-Stubbs S, Suzuki T, Yamamoto M, Blackwell TK, Curran SP (2012) Mitochondrial SKN-1/Nrf mediates a conserved starvation response. Cell Metab 16 (4):526–537. https://doi.org/10.1016/j.cmet.2012.09.007
5. Pang S, Curran SP (2014) Adaptive capacity to bacterial diet modulates aging in C. elegans. Cell Metab 19(2):221–231. https://doi.org/10.1016/j.cmet.2013.12.005
6. Pang S, Lynn DA, Lo JY, Paek J, Curran SP (2014) SKN-1 and Nrf2 couples proline catabolism with lipid metabolism during nutrient

deprivation. Nat Commun 5:5048. https://doi.org/10.1038/ncomms6048

7. Nhan JD, Turner CD, Anderson SM, Yen CA, Dalton HM, Cheesman HK, Ruter DL, Uma Naresh N, Haynes CM, Soukas AA, Pukkila-Worley R, Curran SP (2019) Redirection of SKN-1 abates the negative metabolic outcomes of a perceived pathogen infection. Proc Natl Acad Sci U S A 116(44):22322–22330. https://doi.org/10.1073/pnas.1909666116
8. Kadandale P, Singson A (2004) Oocyte production and sperm utilization patterns in semi-fertile strains of Caenorhabditis elegans. BMC Dev Biol 4:3. https://doi.org/10.1186/1471-213X-4-3
9. Luo S, Kleemann GA, Ashraf JM, Shaw WM, Murphy CT (2010) TGF-beta and insulin signaling regulate reproductive aging via oocyte and germline quality maintenance. Cell 143 (2):299–312. https://doi.org/10.1016/j.cell.2010.09.013
10. Sharma R, Agarwal A, Rohra VK, Assidi M, Abu-Elmagd M, Turki RF (2015) Effects of increased paternal age on sperm quality, reproductive outcome and associated epigenetic risks to offspring. Reprod Biol Endocrinol 13:35. https://doi.org/10.1186/s12958-015-0028-x
11. Ward S, Carrel JS (1979) Fertilization and sperm competition in the nematode Caenorhabditis elegans. Dev Biol 73(2):304–321
12. LaMunyon CW, Ward S (1995) Sperm precedence in a hermaphroditic nematode (Caenorhabditis elegans) is due to competitive superiority of male sperm. Experientia 51 (8):817–823
13. LaMunyon CW, Ward S (1998) Larger sperm outcompete smaller sperm in the nematode Caenorhabditis elegans. Proc Biol Sci 265 (1409):1997–2002. https://doi.org/10.1098/rspb.1998.0531
14. Nelson GA, Ward S (1980) Vesicle fusion, pseudopod extension and amoeboid motility are induced in nematode spermatids by the ionophore monensin. Cell 19(2):457–464. https://doi.org/10.1016/0092-8674(80)90520-6
15. Shakes DC, Ward S (1989) Initiation of spermiogenesis in C. elegans: a pharmacological and genetic analysis. Dev Biol 134(1): 189–200
16. Porta-de-la-Riva M, Fontrodona L, Villanueva A, Ceron J (2012) Basic Caenorhabditis elegans methods: synchronization and observation. J Vis Exp (64):e4019. https://doi.org/10.3791/4019
17. Brenner S (1974) The genetics of Caenorhabditis elegans. Genetics 77(1):71–94
18. Yen C-A, Ruter DL, Turner CD, Pang S, Curran SP (2020) Loss of flavin adenine dinucleotide (FAD) impairs sperm function and male reproductive advantage in C. elegans. eLife 9

Chapter 9

Metabolic Assessment of Lipid Abundance and Distribution

James D. Nhan and Sean P. Curran

Abstract

Lipids are an essential macromolecule used for diverse functions including use for structural components of membranes, energy storage, and signaling molecules. The regulation of cellular lipid stores is critical for maintaining organismal metabolic homeostasis. Lipid homeostasis can decline with age, which can lead to poor health outcomes and accelerate the progression of disease states. *C. elegans* represents an excellent model to study age-related decline in lipid homeostasis due to its short lifespan and remarkably well-conserved metabolic pathways. Due to their ease of use and similarities, there have been numerous developments in methodologies to study intracellular lipid abundance and tissue distribution in *C. elegans*.

Key words Lipids, *C. elegans*, Fat, Distribution, Abundance, Nile red, Oil red O, Germline, Intestine, Aging

1 Introduction

As an organism ages, there comes a decline in many cellular process, one of which includes lipid homeostasis [1–4]. With a short lifespan of about 2 weeks, *C.elegans* have become a popular model organism to study age-related decline in lipid metabolism [5]. Because of its popularity, many techniques have been developed to study the lipid content of worms, such as high-performance liquid chromatography–mass spectrophotometry and gas chromatography–mass spectrophotometry, which allows for the analyzation of specific lipid species [6, 7]. Although these methods are useful for determining the complexity of the lipid extract, they require expensive machinery that may not be readily available. The transparency of *C. elegans* makes them amenable to visual measures of lipids via staining with lipophilic dyes [4, 7–15]. Here we describe two inexpensive and rapid methods for visualizing the amount and tissue distribution of intracellular lipids in fixed animal samples.

Nile red, 9-diethylamino-5H-benzo[α]phenoxazine-5-one, is a lipophilic dye that can be used to stain intracellular neutral lipid droplets [16]. Lipids that are stained with Nile red emit green light

Sean P. Curran (ed.), *Aging: Methods and Protocols*, Methods in Molecular Biology, vol. 2144,
https://doi.org/10.1007/978-1-0716-0592-9_9,

following excitation, allowing for the quantification of lipid abundance. Oil Red O (ORO) is a fat-soluble dye that can be used to stain neutral lipids a bright red color [17]. Due to the transparent body of the worm, the lipids stained with ORO can be easily visualized, allowing for qualitative assessment of lipid droplet size and distribution across different tissues [4]. Using these two dyes allows for the determination of changes to the amount and distribution of lipids across the lifespan, following environmental perturbation, or between genetic mutants.

2 Materials

Prepare all solutions using ultrapure water (prepared by purifying deionized water, to attain a sensitivity of 18 MΩ-cm at 25 °C). Prepare and store all reagents at room temperature (unless indicated otherwise). Filter-sterilize with 0.22 μM filter or autoclave to sterilize (as indicated).

1. Stock Nile Red (5 mg/mL) dissolved in 100% acetone (*see* **Note 1**).
2. Stock Oil Red O (5 mg/mL) dissolved in 100% isopropanol (*see* **Note 2**).
3. Isopropanol (100%, 60%, and 40%).
4. Phosphate Buffered Saline Triton (PBST): 137 mM NaCl, 10 mM phosphate, 2.7 mM KCl, pH 7.4, 0.01% Triton X-100.
5. Autoclaved water.
6. 10 mL syringe
7. 0.2 μm cellulose acetate sterile syringe filter.
8. DAPI (2-(4-amidinophenyl)-1H-indole-6-carboxamidine).
9. 1.5 mL microcentrifuge tubes.
10. Pipettes (1 mL and 10 μL).
11. Microcentrifuge.
12. Stir plate.
13. Magnetic stir bars.
14. Rocker/Nutator for Eppendorf tubes.
15. Microscope slide—75 × 25 × 1 mm.
16. Coverslip—22 × 22 mm.
17. Clear nail polish.
18. Compound microscope with brightfield/DIC, FITC, and DAPI filter sets, 10×, 20×, and 64× objectives.
19. Camera for fluorescent image acquisition when using Nile red staining.
20. Color capable camera when using Oil red O staining.

3 Methods

3.1 Nile Red Staining

3.1.1 Preparing Stock Dyes for Staining

1. Working solution of Nile Red (NR) should always be prepared the day of staining.
2. Prepare working solution by adding 6 μL of NR stock solution to 1 mL of 40% isopropanol for every sample to be stained.
3. For every 1 mL of NR working solution add 1 μL of DAPI to counterstain nuclei as an assessment of permeability and dye accessibility.

3.1.2 Staining Worms with Nile Red

1. Collect worms from plate by adding 1 mL of PBST and swirl until all worms are dislodged off the media. Tilt the plate so that all the worms collect on the edge and rinse the plate with an additional 1 mL of PBST. Transfer the worms to a microcentrifuge tube.
2. Allow worms to settle by gravity.
3. Remove the supernatant with a pipette until just above the pellet of the worms without disturbing the pellet. Add 1 mL fresh PBST to wash.
4. Repeat **steps 2–3** three more times (*see* **Note 3**).
5. Following the final wash, remove the supernatant until 100 μL remains.
6. Add 600 μL of 60% isopropanol to the tube to fix and permeabilize the worms and gently rock on nutator for 3 min at room temperature.
7. Following permeabilization, centrifuge sample for 30 s at 50 × *g*.
8. Remove the supernatant until 100 μL is left.
9. Add 600 μL of NR working solution to the samples.
10. Incubate samples at room temperature in the dark for 2 h.
11. Following the 2-h incubation, spin down samples for 30 s at 50 × *g*.
12. Remove supernatant until 100 μL is left and destain by adding 600 μL of PBST and incubating in the dark for 30 min.

3.1.3 Imaging and Quantification of Lipids Stained with Nile Red

1. Worms stained with Nile red should be imaged the day of staining.
2. After destaining (Subheading 3.1.2, **step 12**), allow worms to settle by gravity and remove the supernatant down to 100 μL.
3. Resuspend the stained worms in this reduced volume by gentle agitation.
4. Remove 10 μL of the sample onto a microscope slide (*see* **Note 4**).

5. Carefully place a coverslip over the sample to ensure no air bubbles form, and seal with clear nail polish (*see***Note 5**).
6. Image worms on the microscope using a camera capable of fluorescent image acquisition at 10× magnification in order for better quantification of individual worms. Use bright-field/DIC transmitted light to visualize the entire region being imaged, the FITC filter set to visualize lipids from NR staining, and a DAPI filter set to visualize the nucleus from the DAPI staining (*see* **Note 6**).
7. Autoexpose worms to determine the best exposure times but keep the same exposure settings across all samples.
8. To quantify intensity of fluorescence, open the image in ImageJ. Use the polygon tool to outline the shape of the worm from the DIC image and use the measure function under the analysis tab on the green fluorescence image to determine the integrated density (ID) of the lipids. (Fig. 1a–d).
9. Take a measurement of the background to determine the mean ID of the background.
10. To calculate the intensity of the lipids, take the ID of the worm image and subtract from the area of the worm multiplied by the mean background ID to get the CTCF value, and divide by the area of the worm image to get CTCF/area (*see* **Note 7**).

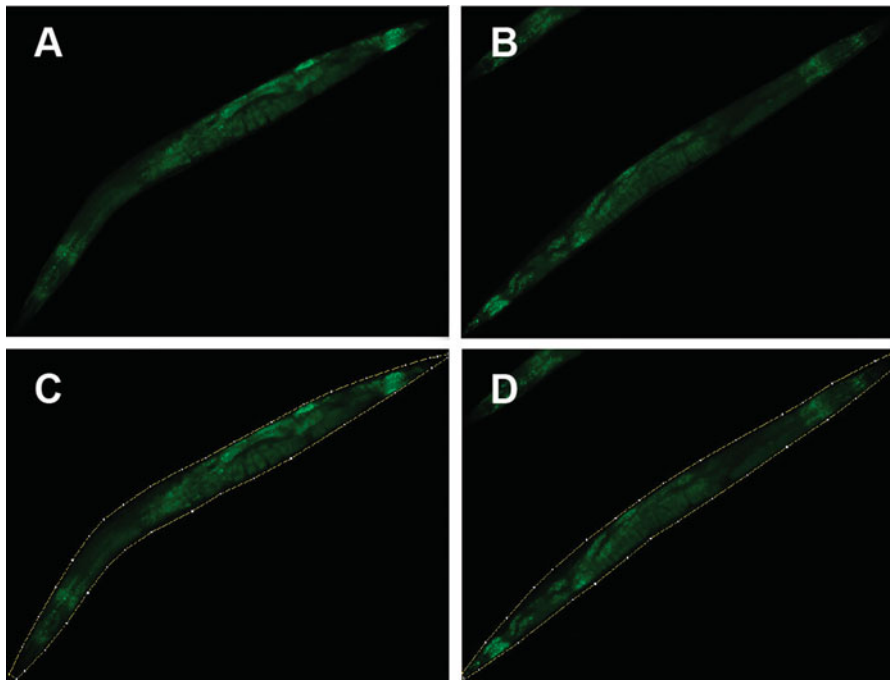

Fig. 1 Images of Nile red stained worm with high (**a**) or low (**b**) fluorescent intensity. (**c**, **d**) Example of worms outlined using the polygon tool on ImageJ

3.2 Oil Red O Staining

3.2.1 Preparing ORO Stock Dyes for Staining

1. Prepare a working solution of ORO by diluting three parts of the ORO stock solution with two parts of autoclaved water (3:2 ratio). 1 mL of working solution should be prepared for every sample being stained (*see***Notes 8** and **9**).
2. Fill a 10 mL syringe with working solution of ORO and pass through a 0.2 μm syringe filter (*see* **Note 10**).

3.2.2 Staining Worms with ORO

1. Collect worms from plate by adding 1 mL of PBST and swirl until all worms are dislodged off the media. Tilt the plate so all the worms collect on the edge and rinse the plate with an additional 1 mL of PBST. Transfer the worms to a microcentrifuge tube.
2. Allow worms to settle by gravity.
3. Remove the supernatant with a pipette until just above the pellet of the worms without disturbing the pellet. Add 1 mL fresh PBST to wash.
4. Repeat **steps 2–3** three more times (*see* **Note 3**).
5. Following the final wash, remove the supernatant until 100 μL remains.
6. Add 600 μL of 60% isopropanol to the tube to fix and permeabilize the worms and gently rock on nutator for 3 min at room temperature.
7. Following permeabilization, centrifuge the worms for 30 s at 50 × *g*.
8. Remove the supernatant until 100 μL is left.
9. Add 600 μL of ORO working solution to the samples.
10. Place samples on a rotator and incubate for 2 h at room temperature.
11. Following the 2-h incubation, spin down samples for 30 s at 50 × *g*.
12. Remove supernatant until 100 μL is left and add 600 μL of PBST and place back on rotator for 30 min to destain.

3.2.3 Imaging ORO Stained Worms

1. Worms stained with ORO can be stored at 4 °C, up to 24 h following staining before being used for imaging, but all samples should be stored for the same amount of time.
2. Remove the supernatant down to 100 μL, resuspend the stained worms, and drop 10 μL of the sample onto a microscope slide (*see* **Note 4**).
3. Carefully place a coverslip over the sample to ensure no air bubbles form, and seal with clear nail polish (*see* **Note 5**).

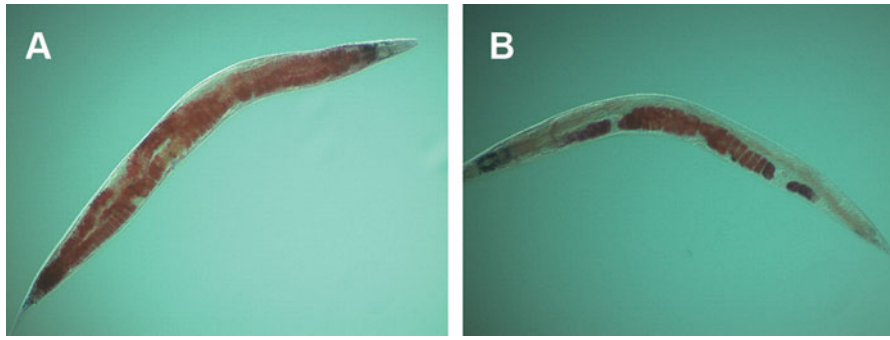

Fig. 2 (**a**) Image of an ORO-stained adult worm with normal distribution of lipids throughout the intestine and germline. (**b**) Image of an ORO-stained adult worm with lipid dysregulation resulting in depleted intestinal lipids (devoid of stain) but intact germline lipid pools

4. Image samples using the microscope with a color capable camera at 10× magnification for best resolution for whole worm imaging and qualitative assessment of lipid distribution (Fig. 2).

4 Notes

1. Dissolve Nile red powder in 100% acetone to achieve a concentration of 5 mg/mL and stir overnight. Nile red stock solution is light sensitive, so it should be kept in the dark at all time. Wrap a bottle with aluminum foil to block out all light. The stock solution can be kept for several months in the dark.
2. Dissolve Oil red O powder in 100% isopropanol to achieve a stock solution concentration of 5 mg/mL and let stir overnight to ensure it properly dissolves. Stock solution can be kept in the dark for several months.
3. The wash step removes any bacteria that may have been washed off from the plate. Worms are allowed to gravity settle in order to separate parents from any progeny that may have been on the plate.
4. Following staining the worms become rigid and may be difficult to pipette with a normal tip. Making a wider opening by using a pair of scissors to cut off a section of the pipette tip allows for easier pipetting of the sample.
5. Nail polish is used to prevent evaporation of liquid. Worms close to the edge of the coverslip may be exposed to the nail polish and affect results, and should be excluded.
6. DAPIstaining is used to assess the location of cells by staining the nucleus but can also be used to determine the permeability of the staining.

7. Equation to determine CTCF/area value of Nile red stained worms
   (Worm_ID-(Background_Mean_ID ∗ Worm_area))/ Worm_area.
8. For example, if five samples are to be stained, dilute 3 mL of stock ORO with 2 mL autoclaved water.
9. Working solution of ORO should be prepared preferably overnight but can be made up to 2 h before staining. After diluting the stock ORO, the working stock should rotate until it is ready to use.
10. Filtering the working stock of ORO removes any debris that may have formed during the rotation. The solution should only be filtered right before use.

Acknowledgments

This work was supported by NIH grants R01GM109028 (S.P.C.) and R01AG058610 (S.P.C.) and T32AG000037 (J.D.N.).

References

1. Zhao YY, Miao H, Cheng XL, Wei F (2015) Lipidomics: novel insight into the biochemical mechanism of lipid metabolism and dysregulation-associated disease. Chem Biol Interact 240:220–238. https://doi.org/10.1016/j.cbi.2015.09.005
2. Johnson AA, Stolzing A (2019) The role of lipid metabolism in aging, lifespan regulation, and age-related disease. Aging Cell 18:e13048. https://doi.org/10.1111/acel.13048
3. Toth MJ, Tchernof A (2000) Lipid metabolism in the elderly. Eur J Clin Nutr 54(Suppl 3): S121–S125
4. Lynn DA, Dalton HM, Sowa JN, Wang MC, Soukas AA, Curran SP (2015) Omega-3 and -6 fatty acids allocate somatic and germline lipids to ensure fitness during nutrient and oxidative stress in Caenorhabditis elegans. Proc Natl Acad Sci U S A 112(50):15378–15383. https://doi.org/10.1073/pnas.1514012112
5. Zhang Y, Zou X, Ding Y, Wang H, Wu X, Liang B (2013) Comparative genomics and functional study of lipid metabolic genes in Caenorhabditis elegans. BMC Genomics 14:164. https://doi.org/10.1186/1471-2164-14-164
6. Castro C, Sar F, Shaw WR, Mishima M, Miska EA, Griffin JL (2012) A metabolomic strategy defines the regulation of lipid content and global metabolism by Delta9 desaturases in Caenorhabditis elegans. BMC Genomics 13:36. https://doi.org/10.1186/1471-2164-13-36
7. Pino EC, Webster CM, Carr CE, Soukas AA (2013) Biochemical and high throughput microscopic assessment of fat mass in Caenorhabditis elegans. J Vis Exp (73). https://doi.org/10.3791/50180
8. Pang S, Curran SP (2014) Adaptive capacity to bacterial diet modulates aging in C. elegans. Cell Metab 19(2):221–231. https://doi.org/10.1016/j.cmet.2013.12.005
9. Pang S, Lynn DA, Lo JY, Paek J, Curran SP (2014) SKN-1 and Nrf2 couples proline catabolism with lipid metabolism during nutrient deprivation. Nat Commun 5:5048. https://doi.org/10.1038/ncomms6048
10. Khanna A, Johnson DL, Curran SP (2014) Physiological roles for mafr-1 in reproduction and lipid homeostasis. Cell Rep 9 (6):2180–2191. https://doi.org/10.1016/j.celrep.2014.11.035
11. Pradhan A, Hammerquist AM, Khanna A, Curran SP (2017) The C-box region of MAF1 regulates transcriptional activity and protein stability. J Mol Biol 429(2):192–207. https://doi.org/10.1016/j.jmb.2016.12.012
12. Nhan JD, Turner CD, Anderson SM, Yen CA, Dalton HM, Cheesman HK, Ruter DL, Uma Naresh N, Haynes CM, Soukas AA, Pukkila-

Worley R, Curran SP (2019) Redirection of SKN-1 abates the negative metabolic outcomes of a perceived pathogen infection. Proc Natl Acad Sci U S A 116(44):22322–22330. https://doi.org/10.1073/pnas.1909666116

13. Escorcia W, Ruter DL, Nhan J, Curran SP (2018) Quantification of lipid abundance and evaluation of lipid distribution in Caenorhabditis elegans by Nile red and oil red O staining. J Vis Exp (133). https://doi.org/10.3791/57352
14. Soukas AA, Kane EA, Carr CE, Melo JA, Ruvkun G (2009) Rictor/TORC2 regulates fat metabolism, feeding, growth, and life span in Caenorhabditis elegans. Genes Dev 23 (4):496–511. https://doi.org/10.1101/gad.1775409
15. Webster CM, Pino EC, Carr CE, Wu L, Zhou B, Cedillo L, Kacergis MC, Curran SP, Soukas AA (2017) Genome-wide RNAi screen for fat regulatory genes in C. elegans identifies a proteostasis-AMPK axis critical for starvation survival. Cell Rep 20(3):627–640. https://doi.org/10.1016/j.celrep.2017.06.068
16. Greenspan P, Mayer EP, Fowler SD (1985) Nile red: a selective fluorescent stain for intracellular lipid droplets. J Cell Biol 100 (3):965–973. https://doi.org/10.1083/jcb.100.3.965
17. O'Rourke EJ, Soukas AA, Carr CE, Ruvkun G (2009) C. elegans major fats are stored in vesicles distinct from lysosome-related organelles. Cell Metab 10(5):430–435. https://doi.org/10.1016/j.cmet.2009.10.002

Chapter 10

Quantitative Profiling of Lipid Species in *Caenorhabditis elegans* with Gas Chromatography–Mass Spectrometry

Elizabeth C. Pino and Alexander A. Soukas

Abstract

Gas chromatography–mass spectrometry (GC-MS) enables sensitive detection and relative quantification of fatty acids. In *Caenorhabditis elegans*, the use of GC-MS can corroborate findings from common staining methodologies, providing great resolution on the lipid species altered in abundance in aging, genetic mutants, or with dietary or pharmacologic manipulation. Here we describe a method to quantitate relative abundance of fatty acids in total worm lipid extracts, as well as a method that quantitates fatty acids following separation into neutral lipid pools (triacylglycerols and cholesteryl esters) versus more polar lipids (phospholipids) by solid-phase extraction (SPE).

Key words *C. elegans*, Aging, Fatty acids, Lipids, Fat, Triglycerides, Phospholipids, Gas chromatography–mass spectrometry, Solid-phase chromatography

1 Introduction

Lipid homeostasis plays important roles in the aging process and in susceptibility to aging-related diseases [1–6]. In the round worm *C. elegans*, a facile organism for genetic studies of aging, various methods have been used to indicate lipid stores. The use of vital dyes to indicate lipid stores in the worm [7] proved to be confounded by the fact that these dyes undergo sequestration in acidified compartments in the worm, acting as indicators of lysosome-related organelles rather than lipid droplets [6, 8–11]. Alternatively, fixative-based lipid staining and the use of transgenic worms carrying lipid droplet-GFP reporters have proven to be more reliable indicators of lipid storage in *C. elegans*, but is limited in the resolution of exactly which lipid species are being studied [9, 12–15]. Label-free methods such as coherent anti-Stokes Raman scattering and stimulated Raman scattering type microscopy can provide information on lipid amount, localization, as well as the degree of lipid desaturation [12, 15, 16], but ultimately do not provide high resolution on the precise lipid species present.

Sean P. Curran (ed.), *Aging: Methods and Protocols*, Methods in Molecular Biology, vol. 2144,
https://doi.org/10.1007/978-1-0716-0592-9_10,

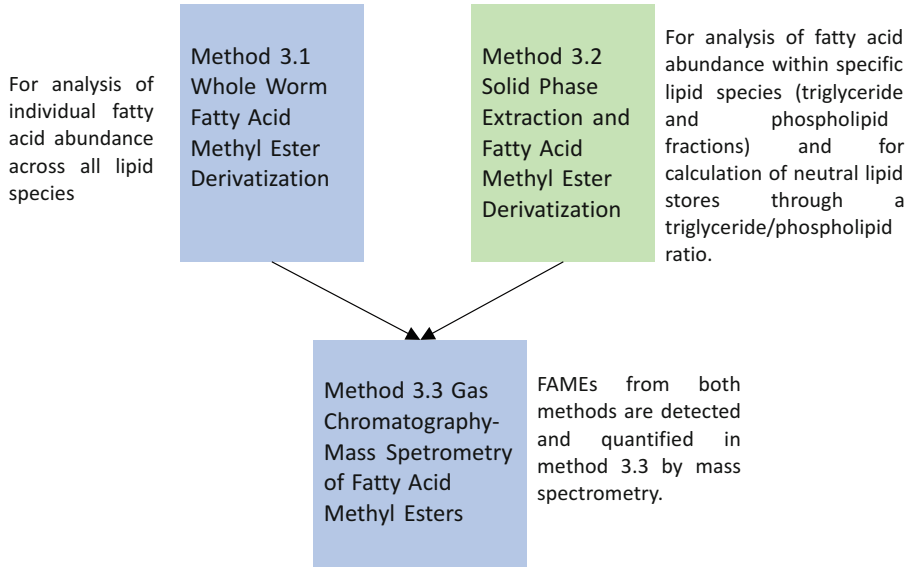

Fig. 1 The choice of method depends upon whether the investigator would like to determine the percentage of specific fatty acids within the whole organism (Subheading 3.1), or whether the quantification of fatty acids within specific lipid species or for calculation of a triglyceride–phospholipid ratio, which can be used to corroborate changes seen by neutral lipid staining (Subheading 3.2). In either case, fatty acid methyl esters derived as the final product of both protocols are quantitatively analyzed in Subheading 3.3 on the gas chromatograph-mass spectrometer (GC-MS)

As such, quantitative lipid biochemistry remains the gold standard in the *C. elegans* aging and metabolism fields [6, 9, 17, 18], and an important supportive corollary to studies completed with fixative-based stains or label-free methods. While more laborious than staining for lipid mass or the use of enzymatic assays for triglycerides [2, 19], GC-MS based methods can provide precise quantification of individual fatty acid species present in either whole worm extracts [20, 21] or in individual lipid species such as triacylglycerols and phospholipids separated by chromatographic methods [6, 9, 22] (Fig. 1). Study of individual fatty acids present in either whole-worm lipid extracts or chromatographically separated lipid species requires subsequent fatty acid methyl ester (FAME) derivatization. FAMEs transition to the gas phase upon heating, where upon they are separated by gas chromatography and subsequently detected on a GC-coupled mass spectrometer.

Uses of whole worm GC-MS include determination of precise lipid alterations due to genetic, dietary, or pharmacologic manipulation (e.g., fatty acid dietary supplementation). Alternatively, separation of lipid species into neutral lipid pools and polar lipids by solid phase extraction followed by GC-MS has the advantage of being able to quantify the amount of fatty acid in triglycerides relative to membrane lipids, providing an indication of long term energy stores as triglycerides in the worm.

2 Materials

Prepare all solutions using ultrapure water (prepared by purifying deionized water, to attain a sensitivity of 18 MΩ-cm at 25 °C) and chromatography-grade reagents. Prepare and store all reagents at room temperature (unless indicated otherwise). Organic solvents are highly flammable and should be stored in a proper explosion-proof safety cabinet. All work with solvents should be done in a properly functioning fume hood and organic waste disposed of according to waste disposal regulations. All organics should be pipetted with borosilicate glass pipettes or borosilicate glass Pasteur pipettes.

2.1 Whole Worm Fatty Acid Methyl Ester Preparation

1. M9W buffer: 3 g KH_2PO_4, 6 g Na_2HPO_4, 5 g NaCl, H_2O to 1 L. Sterilize by autoclaving. Add 1 mL sterile 1 M $MgSO_4$ in sterile fashion after cooling to room temperature.
2. 10 mL Borosilicate glass centrifuge tubes with phenolic caps (*see* **Note 1**).
3. Borosilicate glass 5 and 10 mL serological pipettes.
4. Nine inch Pasteur pipettes, cotton plugged.
5. Fifty and two hundred microliter Wiretrol calibrated microcapillary pipettes.
6. 75% (v/v) Methanol: 25% (v/v) methylene chloride (3:1), made fresh in clean glassware rinsed beforehand with a few milliliters of methanol. Make sure solvents are of chromatography grade.
7. Fatty acid internal standard heptadecanoic acid, 1.1 mM in 75% methanol:25% methylene chloride, prepared in a borosilicate glass screw-cap tube with phenolic cap. The standard may be stored at −20 °C under nitrogen, wrapped in Parafilm for up to 1 year (*see* **Note 2**).
8. Acetyl chloride.
9. Acetonitrile, chromatography grade.
10. 7% potassium carbonate (K_2CO_3) in water, analytical grade.
11. Chromatography grade hexane.
12. Nitrogen gas with evaporator manifold.

2.2 Solid-Phase Extraction and Fatty Acid Methyl Ester Derivatization

1. M9W buffer: 3 g KH_2PO_4, 6 g Na_2HPO_4, 5 g NaCl, H_2O to 1 L. Sterilize by autoclaving. Add 1 mL sterile 1 M $MgSO_4$ in sterile fashion after cooling to room temperature.
2. 10 mL Borosilicate glass centrifuge tubes with phenolic caps (*see* **Note 1**).
3. Borosilicate glass 5 and 10 mL serological pipettes.
4. Nine-inch Pasteur pipettes, cotton plugged.

5. Fifty-microliter Wiretrol calibrated microcapillary pipettes.
6. Prepacked silica gel 60 columns, 100 mg resin size.
7. Chromatography grade chloroform, methanol, acetone, and hexane.
8. Chloroform (66%):methanol (33%), prepared by mixing two parts chloroform with one part methanol. Store in clean, methanol-rinsed amber glass bottles, or prepare immediately before use.
9. Acetone (90%):methanol (10%), prepared by mixing nine parts acetone with one part methanol. Store in clean, methanol-rinsed amber glass bottles or prepare immediately before use.
10. Sodium chloride solution, 0.9% (w/v), prepared by adding 9 g of analytical grade sodium chloride to 900 mL water, dissolving by stirring or shaking, bringing final volume to 1 L and sterilizing by autoclave on liquid cycle.
11. Phospholipid standard: 0.5 mM 1,2-diheptadecanoyl-s*n*-glycero-3-phosphocholine, prepared by dissolving 7.6 mg standard to 30 mL 66% chloroform: 33% methanol in clean, methanol-rinsed glassware (*see* **Note 2**).
12. Triglyceride standard: 0.33 mM tritridecanoin, prepared by dissolving 6.8 mg in 30 mL 66% chloroform: 33% methanol in clean, methanol-rinsed glassware.
13. Acidified methanol (2.5%), prepared by slowly adding one part concentrated hydrochloric acid (37%, analytical grade) to 39 parts chromatography grade methanol (*see* **Note 3**).
14. Rack or solid-phase extraction manifold for holding silica gel columns.
15. Nitrogen gas with evaporator manifold.

2.3 Gas Chromatography–Mass Spectrometry

1. GC-MS amber autosampler vials with glass inserts and caps with PTFE/red rubber septa.
2. Chromatography grade hexane.
3. Gas chromatograph-mass spectrometer (e.g., Agilent GCMS model 6890/5973N) outfitted with a Supelcowax-10 (24079) 30 m, 250 μm fused silica capillary column, equipped with ultrapure helium carrier gas.

3 Methods

3.1 Whole Worm Fatty Acid Methyl Ester Production

1. For each sample, wash 1000–3000 *C. elegans* L4 to adult worms three times in a 15 mL conical polypropylene tube (*see* **Note 4**).

2. On the final wash, leave worms in no more than 250 μL total volume. Transfer worms and the entire volume of M9 buffer to a 10 mL borosilicate glass tube with phenolic cap (*see* **Note 5**).
3. Add 1 mL 75% methanol:25% methylene chloride to each sample using a borosilicate glass pipette (reminder *see* **Note 1**).
4. Add 50 μL of the fatty acid internal standard heptadecanoic acid to each sample in the borosilicate glass tube using a 50 μL Wiretrol capillary pipette.
5. In the fume hood, while vortexing gently, add 200 μL acetyl chloride dropwise slowly to each sample in its borosilicate glass tube using a 200 μL Wiretrol capillary pipette. The acetyl chloride must be added slowly while vortexing to prevent the sample from boiling and popping. Expect the sample to get quite warm after acetyl chloride addition. Cap the sample and vortex well. Incubate in a 75 °C water bath for 1 h to generate FAMEs (*see* **Note 6**).
6. Remove samples from the water bath, and cool samples on the bench for 5 min.
7. Add 4 mL 7% potassium carbonate to each sample, recap, and vortex.
8. Add 2 mL chromatography grade hexane to each sample, recap, and vortex well for 1 min. Shake vigorously for 30 s, and repeat vortexing for 1 min. FAMEs will partition into the hexane at this point.
9. Centrifuge samples in a swing-bucket rotor for 5 min at 1000 × *g*.
10. Transfer the upper hexane layer to a new borosilicate tube with phenolic cap using a borosilicate glass Pasteur pipette, avoiding the interphase.
11. Add 2 mL of chromatography-grade acetonitrile to each sample, cap, and vortex vigorously. Centrifuge samples in a swing-bucket rotor for 5 min at 1000 × *g* to separate phases fully.
12. Transfer the upper hexane layer to a new borosilicate glass tube with a Pasteur pipette. Be absolutely certain no acetonitrile is carried over into the new tube.
13. Dry down the hexane using nitrogen gas evaporator manifold. Although it is possible to dry the sample to an approximate volume of 100–200 μL, it is more straightforward to evaporate it entirely and resuspend the FAMEs (which are often faintly visible as a cloudy film on the glass tube bottom) in 200 μL (100 μL may be used if sample size was very small). Transfer the entirety of the hexane to an autosampler tube with a glass insert, and cap tightly with a PTFE/red rubber septa cap. Proceed to Subheading 3.3. Samples may be stored at −80 °C at this point if desired.

3.2 Solid Phase Extraction and Fatty Acid Methyl Ester Derivatization

For validation of lipid levels based on Nile red fluorescence, gas chromatography followed by mass spectrometry analysis (GC-MS) can be performed on fatty acid methyl esters (FAME) derived from triglycerides and phospholipids from worm pellets. Steps involving organics should be performed under a fume hood. Care should be taken that lipids are kept under nitrogen protected from light during extended storage or incubation steps as they are very vulnerable to oxidation.

1. For each sample, wash 5000–10,000 *C. elegans* L4 to adult worms three times in a 15 mL conical polypropylene tube (*see* **Note 4**).
2. On the final wash, leave worms in no more than 250 μL total volume. Transfer worms and the entire volume of M9 buffer to a 10 mL borosilicate glass tube with phenolic cap (*see* **Notes 5** and **7**).
3. Add 1.5 mL of chloroform (66%):methanol (33%) to each sample using a borosilicate glass pipette (*see* **Note 1**).
4. Using Wiretrol capillary 50 μL pipettes, add 50 μL of phospholipid standard and 50 μL of triglyceride standard to each sample (*see* **Note 2**).
5. Cap the samples with phenolic caps and vortex each vigorously. Extract lipids for 1 h at room temperature, vortexing the sample every 15 min.
6. Centrifuge samples at 1000 × *g* for 5 min to separate phases. Transfer the lower organic phase without residual worm debris or carcasses to a new borosilicate glass tube.
7. Add 0.3 mL 0.9% NaCl to each sample, cap, and vortex vigorously. Centrifuge samples at 1000 × *g* for 5 min to separate phases.
8. Transfer the bottom, organic layer, which contains the extracted lipids, to a fresh borosilicate culture tube, making sure not to transfer over any of the aqueous phase. Dry the organic phase using nitrogen gas in an evaporator manifold.
9. Resuspend dried lipids in 1 mL chloroform (*see* **Note 8**).
10. Assemble silica gel solid-phase extraction (SPE) column on SPE manifold (Fig. 2). Preequilibrate one column for each lipid sample by adding 3 mL chloroform in 1 mL increments using a glass pipette, allowing the solvent to flow by gravity.
11. Load each lipid sample in chloroform onto its own SPE column using a glass pipette, collecting flow-through in a threaded borosilicate tube as part of the first, triglyceride fraction. Most neutral lipids will come through in this first 1 mL flow-through. Add an additional 3 mL chloroform, 1 mL at a

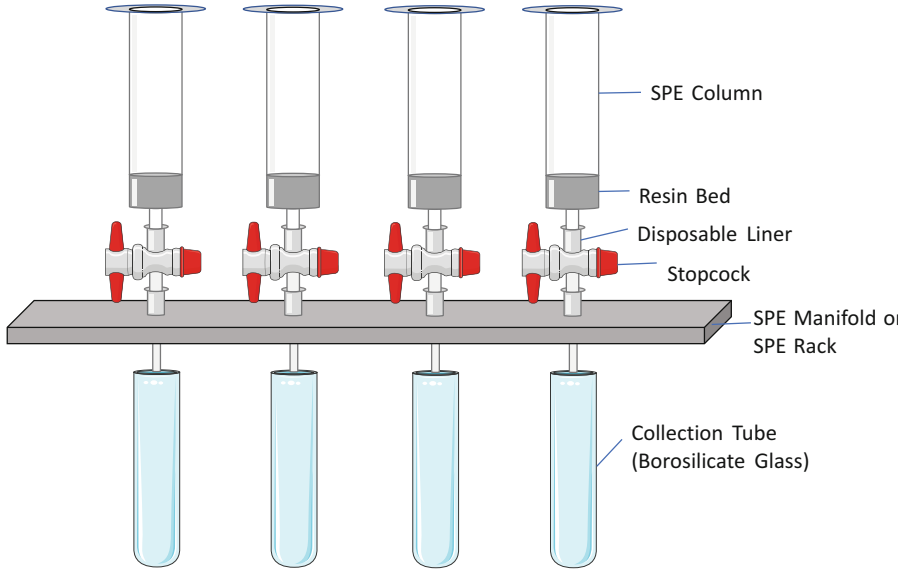

Fig. 2 Solid-phase chromatography is set up by inserting the solid-phase extraction (SPE) column into the luer-lok port of a disposable manifold liner (ensures non-cross-contamination of samples) through a stopcock capable of regulating flow within a SPE manifold or SPE rack. We use an SPE manifold from Sigma-Aldrich that has the capability of accelerating flow through the use of vacuum pressure, but we do not make use of this feature as gravity flow of solvents is generally fast enough and solvent volumes are low in this procedure. All collection is done into threaded, borosilicate glass tubes (not plastic) so that phthalates that are extractable from plastic do not contaminate the lipid extract mixture

time, to fully elute triglycerides using a borosilicate glass pipette, collecting flow-through in the same triglyceride fraction tube.

12. Remove and cap the first collection tube, and replace the tube with a clean collection tube. Elute glycosphingolipids by adding a total of 5 mL of acetone (90%)–methanol (10%), 1 mL at a time using a borosilicate glass pipette (*see* **Note 9**).
13. Replace glycosphingolipid collection tube with a third threaded borosilicate collection tube. Elute phospholipids by adding 3 mL of 100% methanol, 1 mL at a time. This fraction represents the phospholipid fraction. Fractions can be stored at −80 °C at this point capped tightly under nitrogen (*see* **Note 2**).
14. Dry the triglyceride and phospholipid fractions under nitrogen in an evaporation manifold. To speed drying, especially of the less volatile methanol-containing phospholipid fraction, we perform this in a dry heating block at 33 °C.
15. To derivatize lipids and generate FAMEs, add 2 mL acidified methanol to each lipid fraction and resuspend by vortexing. Incubate capped tightly for 1 h in a 75 °C water bath (*see* **Note 10**).

16. Remove samples from the water bath, and cool samples on the bench for 5 min.
17. Add 1.5 mL water to each sample to quench the FAME reaction and then 0.3 mL chromatography-grade hexane to each triglyceride and phospholipid fraction. Shake vigorously and centrifuge at 1000 × *g* for 5 min. FAMEs will partition into the hexane at this point.
18. Very carefully remove only top hexane layer using a Pasteur pipette. Plastic pipette tips may be used very cautiously at this point, as polypropylene is resistant to hexane, however, great caution must be taken to not touch plastic to the lower, methanol phase (*see* **Note 1**). Transfer the hexane layer to an autosampler tube with a glass insert, and cap tightly with a PTFE/red rubber septa cap. Make absolutely certain not to carry over any acidified methanol as this will destroy the GC column and MSD. Proceed to Subheading 3.3. Samples may be stored tightly capped at −80 °C at this point if desired.

3.3 Gas Chromatography–Mass Spectrometry of Fatty Acid Methyl Esters

1. Cap and load samples onto GC-MS.
2. On an Agilent GC-MS model 6890/5973N outfitted with a Supelcowax-10 (24079) 30 M, 250 μm fused silica capillary column, following three injection needle washes, 1 μL of sample is injected into a splitless inlet set at 250 °C and 13.33 pounds per square inch. Ultrapure helium is used a carrier gas.
3. The protocol run is as follows at a constant flow of helium at 1 mL per min:

Step	Instruction	Goal temperature (°C)
1	Hold 2 min	150
2	Ramp 10 °C per min	200
3	Hold 4 min	200
4	Ramp 5 °C per min	240
5	Hold 3 min	240
6	Ramp 10 °C per min	270
7	Hold 5 min	270

4. For mass spectrometry detection, a 3 min solvent delay is used to minimize wear on the filament. Thereafter, masses between 50 and 550 Da are detected with the MS quadrupole set at 150 °C and the MS source set at 230 °C, with a thermal auxiliary temperature of 270 °C.

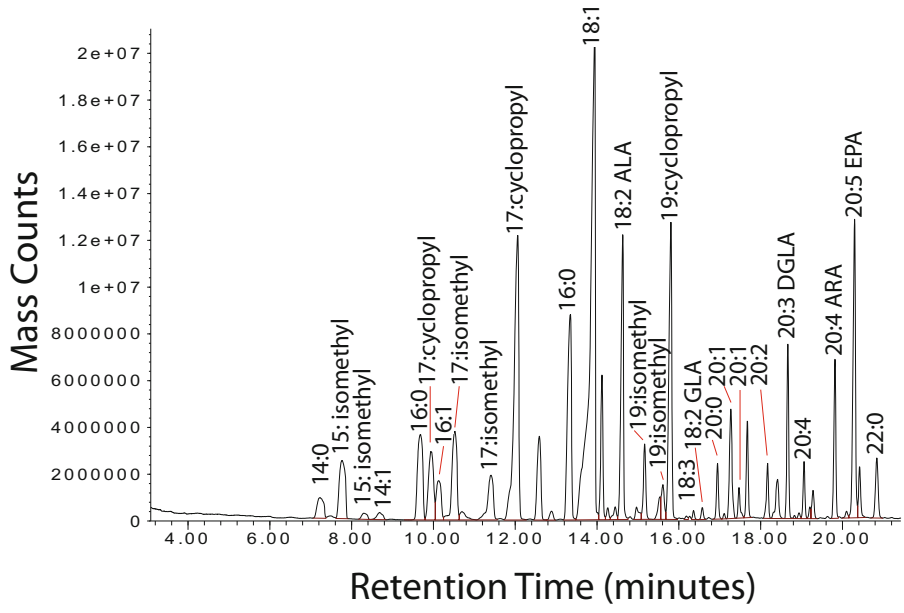

Fig. 3 Representative tracing of FAMEs detected by GC-MS analysis of whole worm lipid extracts (Subheadings 3.1 and 3.3). The individual peak areas are integrated giving an approximate measure of the relative abundance of fatty acid species. Note that the percentage of any particular fatty acid present can be relatively quantitated by dividing the peak area for that FAME by the total area of other fatty acids present. Several fatty acids, such as 15:isomethyl branch chain fatty acids, fatty acids with double bonds (e.g. 18:2, 20:1) and cyclopropyl fatty acids have multiple isomers, showing up as peaks that have distinct retention times but on MS analysis have the same parent ion mass. These are difficult to definitively identify except with internal standards. Note that some peaks are not labeled because they do not correspond to FAMEs based upon their mass spectra. We do not routinely include these in our calculations

5. Fatty acids are identified and quantified based upon mass spectra and characteristic retention times (Fig. 3). To determine the percentage of fatty acids present in whole worm extracts or in individual fatty acid fractions, mass counts for individual fatty acids divided by the sum of all mass counts for all fatty acids (without the internal standard). To corroborate that neutral lipid stores are altered in a biological sample, a ratio of normalized triglyceride content to phospholipid content is calculated, taking into consideration recovery of the internal standards (Fig. 4). In this case, the sum of all mass counts for all triglyceride peaks except tridecanoate (13:0, internal standard) is divided by the mass count for the tridecanoate peak. This "normalized" triglyceride amount is then divided by the value obtained by summing all phospholipid fatty acid peaks (exclusive of 17:0 heptadecanoate, internal standard) divided by the mass count for the heptadecanoate peak. This permits the investigator to determine alterations in this ratio in different genetic, nutritional, or pharmacologic manipulations that alter neutral lipid stores [6, 9, 17, 18].

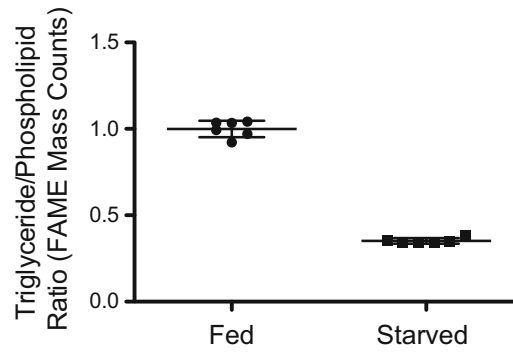

Fig. 4 Representative data from fed and 24-h starved L4 stage *C. elegans* from Subheadings 3.2 and 3.3 where FAMEs are analyzed from triglyceride and phospholipid fractions separated by solid-phase extraction. In this case, total area of all fatty acid peaks in the triglyceride fraction are summed, and divided by the area of the tridecanoate triglyceride standard peak. The result of this calculation is divided by the sum total area of all phospholipid fatty acid peaks divided by the heptadecanoate phospholipid standard peak. The result (in this case normalized to 1.0 for the mean of the fed animals) gives an indication of neutral lipid stores (triglycerides) relative to membrane lipids (phospholipids). We have found that this ratio corroborates data obtained by neutral lipid staining well and is reflective of nutritional state. In this case, fasting for 24 h leads to a reduction of triglyceride–phospholipid ratio to ~0.3 of the fed state ($N = 6$ biological replicates per group, bars represent mean $\pm$ standard deviation, $P < 0.0001$ by unpaired, two-tailed *t*-test with Welch's correction)

4 Notes

1. When using organic solvents, great care must be taken to not expose the solvent to plastics known to be nonresistant to organics. Failure to exercise this caution can lead to inadvertent extraction of phthalates from the plastic into the sample, confounding downstream mass spectrometry analysis. Thus, for pipetting chloroform, methanol, acetone, acetonitrile, and mixtures of the above, we take care to use all glass pipettes, and to making all samples in glassware rinsed clean prior to use (to remove fatty acids present in soap), and to using borosilicate glass sample tubes with organic solvent-resistant phenolic caps. The only point in this proposal where we use plastic pipettes to pipet organics is on the final step in protocol 3.2 as indicated to remove the hexane layer containing derivatized FAMES, but great care must be taken to not expose the pipette tip to the underlying acid-methanol layer as this can lead to interfering contaminants in subsequent GC-MS analyses.
2. Lipids oxidize upon exposure to air. Therefore, all lipids should be kept at reduced storage temperatures (−20 or −80 °C) and stored under nitrogen gas (performed by gently blowing a

nitrogen gas source over the sample and promptly closing the cap, and wrapping the sealed tube with Parafilm). Lipids should never be stored dry unless sealed in an inert gas environment. Fatty acid, triglyceride, and phospholipid standards can be stored up to 1 year at −20 °C under nitrogen in a borosilicate glass tube with a phenolic cap.

3. When making a diluted acid solution, always add acid slowly to the solvent (in this case methanol) and not vice versa, as adding solvent to acid may result in a violent reaction and serious injury.
4. When analyzing lipid content in worms, 1000–3000 L4-adult worms is sufficient for whole worm FAME analysis, and 5000–10,000 L4-adult worms is sufficient for lipid species separation by SPE followed by FAME analysis. Because *C. elegans* accumulate lipid over time through development, if younger, larval stage animals are to be analyzed, the number may need to be scaled for sufficient detection of FAMEs by GC-MS.
5. Frozen pellets of *C. elegans* collected and washed clear of the bacterial food source may be kept for many months or even years at −80 °C in either plastic or glass tubes.
6. Examine tubes shortly after transferring to the 75 °C water bath to be sure the liquid level is not falling, as we have found that some tubes and caps leak, leading to rapid evaporation of the sample at elevated temperatures.
7. We usually normalize triglyceride mass (neutral lipid stores) to phospholipid mass. The worm pellet may be taken directly to chloroform–methanol based lipid extraction if triglyceride mass is to be normalized to phospholipid mass. However, if the investigator desires normalization to protein content, the worm pellet should be sonicated on the highest intensity in a bath sonicator for 10 min, 30 s on, 30 s off, at 4 °C. Remove a 5 μL aliquot after determining the total sample volume and determine total protein concentration using a BCA assay, Bradford reagent, or similar in order to normalize FAME mass counts to total protein content.
8. Alternative methods for separating lipids include thin layer chromatography and HPLC [23]. Where we separate neutral lipids (dominated by triglycerides) and phospholipids, alternative methods can resolve different phospholipid classes, glycolipids, sphingolipids, diacylglycerols, triacylglycerols, free fatty acids, and cholesterol esters. Sophisticated methods of whole-lipidome profiling by liquid-chromatography/MS (LCMS) can also be used [24].

9. We do not routinely analyze the fatty acid composition of the glycosphingolipid fraction, however, it may contain valuable information and can be saved for preparation of methyl esters and free sphingoid bases for further analysis utilizing specialized procedures distinct from those for TAG and PL [25].
10. Care must be taken to get absolutely no water in the FAME reaction as this will greatly inhibit derivatization of lipids. As an alternative to 75 °C incubation for 1 h, we have found equally efficient derivatization by overnight incubation at 55 °C, and the literature suggests less lipid oxidation occurs at lower temperatures during FAME preparation [26].

Acknowledgments

This work was supported by NIH Grants K08DK087941, R01DK101522, and R01AG058256, by a Glenn Award for Research in the Biological Mechanisms of Aging, and by the Weissman Family MGH Research Scholar award to A.A.S.

References

1. Wang MC, O'Rourke EJ, Ruvkun G (2008) Fat metabolism links germline stem cells and longevity in C. elegans. Science 322 (5903):957–960
2. Lapierre LR, Gelino S, Melendez A, Hansen M (2011) Autophagy and lipid metabolism coordinately modulate life span in germline-less C. elegans. Curr Biol 21(18):1507–1514. https://doi.org/10.1016/j.cub.2011.07.042
3. Lapierre LR, Melendez A, Hansen M (2012) Autophagy links lipid metabolism to longevity in C. elegans. Autophagy 8(1):144–146. https://doi.org/10.4161/auto.8.1.18722
4. Pang S, Curran SP (2014) Adaptive capacity to bacterial diet modulates aging in C. elegans. Cell Metab 19(2):221–231. https://doi.org/10.1016/j.cmet.2013.12.005
5. Watts JL (2009) Fat synthesis and adiposity regulation in Caenorhabditis elegans. Trends Endocrinol Metab 20(2):58–65. https://doi.org/10.1016/j.tem.2008.11.002. S1043-2760(09)00004-6 [pii]
6. Soukas AA, Kane EA, Carr CE, Melo JA, Ruvkun G (2009) Rictor/TORC2 regulates fat metabolism, feeding, growth, and life span in Caenorhabditis elegans. Genes Dev 23 (4):496–511. https://doi.org/10.1101/gad.1775409.23/4/496
7. Ashrafi K, Chang FY, Watts JL, Fraser AG, Kamath RS, Ahringer J, Ruvkun G (2003) Genome-wide RNAi analysis of Caenorhabditis elegans fat regulatory genes. Nature 421 (6920):268–272
8. O'Rourke EJ, Soukas AA, Carr CE, Ruvkun G (2009) C. elegans major fats are stored in vesicles distinct from lysosome-related organelles. Cell Metab 10(5):430–435. https://doi.org/10.1016/j.cmet.2009.10.002. S1550-4131 (09)00301-5 [pii]
9. Pino EC, Webster CM, Carr CE, Soukas AA (2013) Biochemical and high throughput microscopic assessment of fat mass in Caenorhabditis elegans. J Vis Exp (73). https://doi.org/10.3791/50180
10. Soukas AA, Carr CE, Ruvkun G (2013) Genetic regulation of Caenorhabditis elegans lysosome related organelle function. PLoS Genet 9(10):e1003908. https://doi.org/10.1371/journal.pgen.1003908
11. Brooks KK, Liang B, Watts JL (2009) The influence of bacterial diet on fat storage in C. elegans. PLoS One 4(10):e7545. https://doi.org/10.1371/journal.pone.0007545
12. Yen K, Le TT, Bansal A, Narasimhan SD, Cheng JX, Tissenbaum HA (2010) A comparative study of fat storage quantitation in nematode Caenorhabditis elegans using label and label-free methods. PLoS One 5(9):e12810. https://doi.org/10.1371/journal.pone.0012810

13. Zhang SO, Trimble R, Guo F, Mak HY (2010) Lipid droplets as ubiquitous fat storage organelles in C. elegans. BMC Cell Biol 11:96. https://doi.org/10.1186/1471-2121-11-96
14. Klapper M, Ehmke M, Palgunow D, Bohme M, Matthaus C, Bergner G, Dietzek B, Popp J, Doring F (2011) Fluorescence-based fixative and vital staining of lipid droplets in Caenorhabditis elegans reveal fat stores using microscopy and flow cytometry approaches. J Lipid Res 52 (6):1281–1293. https://doi.org/10.1194/jlr.D011940
15. Wang MC, Min W, Freudiger CW, Ruvkun G, Xie XS (2011) RNAi screening for fat regulatory genes with SRS microscopy. Nat Methods 8(2):135–138. https://doi.org/10.1038/nmeth.1556
16. Hellerer T, Axang C, Brackmann C, Hillertz P, Pilon M, Enejder A (2007) Monitoring of lipid storage in Caenorhabditis elegans using coherent anti-Stokes Raman scattering (CARS) microscopy. Proc Natl Acad Sci U S A 104 (37):14658–14663. https://doi.org/10.1073/pnas.0703594104
17. Perez CL, Van Gilst MR (2008) A 13C isotope labeling strategy reveals the influence of insulin signaling on lipogenesis in C. elegans. Cell Metab 8(3):266–274
18. Webster CM, Pino EC, Carr CE, Wu L, Zhou B, Cedillo L, Kacergis MC, Curran SP, Soukas AA (2017) Genome-wide RNAi screen for fat regulatory genes in C. elegans identifies a proteostasis-AMPK axis critical for starvation survival. Cell Rep 20(3):627–640. https://doi.org/10.1016/j.celrep.2017.06.068
19. Srinivasan S, Sadegh L, Elle IC, Christensen AG, Faergeman NJ, Ashrafi K (2008) Serotonin regulates C. elegans fat and feeding through independent molecular mechanisms. Cell Metab 7(6):533–544. https://doi.org/10.1016/j.cmet.2008.04.012
20. Watts JL, Browse J (2002) Genetic dissection of polyunsaturated fatty acid synthesis in Caenorhabditis elegans. Proc Natl Acad Sci U S A 99(9):5854–5859
21. Brock TJ, Browse J, Watts JL (2006) Genetic regulation of unsaturated fatty acid composition in C. elegans. PLoS Genet 2(7):e108. https://doi.org/10.1371/journal.pgen.0020108
22. Walker AK, Jacobs RL, Watts JL, Rottiers V, Jiang K, Finnegan DM, Shioda T, Hansen M, Yang F, Niebergall LJ, Vance DE, Tzoneva M, Hart AC, Naar AM (2011) A conserved SREBP-1/phosphatidylcholine feedback circuit regulates lipogenesis in metazoans. Cell 147(4):840–852. https://doi.org/10.1016/j.cell.2011.09.045
23. Watts JL, Browse J (2006) Dietary manipulation implicates lipid signaling in the regulation of germ cell maintenance in C. elegans. Dev Biol 292(2):381–392. https://doi.org/10.1016/j.ydbio.2006.01.013
24. Wang TJ, Larson MG, Vasan RS, Cheng S, Rhee EP, McCabe E, Lewis GD, Fox CS, Jacques PF, Fernandez C, O'Donnell CJ, Carr SA, Mootha VK, Florez JC, Souza A, Melander O, Clish CB, Gerszten RE (2011) Metabolite profiles and the risk of developing diabetes. Nat Med 17(4):448–453. https://doi.org/10.1038/nm.2307
25. Gerdt S, Lochnit G, Dennis RD, Geyer R (1997) Isolation and structural analysis of three neutral glycosphingolipids from a mixed population of Caenorhabditis elegans (Nematoda:Rhabditida). Glycobiology 7(2):265–275
26. Christie WW (1993) Advances in lipid methodology – two. Oily Press, Dundee

Chapter 11

Assessing Insulin and Glucose Tolerance in the Aging Mouse

Roberta Buono and Sebastian Brandhorst

Abstract

Basic preclinical research on the pathophysiology of aging-related and/or metabolic diseases, including type 2 diabetes, largely relies on animal models. Mice, the most commonly used species to study the biological processes that regulate aging and its associated functional decline, have helped researchers to identify pathways, mechanisms, and genes that regulate aging-related diseases and aging itself and thus are intervention targets. Changes in energy metabolism are a central component of the biological processes that undergo significant alterations with age. For example, the prevalence of type 2 diabetes and impaired glucose tolerance increases with aging. Not surprisingly, the characterization of these changes for metabolic phenotyping is commonly found in laboratories around the world. Glucose tolerance tests (GTT) and insulin tolerance tests (ITT) do not require surgery, are relatively easy to perform, and, most importantly, are minimally invasive and are thus the preferred method to evaluate glucose homeostasis in the aging animal. Both assays measure blood glucose following the bolus injection of either glucose (for GTT) or insulin (for ITT). Although they are standard procedures, the interpretation of both assays is strongly influenced by laboratory practices and variable experimental conditions. Here, we aim to provide simple guidelines that can be useful to standardize GTT and ITT in the aging mouse.

Key words Mice, Aging, Glucose, Insulin, Metabolic homeostasis

1 Introduction

Aging is associated with distortions in glucose metabolism, including insulin resistance and/or insulin-secreting pancreatic beta cell dysfunction [1–3]. Nearly 13% of adults 70 years or older have diabetes, and 11% of adults between the ages of 60 and 74 years are estimated to have diabetes but are undiagnosed [4]. Insulin secretion and insulin sensitivity play a crucial role in the maintenance of normal glucose tolerance, and insulin secretion as well as beta cell mass increase as a compensatory mechanism when insulin sensitivity decreases [5]. However, when the functional threshold of beta cells is surpassed and when beta cells fail, type 2 diabetes develops. Not surprisingly, diabetes and impaired glucose tolerance affect a substantial proportion of the elderly population. Continuous research efforts are aimed at exploring the association of

Sean P. Curran (ed.), *Aging: Methods and Protocols*, Methods in Molecular Biology, vol. 2144,
https://doi.org/10.1007/978-1-0716-0592-9_11,

dysglycemia and insulin resistance with aging-related comorbidities, decreased quality of life, and shortened life expectancy [6–8]. Factors that may predispose to glucose intolerance in the aged are increased body weight, decreased physical activity, decreased insulin secretion, and lack of glucagon suppression [9].

Functional assays to measure glucose tolerance and insulin sensitivity remain essential tools to determine the age-related effects on glucose metabolism. The Baltimore Longitudinal Study of Aging demonstrates an age-related increase in the rate of progression from normal glucose metabolism to impaired glucose tolerance which is nearly two times the rate observed when progressing from normal to impaired fasting glucose after 20 years of follow-up [10]. These findings suggest that oral glucose tolerance testing, in particular, is important to consider when characterizing abnormal glucose status in the elderly.

Interventions continue to rely on preclinical experiments that include mouse models to test for treatment efficacy. To compare studies and interventions, it is paramount that standardized assays are utilized. Here, we outline the experimental setups for the intraperitoneal glucose tolerance test (IPGTT) and the insulin tolerance test (ITT) which can be applied to mice regardless of age. As for all studies utilizing aged animals, investigators should take special care of old animals and need to rely on experienced personnel to evaluate if the added handling and procedure stress may cause harm to individual mice. Due to the anticipated increase in animal deaths with age, it should also be considered to increase the number of animals maintained in the colony to ensure sufficient statistical power for the investigation.

2 Materials

1. 20% D-glucose solution (Sigma-Aldrich).
2. Insulin 100 U/ml (Sigma-Aldrich).
3. Saline solution (0.9% NaCl).
4. 1 ml insulin syringes (BD Insulin syringes: 0.5 cc, 31 G).
5. Sharp scalpel blade.
6. Glucometer and Glucose test sticks (OneTouch UltraMini Blood Glucose Monitoring System; Lifescan, Milpitas, CA, USA).
7. Sterile alcohol pads.
8. Heparinized tubes (MiniCollect® Serum and Plasma Tubes, Greiner Bio-One K3EDTA).
9. Eppendorf tubes, prelabeled.
10. Scale.

11. Timer.
12. Clean mouse cages.
13. 4 °C chilled centrifuge.

3 Methods

3.1 Intraperitoneal Glucose Tolerance Test (IPGTT)

1. Fast mice for 6 h (morning fasting) before blood glucose measurements with standard light–dark cycle and free access to water at all times (*See* **Notes 1–3**).
2. Weight the mice and annotate body weight (BW) in a record book.
3. Calculate the volume of 20% glucose solution to be injected intraperitoneally (i.p.) for a final dose of 2 g of glucose/kg of BW. In other words, for each mouse, the volume in μl of 20% glucose solution to be injected is ten times the mouse BW in grams (*See* **Note 4**).
4. Prepare syringes loaded with the required volume of the glucose solution, glucometer, and glucose sticks for measurements (*See* **Note 5**).
5. Clean the tip of the mouse tail with an alcohol pad and perform a small cut at the tip of the tail with a sharp scalpel. Allow the blood to flow directly into the glucose test stick inserted into the glucometer and report the glucose value at time point 0 ($t = 0$).
6. Collect up to 4 0 μl of blood using heparinized tubes and store at 4 °C.
7. To avoid excessive blood loss, apply pressure to the incision site after each measurement or, alternatively, use silver nitrate sticks to chemically cauterize the skin.
8. Clean the ventral side of the mouse using sterile alcohol pads.
9. Intraperitoneally inject mice with syringes with a final dose of 2 g of glucose/kg of BW.
10. Start the timer.
11. Measure the glucose levels at time points $t = 30$, $t = 60$, $t = 90$, and $t = 120$ min as in **step 5**. Record the glucose values for each mouse in a record table. You may collect blood as in **step 6** if needed.
12. At the end of the experiment, clean the mouse tail tips with sterile pads and place the mice in clean cages with free access to food and water.
13. Monitor the animals during the following 2 h to report any abnormal behavior.

14. Centrifuge blood at 4 °C 10 min at 14,000 × *g* speed to obtain plasma from the different time points.
15. Collect plasma into a new labeled tube and measure insulin concentrations by ELISA.
16. The IPGTT results are represented in a graph depicting glucose levels versus time.

3.2 Insulin Tolerance Test (ITT)

1. Fast mice for 4 h (morning fasting) before blood glucose measurements with standard light–dark cycle and free access to water at all times. *See* **Notes 1**-**3**.
2. Weight the mice and annotate body weight (BW) in a record book.
3. Calculate the volume of insulin to be injected to each mouse for a dose of 0.5 U/kg of BW. For a working solution of 0.1 U/ml, the volume of insulin to be injected (μl) is five times the mouse BW (g). *See* **Note 4**.
4. Prepare syringes with the appropriate amount of insulin solution and prepare the glucose test strips and glucometer. *See* **Note 5**.
5. Clean the tip of the mouse tail with alcohol pads and perform a small cut at the tip of the tail with a sharp scalpel. Allow the blood flow directly into the glucose test stick and report the glucose value at time point 0 ($t = 0$).
6. To avoid excessive blood loss, apply pressure to the incision site after each measurement or, alternatively, use silver nitrate sticks to chemically cauterize the skin.
7. Clean the ventral side of the mouse using sterile alcohol pads and inject mice with syringes loaded with insulin.
8. Measure the glucose levels at time points $t = 5$, $t = 15$, $t = 30$, $t = 60$, $t = 90$, and $t = 120$ min as in **step 5**. Record the glucose values for each mouse in a record table.
9. At the end of the experiment, clean the mouse tail tips with sterile pads and place the mice in clean cages with free access to food and water.
10. Monitor the animals during the following 2 h.
11. The ITT results are represented in a graph depicting relative glucose levels in percentage versus time.

4 Notes

1. IPGTT and ITT should never be performed in anesthetized mice. Anesthesia affects heart rate and induces hyperglycemia.
2. Trained and experienced personnel is highly recommended in order to reduce anxiety levels in the mice.

3. It is recommended that metabolic studies are performed at approximately the same hour in the morning because physiological and biochemical parameters change throughout the day.
4. Use room temperature glucose and insulin solution before injection in the mice.
5. Space the injections of each mouse about 1–2 min to facilitate glucose measurements and to avoid overlaps for all subsequent bleedings.

References

1. Kalyani RR, Egan JM (2013) Diabetes and altered glucose metabolism with aging. Endocrinol Metab Clin North Am 42(2):333–347. https://doi.org/10.1016/j.ecl.2013.02.010
2. Shimokata H, Muller DC, Fleg JL, Sorkin J, Ziemba AW, Andres R (1991) Age as independent determinant of glucose tolerance. Diabetes 40(1):44–51. https://doi.org/10.2337/diab.40.1.44
3. Cowie CC, Rust KF, Ford ES, Eberhardt MS, Byrd-Holt DD, Li C, Williams DE, Gregg EW, Bainbridge KE, Saydah SH, Geiss LS (2009) Full accounting of diabetes and pre-diabetes in the U.S. population in 1988–1994 and 2005–2006. Diabetes Care 32(2):287–294. https://doi.org/10.2337/dc08-1296
4. Mokdad AH, Ford ES, Bowman BA, Nelson DE, Engelgau MM, Vinicor F, Marks JS (2000) Diabetes trends in the U.S.: 1990–1998. Diabetes Care 23 (9):1278–1283. https://doi.org/10.2337/diacare.23.9.1278
5. Kahn SE, Prigeon RL, McCulloch DK, Boyko EJ, Bergman RN, Schwartz MW, Neifing JL, Ward WK, Beard JC, Palmer JP et al (1993) Quantification of the relationship between insulin sensitivity and beta-cell function in human subjects. Evidence for a hyperbolic function. Diabetes 42(11):1663–1672. https://doi.org/10.2337/diab.42.11.1663
6. Rubin RR, Peyrot M (1999) Quality of life and diabetes. Diabetes Metab Res Rev 15 (3):205–218
7. Long AN, Dagogo-Jack S (2011) Comorbidities of diabetes and hypertension: mechanisms and approach to target organ protection. J Clin Hypertens (Greenwich) 13(4):244–251. https://doi.org/10.1111/j.1751-7176.2011.00434.x
8. Chentli F, Azzoug S, Mahgoun S (2015) Diabetes mellitus in elderly. Indian J Endocrinol Metab 19(6):744–752. https://doi.org/10.4103/2230-8210.167553
9. Stevic R, Zivkovic TB, Erceg P, Milosevic D, Despotovic N, Davidovic M (2007) Oral glucose tolerance test in the assessment of glucose-tolerance in the elderly people. Age Ageing 36 (4):459–462. https://doi.org/10.1093/ageing/afm076
10. Meigs JB, Muller DC, Nathan DM, Blake DR, Andres R (2003) The natural history of progression from normal glucose tolerance to type 2 diabetes in the Baltimore Longitudinal Study of Aging. Diabetes 52(6):1475–1484. https://doi.org/10.2337/diabetes.52.6.1475

Chapter 12

High-Throughput Assessment of Changes in the *Caenorhabditis elegans* Gut Microbiome

Fan Zhang, Jessica L. Weckhorst, Adrien Assié, Anastasia S. Khodakova, Mario Loeza-Cabrera, Daniela Vidal, and Buck S. Samuel

Abstract

The gut microbiome is an important driver of host physiology and development. Altered abundance or membership of this microbe community can influence host health and disease progression, including the determination of host lifespan and healthspan. Here, we describe a robust pipeline to measure microbiome abundance and composition in the *C. elegans* gut that can be applied to examine the role of the microbiome on host aging or other physiologic processes.

Key words Microbiome, Bacteria, *C. elegans*, Colonization, Amplicon sequencing, High-throughput methods

1 Introduction

Animals have partnered with microbes in mutualistic or commensal relationships throughout evolution. Microbial input is required for normal animal function and shapes many central systems, including metabolism, immunity, and even the nervous system. Conversely, bacterial colonization also contributes to aging and disease, especially when microbial composition becomes perturbed [1, 2].

With its powerful genetic tools and short lifespan, the roundworm *C. elegans* has become an instrumental model system in longevity research and led to the discovery of several key aging regulators. Several links between microbes and the regulation of *C. elegans* lifespan and/or healthspan have also been observed [3–8]. Assessments of bacteria from wild isolates by non-culture-based sequencing indicate that *C. elegans* harbors a natural microbiome that is distinct and likely to be deterministically acquired from its natural habitats of rotting fruits and vegetation [9–

Fan Zhang, Jessica L. Weckhorst and Adrien Assié contributed equally.

Sean P. Curran (ed.), *Aging: Methods and Protocols*, Methods in Molecular Biology, vol. 2144,
https://doi.org/10.1007/978-1-0716-0592-9_12,

11]. Further meta-analyses indicate that its core microbiome comprises 12 families of bacteria that consistently colonize the *C. elegans* gut [12], and has spurred the development of a model 12-member microbiome (CeMbio—http://www.cembio.uni-kiel.de/). Therefore, *C. elegans* is a promising model to explore the role of the microbiome in the aging process.

Microbial colonization of the *C. elegans* gut has previously been measured by a classic mortar and pestle method [13]. However, labor-intensive CFU counting limits throughput of the assay and makes it difficult to assess the diversity of complex mixtures of the microbiome. Here, we address these challenges and describe a high-throughput pipeline (Fig. 1) to examine microbiome abundance and composition in *C. elegans*.

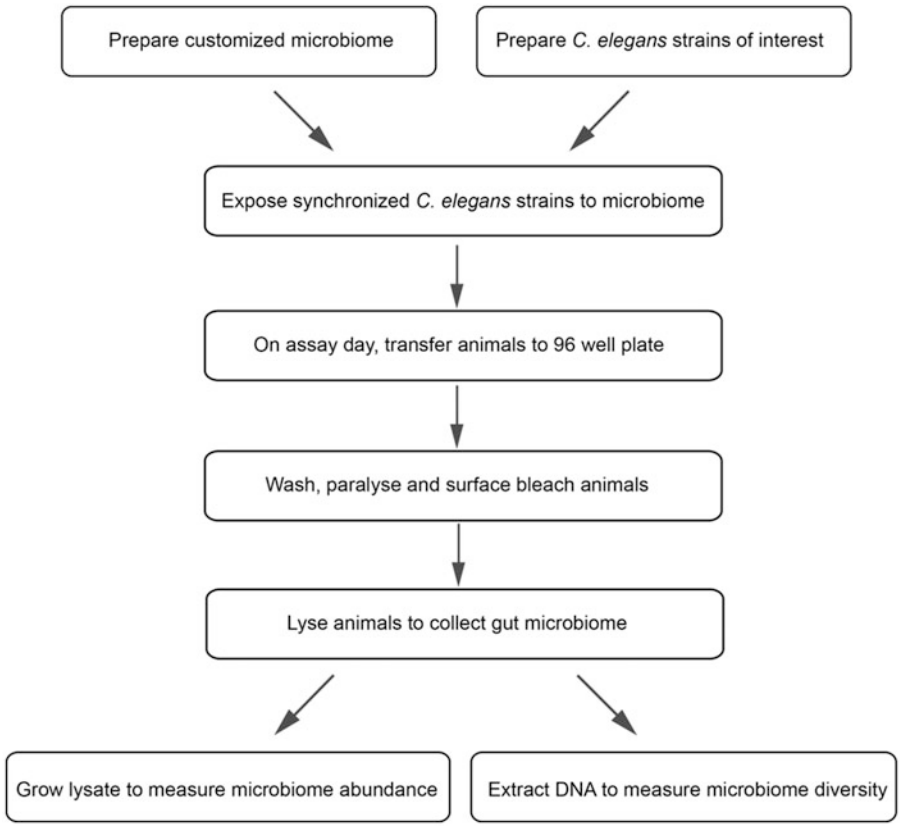

Fig. 1 Schematic pipeline to measure microbiome abundance and diversity

2 Materials

Prepare all solutions using MilliQ water and store all reagents at room temperature, unless otherwise noted.

2.1 Bacterial Culture and Maintenance

1. *LB Medium*: Add 10 g Bacto tryptone to 900 mL water in 1 L glass autoclavable bottle (e.g., Pyrex), then add 5 g Bacto yeast, 5 g NaCl and adjust pH to 7.0 using 5 M NaOH. For LB agar, add 15 g of agar, adjust volume to 1000 mL and autoclave.
2. *Rectangular plates*: Stamp out bacterial culture stock in 96-well plate format.
3. *Deep well plates*: Grow bacterial culture in 96-well plate format (Axygen).

2.2 C. elegans Culture and Maintenance

1. *Nematode Growth Medium (NGM) Agar*: Start with 975 mL water in 1 L glass autoclavable bottle (Pyrex, etc.), add 3.0 g NaCl, 2.5 g peptone, and 17 g agar, and autoclave with a magnetic stir bar. Cool the mixture down to 55 °C on a heat plate preheated to 55 °C and add the following while stirring it: 0.5 mL of 1 M $CaCl_2$ (sterile), 1 mL of 5 mg/mL cholesterol (dissolved in ethanol), 1 mL of 1 M $MgSO_4$ (sterile), 25 mL of 1 M potassium phosphate buffer, pH 6.0 (sterile); pour into petri dishes or multiple-well plate using sterile technique [14].
2. *M9 buffer*: Start with 700 mL water in 1 L glass autoclavable bottle (Pyrex, etc.), add 6 g Na_2HPO_4, 3 g KH_2PO_4, 5 g NaCl, 0.25 g $MgSO_4{\cdot}7H_2O$ or 1 mL of 1 M $MgSO_4$, add water to 1000 mL, and autoclave [14].
3. *Multiwell plates*: 12- or 24-well plates with NGM agar for cultivation of *C. elegans*.

2.3 Measurement of Microbiome Colonization Levels

1. *M9-wash solution*: Prepare 0.01% Triton X-100 solution in M9 buffer form 5% Triton X-100 stock solution in M9 buffer. Sterilize by filtration through 0.22 μm filter (*see* **Note 1**).
2. *Levamisole solution*: Prepare 100 mM stock solution of levamisole in M9 buffer and dilute it to 10 mM to be used as working solution. Sterilize by filtration through 0.22 μm filter. Prepare fresh before use.
3. *Egg prep bleach solution*: Mix two parts of Clorox bleach and one part of 5 M NaOH. Prepare fresh before use.
4. *Wash bleach solution*: Prepare a 4% Bleach solution in M9 buffer. Prepare fresh before use.
5. *Garnet beads* (1.0 mm): For mechanical lysis of worms by bead beating. Sterilize by autoclaving before use.
6. *Phosphate buffer saline* (PBS; 1×): pH 7.2, 0.22 μm filter sterilized.

Table 1
PCR reaction master mixture

Reagent	Volume (μL) per reactions
2× TAQ mixture	12.5
PCR grade water	10.5
806r (10 μM) primer	0.5
515f (10 μM) barcoded primer[a]	0.5
DNA template[a]	1
Total	25

[a]Added separately

2.4 Measurement of Microbiome Composition and Diversity

1. *PCR primers*: A list of sequences for the primers used in this study can be found in Table 2 (*see* **Note 2**).
2. *Silica beads* (0.1 mm): For mechanical lysis of bacterial cells by bead-beating prior to DNA isolation. Sterilize by autoclaving before use.
3. *96-Well PCR plates*: For use in Proteinase K treatments during microbiomeDNA extraction and PCR amplifications.
4. *PCR master mix*: *See* Table 1 for a detailed recipe.
5. *Agarose gel electrophoresis supplies*:
   (a) Low-melting point agarose powder.
   (b) TAE buffer (40 mM Tris–acetate, 1 mM EDTA).
   (c) 1 kb ladder (NEB).
   (d) Gel loading dye (NEB).
6. *PCR purification kit*: Removes primers, nucleotides, enzymes, and other impurities from PCR product before sequencing.

2.5 Equipment

1. *Multiple channel pipette*: 12-channel pipettes (1000 and 200 μL) are commonly used in the assay to dispense liquid reagents and transfer volumes between plates.
2. *Plate reader*: For assessment of optical density (OD) in 96-well clear flat bottom plates.
3. *PCR thermocycler*: For use in Proteinase K treatment during microbiomeDNA extraction and generation of 16S rRNA gene amplicon libraries.
4. *Mixer mill*: For use in lysis of animals and microbial cells by bead beating (Retsch MM400).
5. *Microplate aspiration manifold*: For use in rapid removal of supernatants during wash steps (VP1171A V&P scientific).

3 Method

Since the main goals of these protocols is to monitor the levels and composition of desired microbes within the *C. elegans* gut, great care should be taken to prevent or minimize contamination by other microbes. We suggest carrying out all procedures under sterile conditions (e.g., laminar flow hood), use of sterile filter tips, filter-sterilize all reagents before use, and include appropriate negative controls during bacterial growth and preparation of microbiome plates.

3.1 Preparation of Microbiome Mixtures

1. Stamp or streak bacteria out of glycerol stocks onto LB plate(s), and grow overnight at optimum temperature (e.g., 28 °C for *C. elegans* natural microbiome) (*see* **Note 3**).
2. From the plate(s), inoculate one colony from each bacterial isolate (e.g., 12 bacteria of CeMbio collection [http://www.cembio.uni-kiel.de/]) into separate wells of 800 μL LB medium in a 1 mL deep well plate. Incubate overnight at optimum temperature, shaking at 250 rpm/min.
3. Assess growth of each microbe by spectrophotometry: transfer 20 μL aliquot into 80 μL of LB into a clear flat bottom 96-well plate and measure OD600 on a plate reader.
4. Centrifuge deep well culture plate (4000 × *g* for 10 min) to pellet bacteria and remove supernatant by aspiration (e.g., 96-well aspiration manifold).
5. Using OD600 values, normalize concentration of each well individually to an OD600 of 1.0 using sterile-filtered M9.
6. Determine the amount of bacterial culture needed for the experiment and create microbiome master mix by combining equal volumes of each bacterial strain into a tube of sufficient size (e.g., 5 mL or 15 mL tubes).
7. Spot 30–50 μL of the microbiome mixture onto the center of each well of a 12- or 24-well plate. Allow seeded microbiome to grow overnight at optimum temperature. Be sure to prepare enough plates for all transfer steps (keep at 4 °C).
8. [O*ptional*, Control Samples] Save bacterial pellets of single cultures and microbiome master mix. Centrifuge deep well culture plate and master mix (4000 × *g* for 10 min) to pellet bacteria and remove the supernatant by aspiration. Freeze at −80 °C (*see* **Note 4**).

3.2 Exposure of Animals to Microbiome Mixtures

1. Grow worm strains of interest on NGM plates seeded with *E. coli* OP50 (or another bacteria of interest) until worms reach gravid adulthood. Wash off and bleach strains to perform an egg prep [14]. Allow eggs to hatch and synchronize at L1 stage overnight (*see* **Note 5**).

2. Drop ~50–100 synchronized L1 larvae per condition and replicate on microbiome seeded NGM plates, allow to dry, and incubate at 20 °C or other desired temperature.
3. Allow worms to grow until desired age (*see* **Note 6**).
4. Transfer animals away from progeny as needed to avoid starvation and monitor microbiome in adult animals (*see* **Note 7**).

3.3 Creation of Microbiome Colonization Standard Curves

The method below is adapted from a protocol by Hazan et al. [15] in order to generate a standard curve for microbiome abundance determinations.

1. Continue using aliquot from existing microbiome mixture in **step 6** of Subheading 3.1 or create similar microbiome mixture.
2. *Prepare a dilution series*:
   (a) Fill a flat bottom 96-well plate with 180 μL of sterile filtered PBS. Pipette 20 μL of the microbiome mixture (same as 3.1) into four replicate wells in column 1 of the plate (e.g., A1, B1, C1, and D1). For controls, pipet 20 μL of LB in the remaining wells of column 1.
   (b) Using a multichannel pipette, serially dilute the microbiome mixture (1:10) in columns 2–12 to create a dilution series for all wells of the plate. Change tips between each dilution/column.
3. *CFU measurement*: From the serial dilution plate, plate 10 μL of each dilution onto a rectangular LB plate using a multichannel pipette. Incubate at optimal temperature overnight. Count colonies for each of the wells where possible (*see* **Note 8**).
4. *Liquid growth assay measurement*: Prepare a growth plate by filling each well of a flat bottom 96-well plate with 180 μL of LB. Transfer 20 μL from the serial dilution plate to the corresponding well of the growth plate. Incubate at optimal temperature with intermittent shaking and monitor OD600 regularly (e.g., every 15–30 min) until growth is observed in all wells (*see* **Note 9**).
5. Use a plotting software (Microsoft Excel, R, or other), to visualize growth curves by plotting OD600 reading vs time for each well on a single chart. Verify that growth patterns are consistent between replicates and growth curves are ordered by dilution factor.
6. Identify the range of OD600 values within the linear portion of the growth curves (*see* Fig. 2). Use the linear range identified and the following equation to calculate the optical density *Threshold*:

$$\text{Threshold} = (\text{OD600}_{\max} - \text{OD600}_{\min})/2 + \text{OD600}_{\min}$$

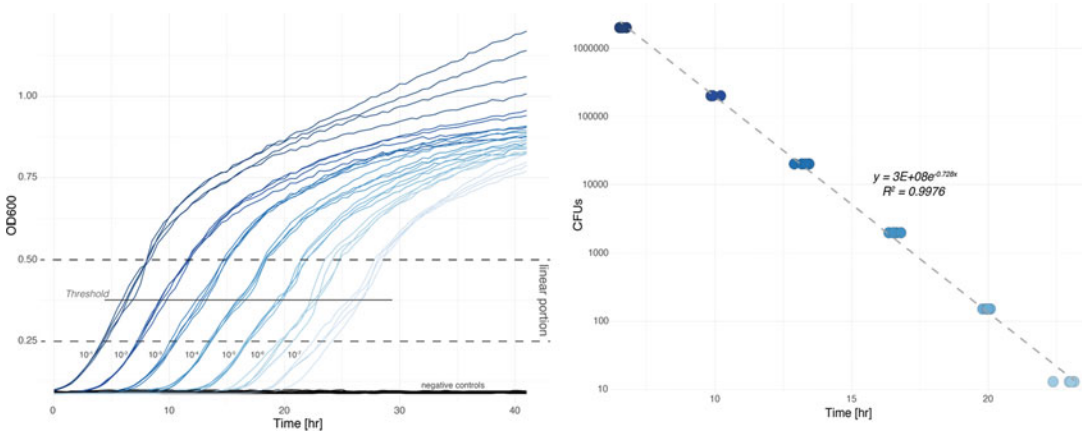

Fig. 2 Growth curve of microbiome mixture in serial dilutions and standard curve for CFU value conversion

7. Using the only data points where the OD600 readings for each well fall between the linear portion, calculate the *Slope* and *Intercept* for each well.
8. To calculate the time at which each well reached the threshold (Υ axis of calibration curve), use the following equation for each well:

$$\text{Time} = (\text{Threshold} - \text{Intercept})/\text{Slope}$$

9. Plot CFU values collected in **step 3** vs. *Time* of *Threshold* crossing for each well, and calculate the R squared value and exponential *Trendline* equation (*see* **Note 10**).

3.4 Measurement of Microbiome Gut Colonization

1. On the day worms reach desired age, use 600 μL of M9-wash solution to transfer worms from bacterial lawns to a sterilized 2 mL 96-well deep plate.
2. Wash worms by adding M9-wash solution to each well to a total volume of 1.8 mL.
3. Centrifuge the deep well plate at 300 × *g* for 1 min to pellet down worms, then remove liquid by using the aspiration manifold (*see* **Note 11**).
4. Repeat **steps 2** and **3** five more times.
5. After the final wash, aspirate each well to final volume of 100 μL.
6. Add 100 μL of levamisole solution to each well and allow the worms to paralyze for 1–5 min. Confirm paralysis by microscopy before proceeding to the next step (*see* **Note 12**).
7. Surface sterilize the worms by adding 200 μL of a 4% bleach solution in M9 to each well for 2 min.

8. Repeat **steps 2** and **3** two more times to wash away bleach and levamisole solutions. Do *not* aspirate after final centrifugation.
9. [*Optional*] Save 100 μL of supernatant from the last wash as control for background bacterial residual before host lysis (*see* **Note 13**).
10. To estimate animal numbers per well, mix by pipetting and transfer 100 μL to a flat bottom 96 well plate using a multichannel pipette. Count worms by microscopy.
11. Aspirate remaining liquid volume to 300 μL and add 1.0 mm sterilized garnet beads to each well (i.e., enough to barely cover the bottom of each well, or ~5–10 beads).
12. Seal the plate with an autoclaved plastic mat and lyse worms in Mixer Mill at a speed of 25 Hz for 5 min.
13. Briefly spin (pulse) plate in a centrifuge, allowing plates to come to max speed and allow to stop gently (with brakes).
14. Mix by pipetting and dilute the lysate by transferring 20 μL of each well into a 96-well plate containing 180 μL 1× PBS solution.
15. Transfer 20 μL of the dilution to 180 μL LB in 96 well flat bottom plate for liquid OD growth measurements. As in **step 4** of Subheading 3.3, monitor OD regularly (e.g., every 15–30 min) using a plate reader until growth is observed in all wells (12–18 h).
16. Calculate the colonization levels of bacteria per worm using the standard curve created previously. Use OD measurements and previously generated standard curves (trendline equation) to calculate CFU (*y)* values based on the time point the curve for each well crossed the threshold (*x*) (*see* **Note 14**).
17. Determine colonization levels on a per animal basis using the following formula:

$$\text{CFU/animal} = (\text{CFU} * \text{Dilution factor})/\text{of Animals}$$

18. For the remaining lysate, either proceed directly to Subheading 3.5 or freeze at −80 °C (*see* **Note 15**).

3.5 Preparation of Amplicon Libraries for Microbiome Sequencing

There are a plethora of tools and protocols for microbiome analyses [16]. We briefly describe our pipeline here that is based heavily on protocols targeting the 16S rRNA gene for amplification and originally developed for the Earth Microbiome Project (www.earthmicrobiome.org).

1. [*Optional*] Control samples (from **step 8** of Subheading 3.1) can be processed as below.
2. [*Optional*] If frozen, thaw the plate.

Table 2
Primer sequences for 16S rRNA amplification and high-throughput sequencing

1. **16S rDNA v4 amplification primers:**

515F forward primer, barcoded				
5′ Illumina adapter	Golay barcode	Forward primer pad	Forward primer linker	Forward primer (515F)
AATGATACGGCGACCACCGAGATCTACACGCT	XXXX*	TATGGTAATT	GT	GTGYCAGCMGCCGCGGTAA
806R reverse primer				
Reverse complement of 3′ Illumina adapter		Reverse primer pad	Reverse primer linker	Reverse primer (806R)
AATGATACGGCGACCACCGAGATCTACACGCT		AGTCAGCCAG	CC	GGACTACNVGGGTWTCTAAT

*See note 2

2. **Sequencing primers:**

Read 1 sequencing primer		
Forward primer pad	Forward primer linker	Forward primer
TATGGTAATT	gt	GTGYCAGCMGCCGCGGTAA
Read 2 sequencing primer		
Reverse primer pad	Reverse primer linker	Reverse primer
AGTCAGCCAG	cc	GGACTACNVGGGTWTCTAAT
Index sequencing primer		
AATGATACGGCGACCACCGAGATCTACACGCT		

3. Add 0.1 mm sterile zirconia/silica beads to each well (enough to barely cover well bottom with a thin layer of beads). Place in Mixer Mill for 5 min (25 Hz) to lyse bacterial cells.
4. Transfer 190 μL to a PCR plate. Add 10 μL of 20 mg/mL proteinase K to each well and mix by vortexing.
5. Place the plate in a PCR machine for 60 min at 60 °C for digestion then 15 min at 95 °C to deactivate the proteinase K. Store on ice until use.
6. For *amplicon* PCRsequencing:
   (a) Prepare the PCR reaction mixture as on Table 2.
   (b) Mix and add 23 μL of master mix into each well of a new 96 well PCR plate.
   (c) Add 1 μL of forward barcoded primer 515F to each well.
   (d) Add 1 μL of the supernatant from the PCR plate prepared in **step 5** of Subheading 3.5; the remaining supernatant is frozen in −80 °C for storage or future use (*see* **Note 16**).
   (e) Place the PCR plate in the ThermoCycler, run program described in Table 3.
7. Verify PCR amplification results with an agarose gel. Prepare a 1.5% agarose gel as described [17]. Mix 2 μL of loading dye with 4 μL of PCR product per sample and load 5 μL in the gel along with 1 kb ladder.
8. Purify PCR product using commercial PCR purification kit.

Table 3
PCR program for 16S rRNA amplification

Temperature (°C)	Time, 96-well	Repeat
94	3 min	
94	45 s	×35
50	60 s	×35
72	90 s	×35
72	10 min	
4	Hold	

9. Quantify intensity of PCR product band from each library (gel or fluorometry), normalize PCR product amount by volume and pool libraries together at equivalent concentrations into a single tube.
10. Submit samples for sequencing along with sequencing primers (*see* Subheading 2).

3.6 Analysis of Microbiome Sequencing Data

For analysis of sequencing datasets, we outline procedures using a QIIME2-based pipeline (https://docs.qiime2.org/; [18]).

1. Acquire sequencing dataset files (e.g., raw fastq forward, reverse, and index read files from an Illumina Miseq run).
2. *Perform quality control on amplicon sequences.* We perform a manual inspection of sequence quality using FastQC (https://www.bioinformatics.babraham.ac.uk/projects/fastqc/) (*see* **Note 17**).
3. [*Optional*] *PCR primer trimming*: Depending on the sequencing approach used if PCR primers are still present in the sequences they need to be removed. We trimmed the sequences using the cutadapt software [19].
4. *Process and demultiplex sequencing project(s).* We recommend using Deblur in QIIME2 (*see* **Note 18**). Briefly, we process the data with the following steps:
   (a) Load the sequencing read files and metadata table into QIIME2.
   (b) If using Deblur, merge reads and filter low-quality reads.
   (c) Run denoising algorithm.
   (d) Filter low abundance Amplicon Sequence Variant (ASV).
   (e) Summarize final table.
   (f) Build quick phylogeny with FastTree.
   (g) Assign Taxonomy with the SILVA database.

5. *Perform statistical analyses.* The following steps are completed using QIIME2.
   (a) *Estimate sequencing depth*: A key quality control step is to control if enough sequencing was performed on the samples. We generate rarefaction curves that plot of the number of species as a function of the number of samples.
   (b) *Calculate diversity metrics and generate ordination plots* (*see* **Note 19**) using the following steps:
   - Rarefy samples to the lowest reasonable sample depth (typically 1000–2000 reads is sufficient for simple microbiome samples).
   - Calculate alpha and beta diversity metrics.
   - Generate ordination plots, such as PCoA plots of Unifrac distances between samples.
   - Export table for further statistical analyses.

4 Notes

1. Adding Triton X-100 to M9 buffer reduces adherence of worms to pipette tips during their transfer.
2. A complete list of primers used for 16S rDNA amplification can be found on the Earth Microbiome project website: http://www.earthmicrobiome.org/protocols-and-standards/16s/. Forward primer-barcoded constructs were redesigned by Walters et al. [20] based upon the original constructs generated by Caporaso et al. [21]. A full list of primers can be found here: https://figshare.com/articles/EMP_16S_rRNA_V4_515F_806R_Parada_Appil/8794931.
3. Bacteria should be freshly stamped before starting each experiment.
4. Inclusion of control samples in the sequencing project provides an additional quality control step. Seed sample controls provides information about potential contamination of initial cultures. No worm lawn samples can also be included and washed off at the time of worm sampling to assess how the microbiome mixture has changed on the plates over time. Both can be processed as bacterial cell pellets using the same protocol outlined for worm lysates.
5. Alternatively, nonsynchronized and washed eggs can also be added directly to the microbiomeplates to avoid the influence of starvation during synchronization.
6. FUDR should be avoided as it influences microbial viability and metabolism [22, 23].

7. Initial colonization of animals for most strains occurs in early adulthood (day 1) with peak colonization levels by days 5–7 of adulthood. Studies in liquid also suggest more stochastic colonization of the *C. elegans* gut [24].
8. For hard-to-count bacteria or dense cultures, more accurate counts can be obtained by spotting 10 μL onto the top of the plate and tilting it vertically such that the droplets run toward the bottom of the plate.
9. Growth rates can vary by bacterial strain and can be greater than 24 h.
10. For dilutions too confluent to count, it may be necessary to impute those CFU values from the countable dilutions.
11. Alternatively worms can be allowed to settle without centrifugation to separate adults from progeny.
12. Worms that are not paralyzed will take up bleach solution and sterilize the guts of these animals in the next step.
13. This is an important control when setting up the protocol and can be used to troubleshoot effectiveness of the bleach solution.
14. The threshold value should be the same as the one used to build standard curves (e.g., OD600 = 0.25).
15. If using the plate again on the same day, place in 4 °C, otherwise, store in −80 °C. Use filter tips for this step, and do not allow the area above the "groove" of the tips to enter the plate.
16. As an option, the lysates can be used in alternative sequencing projects such as amplicon sequencing of a different region (such as ITS and 18S rRNA regions), shallow metagenomic sequencing [25] or RNA extraction, to only cite a few.
17. This first step is important and informs about the overall quality of the sequencing project and determine how we should trim the reads in downstream steps. The information provided by FastQC helps us determine at what length we can trim the reads so that we can discard low-quality bases.
18. Detailed protocols on how to fully process the data can be found on the QIIME2 documentation website (https://docs.qiime2.org/). QIIME2 offers two denoising algorithms to process the data, Deblur [26] and DaDa2 [27]. Denoising algorithms perform differently on certain datasets, however [29]. Although we recommend using Deblur in most cases, comparison of Deblur and DaDa2 for your samples should be tested to identify which is best in identifying the bacteria you have included in your microbiome mixtures.

19. The QIIME2 pipeline generates a file summarizing each individual amplicon sequence found in the analysis. You can compare those sequence to the individual 16S rRNA reference from your custom microbiome mixture in order to identify which amplicon sequence correspond to which reference. This can be performed with an alignment, using a tool such as MAAFT (https://mafft.cbrc.jp/), or custom blastn search [28].

Acknowledgements

This work was supported by an NIH New Innovator Award [DP2 DK116645] and seed funding from the Alkek Foundation to B. Samuel.

References

1. Lu M, Wang Z (2018) Linking gut microbiota to aging process: a new target for anti-aging. Food Sci Human Wellness 7:111–119
2. Gomez F, Monsalve GC, Tse V et al (2012) Delayed accumulation of intestinal coliform bacteria enhances life span and stress resistance in *Caenorhabditis elegans* fed respiratory deficient *E. coli*. BMC Microbiol 12:300
3. Sonowal R, Swimm A, Sahoo A et al (2017) Indoles from commensal bacteria extend healthspan. Proc Natl Acad Sci U S A 114: E7506–E7515
4. Sánchez-Blanco A, Rodríguez-Matellán A, González-Paramás A et al (2016) Dietary and microbiome factors determine longevity in *Caenorhabditis elegans*. Aging 8:1513–1539
5. Gusarov I, Gautier L, Smolentseva O et al (2013) Bacterial nitric oxide extends the lifespan of *C. elegans*. Cell 152:818–830
6. Han B, Sivaramakrishnan P, Lin C-CJ et al (2017) Microbial genetic composition tunes host longevity. Cell 169:1249–1262.e13
7. Virk B, Jia J, Maynard CA et al (2016) Folate acts in *E. coli* to accelerate *C. elegans* aging independently of bacterial biosynthesis. Cell Rep 14:1611–1620
8. Cabreiro F, Au C, Leung K-Y et al (2013) Metformin retards aging in *C. elegans* by altering microbial folate and methionine metabolism. Cell 153:228–239
9. Samuel BS, Rowedder H, Braendle C et al (2016) *Caenorhabditis elegans* responses to bacteria from its natural habitats. Proc Natl Acad Sci U S A 113:E3941–E3949
10. Dirksen P, Marsh SA, Braker I et al (2016) The native microbiome of the nematode *Caenorhabditis elegans*: gateway to a new host-microbiome model. BMC Biol 14:38
11. Berg M, Stenuit B, Ho J et al (2016) Assembly of the *Caenorhabditis elegans* gut microbiota from diverse soil microbial environments. ISME J 10:1998–2009
12. Zhang F, Berg M, Dierking K et al (2017) *Caenorhabditis elegans* as a model for microbiome research. Front Microbiol 8:485
13. Portal-Celhay C, Bradley ER, Blaser MJ (2012) Control of intestinal bacterial proliferation in regulation of lifespan in *Caenorhabditis elegans*. BMC Microbiol 12:49
14. Stiernagle T (2006) Maintenance of *C. elegans*. WormBook
15. Hazan R, Que Y-A, Maura D, Rahme LG (2012) A method for high throughput determination of viable bacteria cell counts in 96-well plates. BMC Microbiol 12:259
16. Pollock J, Glendinning L, Wisedchanwet T, Watson M (2018) The madness of microbiome: attempting to find consensus "best practice" for 16S microbiome studies. Appl Environ Microbiol 84. https://doi.org/10.1128/AEM.02627-17
17. Lee PY, Costumbrado J, Hsu C-Y, Kim YH (2012) Agarose gel electrophoresis for the separation of DNA fragments. J Vis Exp (62). https://doi.org/10.3791/3923
18. Bolyen E, Rideout JR, Dillon MR, et al (2018) QIIME 2: reproducible, interactive, scalable, and extensible microbiome data science. PeerJ Preprints
19. Martin M (2011) Cutadapt removes adapter sequences from high-throughput sequencing reads. EMBnet J 17:10

20. Walters W, Hyde ER, Berg-Lyons D et al (2016) Improved bacterial 16S rRNA gene (V4 and V4-5) and fungal internal transcribed spacer marker gene primers for microbial community surveys. mSystems 1. https://doi.org/10.1128/mSystems.00009-15
21. Caporaso JG, Lauber CL, Walters WA et al (2012) Ultra-high-throughput microbial community analysis on the Illumina HiSeq and MiSeq platforms. ISME J 6:1621–1624
22. García-González AP, Ritter AD, Shrestha S et al (2017) Bacterial metabolism affects the *C. elegans* response to cancer chemotherapeutics. Cell 169:431–441.e8
23. Scott TA, Quintaneiro LM, Norvaisas P et al (2017) Host-microbe co-metabolism dictates cancer drug efficacy in *C. elegans*. Cell 169:442–456.e18
24. Vega NM, Gore J (2017) Stochastic assembly produces heterogeneous communities in the *Caenorhabditis elegans* intestine. PLoS Biol 15:e2000633
25. Hillmann B, Al-Ghalith GA, Shields-Cutler RR et al (2018) Evaluating the information content of shallow shotgun metagenomics. mSystems 3. https://doi.org/10.1128/mSystems.00069-18
26. Amir A, McDonald D, Navas-Molina JA et al (2017) Deblur rapidly resolves single-nucleotide community sequence patterns. mSystems 2. https://doi.org/10.1128/mSystems.00191-16
27. Callahan BJ, McMurdie PJ, Rosen MJ et al (2016) DADA2: High-resolution sample inference from Illumina amplicon data. Nat Methods 13:581–583
28. Camacho C, Coulouris G, Avagyan V, Ma N, Papadopoulos J, Bealer K, Madden TL (2009) BLAST+: architecture and applications. BMC Bioinformatics 10:421
29. Nearing JT, Douglas GM, Comeau AM, Langille MGI (2018) Denoising the Denoisers: an independent evaluation of microbiome sequence error-correction approaches. PeerJ 6:e5364

Chapter 13

Measurements of Innate Immune Function in *C. elegans*

Kyle J. Foster, Deborah L. McEwan, and Read Pukkila-Worley

Abstract

The microscopic nematode *Caenorhabditis elegans* has emerged as a powerful system to characterize evolutionarily ancient mechanisms of pathogen sensing, innate immune activation, and protective host responses. Experimentally, *C. elegans* can be infected with a wide variety of human pathogens, as well as with natural pathogens of worms that were isolated from wild-caught nematodes. Here, we focus on an experimental model of bacterial pathogenesis that utilizes the human opportunistic bacterial pathogen *Pseudomonas aeruginosa* and present an algorithm that can be used to study mechanisms of immune function in nematodes. An initial comparison of the susceptibility of a *C. elegans* mutant to *P. aeruginosa* infection with its normal lifespan permits an understanding of a mutant's effect on pathogen susceptibility in the context of potential pleotropic consequences on general worm fitness. Assessing the behavior of nematodes in the presence of *P. aeruginosa* can also help determine if a gene of interest modulates pathogen susceptibility by affecting the host's ability to avoid a pathogen. In addition, quantification of the pathogen load in the *C. elegans* intestine during infection, characterization of immune effector transcription that are regulated by host defense pathways and an initial assessment of tissue specificity of immune gene function can refine hypotheses about the mechanism of action of a gene of interest. Together, these protocols offer one approach to characterize novel host defense mechanisms in a simple metazoan host.

Key words Innate immunity, *C. elegans*, Pathogens, Aging

1 Introduction

In their natural habitats, the microscopic nematode *Caenorhabditis elegans* forage microorganisms within decomposing organic matter. As a result, their evolution has been shaped by interactions with pathogenic and nonpathogenic bacteria. For over two decades, researchers have exploited a wealth of genetic tools available in *C. elegans* to characterize the host defense mechanisms utilized by nematodes to survive challenge from pathogenic microbes. This effort has revealed that *C. elegans* mount inducible antipathogen defenses toward diverse pathogens, which involve the elaboration of secreted immune effectors, and also program behavioral avoidance responses to minimize exposure to pathogens [1–5]. Interestingly, detection of pathogens in these contexts involves surveillance

Sean P. Curran (ed.), *Aging: Methods and Protocols*, Methods in Molecular Biology, vol. 2144,
https://doi.org/10.1007/978-1-0716-0592-9_13,

of core host processes that are often disrupted during microbial infection (e.g., translation and mitochondrial respiration) [6–10], monitoring for host damage associated with pathogen invasion [11], and sensory nervous system activation by microbial molecules [12–16]. Moreover, anti-pathogen immune defenses are induced following physical damage to core cellular structures; as a host protective response after DNA damage or disruption of the ubiquitin proteasome system [8, 9, 17]; and by a nuclear hormone receptor following activation by ligands in the chemical environment [18]. These studies have revealed that multiple biological processes are connected with pathogen defense mechanisms and have fueled interest in using genetic approaches in *C. elegans* to define new mechanisms of innate immune regulation. In this chapter, we aim to provide a framework for the experimental assessment of innate immune function in *C. elegans* by assimilating commonly used protocols in the field.

In the laboratory, *C. elegans* can be infected with a variety of human pathogens, as well as with natural pathogens isolated from nematode habitats in the wild [5, 19–21]. Here, we will focus on *C. elegans* experimental models that use the human opportunistic bacterial pathogen *Pseudomonas aeruginosa*, a widely used assay that has been the subject of several published protocols [22–24]. A *C. elegans–P. aeruginosa* pathogenesis assay can be used to determine if a gene of interest leads to enhanced susceptibility of *C. elegans* to bacterial infection when it is mutated or knocked down by RNAi [19, 25]. Interpretation of a phenotype in *C. elegans–P. aeruginosa* pathogenesis assay should be made with an understanding of how the gene affects the longevity of *C. elegans* growing under standard laboratory conditions to assess pleiotropic effects of the mutant or gene knockdown on general nematode fitness.

An assessment of *C. elegans* behavior in the presence of pathogenic bacteria is an important next step to determine if a gene affects susceptibility to *P. aeruginosa* infection by modulating the ability of the host to avoid the pathogen or by modulating some aspect of the inducible immune response [14, 15, 26]. Upon exposure to pathogenic food sources or noxious compounds, neuronal receptors induce programmed behavioral avoidance responses to minimize exposure to the insult [14, 27–30]. Avoidance behaviors are both innately programmed and learned as the result of prior exposure to toxic stimuli [15, 16, 27]. One way to determine if a gene of interest modifies the behavior of nematodes is to perform a lawn occupancy assay whereby *C. elegans* are exposed to a small lawn of a pathogenic bacteria and their behavioral response is assayed [26, 31, 32].

Does a gene of interest affect intestinal colonization of the bacterial pathogen? Mutations in key immune defense pathways in *C. elegans* cause an increased burden of bacteria in the nematode intestine, presumably as a consequence of the failed immune response [33, 34]. Alternatively, mutations can modify the ability of the host to tolerate infection or affect postinfection wound healing in a manner that does not modulate the burden of bacteria in the intestine [15, 35]. Measurements of bacterial colonization within the *C. elegans* intestine can help distinguish between these possibilities.

An important next step is to determine whether a gene of interest affects the function of known immune pathways. Multiple pathways operate in parallel in *C. elegans* to control protective host defenses during bacterial infection. Transgenic *C. elegans* strains that express green fluorescent protein under the control of a promoter for an innate immune effector, called transcriptional immune reporters, can provide a visual readout of host defense activation [18, 36–39]. Assessing a panel of these immune reporters in a mutant background can help focus subsequent genetic epistasis analyses.

When it is established that a gene of interest affects host defense mechanisms toward *P. aeruginosa*, it is often useful to determine the tissues where gene function is necessary to modulate antipathogen defenses. Transgenic *C. elegans* strains in which the RNAi machinery has been reconstituted in specific tissues are available and can provide a useful starting point to assess the tissue-specific roles for a gene of interest [8, 40]. We discuss the benefits and pitfalls of this method.

Together, these protocols offer an approach to assess immune gene function in *C. elegans*.

2 Materials

1. Worm Pick: Carefully break off the tip of a Pasteur pipette just below the neck. Over a flame, use forceps to slowly insert a 2-in. long segment of 90% platinum/10% iridium wire into the fractured end of the Pasteur pipette. Heat until the Pasteur pipette melts around the platinum wire, securing it in place. Once cooled, the wire tip can be hammered flat or pressed with jewelry pliers in order to increase its surface area.
2. 1-mm silicon carbide beads.
3. Streptomycin (2.5% w/v): Dissolve 1.25-g streptomycin sulfate in 50-mL ddH_2O. Filter-sterilize and store in the dark at 4 °C.

4. Nystatin (50 × 10 mg/mL stocks): Suspend 500-mg nystatin in 50-mL 70% EtOH. Aliquot into 1-mL tubes and store at −20 °C. Nystatin will precipitate out of the ethanol. Resuspend prior to use.
5. M9W (1 L): Dissolve 3-g of KH_2PO_4, 6-g of Na_2HPO_4, and 5-g NaCl in 1-L of ddQ H_2O. Autoclave and cool in a 55 °C water bath. Once solution has cooled, add 1-mL of filter-sterilized 1 M $MgSO_4$.
6. 5-Fluoro-2′-deoxyuridine [FUDR] (50 × 10 mg/mL stocks): Dissolve 0.5-g of 5-fluoro-2′-deoxyuridine in 50-mL ddQ H_2O. Filter-sterilize and aliquot into 1-mL tubes.
7. 5 mg/mL cholesterol in Ethanol (50-mL): Dissolve 0.25-g cholesterol in 50-mL of 99.5% EtOH. Filter-sterilize.
8. 1 M magnesium sulfate (100-mL): Dissolve 12.04-g $MgSO_4$ in 100-mL of ddH_2O. Autoclave.
9. 1 M Calcium Chloride (100-mL): Dissolve 14.7-g $CaCl_2$ in 100-mL of ddH_2O. Autoclave.
10. 2 N NaOH (50-mL): Dissolve 4-g NaOH in 50-mL of ddH_2O.
11. 5 M NaOH (50-mL): Dissolve 14.6-g NaOH in 50-mL of ddH_2O.
12. LB Broth (1 L): Dissolve 10-g Bacto tryptone, 5-g Bacto yeast extract, and 5-g NaCl in 1 L of ddQ H_2O. Autoclave.
13. LB Agar Plate Media (1 L): Dissolve 10-g Bacto tryptone, 5-g Bacto yeast extract, 5-g NaCl, 15-g Bacto agar, and dispense 1.5-mL 2 N NaOH in 1 L of ddQ H_2O. Autoclave. Place media in a 55 °C water bath for 30 min to cool before using.
14. "Slow Killing" Plate Media (1 L): Dissolve 3-g NaCl, 3.5-g Bacto peptone, and 17-g Bacto agar, in 1 L of ddH_2O. Autoclave. Place media in a 55 °C water bath for 30 min to cool. Once media is cool enough to be handled, add 1-mL 1 M $MgSO_4$, 1-mL 1 M $CaCl_2$, 1-mL 5 mg/mL cholesterol in EtOH, and 25-mL 1 M KPO_4 buffer. Using a Unispense plate pourer or repeater pipette, pour media into the desired plates.
15. Nematode Growth Media Plates (1 L): Dissolve 3-g NaCl, 2.5-g Bacto Peptone, and 17-g Bacto Agar, in 1 L of ddH_2O. Autoclave. Place media in a 55 °C water bath for 30 min to cool. Once media is cool enough to be handled, add 1-mL 1 M $MgSO_4$, 1-mL 1 M $CaCl_2$, 1-mL 5 mg/mL cholesterol in EtOH, 25-mL 1 M KPO_4 Buffer, 7.5-mL 2.5% (w/v) Streptomycin, and 1-mL 10 mg/mL Nystatin. Using a Unispense plate pourer or repeater pipette, pour media into the desired plates.

3 *C. elegans* Maintenance and Plate Preparation

3.1 NGM-OP50 Plate Preparation

1. Inoculate a single colony of *E. coli* OP50 in LB broth + Streptomycin (10 μg/mL). Incubate the culture at 37 °C overnight while shaking continuously at 250 rpm.
2. Spin resulting bacterial culture at 3000 × *g* for 10 min at 4 °C and pour off the supernatant. Ensure that the bacterial pellet is not disturbed. Resuspend bacterial pellet in appropriate volume of M9W so that the resulting OP50 concentration is 10×. Less concentrated OP5O can be used; however, worms may exhaust the food source and starve.
3. Spread between 100–500-μL of 10× OP50 onto the surface of 6- or 10-cm petri dishes containing NGM media, ensuring that the bacterial lawn does not reach the sides of the plates. Allow plates to dry completely before using. Seeded plates can be stored for 1–2 weeks at 15 °C.

3.2 P. aeruginosa PA14 Pathogenesis Assay Plate Preparation

1. Inoculate one *P. aeruginosa*, strain PA14 colony in 5-mL LB broth. Incubate culture overnight (16 h maximum) at 37 °C while shaking at 250 rpm.
2. Dry the *P. aeruginosa* PA14 plates uncovered in a biologic hood for 10 min.
3. Using a pipette, drop 10-μL of *P. aeruginosa* PA14 culture onto the center of Slow Kill (SK) plates. Carefully tip the plates from side to side in order to increase the surface area of the bacterial lawn, ensuring that the bacterial lawn does not reach the sides of the plates.
4. Incubate seeded *P. aeruginosa* PA14 plates at 37 °C for 24 h and then 24 h at 25 °C.

3.3 C. elegans Maintenance and Synchronization

3.3.1 Carry out all Centrifugation Steps at 900 × g Unless Otherwise Specified

1. From NGM plates containing starved L1-stage *C. elegans*, remove a "chunk" of agar and place on a 6- or 10-cm NGM plate containing *E. coli* OP50, prepared as described above. Incubate plates at 20 °C until they reach the gravid adult stage (approximately 3 days).
2. Using a serological pipette, add 3-mL of M9W to each NGM plate and rinse worms off into 15-mL conical tubes (combine plates of the same condition into one tube).
3. Pellet worms by spinning down tubes at 900 × *g* for 30 s. Remove supernatant until 500-μL liquid remains.
4. Add 400-μL of ~8% bleach and 100-μL 5 M NaOH into each tube and gently agitate by hand for 2–3 min. Check under a microscope to ensure that the carcasses have broken open and that eggs have been released. Do not expose eggs to concentrated bleach solution for more than 5 min. Quench the bleach by adding M9W up to 15-mL total volume.

5. Centrifuge for 30 s. Aspirate supernatant down to egg pellet.
6. Wash pellet with M9W 3–4 times.
7. Resuspend purified eggs in 5-mL of M9W and place on a rocker overnight at room temperature to allow the eggs to hatch and arrest at the L1 stage.
8. Drop approximately 200 L1-stage nematodes onto 6-cm NGM-OP50 plates and incubate at 20 °C until animals reach the L4 stage. *Note: You may need to concentrate the egg isolation if the volume required to obtain 200 eggs is greater than 200 μL. Volumes of buffer added to plates in excess of this amount may not dry completely.*

3.4 Pseudomonas aeruginosa PA14 Pathogenesis and C. elegans Lifespan Assays

The *P. aeruginosa* PA14 pathogenesis assay described here is also referred to as the "slow killing" assay [19, 23]. In this assay, *P. aeruginosa* kills *C. elegans* via an infection-like process that requires live bacteria and engages host defense mechanisms in the worm.

3.4.1 P. aeruginosa PA14 Pathogenesis Assay Setup

1. Prepare NGM-OP50 and *P. aeruginosa* PA14 pathogenesis assay plates as described in Subheadings 3.1 and 3.2, respectively.
2. Obtain synchronized populations of strains to be assessed as described in Subheading 3.3.
3. Spot the seeded *P. aeruginosa* PA14 plate with four 10-μL drops of 10 mg/mL FUDR around the perimeter of the bacterial lawn (final concentration 40 μg/mL). Leave plates to dry at room temperature for 30 min to allow the FUDR to absorb into the plates. Adding FUDR prevents the hatching of progeny during the assay.
4. Pick 50 *C. elegans* at the L4 stage to each of three separate *P. aeruginosa* PA14-seeded plates. Be careful not to injure the worms during assay setup. After animals are transferred to assay plates, ensure that residual OP50 is removed from the *P. aeruginosa* PA14-seeded plates.
5. Incubate assay plates at 25 °C for the duration of the pathogenesis assay.

3.4.2 Assay Scoring and Statistical Analyses

1. Score assay twice daily, by counting the total number of live and dead animals on each assay plate. Animals may need to be prodded in order to determine whether they have succumbed to the infection. Remove all carcasses by picking them into a flame.
2. Calculate the cumulative number of dead worms at each time point for each condition. Subsequently, determine the percent survival of each condition and plot this versus time.

3. Mean Lifespan, Kaplan–Meier Estimator, and Log-rank test calculations can be performed by inputting survival data into the Online Application for Survival Analysis (OASIS) [41].

3.4.3 C. elegans *Lifespan Assay Setup*

1. Prepare NGM-OP50 as described in Subheading 3.1.
2. Obtain synchronized populations of strains to be assessed as described in Subheading 3.3.
3. From synchronized NGM-OP50 plates, pick 50 synchronized L4 animals of each condition to three separate freshly seeded NGM-OP50 plates that contain 40 μg/mL FUDR). Be careful not to injure the worms during assay setup. FUDR is used in the *C. elegans* lifespan assays to mirror the conditions in the *P. aeruginosa* PA14 pathogenesis assays.
4. Incubate assay plates at 20 °C for the duration of the lifespan assay. A lifespan assay typically take several weeks. It is advised to wrap assay plates in aluminum foil in order to limit contamination for the duration of the experiment.

3.4.4 C. elegans *Lifespan Assay Scoring and Statistical Analyses*

1. Score lifespan assays once daily by counting the total number of live and dead animals on each assay plate. Animals may need to be tapped on the head in order to determine if they are alive. Remove all carcasses by picking them into a flame.
2. Data processing and statistical analyses can be performed as described in Subheading 3.4.2.

3.5 Lawn Occupancy Assay

3.5.1 Assay Setup

1. Prepare NGM-OP50 and *P. aeruginosa* assay plates as described in Subheadings 3.1 and 3.2, respectively.
2. Obtain synchronized populations of strains to be assessed as described in Subheading 3.3.
3. From synchronized OP50-NGM plates, pick 50 synchronized L4 animals of each strain to three separate *P. aeruginosa* assay plates. Be careful not to injure the worms during assay setup. After animals are transferred to assay plates, ensure that residual OP50 is removed from the *P. aeruginosa* assay plates..
4. Flip over assays plates and use a fine tip marker to carefully trace the perimeter of the pathogenic lawn.
5. Incubate plates at 25 °C for the duration of the assay.

3.5.2 Scoring and Statistical Analysis

1. Score assay at several time points by counting the total number of animals that reside off and on the bacterial lawn (Fig. 1). Typically, scoring the assay at 4, 8, 16, 24, and 30 h is sufficient to define the dynamics of behavioral avoidance to *P. aeruginosa*.

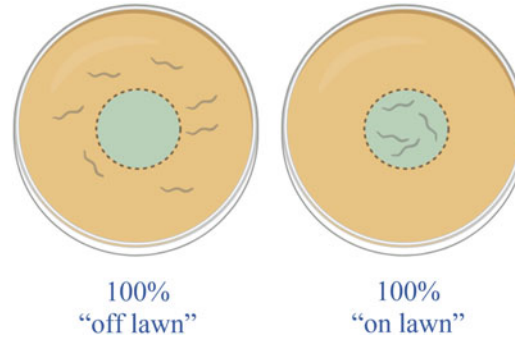

Fig. 1 Lawn avoidance assay. The figure shows how a typical lawn avoidance assay is scored

3.6 Quantification of P. aeruginosa *in the* C. elegans *Intestine*

3.6.1 Bacterial Isolation and Plating

1. Prepare NGM-OP50 and *P. aeruginosa* PA14 pathogenesis assay plates as described in Subheadings 3.1 and 3.2, respectively.
2. Obtain synchronized populations of the strains to be studied, as described in Subheading 3.3.
3. Pick 50 synchronized L4 animals of each strain to three separate *P. aeruginosa* PA14 pathogenesis assay plates. After animals are transferred to assay plates, ensure that residual OP50 is removed from the *P. aeruginosa* PA14-seeded plates.
4. Incubate *P. aeruginosa* PA14-seeded plates at 25 °C overnight.
5. Make bacterial isolation buffer by adding 300-mg tetramisole hydrochloride to 50-mL M9W. Vortex. Add 50-μL of 10% Triton X-100.
6. Pick 10–20 L4 worms from *P. aeruginosa* PA14 plates to unseeded NGM plates (one plate per condition per replicate) and let them crawl around for 10 min to dislodge bacteria attached to cuticle.
7. After 10 min, pick worms to another unseeded NGM plates and let them crawl around for 10 more minutes.
8. Dispense 150-μL of bacterial isolation buffer into 1.5-mL tubes (1 tube per condition).
9. Pick at minimum ten L4 animals of each condition from unseeded NGM plates into each 1.5-mL tube.
10. Important: Count the worms after transferring to ensure that you have an accurate worm count for each tube.
11. Spin down worms at 900 × *g* for 30 s. Remove supernatant down to 50-μL. Add 1-mL M9W. Repeat wash steps five times.
12. Perform one final wash. After last wash, transfer 200-μL of supernatant from each sample to clean Eppendorf tube before aspirating volume down to 100-μL. This aliquot will be used to assess the effectiveness of the wash steps at removing surface bacteria from the animals.

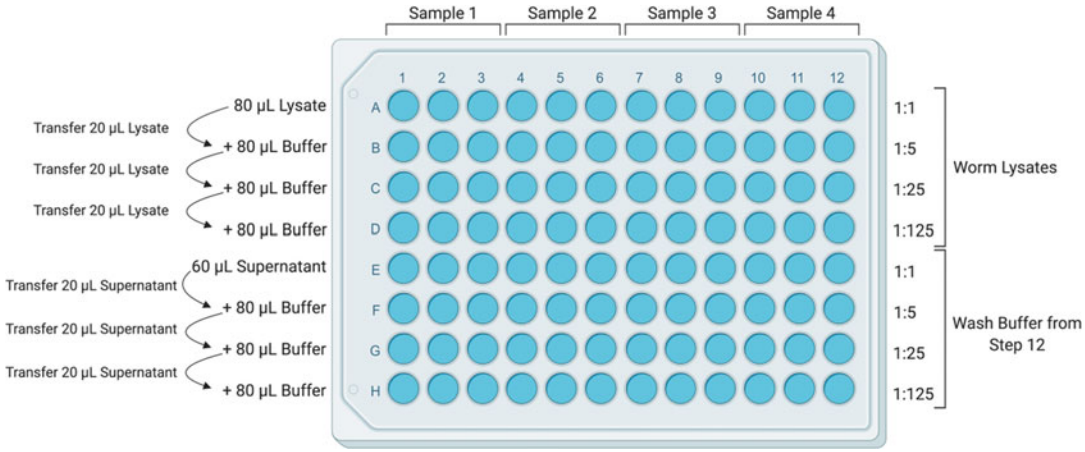

Fig. 2 Quantification of *P. aeruginosa* in the *C. elegans* intestine. The figure shows how to set up a 96-well plate to quantify *P. aeruginosa* CFUs in the *C. elegans* intestine

13. Count worms and record the final number present in each tube. Add 80-µL of bacterial isolation buffer + 20-µL of 10% Triton.
14. Add 400-mg (~0.5 mL mark) of 1.0-mm silicon carbide beads to 1.5-mL screw top Eppendorf tubes (1 tube per condition).
15. Transfer animals and liquid to bead-filled tubes by pipetting and vortex for 1 min to homogenize worms. Hold the tube vertically while vortexing to limit foam formation.
16. Transfer foam and liquid to new tube. Try to remove as much liquid as possible to ensure all bacteria are collected.
17. Spin tubes at 6000 × *g* for 2 min to reduce foam that formed during homogenization. Vortex solution briefly to resuspend bacterial pellet.
18. Perform three 1:5 serial dilutions of worm lysate for each sample in a 96 well plate. Dispense 60-µL of wash buffer (isolated form **step 12**) into row E and perform three 1:5 serial dilutions. Refer to plate diagram below (Fig. 2).
19. Plate 10-µL liquid from all wells onto agar plates. Tilt the plate and let the liquid spread down the plate. Incubate plates at 25 °C overnight.

3.6.2 Intestinal CFU Calculations

1. Count the number of colonies for each dilution under a dissecting microscope.
2. Calculate CFUs/worm by multiplying the number of colonies for each lysate dilution by its respective dilution factor, followed by a factor of 20 (each plated well contained 10-µL of the total 200-µL lysate volume).
3. Divide the total CFU count by the number of worms counted in **step 13** of Subheading 3.6.1.

4. Perform the calculations on wells containing the isolated wash buffer (**step 12** of Subheading 3.6.1) for each condition and subtract this result from the result obtained from plating the worm lysate. This step ensures that bacteria that may have been attached to the cuticle are not counted.

3.7 Utilizing Transcriptional Readouts to Examine Immune Pathway Function

Multiple pathways operate in parallel in *C. elegans* to promote host defense toward diverse pathogens. Understanding how putative immune regulators function together with these known host defense mechanisms can be challenging given the number of pathways that have been implicated. One approach to streamline this characterization is to examine the regulation of specific genes, which are known to be downstream of different host defense pathways in *C. elegans*. This approach can give an initial understanding of the mechanisms underlying immune misregulation in a particular mutant strain and can be accomplished using quantitative real time-PCR (qRT-PCR) to study the expression of these genes upon pathogen exposure in mutant or RNAi-knockdown animals. Alternatively, transgenic, GFP-based transcriptional reporters, in which the promoter for an immune effector has been fused to GFP, can provide a visual readout of pathway regulation. In Table 1, we have included a list of genes and available transcriptional reporters that are regulated downstream of different pathways, which have been implicated in *C. elegans* immune defenses.

It is important to note that this is not an exhaustive list of immune effectors or host defense pathways in *C. elegans*, and some of the listed genes are regulated by more than one pathway. In addition, depending on the context and pathogen used, the transcription of the listed putative immune effectors can be induced in other ways. For example, upon activation with a chemical ligand, the nuclear hormone receptor NHR-86 traffics to the promoters of genes whose basal expression is ensured by the p38 MAPK PMK-1 pathway. NHR-86 drives the induction of these genes in a manner independent of the PMK-1 immune pathway [18]. In addition, many of the genes listed in the table are not induced during infection with *P. aeruginosa*, but are upregulated during infection with other pathogens. For example, *clec-60* is important for defense against *Staphylococcus aureus* in a manner dependent on Wnt/β-catenin BAR-1 signaling [39, 42]. Therefore, we suggest that this list should be employed as a hypothesis-generating tool and as a prelude to further characterization of a new immune regulator with classic epistasis experiments, biochemical analyses of pathway activation and whole-genome transcriptome profiling studies.

3.8 An Initial Evaluation of Tissue Specificity in Immune Function

Innate immune defenses in *C. elegans* are controlled via tissue-autonomous mechanisms at sites of pathogen encounter, such as the intestine and hypodermis, and are also regulated tissue non-autonomously from neurons and the germ line. One commonly used method for the initial examination of tissue specificity of gene

Table 1
Genes and transcriptional immune reporters that are regulated downstream of pathways that have been implicated in *C. elegans* host defense

Pathway implicated in *C. elegans* immune defense	Selected genes downstream of indicated pathway	Selected transcriptional immune reporters	References
DBL-1/DAF-7 (TGFβ)	*clec-66, clec-67, lys-1*	P*clec-67::GFP* P*sma-6::GFP*	[43–49]
DAF-2/DAF-16 (Insulin Signaling)	*lys-7, dod-22, nlp-31*	P*lys-7::GFP* P*dod-24::GFP* P*nlp-31::GFP*	[50–53]
PMK-1 MAPK (basal regulation in the intestine)	*irg-4, irg-5, T24B8.5*	P*irg-4::GFP* P*irg-5::GFP* P*T24B8.5::GFP*	[18, 25, 36, 54]
PMK-1 MAPK (hypodermis)	*nlp-29, sta-2, elt-3*	P*nlp-29::GFP* P*elt-3::GFP*	[48, 55]
Wnt/β-catenin BAR-1	*ilys-3, lys-5, clec-60*	P*clec-60::GFP*	[13, 42]
ZIP-2	*irg-1, irg-2*	P*irg-1::GFP*	[38]
FSHR-1	*F01D5.5, clec-67, irg-5*	P*irg-5::GFP* P*clec-67::GFP*	[56, 57]
HLH-30 (TFEB)	*ilys-2, lys-3 lys-5*	P*ilys-2::GFP* HLH-30::GFP	[58]
SKN-1 (Nrf1)	*gst-4, gcn-1*	P*gst-4::GFP*	[59, 60]
ATFS-1 Mitochondrial Unfolded Protein Response (UPR^{MT})	*hsp-6*	P*hsp-6::GFP*	[61]
Endoplasmic Reticulum Protein Response (UPR^{ER})	*xbp-1* (activated splice form), *hsp-4*	P*hsp-4::GFP*	[62]

function is to use a panel of transgenic *C. elegans* strains in which the RNAi machinery has been reconstituted only in specific tissues, thereby permitting tissue-specific gene knockdown; however, an important caveat with this approach is discussed below.

We examined the ability of a panel of *C. elegans* strains that were engineered for tissue specific RNAi-mediated gene knockdown to perform RNAi in different tissues. We exposed these strains to *E. coli* RNAi-feeding bacteria that target genes, which confer visible phenotypes that are scorable under a dissecting microscope: RNAi-mediated knockdown of *act-5*, a gene required for intestinal development, causes developmental arrest; *unc-22(RNAi)*, a gene expressed in body wall muscle, causes a twitching phenotype in levamisole; knockdown of *bli-1* in the hypodermis causes blistering of the cuticle; and *pos-1(RNAi)*, a gene expressed in the germline,

Table 2
Assessing the specificity of transgenic *C. elegans* engineered for tissue-restricted RNAi

	Percent of animals with the phenotype associated with the indicated RNAi strain (total *n* counted)			
	Strains			
	Wild-type **N2** **Capable of RNAi in intestine, germline and hypodermis**	**MGH167** ***sid-1(qt9); alxIs9 [Pvha-6p::sid-1::SL2::GFP]*** **Designed to perform RNAi only in intestine [8]**	**VP303** ***rde-1(ne219); kbIs7 [Pnhx-2::rde-1+ rol-6(su1006)]*** **Designed to perform RNAi only in intestine [8]**	**JM43** ***rde-1(ne219); Is [Pwrt-2::rde-1; Pmyo-2::rfp]*** **Designed to perform RNAi only in hypodermis [40]**
L4440(RNAi) Control vector	0% (82)	0% (96)	0% (199)	0% (151)
act-5(RNAi) Affected tissue in *act-5(RNAi)*: intestine Phenotype scored: developmental arrest [63]	100% (74)	99% (70)	100% (170)	No arrest: 67% (77) Intermediate arrest: 16% (18) N2-like arrest: 17% (20)
unc-22(RNAi) Affected tissue in *unc-22(RNAi)*: body wall muscle Phenotype scored: twitching in 10 mM levamisole	100% (100)	0% (100)	0% (100)	13% (100)
bli-1(RNAi) Affected tissue in *bli-1(RNAi)*: hypodermis Phenotype scored: blistered cuticle	100% (97)	0% (168)	36% (168)	100% (214)
pos-1(RNAi) Affected tissue in *pos-1(RNAi)*: germ line Phenotype scored: >50 unhatched eggs	100% (10)	0% (10)	0% (10)	20% (10)

prevents eggs from hatching (Table 2). We found that *C. elegans* strain MGH167, in which machinery essential for RNAi was reconstituted only in the intestine, demonstrated excellent tissue specificity in RNAi-mediated gene knockdown with no detectable RNAi-mediated gene knockdown outside of the intestine [63]. In contrast, RNAi in *C. elegans* strain VP303, which also reports intestinal specificity, occurs efficiently in the intestine and not in body wall muscle or the germline; however, 36% of VP303 animals exposed to *bli-1(RNAi)* had cuticle blistering. Likewise, RNAi in the *C. elegans* strain JM43 is primarily restricted to hypodermal cells, although a subset of animals showed evidence of some RNAi-mediated gene knockdown in the intestine (33%) or body-wall muscle (13%). These data indicate that results with *C. elegans* JM43 and VP303 strains should be interpreted with caution. For these reasons, it can be useful to confirm results with tissue-restricted RNAi strains by generating mosaic *C. elegans* with a tissue-specific mutation in a given gene [64].

Experiments with tissue-restricted RNAi can help determine if expression of a gene is necessary in a given tissue for a particular immune-related phenotype (e.g., resistance to pathogen infection or induction of an immune effector). It is also important to determine if gene expression in a particular tissue is sufficient for the phenotype by generating transgenic *C. elegans* strains in which the gene of interest is only expressed in a particular tissue. Most commonly, this is accomplished by introducing an extrachromosomal array, which expresses the gene of interest under the control of a tissue-specific promoter, into a loss-of-function mutant and assaying for complementation of the immune-related phenotype.

References

1. Kim DH, Ewbank JJ (2018) Signaling in the innate immune response. WormBook 2018:1–35. https://doi.org/10.1895/wormbook.1.83.2
2. Meisel JD, Kim DH (2014) Behavioral avoidance of pathogenic bacteria by *Caenorhabditis elegans*. Trends Immunol 35(10):465–470. https://doi.org/10.1016/j.it.2014.08.008
3. Cohen LB, Troemel ER (2015) Microbial pathogenesis and host defense in the nematode *C. elegans*. Curr Opin Microbiol 23:94–101. https://doi.org/10.1016/j.mib.2014.11.009
4. Ewbank JJ, Pujol N (2016) Local and long-range activation of innate immunity by infection and damage in *C. elegans*. Curr Opin Immunol 38:1–7. https://doi.org/10.1016/j.coi.2015.09.005
5. Pukkila-Worley R, Ausubel FM (2012) Immune defense mechanisms in the *Caenorhabditis elegans* intestinal epithelium. Curr Opin Immunol 24(1):3–9. https://doi.org/10.1016/j.coi.2011.10.004
6. McEwan DL, Kirienko NV, Ausubel FM (2012) Host translational inhibition by *Pseudomonas aeruginosa* Exotoxin A Triggers an immune response in Caenorhabditis elegans. Cell Host Microbe 11(4):364–374. https://doi.org/10.1016/j.chom.2012.02.007
7. Dunbar TL, Yan Z, Balla KM, Smelkinson MG, Troemel ER (2012) *C. elegans* detects pathogen-induced translational inhibition to activate immune signaling. Cell Host Microbe 11(4):375–386. https://doi.org/10.1016/j.chom.2012.02.008
8. Melo JA, Ruvkun G (2012) Inactivation of conserved *C. elegans* genes engages pathogen- and xenobiotic-associated defenses. Cell 149(2):452–466. https://doi.org/10.1016/j.cell.2012.02.050

9. Reddy KC, Dunbar TL, Nargund AM, Haynes CM, Troemel ER (2016) The *C. elegans* CCAAT-enhancer-binding protein gamma is required for surveillance immunity. Cell Rep 14(7):1581–1589. https://doi.org/10.1016/j.celrep.2016.01.055
10. Pukkila-Worley R (2016) Surveillance immunity: an emerging paradigm of innate defense activation in *Caenorhabditis elegans*. PLoS Pathog 12(9):e1005795. https://doi.org/10.1371/journal.ppat.1005795
11. Zugasti O, Bose N, Squiban B, Belougne J, Kurz CL, Schroeder FC, Pujol N, Ewbank JJ (2014) Activation of a G protein-coupled receptor by its endogenous ligand triggers the innate immune response of *Caenorhabditis elegans*. Nat Immunol 15(9):833–838. https://doi.org/10.1038/ni.2957
12. Meisel JD, Panda O, Mahanti P, Schroeder FC, Kim DH (2014) Chemosensation of bacterial secondary metabolites modulates neuroendocrine signaling and behavior of *C. elegans*. Cell 159(2):267–280. https://doi.org/10.1016/j.cell.2014.09.011
13. Labed SA, Wani KA, Jagadeesan S, Hakkim A, Najibi M, Irazoqui JE (2018) Intestinal epithelial Wnt signaling mediates acetylcholine-triggered host defense against infection. Immunity 48(5):963–978. e964. https://doi.org/10.1016/j.immuni.2018.04.017
14. Aballay A (2009) Neural regulation of immunity: role of NPR-1 in pathogen avoidance and regulation of innate immunity. Cell Cycle 8(7):966–969. https://doi.org/10.4161/cc.8.7.8074
15. Cao X, Kajino-Sakamoto R, Doss A, Aballay A (2017) Distinct roles of sensory neurons in mediating pathogen avoidance and neuropeptide-dependent immune regulation. Cell Rep 21(6):1442–1451. https://doi.org/10.1016/j.celrep.2017.10.050
16. Hoffman C, Aballay A (2019) Role of neurons in the control of immune defense. Curr Opin Immunol 60:30–36. https://doi.org/10.1016/j.coi.2019.04.005
17. Ermolaeva MA, Segref A, Dakhovnik A, Ou HL, Schneider JI, Utermohlen O, Hoppe T, Schumacher B (2013) DNA damage in germ cells induces an innate immune response that triggers systemic stress resistance. Nature 501(7467):416–420. https://doi.org/10.1038/nature12452
18. Peterson ND, Cheesman HK, Liu P, Anderson SM, Foster KJ, Chhaya R, Perrat P, Thekkiniath J, Yang Q, Haynes CM, Pukkila-Worley R (2019) The nuclear hormone receptor NHR-86 controls anti-pathogen responses in *C. elegans*. PLoS Genet 15(1):e1007935. https://doi.org/10.1371/journal.pgen.1007935
19. Tan MW, Mahajan-Miklos S, Ausubel FM (1999) Killing of *Caenorhabditis elegans* by *Pseudomonas aeruginosa* used to model mammalian bacterial pathogenesis. Proc Natl Acad Sci U S A 96(2):715–720
20. Troemel ER, Felix MA, Whiteman NK, Barriere A, Ausubel FM (2008) Microsporidia are natural intracellular parasites of the nematode *Caenorhabditis elegans*. PLoS Biol 6(12):2736–2752. https://doi.org/10.1371/journal.pbio.0060309
21. Troemel ER (2011) New models of microsporidiosis: infections in Zebrafish, *C. elegans*, and honey bee. PLoS Pathog 7(2):e1001243. https://doi.org/10.1371/journal.ppat.1001243
22. Powell JR, Ausubel FM (2008) Models of *Caenorhabditis elegans* infection by bacterial and fungal pathogens. Methods Mol Biol 415:403–427. https://doi.org/10.1007/978-1-59745-570-1_24
23. Conery AL, Larkins-Ford J, Ausubel FM, Kirienko NV (2014) High-throughput screening for novel anti-infectives using a *C. elegans* pathogenesis model. Curr Protoc Chem Biol 6(1):25–37. https://doi.org/10.1002/9780470559277.ch130160
24. Kirienko NV, Cezairliyan BO, Ausubel FM, Powell JR (2014) *Pseudomonas aeruginosa* PA14 pathogenesis in *Caenorhabditis elegans*. Methods Mol Biol 1149:653–669. https://doi.org/10.1007/978-1-4939-0473-0_50
25. Troemel ER, Chu SW, Reinke V, Lee SS, Ausubel FM, Kim DH (2006) p38 MAPK regulates expression of immune response genes and contributes to longevity in *C. elegans*. PLoS Genet 2(11):e183. https://doi.org/10.1371/journal.pgen.0020183
26. Sun J, Singh V, Kajino-Sakamoto R, Aballay A (2011) Neuronal GPCR controls innate immunity by regulating noncanonical unfolded protein response genes. Science 332(6030):729–732. https://doi.org/10.1126/science.1203411
27. Zhang Y, Lu H, Bargmann CI (2005) Pathogenic bacteria induce aversive olfactory learning in *Caenorhabditis elegans*. Nature 438(7065):179–184. https://doi.org/10.1038/nature04216
28. Lee K, Mylonakis E (2017) An intestine-derived neuropeptide controls avoidance behavior in *Caenorhabditis elegans*. Cell Rep 20(10):2501–2512. https://doi.org/10.1016/j.celrep.2017.08.053

29. Singh J, Aballay A (2019) Microbial colonization activates an immune fight-and-flight response via neuroendocrine signaling. Dev Cell 49(1):89–99.e84. https://doi.org/10.1016/j.devcel.2019.02.001
30. Kumar S, Egan BM, Kocsisova Z, Schneider DL, Murphy JT, Diwan A, Kornfeld K (2019) Lifespan extension in *C. elegans* caused by bacterial colonization of the intestine and subsequent activation of an innate immune response. Dev Cell 49(1):100–117.e106. https://doi.org/10.1016/j.devcel.2019.03.010
31. Chang HC, Paek J, Kim DH (2011) Natural polymorphisms in *C. elegans* HECW-1 E3 ligase affect pathogen avoidance behaviour. Nature 480(7378):525–529. https://doi.org/10.1038/nature10643
32. Styer KL, Singh V, Macosko E, Steele SE, Bargmann CI, Aballay A (2008) Innate immunity in *Caenorhabditis elegans* is regulated by neurons expressing NPR-1/GPCR. Science 322 (5900):460–464. https://doi.org/10.1126/science.1163673
33. Kim DH, Feinbaum R, Alloing G, Emerson FE, Garsin DA, Inoue H, Tanaka-Hino M, Hisamoto N, Matsumoto K, Tan MW, Ausubel FM (2002) A conserved p38 MAP kinase pathway in *Caenorhabditis elegans* innate immunity. Science 297(5581):623–626. https://doi.org/10.1126/science.1073759
34. Portal-Celhay C, Bradley ER, Blaser MJ (2012) Control of intestinal bacterial proliferation in regulation of lifespan in *Caenorhabditis elegans*. BMC Microbiol 12:49. https://doi.org/10.1186/1471-2180-12-49
35. Head B, Aballay A (2014) Recovery from an acute infection in *C. elegans* requires the GATA transcription factor ELT-2. PLoS Genet 10 (10):e1004609. https://doi.org/10.1371/journal.pgen.1004609
36. Cheesman HK, Feinbaum RL, Thekkiniath J, Dowen RH, Conery AL, Pukkila-Worley R (2016) Aberrant activation of p38 MAP kinase-dependent innate immune responses is toxic to *Caenorhabditis elegans*. G3 (Bethesda) 6(3):541–549. https://doi.org/10.1534/g3.115.025650
37. Pukkila-Worley R, Feinbaum R, Kirienko NV, Larkins-Ford J, Conery AL, Ausubel FM (2012) Stimulation of host immune defenses by a small molecule protects *C. elegans* from bacterial infection. PLoS Genet 8(6): e1002733. https://doi.org/10.1371/journal.pgen.1002733
38. Estes KA, Dunbar TL, Powell JR, Ausubel FM, Troemel ER (2010) bZIP transcription factor zip-2 mediates an early response to *Pseudomonas aeruginosa* infection in *Caenorhabditis elegans*. Proc Natl Acad Sci U S A 107(5):2153–2158. https://doi.org/10.1073/pnas.0914643107
39. Irazoqui JE, Troemel ER, Feinbaum RL, Luhachack LG, Cezairliyan BO, Ausubel FM (2010) Distinct pathogenesis and host responses during infection of *C. elegans* by *P. aeruginosa* and *S. aureus*. PLoS Pathog 6: e1000982. https://doi.org/10.1371/journal.ppat.1000982
40. Espelt MV, Estevez AY, Yin X, Strange K (2005) Oscillatory Ca^{2+} signaling in the isolated *Caenorhabditis elegans* intestine: role of the inositol-1,4,5-trisphosphate receptor and phospholipases C beta and gamma. J Gen Physiol 126(4):379–392. jgp.200509355 [pii]. https://doi.org/10.1085/jgp.200509355
41. Han SK, Lee D, Lee H, Kim D, Son HG, Yang JS, Lee SV, Kim S (2016) OASIS 2: online application for survival analysis 2 with features for the analysis of maximal lifespan and healthspan in aging research. Oncotarget 7 (35):56147–56152. https://doi.org/10.18632/oncotarget.11269
42. Irazoqui JE, Ng A, Xavier RJ, Ausubel FM (2008) Role for beta-catenin and HOX transcription factors in *Caenorhabditis elegans* and mammalian host epithelial-pathogen interactions. Proc Natl Acad Sci U S A 105 (45):17469–17474. https://doi.org/10.1073/pnas.0809527105
43. Mallo GV, Kurz CL, Couillault C, Pujol N, Granjeaud S, Kohara Y, Ewbank JJ (2002) Inducible antibacterial defense system in *C. elegans*. Curr Biol 12(14):1209–1214
44. Mochii M, Yoshida S, Morita K, Kohara Y, Ueno N (1999) Identification of transforming growth factor-beta-regulated genes in *Caenorhabditis elegans* by differential hybridization of arrayed cDNAs. Proc Natl Acad Sci U S A 96 (26):15020–15025
45. Alper S, McBride SJ, Lackford B, Freedman JH, Schwartz DA (2007) Specificity and complexity of the *Caenorhabditis elegans* innate immune response. Mol Cell Biol 27 (15):5544–5553. MCB.02070-06 [pii]. https://doi.org/10.1128/MCB.02070-06
46. Liang J, Yu L, Yin J, Savage-Dunn C (2007) Transcriptional repressor and activator activities of SMA-9 contribute differentially to BMP-related signaling outputs. Dev Biol 305 (2):714–725. https://doi.org/10.1016/j.ydbio.2007.02.038
47. Roberts AF, Gumienny TL, Gleason RJ, Wang H, Padgett RW (2010) Regulation of genes affecting body size and innate immunity

by the DBL-1/BMP-like pathway in *Caenorhabditis elegans*. BMC Dev Biol 10:61. https://doi.org/10.1186/1471-213X-10-61

48. Pujol N, Zugasti O, Wong D, Couillault C, Kurz CL, Schulenburg H, Ewbank JJ (2008) Anti-fungal innate immunity in *C. elegans* is enhanced by evolutionary diversification of antimicrobial peptides. PLoS Pathog 4(7): e1000105. https://doi.org/10.1371/journal.ppat.1000105
49. Kerry S, TeKippe M, Gaddis NC, Aballay A (2006) GATA transcription factor required for immunity to bacterial and fungal pathogens. PLoS One 1:e77. https://doi.org/10.1371/journal.pone.0000077
50. Evans EA, Kawli T, Tan MW (2008) *Pseudomonas aeruginosa* suppresses host immunity by activating the DAF-2 insulin-like signaling pathway in *Caenorhabditis elegans*. PLoS Pathog 4(10):e1000175. https://doi.org/10.1371/journal.ppat.1000175
51. Murphy CT, McCarroll SA, Bargmann CI, Fraser A, Kamath RS, Ahringer J, Li H, Kenyon C (2003) Genes that act downstream of DAF-16 to influence the lifespan of *Caenorhabditis elegans*. Nature 424(6946):277–283
52. Ookuma S, Fukuda M, Nishida E (2003) Identification of a DAF-16 transcriptional target gene, scl-1, that regulates longevity and stress resistance in *Caenorhabditis elegans*. Curr Biol 13(5):427–431
53. Nathoo AN, Moeller RA, Westlund BA, Hart AC (2001) Identification of neuropeptide-like protein gene families in *Caenorhabditis elegans* and other species. Proc Natl Acad Sci U S A 98 (24):14000–14005. https://doi.org/10.1073/pnas.241231298
54. Pukkila-Worley R, Feinbaum RL, McEwan DL, Conery AL, Ausubel FM (2014) The evolutionarily conserved mediator subunit MDT-15/MED15 links protective innate immune responses and xenobiotic detoxification. PLoS Pathog 10(5):e1004143. https://doi.org/10.1371/journal.ppat.1004143
55. Dierking K, Polanowska J, Omi S, Engelmann I, Gut M, Lembo F, Ewbank JJ, Pujol N (2011) Unusual regulation of a STAT protein by an SLC6 family transporter in *C. elegans* epidermal innate immunity. Cell Host Microbe 9(5):425–435. https://doi.org/10.1016/j.chom.2011.04.011
56. Miller EV, Grandi LN, Giannini JA, Robinson JD, Powell JR (2015) The conserved G-protein coupled receptor FSHR-1 regulates protective host responses to infection and oxidative stress. PLoS One 10(9):e0137403. https://doi.org/10.1371/journal.pone.0137403
57. Powell JR, Kim DH, Ausubel FM (2009) The G protein-coupled receptor FSHR-1 is required for the *Caenorhabditis elegans* innate immune response. Proc Natl Acad Sci U S A 106(8):2782–2787. 0813048106 [pii]. https://doi.org/10.1073/pnas.0813048106
58. Visvikis O, Ihuegbu N, Labed SA, Luhachack LG, Alves AF, Wollenberg AC, Stuart LM, Stormo GD, Irazoqui JE (2014) Innate host defense requires TFEB-mediated transcription of cytoprotective and antimicrobial genes. Immunity 40(6):896–909. https://doi.org/10.1016/j.immuni.2014.05.002
59. Lynn DA, Dalton HM, Sowa JN, Wang MC, Soukas AA, Curran SP (2015) Omega-3 and -6 fatty acids allocate somatic and germline lipids to ensure fitness during nutrient and oxidative stress in *Caenorhabditis elegans*. Proc Natl Acad Sci U S A 112(50):15378–15383. https://doi.org/10.1073/pnas.1514012112
60. Hoeven R, McCallum KC, Cruz MR, Garsin DA (2011) Ce-Duox1/BLI-3 generated reactive oxygen species trigger protective SKN-1 activity via p38 MAPK signaling during infection in *C. elegans*. PLoS Pathog 7(12): e1002453. https://doi.org/10.1371/journal.ppat.1002453
61. Nargund AM, Pellegrino MW, Fiorese CJ, Baker BM, Haynes CM (2012) Mitochondrial import efficiency of ATFS-1 regulates mitochondrial UPR activation. Science 337 (6094):587–590. https://doi.org/10.1126/science.1223560
62. Richardson CE, Kooistra T, Kim DH (2010) An essential role for XBP-1 in host protection against immune activation in *C. elegans*. Nature 463(7284):1092–1095. https://doi.org/10.1038/nature08762. nature08762 [pii]
63. McEwan DL, Feinbaum RL, Stroustrup N, Haas W, Conery AL, Anselmo A, Sadreyev R, Ausubel FM (2016) Tribbles ortholog NIPI-3 and bZIP transcription factor CEBP-1 regulate a *Caenorhabditis elegans* intestinal immune surveillance pathway. BMC Biol 14(1):105. https://doi.org/10.1186/s12915-016-0334-6
64. Besseling J, Bringmann H (2016) Engineered non-Mendelian inheritance of entire parental genomes in *C. elegans*. Nat Biotechnol 34 (9):982–986. https://doi.org/10.1038/nbt.3643

Chapter 14

Measuring Phagocytosis in Bone Marrow-Derived Macrophages and Peritoneal Macrophages with Aging

Ryan Lu, Nirmal K. Sampathkumar, and Bérénice A. Benayoun

Abstract

The majority of age-related diseases share common inflammatory mechanisms, a phenomenon which has been described as "inflamm-aging," and genetic variants in immune and inflammatory genes are significantly associated with exceptional human longevity and/or age-related diseases. Consistently, aging is associated with increased macrophage infiltration into tissues. Macrophages are a key component of the innate immune system and the inflammatory response, which accomplish key tasks such as phagocytosis, antigen presentation, and cytokine production. Phagocytosis is the process by which specialized cells that can clear harmful foreign particles, pathogens, and dead or dying cells. Upon phagocytosis, foreign particles are internalized in vesicles, forming phagosomes. Phagosomes go on to fuse with lysosomes, and the ingested particles are neutralized by lysosomal enzymes. Macrophages have two main origins: tissue-resident macrophages differentiate from specific embryonic progenitors, whereas monocyte-derived macrophages differentiate from bone-marrow progenitors. Because of their key role in inflammation and damage repair, macrophages are a key cell type in age-related inflammatory diseases. Here, we describe an efficient method to quantify the phagocytotic ability of two types of primary macrophages in aging mice: bone marrow-derived macrophages (BMDMs) and tissue-resident peritoneal macrophages.

Key words Phagocytosis, Macrophages, Aging, Peritoneal macrophages, Bone marrow-derived macrophages, Zymosan, Innate immunity

1 Introduction

The majority of age-related diseases share common inflammatory mechanisms [1, 2], a phenomenon which has been described as "inflamm-aging" [1, 2], and genetic variants in immune and inflammatory genes are significantly associated with exceptional human longevity and/or age-related diseases [3, 4]. Macrophages are a key component of the innate immune system and the inflammatory response, which accomplish key tasks such as phagocytosis, antigen presentation and cytokine production [5]. Consistently,

Ryan Lu and Nirmal K. Sampathkumar contributed equally to this work.

Sean P. Curran (ed.), *Aging: Methods and Protocols*, Methods in Molecular Biology, vol. 2144,
https://doi.org/10.1007/978-1-0716-0592-9_14,

aging is associated with increased macrophage infiltration into tissues [6]. Phagocytosis is a phenomenon where a cell engulfs a foreign particle (bacteria, fungi, etc.) or dead cells, subsequently forming a phagosome, which later fuses with lysosome to process the cargo, then known as the phagolysosome. Macrophages are one of the key components of innate immunity and play a major role in cytokine production, antigen presentation, and clearing of pathogens/dead cells due to infection/injury through phagocytosis [7, 8].

Macrophages have two main origins: tissue-resident macrophages differentiate from specific embryonic progenitors, whereas monocyte-derived macrophages differentiate from bone-marrow progenitors [5, 9]. Resident macrophagepopulations exist across tissues (microglia in the brain, Kupffer cells in the liver, osteoclasts in the bone matrix, etc.) [9]. Because of their key role in inflammation and damage repair, macrophages are a key cell type in age-related inflammatory diseases [10]. Depending on the context, activated macrophages can promote a more proinflammatory state vs. prorepair or wound-healing environment [5]. Macrophages activated with proinflammatory signals (e.g., lipopolysaccharide, interferon gamma), are known as "classically activated" or "M1" macrophages [5]. In contrast, macrophages activated with tissue-remodeling signals (e.g., IL-4) are classified as "alternatively activated" or "M2" macrophage subsets [5]. Interestingly, M1 and M2 macrophages are associated to distinct metabolic and secretory outputs [5]. For instance, classically activated M1 macrophages secrete inflammatory cytokines (e.g., IL-6) and promote extra-cellular matrix hydrolysis through secretion of metalloproteinases, whereas alternatively activated M2 macrophages secrete anti-inflammatory cytokines, and promote extracellular matrix deposition [5]. Macrophages are diverse in their morphology, number and response to LPS activation with aging depending on their origin. For instance, macrophages from lungs show elevated response to LPS with age while the macrophages from spleen showed the opposite [11]. Therefore, it is critical to follow a robust method to determine the phagocytotic potential of macrophages throughout life, to evaluate the potential to mount an efficient immune response. Here, we describe an effective method to (1) isolate bone marrow-derived macrophages (BMDMs) in cohorts of aging mice (based on the protocol described in [12]) and peritonealmacrophages [13, 14], and (2) to perform phagocytosis assays to evaluate the phagocytic potential of these cells throughout life.

2 Materials

2.1 Isolation of Bone Marrow-Derived Macrophages (BMDMs)

1. "Column tube" for isolation of bone marrow cells: take a 500 μL centrifuge tube, cut off the cap and make few holes at the bottom of the tube using a 20 G needle. Place this tube in a sterile 1.5 mL microcentrifuge tube (based on the protocol described in [12]).
2. MACS rinsing buffer: MACS resuspension buffer (1× D-PBS, 2 mM EDTA) (Miltenyi Biotec) and 0.5% BSA (Miltenyi Biotec).
3. Red blood cell lysis buffer: dilute 10× RBC lysis buffer (Miltenyi Biotec) to 1× using ddH_2O.
4. MACS filters, 30 μm (Miltenyi Biotec) and 70 μm (Miltenyi Biotec).
5. (Optional) Monocyte isolation kit (Miltenyi Biotec).
6. (Optional) quadroMACS magnet (Miltenyi Biotec).
7. (Optional) LS columns (Miltenyi Biotec).
8. COUNTESS automated cell counter (Thermo Scientific) and slides (or hemocytometer), and trypan blue solution.

2.2 Isolation of Peritoneal Macrophages

1. Peritoneal Wash Buffer: 3% BSA (Akron), in D-PBS (Mg/Ca Free), filter sterile on 0.22 μm membrane.
2. MACS rinsing buffer: MACS resuspension buffer (1× D-PBS, 2 mM EDTA) (Miltenyi) and 0.5% BSA (Miltenyi Biotec).
3. (Recommended) Red blood cell lysis buffer: dilute 10× RBC lysis buffer (Miltenyi) to 1× using ddH_2O (*see***step 10** of Subheading 3.2).
4. Plastics and other supplies: 10 mL sterile syringes, 20 G needles, sterile 15 mL conicals, and serological pipettes.
5. Macrophages isolation kit (Peritoneum)—Miltenyi Biotec.
6. OctoMACS magnet (Miltenyi Biotec).
7. MS columns (Miltenyi Biotec).

2.3 Macrophage Culture Medium

1. DMEM/F12 medium with stabilized glutamine (VWR).
2. Fetal bovine serum [FBS] (Sigma).
3. Penicillin/Streptomycin 100× Solution (Genesee Scientific).
4. L929 cells (ATCC CCL-1).
5. Recombinant mouse M-CSF (Miltenyi Biotec).
6. D-PBS (VWR).
7. Cell cultureplates and other reagents: tissue-culture treated T75 flasks, sterile 15 and 50 mL conical tubes, and serological pipettes.

8. Macrophageculture medium: DMEM/F12, 10% FBS, 10% L929 conditioned medium, 1% Penicillin/Streptomycin, 1 ng/mL recombinant M-CSF.
9. 0.25% trypsin (Corning).

2.4 Phagocytosis Assay

1. Plastics and other supplies: 24-well tissue-culture plates (VWR), glass coverslips diameter 12 mm (Carolina), forceps to handle coverslips.
2. Ice-cold D-PBS: to quench the phagocytosis reaction and wash cells.
3. Fluorescently labeled Zymosan BioParticles® with Alexa 488 (Thermo Fisher scientific).
4. Macrophageculture medium (*see* Subheading 2.3).
5. 10% paraformaldehyde (Makron Fine Chemicals). Dilute to 4% with 1× D-PBS.
6. Microscope charged glass slides (Springside Scientific) and ProLong Diamond Antifade Mountant with DAPI (Thermo Fisher Scientific).

2.5 Animals

All animals are treated and housed in accordance to the Guide for Care and Use of Laboratory Animals. All experimental procedures are approved by the University of Southern California's Institutional Animal Care and Use Committee (IACUC), and are in accordance with institutional and national guidelines. All mice are maintained under specific pathogen-free (SPF) conditions in the AAALAC-accredited Ray R. Irani Hall Animal Facility at USC. C57BL/6N mice at different ages are obtained from the National Institute on Aging (NIA) colony at Charles Rivers and acclimated at the USC animal facility for at least 2 weeks before any processing. All mice are euthanized between 9 and 11 am to limit circadian effects (*see* **Note 1**). No live animal is censored.

We have successfully performed the described procedures in mice of both sexes and across a range of ages (3–29 months), with reasonable viability and visible Zymosan uptake. For the purpose of this method's description, we are focusing on data from male mice aged 4 and 20 months (Figs. 1 and 2).

3 Methods

All the steps involved in isolation of bone marrow cells and peritoneal macrophages are done on ice (unless indicated otherwise) and all centrifugation steps should be performed in centrifuges pre-cooled to 4 °C.

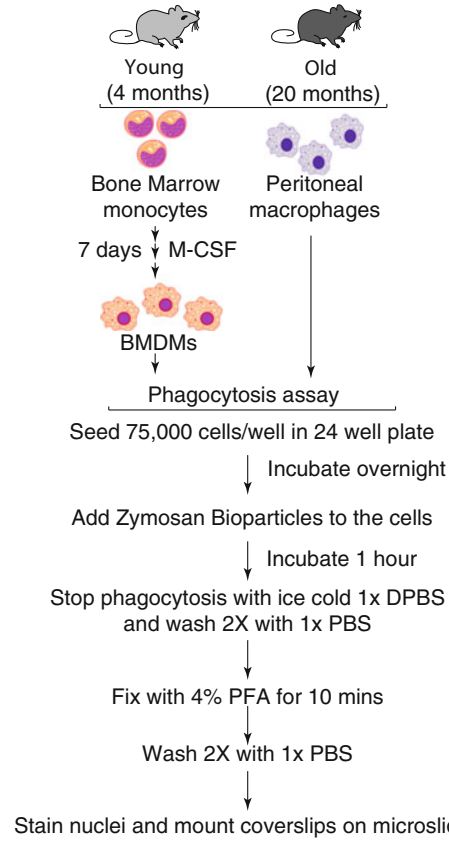

Fig. 1 Overview of phagocytosis assay steps using BMDMs and peritoneal macrophages. Flowchart depicting the steps involved in performing phagocytosis assay using bone marrow-derived macrophages and peritoneal macrophages. *BMDM* bone marrow-derived macrophages. *M-CSF*: macrophage colony-stimulating factor. *PFA* paraformaldehyde solution

3.1 Production of Conditioned Media Containing M-CSF

1. L929 cells are seeded at 50% confluency in a 600 mL cell culture flask (VWR) with 25 mL of DMEM/F12 medium supplemented with FBS.
2. Conditioned media (CM) is collected 2 days after cell seeding.
3. CM is filtered through a 0.45 μm filter to remove cells, and collected into 50 mL conical tubes.
4. CM is stored at −20 °C until use.

3.2 BMDM Isolation, Differentiation, and Culture

1. Euthanize mouse by CO_2 asphyxiation followed by cervical dislocation as a secondary means of euthanasia.
2. Carefully isolate the hind limbs without disturbing/breaking the bones from the euthanized mouse.
3. De-skin the isolated hind limbs and remove all the muscle (*see* **Note 2**).

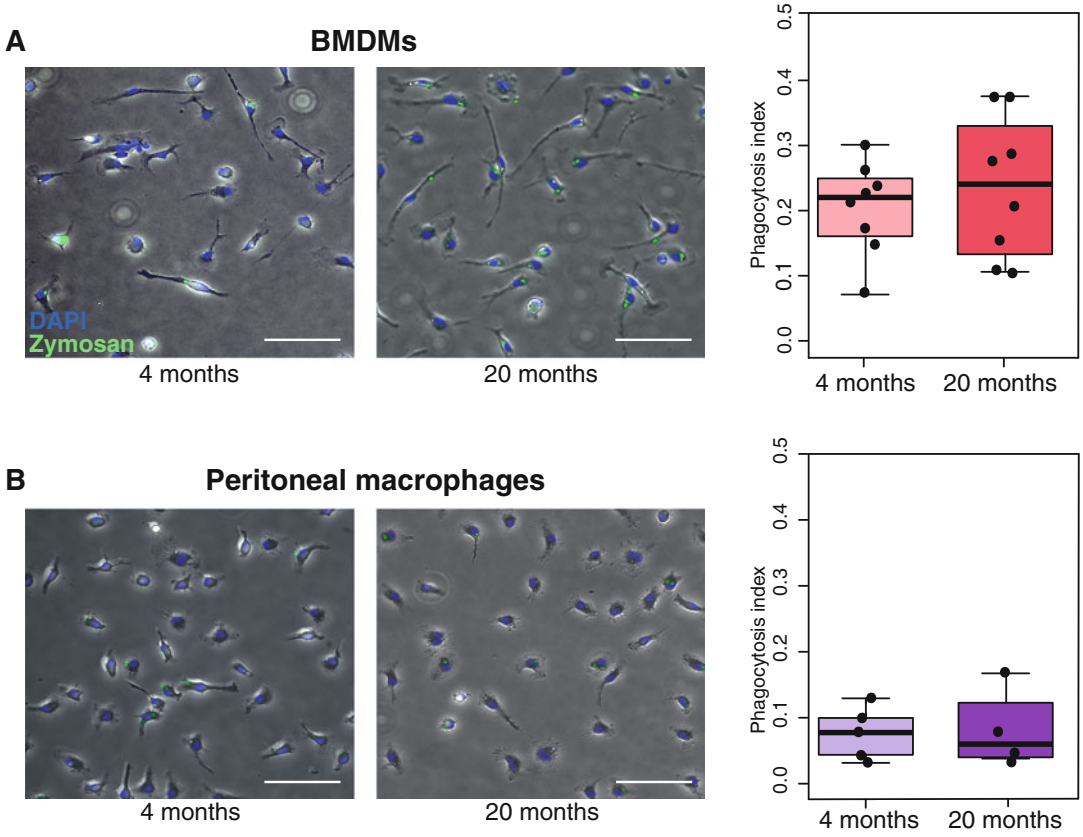

Fig. 2 Microscopy images of BMDM and peritoneal macrophages with Zymosan bioparticles phagocytosed. Representative microscopic images of BMDMs (**a**) or peritoneal macrophages (**b**) from 4- and 20-month-old mice, together with quantification of phagocytosis index. The phagocytosis index is defined as the ratio of cells with visible cargo after 1 h. Scale bar—75 μm

4. Place the cleaned bones in ice-cold D-PBS supplemented with 1% penicillin/streptomycin.
5. Repeat **steps 1–4** for all remaining animals (*see* **Note 2**).
6. Cut at the one end of the bones (knee joint) to expose the bone marrow cells to be collected by centrifugation. Cutting one side is sufficient.
7. Place all four cleaned hind limb bones in the 'Column tube for bone marrow cells isolation'.
8. Centrifuge the bones in their column tubes at 10,000 × *g* for 30 s in a tabletop centrifuge (*see* **Note 3**). All the bone marrow cells will be collected in the 1.5 mL microcentrifuge tubes, and bones will appear white (emptied of the marrow).
9. Resuspend the collected cells in 1 mL of MACS rinsing buffer and filter any chunks of muscle/nondisassociated cells using 70 μm cell strainers.

10. Add 10 mL of 1× RBC lysis buffer (Miltenyi Biotec), mix gently by pipetting up and down. Incubate at room temperature for 2 min. Do not vortex, which can cause undesired immune cell activation.
11. Centrifuge cells at 300 × *g* for 10 min, and carefully remove the supernatant. Wash the pellet twice with MACS rinsing buffer.
12. (Optional) For a purer cell fraction, use the Miltenyi Biotec MACS Monocyte separation kit, according to the manufacturer's instructions. Collect the eluted cells, centrifuge cells at 300 × *g* for 10 min and proceed to **step 13**.
13. Resuspend the cell pellet in 10 mL of macrophageculture medium and plate it in a T75 tissue culture flask. Check cell yield using a hemocytometer or COUNTESS automated cell counter (Thermo Scientific).
14. Incubate cells in a humidified cell culture incubator at 37 °C and 5% CO_2.
15. Do not disturb the flask, until replacement of the differentiation macrophage medium with fresh medium on day 3.
16. On days 7–8, all live cells are considered to be differentiated BMDMs.
17. Wash the cells twice with D-PBS, and detach the cells using 0.25% trypsin at 37 °C for 15 min. Flush the flask with a serological pipette several times to help with cell detachment, as macrophages are highly adherent to cell culture plastics.
18. Estimate the cell concentration. Check cell yield and viability using a hemocytometer or COUNTESS automated cell counter.
19. (Optional) Perform flow cytometry analysis using CD11b and/or F4/80 antibodies to estimate the purity of the cells.

3.3 Peritoneal Macrophage Isolation and Culture

1. Euthanize mouse by CO_2 asphyxiation followed by cervical dislocation as a secondary means of euthanasia.
2. Retract the abdominal skin manually to expose the peritoneal wall taking care to avoid puncturing it.
3. Carefully inject 10 mL of ice-cold Peritoneal Wash medium into the peritoneum using a 10 mL syringe with a 20 G needle. Take care to not puncture any internal organs.
4. Gently shake the mice for 30 s to dislodge any loose cells present in the peritoneal cavity.
5. Collect the peritoneal lavage using a 10 mL syringe with a 20 G needle. This suspension contains peritoneal cells including macrophages, B-cells and T-cells.

6. Remove the needle from the syringe, and slowly dispense peritoneal lavage into a 15 mL conical tube. Place tubes on ice until processing.
7. Repeat **steps 1–6** for all remaining animals.
8. Centrifuge peritoneal lavage at 300 × *g* for 10 min. Carefully aspirate the supernatant while avoiding the cell pellet.
9. Resuspend cells in 1 mL of MACS resuspension buffer.
10. If a red pellet is visible, perform the RBC lysis step (as described in Subheading 3.2).
11. Isolate macrophages following the manufacturer's instruction for MACS peritoneal macrophages isolation kit.
12. Collect the eluted cells, centrifuge cells at 300 × *g* for 10 min. Resuspended cells in 1–2 mL macrophageculture medium.
13. Check cell yield and viability using a hemocytometer or the COUNTESS automated cell counter. We routinely get a yield of 7×10^5–1.2×10^6 cells/mL for both 4- and 20-month-old animals.
14. Proceed to plating cells for different assays.

3.4 Phagocytosis Assay

1. Place one sterile coverslip per well of a 24-well tissue culture plate. Plate 75,000 cells per well in macrophageculture medium for 36–48 h prior to performing phagocytosis assay to allow for the cells to recover (*see* **Note 4** for peritonealmacrophages). We recommend preparing at least duplicate wells for each independent macrophageculture to account for well-to-well variability.
2. Dilute fluorescently labeled Zymosan BioParticles® to a concentration of 1 μg/mL in the complete macrophageculture medium.
3. Remove the medium from the 24-well plate and replace it with 250 μL of the bioparticle mixture in each well.
4. Incubate in the humidified cell culture incubator for 1 h at 37 °C and 5% CO_2.
5. After incubation, quench the phagocytosis process by adding 500 μL of ice-cold D-PBS.
6. Wash coverslip twice with ice-cold D-PBS to remove free bioparticles and decreased background.
7. Fix the cells using a 4% paraformaldehyde solution for 10 min at room temperature.
8. Wash coverslip twice with D-PBS.
9. Mount each coverslip onto a glass slide using a drop of ProLong Diamond Antifade Mounting medium. Allow the microscope slides dry in dark at room temperature for 24 h, and use nail polish to seal coverslips for long term storage at 4 °C.

10. Use an epifluorescence microscope to image the cells. Acquire images for at least 1000 cells per animal across replicate coverslips.
11. Using the ImageJ software (https://imagej.nih.gov/ij/), count the number of green positive cells (Zymosan-internalized cells), and total number of cells in any given image (based on DAPIstaining of nuclei). To note, because a cell may contain more than one phagosome, green positive cells need to be counted by hand in the software rather than with the count particle function.
12. Calculate the ratio of Alexa Fluor 488-positive cells to total number of cells to determine the phagocytosis index.

4 Notes

1. It is best to avoid getting blood into the peritoneal cavity when performing cervical dislocation; however, blood in the peritoneal cavity will not affect the final cell viability. Performing a red blood cell lysis step is then helpful to limit column clogging.
2. Bone marrow isolation and peritoneal lavage are always done at a cold temperature to minimize cell death.
3. Bones can be kept in D-PBS on ice for few hours without overall impact on cell viability and yield.
4. Never centrifuge the bones more than 30 s to get the bone marrow cells and immediately resuspend cells with MACS cell resuspension buffer to avoid clotting of red blood cells from the bone marrow.

Acknowledgments

This work was supported by NIA R00AG049934, an innovator grant from the Rose Hills foundation and a generous gift from the Hanson-Thorell Family to B.A.B.

References

1. Franceschi C, Campisi J (2014) Chronic inflammation (inflammaging) and its potential contribution to age-associated diseases. J Gerontol A Biol Sci Med Sci 69(Suppl 1):S4–S9. https://doi.org/10.1093/gerona/glu057
2. Xia S, Zhang X, Zheng S, Khanabdali R, Kalionis B, Wu J, Wan W, Tai X (2016) An update on inflamm-aging: mechanisms, prevention, and treatment. J Immunol Res 2016:8426874. https://doi.org/10.1155/2016/8426874
3. Franceschi C, Olivieri F, Marchegiani F, Cardelli M, Cavallone L, Capri M, Salvioli S, Valensin S, De Benedictis G, Di Iorio A, Caruso C, Paolisso G, Monti D (2005) Genes involved in immune response/inflammation, IGF1/insulin pathway and response to oxidative stress play a major role in the genetics of human longevity: the lesson of centenarians. Mech Ageing Dev 126(2):351–361. https://doi.org/10.1016/j.mad.2004.08.028

4. Jeck WR, Siebold AP, Sharpless NE (2012) Review: a meta-analysis of GWAS and age-associated diseases. Aging Cell 11 (5):727–731. https://doi.org/10.1111/j.1474-9726.2012.00871.x
5. Murray PJ (2017) Macrophage polarization. Annu Rev Physiol 79:541–566. https://doi.org/10.1146/annurev-physiol-022516-034339
6. Lumeng CN, Liu J, Geletka L, Delaney C, Delproposto J, Desai A, Oatmen K, Martinez-Santibanez G, Julius A, Garg S, Yung RL (2011) Aging is associated with an increase in T cells and inflammatory macrophages in visceral adipose tissue. J Immunol 187 (12):6208–6216. https://doi.org/10.4049/jimmunol.1102188
7. Goudot C, Coillard A, Villani AC, Gueguen P, Cros A, Sarkizova S, Tang-Huau TL, Bohec M, Baulande S, Hacohen N, Amigorena S, Segura E (2017) Aryl hydrocarbon receptor controls monocyte differentiation into dendritic cells versus macrophages. Immunity 47 (3):582–596.e586. https://doi.org/10.1016/j.immuni.2017.08.016
8. Villa A, Gelosa P, Castiglioni L, Cimino M, Rizzi N, Pepe G, Lolli F, Marcello E, Sironi L, Vegeto E, Maggi A (2018) Sex-specific features of microglia from adult mice. Cell Rep 23(12):3501–3511. https://doi.org/10.1016/j.celrep.2018.05.048
9. Gordon S, Pluddemann A (2017) Tissue macrophages: heterogeneity and functions. BMC Biol 15(1):53. https://doi.org/10.1186/s12915-017-0392-4
10. Oishi Y, Spann NJ, Link VM, Muse ED, Strid T, Edillor C, Kolar MJ, Matsuzaka T, Hayakawa S, Tao J, Kaikkonen MU, Carlin AF, Lam MT, Manabe I, Shimano H, Saghatelian A, Glass CK (2017) SREBP1 contributes to resolution of pro-inflammatory TLR4 signaling by reprogramming fatty acid metabolism. Cell Metab 25(2):412–427. https://doi.org/10.1016/j.cmet.2016.11.009
11. van Beek AA, Van den Bossche J, Mastroberardino PG, de Winther MPJ, Leenen PJM (2019) Metabolic alterations in aging macrophages: ingredients for inflammaging? Trends Immunol 40(2):113–127. https://doi.org/10.1016/j.it.2018.12.007
12. Amend SR, Valkenburg KC, Pienta KJ (2016) Murine hind limb long bone dissection and bone marrow isolation. J Vis Exp (110). https://doi.org/10.3791/53936
13. Zhang X, Goncalves R, Mosser DM (2008) The isolation and characterization of murine macrophages. Curr Protoc Immunol. Chapter 14:Unit 14.11. https://doi.org/10.1002/0471142735.im1401s83
14. Gonçalves R, Mosser DM (2015) The isolation and characterization of murine macrophages. Curr Protoc Immunol 111 (1):14.11.11–14.11.16. https://doi.org/10.1002/0471142735.im1401s111

Chapter 15

Chromatin Immunoprecipitation from *Caenorhabditis elegans* Somatic Cells

Mintie Pu and Siu Sylvia Lee

Abstract

Chromatin Immunoprecipitation is a regularly used method to detect DNA–protein interaction in diverse biological samples. Here we describe the application of ChIP for histone modifications in adult-stage *Caenorhabditis elegans* somatic cells.

Key words Chromatin, *Caenorhabditis elegans*, Formaldehyde, Cross-link

1 Introduction

Chromatin Immunoprecipitation (ChIP) is a widely used method to detect the localization of protein factors on chromatin. The interactions between proteins and protein-DNA can be first stabilized by reversible cross-linking by formaldehyde [1] or UV light [2] treatment. Chromatin is then fragmented by sonication or enzyme digestion [3] to generate chromatin fragments. Chromatin fragments that associate with the specific protein mark are then captured by specific antibodyies. The DNA embedded in the chromatin fragment is then recovered by immunoprecipitation. Here we describe the application of ChIP for histone modifications in adult *C. elegans* somatic cells based on the ChIP method in [4].

2 Materials

2.1 Caenorhabditis elegans Collection

M9 buffer: 3.0 g KH_2PO_4, 11.32 g $Na_2HPO_4{\cdot}7H_2O$, 5 g NaCl. Bring to 1 L with distilled water.

2.2 Chromatin Immunoprecipitation

Prepare all solutions using ultrapure water (prepared by purifying deionized water, to attain a sensitivity of 18 MΩ cm at 25 °C). Prepare and store all reagents at room temperature (unless

Sean P. Curran (ed.), *Aging: Methods and Protocols*, Methods in Molecular Biology, vol. 2144,
https://doi.org/10.1007/978-1-0716-0592-9_15,

indicated otherwise). Diligently follow all waste disposal regulations when disposing of waste materials. We do not add sodium azide to reagents.

1. Phosphate-buffered saline (PBS; 10×): 100 mM Na_2HPO_4, 18 mM KH_2PO_4, 1.37 M NaCl, 27 mM KCl (*see* **Note 1**).
2. Protease inhibitors.
3. 1% formaldehyde in PBS: dilute 16% formaldehyde (methanol-free) with PBS to 1% (*see* **Note 2**).
4. 2 M glycine.
5. RNase A.
6. 10% sarkosyl.
7. Protein A-Agarose beads.
8. Elution buffer: 1% SDS in TE with 250 mM NaCl (*see* **Note 3**).
9. 10 mg/mL Proteinase K: dissolve proteinase K with water. Store the aliquots at −20 °C.
10. FA buffer: 50 mM HEPES–KOH (pH 7.5), 1 mM EDTA, 1% Triton X-100, 0.1% sodium deoxycholate, 150 mM NaCl (*see* **Note 4**).
11. FA-1 M salt buffer: 50 mM HEPES–KOH (pH 7.5), 1 mM EDTA, 1% Triton X-100, 0.1% sodium deoxycholate, 1 M NaCl.
12. FA-500 mM salt buffer: 50 mM HEPES-KOH (pH 7.5), 1 mM EDTA, 1% Triton X-100, 0.1% sodium deoxycholate, 500 mM NaCl.
13. TEL buffer: 0.25 M LiCl, 1% NP-40, 1% sodium deoxycholate, 1 mM EDTA, 10 mM Tris–HCl, pH 8.0.

3 Methods

3.1 C. elegans *Collection*

Wash germline-less adult worms off plates with cold M9. Transfer worms in M9 into 15 mL or 50 mL conical tube by using glass pipette. Put the conical tube on ice and wait ~10 min for worms to settle to the bottom of the tube. Aspirate off the M9. Repeat the washing step one more time with adequate amount of M9 to remove as much OP50 as possible. Resuspend worms with cold M9 and centrifuge at 16,400 × *g* for 30 s in a clinical centrifuge to pellet worms. Remove as much M9 as possible. The collection procedure should be finished within 30 min. Snap-freeze worms with liquid nitrogen and store the worm pellet at −80 °C (*see* **Note 5**).

3.2 Chromatin Immunoprecipitation

1. Thaw worms on ice. Resuspend worms with cold M9 and drop worm suspension into liquid nitrogen to make frozen worm beads (*see* **Note 5**).
2. Grind frozen worm beads into fine powder in liquid nitrogen with mortar and pestle. Inspect the fine powder with microscope. When worms are ground into "worm fragment," stop grinding and transfer the fine powder into prechilled 50 mL conical tubes (*see* **Note 6**).
3. Thaw the fine powder on ice. Measure the sample volume (V1).
4. Add 10 × V1 of room temperature 1% formaldehyde in PBS into worm sample and incubate at room temperature for 10 min with gentle rocking.
5. Quench formaldehyde by adding glycine to a final concentration of 125 mM and incubating with gentle rocking for 5 min at room temperature.
6. Spin the sample at 4000 × *g* for 3 min at 4 °C. Wash the pellet with PBS (protease inhibitors added). Repeat this step two more times.
7. Resuspend pellet in FA buffer with protease inhibitors (*see* **Note 7**).
8. Sonicate the sample with Bioruptor (30 s ON and 1 min OFF) for 25–30 cycles (*see* **Note 7**).
9. Spin at 13,200 rpm (around 16,400 × *g*) for 15 min at 4 °C.
10. Quantitate total protein (*see* **Note 8**).
11. Incubate appropriate amount of worm lysate with antibody and 1% sarkosyl overnight at 4 °C with rotation (*see* **Note 8**).
12. Equilibrate Protein A-Agarose beads in FA buffer, preclear them with 10 mg/mL of BSA.
13. Set aside 10% of the worm lysate used in the IP in **step 11**, and store it at 4 °C to be used as "Input" the next day.
14. Next day, add 40 μL of precleared bead slurry (around 20 μL beads) to each IP, and incubate for 3 h at 4 °C with rotation.
15. Spin sample for 1–2 min at 16,400 × *g* at 4 °C.
16. Remove supernatant. Wash the beads with 1 mL of the following buffers with rotation:

    Twice with FA buffer + proteinase inhibitors for 5 min each at 4 °C.

    Once with FA-500 mM NaCl for 10 min at room temperature.

    Once with FA-1 M NaCl for 5 min at room temperature.

    Once with TEL buffer for 10 min at room temperature.

    Twice with TE for 5 min at room temperature.

17. Elute precipitated chromatin from protein A beads by adding 150 μL of elution buffer and incubate at 65 °C for 15 min. Every 5 min resuspend beads by flicking tube or quick vortex. Spin to collect the supernatant. Repeat elution step once. Combine the supernatants.
18. Add 300 μL of elution buffer to input samples from **step 13**.
19. Incubate ChIP samples from **step 17** and Input samples from **step 18** with 20 μg RNase A at 37 °C for 30 min.
20. Add 2 μL of 10 mg/mL proteinase K and incubate at 55 °C for 1 h.
21. Reverse cross-link at 65 °C overnight (*see* **Note 9**).
22. Purify DNA by Qiagen PCR purification columns (QIAquick PCR Purification Kit) and elute with 30 μL elution buffer.
23. Proceed either to Q-PCR (*see* **Note 10**) or to amplification for library construction.

4 Notes

1. PBS can be made as a 1× solution or as a 10× stock. To prepare 1 L of either 1× or 10× PBS, dissolve the reagents listed above in 800 mL of H_2O. Adjust the pH to 7.4 (or 7.2, if required) with HCl, and then add H_2O to 1 L. Dispense the solution into aliquots and sterilize them by autoclaving for 20 min at 15 psi (1.05 kg/cm^2) on liquid cycle or by filter sterilization. Store PBS at room temperature.
2. Prepare the formaldehyde solution in fume hood. Follow the instruction for using formaldehyde in all applications requiring "freshly prepared" formaldehyde solution.
3. TE: 10 mM Tris–HCl (pH 8.0), 1 mM EDTA.
4. Prepare 500 mM EDTA stock. Weigh out 186.12 g of EDTA. $Na_2{\cdot}2H_2O$ (molecular weight: 372.24). Transfer to 2 L beaker/conical flask. Add 800 mL deionized/Milli-Q water. While stirring vigorously on a magnetic stirrer, add NaOH pellet or 10 N NaOH to adjust the solution pH 8.0. ~20 g NaOH pellet is required to adjust the pH 8.0. It is not easy to dissolve EDTA. To dissolve the EDTA completely, solution pH 8.0 is required. Adjust the volume to 1000 mL with deionized water. Mix it again. Transfer the solution to autoclavable bottle. Sterilize the solution by autoclaving (20 min at 15 lb./sq.in. (psi) from 121–124 °C on liquid cycle).
5. For ChIP with protein factors instead of histones, the freezing step needs to be carried out right after cross-linking to preserve protein–protein and protein–DNA interactions.

6. Worms that are overground will be lost in the supernatant in **step 6**.
7. The volume of FA buffer and sonication cycle number are determined by sonication efficiency of the equipment. To determine the appropriate sonication condition, the sonicated chromatin needs to be processed through **steps 18–21**, and the size of the extracted DNA needs to be checked by electrophoresis. For histone modification ChIP, we use the sonication condition that produces DNA fragments ranging from 200 to 500 bp. We start with 10^4 adult worms in 400 μL FA buffer.
8. The optimal antibody amount needs to be empirically determined by comparing the IP specificity and recovery efficiency using Q-PCR. Primers for specific and nonspecific regions are needed for the Q-PCR. The optimal antibody amount should yield the highest recovery at specific regions without causing increased recovery at nonspecific regions.
9. To avoid condensation on tube lid, heat block with heated lid or PCR machine is recommended for overnight incubation at 65 °C.
10. The ChIP and Input DNA can be diluted 1:5 to 1:10 for Q-PCR. Four microliters of diluted DNA can be used for each Q-PCR.

References

1. Jackson V (1978) Studies on histone organization in the nucleosome using formaldehyde as a reversible cross-linking agent. Cell 15:945–954
2. Gilmour DS, Lis JT (1985) In vivo interactions of RNA polymerase II with genes of Drosophila melanogaster. Mol Cell Biol 5:2009–2018
3. Skene PJ, Henikoff S (2015) A simple method for generating high-resolution maps of genome-wide protein binding. Elife 4:e09225
4. Kolasinska-Zwierz P, Down T, Latorre I, Liu T, Liu XS, Ahringer J (2009) Differential chromatin marking of introns and expressed exons by H3K36me3. Nat Genet 41:376–381

Chapter 16

Transcriptional Profiling of *C. elegans* Adult Cells and Tissues with Age

Rachel Kaletsky and Coleen T. Murphy

Abstract

Multicellular organisms are composed of distinct cells and tissues that coordinate highly orchestrated responses to environmental challenges, including those that arise with age. Since *C. elegans* is a premier model system used to study the molecular and cellular regulators of adult and aging phenotypes, cell type- and tissue-specific approaches are needed to characterize the genome-wide expression changes associated with these responses. Here we describe a method for the FACS-based isolation and RNA sequencing of dissociated cells from adult *C. elegans*. This technique is amenable to profiling the cell- and tissue-specific gene expression changes in *C. elegans* mutants, including aging models, such as the *daf-2*/insulin-like signaling (IIS) pathway, and in wild-type animals with age.

Key words *Caenorhabditis elegans*, RNA-seq, Transcriptional profiling, Cell dissociation, FACS, Aging

1 Introduction

Aging is an actively regulated and highly conserved process that is controlled through the integration of genetic and environmental factors. *Caenorhabditis elegans* is widely used to study the processes that regulate aging, including the healthspan- and longevity-regulating insulin/IGF-1 signaling (IIS) pathway, which coordinates the nutritional and stress states of the organism with reproduction, cellular and tissue health, and lifespan [1]. Several studies using whole worms have shown that transcriptional responses are associated with, and in many cases, responsible for various aging phenotypes [2, 3]. However, our understanding of the cell and tissue-specific contributions of gene expression changes to aging is more limited.

Several techniques have emerged to profile individual cell types in *C. elegans*, focusing primarily on larval animals. These include fluorescence-activated cell sorting (FACS) [4–7], nuclear isolation and sorting [8], polyA-binding protein RNA-tagging [4, 9, 10],

Sean P. Curran (ed.), *Aging: Methods and Protocols*, Methods in Molecular Biology, vol. 2144,
https://doi.org/10.1007/978-1-0716-0592-9_16,

spliced-leader RNA-tagging [11], and single cell approaches [12]. While each method exhibits both advantages and limitations, as described elsewhere [13], here we detail the method we developed for rapid transcriptional profiling of *C. elegans* tissues that is specifically optimized for the characterization of adult animals [14, 15]. Since most aging paradigms, including behavioral analyses, are performed in adult animals, our technique is highly suited to assess the adult, tissue-specific gene expression profiles of aging pathway mutants, individual cell types, and animals with age. We have successfully used this technique to profile several of *C. elegans*' adult tissues [14, 15], including neuronal cell subtypes [14, 16] and the neurons of adult IIS mutants [14].

The sample preparation and cell sorting steps are routinely performed within a few hours, using reagents and equipment available to many researchers, including a cell sorter and standard library preparation and sequencing platforms. Importantly, the method can be performed in both young adult and aged animals, allowing comparison of tissue-specific expression profiles across wild-type or mutant populations of various ages. The accessibility of this method should provide researchers with the tools needed to address important questions related to gene expression and aging.

2 Materials

Prepare all solutions at room temperature and using ultrapure water. Cuticle disruption buffer is routinely prepared ahead of time, aliquoted, and stored at −20 °C for future use. L-15/FBS and Pronase solutions are prepared freshly on the day of the experiment.

2.1 Cuticle Disruption and Cell Dissociation

1. M9 buffer: 6 g/L Na_2HPO_4, 3 g/L KH_2PO_4, 5 g/L NaCl, and 1 mL/L of 1 M $MgSO_4$dissolved in distilled water. Filter-sterilize and store at room temperature.
2. Cuticle disruption buffer: 200 mM DTT, 0.25% SDS, 20 mM HEPES pH 8.0, and 3% sucrose. Add 25 mL water to a 100 mL glass beaker. Add 125 mg SDS, 1.5 g sucrose, 1.54 g DTT, and 1 mL of 1 M HEPES, pH 8 to the beaker. Mix to dissolve. Add water to a total volume of 50 mL. Freeze in 1.5 mL aliquots in 1.7 mL microcentrifuge tubes and store at −20 °C. Thaw and bring to room temperature before use.
3. L-15 (Leibovitz) cell sorting buffer: Adjust osmolarity of L-15 to 340 mM. Check lot of L-15 from manufacturer for current osmolarity. Add 1 mM sucrose for every 1 mM mOsM to adjust. For example, if the lot is currently 312 mM, this requires 28 mM mOsM adjustment. In this example, add 4.79 g sucrose to 500 mL bottle of L-15. Stir to dissolve. Filter-sterilize and store at 4 °C until use.

4. Pronase solution: 20 mg/mL in osmolarity-adjusted L-15 media. Cell culture-grade protease from *Streptomyces griseus*, Sigma-Aldrich Cat No: P8811-1G. Dissolve 40 mg of Pronase in 2 mL of L-15 media (*see* **Note 1**). Gently mix to dissolve. Prepare immediately before use.
5. L-15-FBS solution: Add fetal bovine serum (FBS) to a final concentration of 2% in L15. Prepare 25 mL by adding 500 μL of FBS to 25 mL of mOsM-adjusted L-15 media. Keep on ice until use.
6. 5 μm pore size syringe filters for neuron cell sorting: Millex-SV 5.0 μm (Millipore). Prewet the membrane with 500 μL of the L-15-FBS solution immediately before use.
7. Nylon membranes for filtration of muscle, hypodermis, or intestinal cells: Cut nylon mesh (Elko Filtering Co., 03-20/14 for muscle and hypodermis (20 μM pore size), 03-35/16 for intestinal cells (35 μM pore size)) into a 10 × 10 cm square. Carefully fold the membrane into a filtration cone and place into a 50 mL conical centrifuge tube. Pre-wet the membrane with 500 μL of the cold L-15-FBS solution immediately before use.
8. TRIzol LS: Aliquot 850 μL TRIzol LS (Thermo Fisher) per 1.7 mL microcentrifuge tube as needed. Handle with caution and follow the appropriate hazardous waste management protocols.
9. 1 mL Luer-lock syringes.
10. FACS tubes.

2.2 RNA Isolation from Sorted Cells

1. Chloroform: ≥99.8% pure.
2. Isopropanol: 99.5% pure, RNase-free.
3. Ethanol: 100%. Dilute to 75% by adding 750 μL ethanol to 250 μL RNase-free water immediately before use.
4. RNase-free DNase kit for DNA digestion.
5. RNeasy MinElute Cleanup Kit (Qiagen).

2.3 Library Preparation from Isolated RNA

1. SMARTer Stranded Total RNA-Seq Kit v2—Pico Input Mammalian (Takara).

3 Methods

3.1 Isolation of Fluorescently Labeled Cells from Adult C. elegans

1. Wash adult worms into a 1.7 mL clear microcentrifuge tube using M9 (*see* **Note 2**). Be careful not to collect chunks of bacteria with worms. Briefly centrifuge tube to pellet the worms. If worm pellet exceeds 250 μL, split sample between

two tubes and process separately. Rapid washes are performed using a MiniSpin centrifuge and quick pulse settings to pellet worms and minimize the total sample processing time (*see* **Note 3**).

2. Wash worms a minimum of five times using 1 mL of M9 buffer each time (*see* **Note 4**), rapidly centrifuging each time. Washing is complete when the supernatant appears clear of bacteria.
3. Wash worm pellet once in 1 mL of room temp cuticle disruption buffer (*see* **Note 5**). Invert five times to mix. Pellet worms. Remove supernatant and discard.
4. Add 1 mL of room temperature cuticle disruption buffer.
5. Incubate at room temperature for exactly 6.5 min for Day 1 adult worms (*see* **Note 6**). Gently invert the tube frequently during the incubation. Alternatively, incubate the tube on a nutating mixer at low speed. Monitor cuticle disruption by frequently examining 1 μL of the sample on a slide (without a coverslip) using a dissecting microscope. Near the completion of this incubation, worms should appear dead and the head should appear slightly blunt as a result of the weakened cuticle. However, worms should not rupture at this step (*see* **Note 7**).
6. Pellet worms and discard the cuticle disruption buffer.
7. Rapidly wash worms five times in 1 mL of M9 buffer, removing as much of the supernatant as possible during each wash step (*see* **Note 8**).
8. Add 500 μL of freshly made, room temperature, 20 mg/mL Pronase to the worm pellet. Tap the tube to mix.
9. Incubate the samples up to 20 min at room temperature. Dissociation routinely takes between 12 and 20 min depending on the age of the worms, the effectiveness of cuticle disruption, and the lot of Pronase used (*see* **Note 9**). During the incubation, pipette vigorously with P200 tip for 100 times every 2–3 min, rotating between samples. Monitor dissociation after each round of pipetting by checking 2 μL of the worm–Pronase suspension under a dissecting microscope. Large worm chunks will gradually disappear, and the sample will become particulate and cloudy as it becomes a single-cell suspension. Move on to next step when the majority of worm chunks (especially intact heads for neuron isolation) are no longer visible (*see* **Note 10**).
10. Add 500 μL ice-cold L-15-FBS to dilute the Pronase solution and stop the dissociation process (*see* **Note 11**).
11. Use ice-cold L-15-FBS solution to prewet a 5 μM syringe filter (for neuron isolation) using a 1 mL syringe. For other cell types, prewet the appropriate nylon membrane over a conical tube (*see* **Note 12**).

12. Optional: Transfer 50 μL aliquot of dissociated, prefiltered worm sample to a tube containing 850 μL TRIzol LS. This prefiltered sample can serve as a 'whole worm' reference.
13. For syringe filtering, remove the plunger and attach the base of the syringe to the filter. Place the filter over a labeled FACS tube that is on ice. Pipette the dissociated cell suspension into the syringe base and carefully insert the plunger and apply pressure.
14. For filtering over nylon, place the prewet nylon membrane/labeled conical tube on ice. Pipette the cell suspension directly onto the membrane and allow the sample to filter by gravity flow.
15. Wash the syringe or nylon filter with 1 mL of L-15-FBS solution to recover any remaining cells. Additional L-15-FBS can be added directly to the sample or to wash the membrane, depending on the sample dilution requirements for the cell sorter being used. The filtered cell suspension should appear cloudy. For samples in conical tubes, transfer to FACS tubes for cell sorting. Keep samples on ice and in the dark until sorting (*see* **Note 13**).
16. Adjust fluorescence-based sorting gates using a freshly prepared cell suspension from age-matched, nonfluorescent worms (Fig. 1). Sort fluorescently labeled cells directly into TRIzol LS using a 100 μM nozzle. A sorted cell maximum volume of 150 μL can be added to each microcentrifuge tube containing 850 μL of TRIzol LS (*see* **Note 14**). Depending on the cell sorter and sorting conditions used, approximately

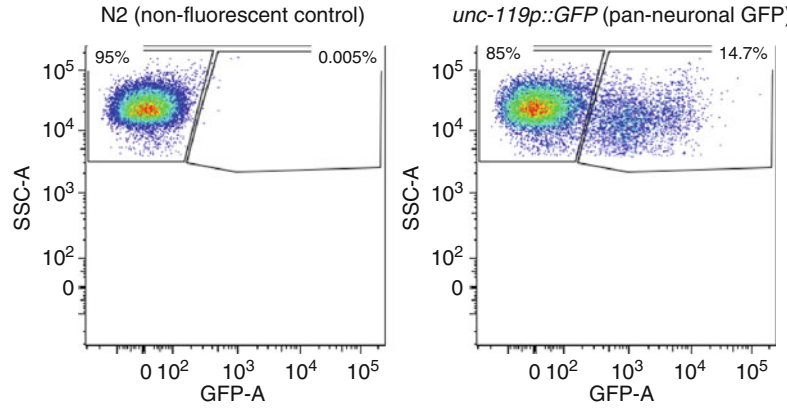

Fig. 1 Dissociated cells from Day 1 adult animals were sorted to collect GFP-labeled neurons. N2 worms that lack fluorescent protein expression were prepared at the same time as age-matched worms expressing GFP in all neurons using the *unc-119* promoter. Sorting gates were set using the N2 nonfluorescent control (left panel), and GFP-positive events (right panel) were collected directly into TRIzol LS

100,000–250,000 fluorescently labeled cells can be collected per tube (*see* **Note 15**). Suitable results have been obtained with at least 25,000 fluorescently labeled cells.

17. Freeze cells in TRIzol at −80 °C until RNA isolation (*see* **Note 16**).

3.2 RNA Extraction from Sorted Cells

All of the following steps are performed using RNase-free conditions.

1. Thaw worm–TRIzol mixture at room temperature. Incubate at 65 °C for 5 min with vortexing every minute.
2. Add 0.2 mL of chloroform to tube. Invert for 15 s. Incubate at room temperature for 2 min.
3. Spin for 10 min at 14,000 × *g* and 4 °C to separate the organic and aqueous phases.
4. Fill a new microcentrifuge tube with 0.55 mL isopropanol.
5. Using a pipette, move the upper aqueous layer to the tube containing isopropanol, and mix thoroughly by inverting the tube. Collect as much of the aqueous phase as possible without TRIzol or interface carryover. Discard the organic phase following appropriate waste handling protocols.
6. Incubate at −20 °C overnight to precipitate the RNA.
7. Pellet the RNA at 14,000 × *g* for 10 min at 4 °C (*see* **Note 17**).
8. Dispose of the supernatant, being careful not to disturb the pellet.
9. Gently wash pellet with 0.1 mL of freshly prepared 75% EtOH.
10. Spin 7,500 × *g* for 5 min at 4 °C.
11. Using a fine tip pipette, dispose of supernatant without disrupting the pellet.
12. Air-dry the pellet for approximately 10 min until little or no liquid is visible.
13. Resuspend the pellet in 87.5 μL RNase-free H_2O.
14. DNase treat the sample in solution using an RNase-Free DNase kit (Qiagen).
15. The RNA is subsequently cleaned up using an RNeasy MinElute Cleanup Kit (Qiagen) following the manufacturer's instructions.
16. Bioanalyze the RNA (Agilent RNA 6000 Pico Kit) to assess the quality of the RNA and to determine the RNA yield (Fig. 2).

3.3 Library Preparation for RNASequencing

1. Strand-specific RNA-seq libraries are prepared using the SMARTer Stranded Total RNA-Seq Kit v2—Pico Input Mammalian kit (Takara), following the manufacturer's instructions (*see* **Note 18**). The maximum volume/quantity of purified RNA is used for each sample.

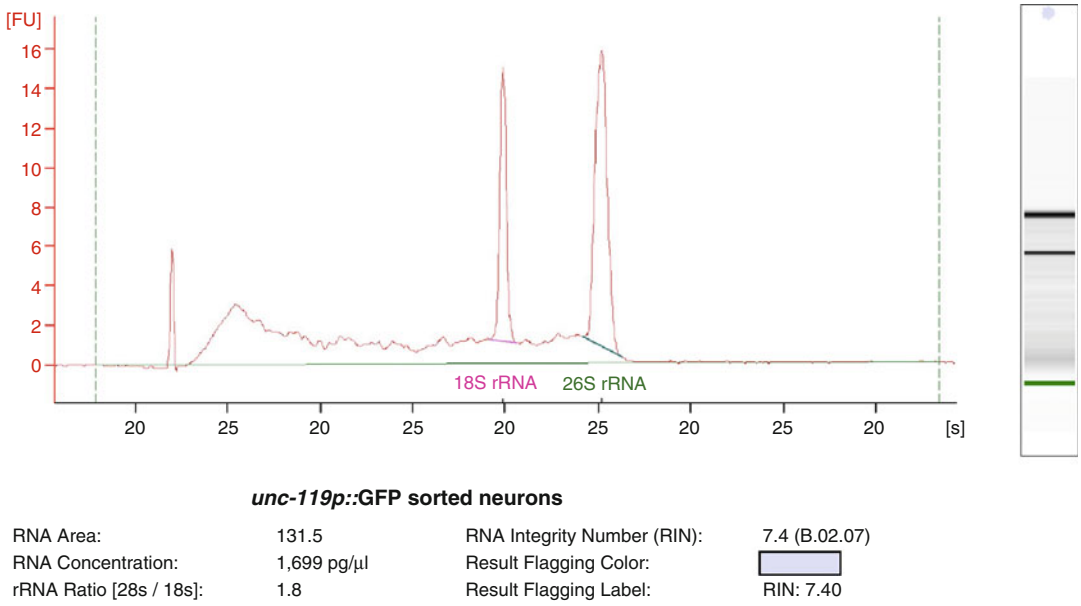

Fig. 2 RNA was isolated from 50,000 GFP-labeled cells collected in TRIzol LS by sorting on a Bio-Rad S3 Cell Sorter. 1 µL of purified RNA was analyzed using the Agilent 2100 Bioanalyzer and Agilent RNA 6000 Pico Reagents. *C. elegans* 18S and 26S rRNA peaks were used to determine the integrity of the RNA sample

2. Suitable results are usually obtained with >25 million reads per sample upon library sequencing.
3. Reads are mapped to the *C. elegans* genome using an alignment program, such as RNA-STAR or HISAT2.
4. The *C. elegans* genomic feature file (GFF) and resulting alignment file are used to generate gene count tables, which are then analyzed for differential gene expression using EdgeR or DESeq2.

4 Notes

1. Pronase and/or salts will precipitate if resuspended in PBS or M9. Dissolve in L-15 for best results. Preparation in distilled water also produces suitable results.
2. Start with approximately three plates (10 cm size) of synchronized, well-fed worms per strain that yields >100 µL of worm pellet when washed into a microcentrifuge tube. Always include an age-matched, nonfluorescent strain control that is prepared simultaneously with the fluorescent strain of interest. This will serve as a negative control for setting the cell sorting gates. We routinely maintain worms on HG (high growth) plates (NGM recipe modified as follows: 20 g/L Bacto peptone, 30 g/L Bacto agar, and 4 mL/L cholesterol (5 mg/mL in ethanol); all other components the same as NGM).

3. Begin the worm washing step approximately 45 min before the planned start of cell sorting to minimize the time between cell harvesting and collection.
4. Cell isolation and sorting can successfully be performed in the presence of Actinomycin D (100 μg/mL) to prevent new transcription that may occur during cell preparation. Act D is added to all solutions (Dissociation buffer, M9, Pronase, and L-15-FBS) immediately before isolation. Solutions are kept in the dark. Act D can diminish GFP intensity and/or increase autofluorescence. Use Act D-treated controls to establish sorting gates.
5. If cuticle disruption buffer was previously prepared and frozen at −20 °C, thaw at room temperature or in a 37 °C water bath until all of the components are completely dissolved and the solution appears clear. Allow enough time for the solution to equilibrate to room temperature before use.
6. Certain *C. elegans* mutant phenotypes, such as *dpy* and *roller* strains, are more sensitive to lysis conditions. Incubation times may vary. For *dpy* and *roller* strains examined, incubation in cuticle disruption buffer for exactly 6 min is sufficient.
7. Overexposure to the SDS-DTT in the cuticle disruption buffer will diminish cell integrity and GFP signal. This is often detected by the reduction or absence of a fluorescent cell signal during cell sorting.
8. The tubes containing the worms should no longer smell like DTT. Carryover of SDS-GFP will damage cells and affect the cell sorting efficiency.
9. Different batches of Pronase exhibit variable levels of activity resulting in different tissue and cell dissociation rates. In rare cases, incubation times sometimes last up to 25 min.
10. Proceed to next step immediately when intact worms are no longer visible and the appropriate level of tissue and cell disruption is achieved. Some large worm fragments may be acceptable depending on the target cell type. Avoid overdigestion, since this may lead to cell damage and loss.
11. The FBS solution can alternatively be made in PBS (phosphate buffered saline, calcium and magnesium free) without any loss in cell sorting efficiency.
12. This step can be performed at any time during the experiment prior to filtration. The mechanical dissociation step is time intensive, especially if multiple samples are being prepared simultaneously. We often prewet the filters at the beginning of the protocol for convenience.

13. It is critical to work rapidly through the entire cell dissociation protocol. Cells and cell fragments are highly fragile. Optimal sorting conditions are achieved when cells are harvested and on ice within 45 min of starting the isolation.
14. Exceeding the volume of sorted cells per tube will dilute the TRIzol LS reagent such that RNases are not effectively neutralized. It is recommended to follow the manufacturer's guidelines for reagent use.
15. Tubes containing TRIzol and sorted cells should be thoroughly mixed by inverting or vortexing. For sorts that last several hours, sorting is periodically paused approximately every hour to mix cells in TRIzol.
16. We have successfully sorted cells and isolated RNA from aged animal tissues (testing up to Day 10 adults) using the same protocol. Incubation times in Pronase may be slightly reduced and should be monitored closely.
17. It is unlikely that enough RNA is present to produce a visible pellet. It is useful to mark the orientation of the tube in the centrifuge so that the location of the RNA pellet can be avoided during pipetting.
18. rRNA depletion using the standard kit protocol is ineffective for *C. elegans*. It is optional to omit this step from the manufacturer's protocol.

Acknowledgments

This work was supported by an NIH Pioneer Award (DP1, 5DP1GM119167) and Cognitive Aging R01 (R01AG034446) to C.T.M.

References

1. Kenyon CJ (2010) The genetics of ageing. Nature 464:504–512
2. Tepper RG, Ashraf J, Kaletsky R, Kleemann G, Murphy CT, Bussemaker HJ (2013) PQM-1 complements DAF-16 as a key transcriptional regulator of DAF-2-mediated development and longevity. Cell 154:676–690
3. Murphy CT, McCarroll SA, Bargmann CI, Fraser A, Kamath RS, Ahringer J, Li H, Kenyon C (2003) Genes that act downstream of DAF-16 to influence the lifespan of *Caenorhabditis elegans*. Nature 424:277–283
4. Spencer WC, Zeller G, Watson JD, Henz SR, Watkins KL, McWhirter RD, Petersen S, Sreedharan VT, Widmer C, Jo J, Reinke V, Petrella L, Strome S, Von Stetina SE, Katz M, Shaham S, Rätsch G, Miller DM (2011) A spatial and temporal map of *C. elegans* gene expression. Genome Res 21:325–341
5. Spencer WC, McWhirter R, Miller T, Strasbourger P, Thompson O, Hillier LW, Waterston RH, Miller DM (2014) Isolation of specific neurons from *C. elegans* larvae for gene expression profiling. PLoS One 9: e112102
6. Fox RM, Von Stetina SE, Barlow SJ, Shaffer C, Olszewski KL, Moore JH, Dupuy D, Vidal M, Miller DM (2005) A gene expression fingerprint of *C. elegans* embryonic motor neurons. BMC Genomics 6:42
7. Zhang Y, Ma C, Delohery T, Nasipak B, Foat BC, Bounoutas A, Bussemaker HJ, Kim SK,

Chalfie M (2002) Identification of genes expressed in *C. elegans* touch receptor neurons. Nature 418:331–335

8. Haenni S, Ji Z, Hoque M, Rust N, Sharpe H, Eberhard R, Browne C, Hengartner MO, Mellor J, Tian B, Furger A (2012) Analysis of *C. elegans* intestinal gene expression and polyadenylation by fluorescence-activated nuclei sorting and 3′-end-seq. Nucleic Acids Res 40:6304–6318
9. Roy PJ, Stuart JM, Lund J, Kim SK (2002) Chromosomal clustering of muscle-expressed genes in *Caenorhabditis elegans*. Nature 418:975–979
10. Blazie SM, Babb C, Wilky H, Rawls A, Park JG, Mangone M (2015) Comparative RNA-Seq analysis reveals pervasive tissue-specific alternative polyadenylation in *Caenorhabditis elegans* intestine and muscles. BMC Biol 13:4
11. Ma X, Zhan G, Sleumer MC, Chen S, Liu W, Zhang MQ, Liu X (2016) Analysis of *C. elegans* muscle transcriptome using trans-splicing-based RNA tagging (SRT). Nucleic Acids Res 44(21):e156
12. Cao J, Packer JS, Ramani V, Cusanovich DA, Huynh C, Daza R, Qiu X, Lee C, Furlan SN, Steemers FJ, Adey A, Waterston RH, Trapnell C, Shendure J (2017) Comprehensive single-cell transcriptional profiling of a multicellular organism. Science 357:661–667
13. Handley A, Schauer T, Ladurner AG, Margulies CE (2015) Designing cell-type-specific genome-wide experiments. Mol Cell 58:621–631
14. Kaletsky R, Lakhina V, Arey R, Williams A, Landis J, Ashraf J, Murphy CT (2016) The *C. elegans* adult neuronal IIS/FOXO transcriptome reveals adult phenotype regulators. Nature 529:92–96
15. Kaletsky R, Yao V, Williams A, Runnels AM, Tadych A, Zhou S, Troyanskaya OG, Murphy CT (2018) Transcriptome analysis of adult *Caenorhabditis elegans* cells reveals tissue-specific gene and isoform expression. PLoS Genet 14:e1007559
16. Wang J, Kaletsky R, Silva M, Williams A, Haas LA, Androwski RJ, Landis JN, Patrick C, Rashid A, Santiago-Martinez D, Gravato-Nobre M, Hodgkin J, Hall DH, Murphy CT, Barr MM (2015) Cell-specific transcriptional profiling of ciliated sensory neurons reveals regulators of behavior and extracellular vesicle biogenesis. Curr Biol 25:3232–3238

Chapter 17

Asessing Tissue-Specific Autophagy Flux in Adult *Caenorhabditis elegans*

Jessica T. Chang, Malene Hansen, and Caroline Kumsta

Abstract

The cellular recycling process of autophagy is essential for survival, development, and homeostasis. Autophagy also plays an important role in aging and has been linked to longevity in many species, including the nematode *C. elegans*. Study of the physiological roles of autophagy during *C. elegans* aging requires methods for the spatiotemporal analysis of autophagy. Here we describe a method for assessing autophagic flux in multiple tissues of *C. elegans* by quantifying the pool of autophagic vesicles using fluorescently labelled Atg8/LGG-1 reporters upon autophagy inhibition using bafilomycin A_1 (BafA). This methodology has revealed that autophagic activity varies in different cell types of *C. elegans* during aging.

Key words Autophagic flux, Aging, Bafilomycin A, *C. elegans*

1 Introduction

Macroautophagy (hereafter referred to as autophagy) facilitates degradation and recycling of cytosolic components, referred to as cargo, in response to nutrient deprivation or other stresses. Autophagy is initiated by the nucleation of a double membrane, which forms the phagophore. Upon completion and maturation, autophagosomes fuse with acidic lysosomes, resulting in the degradation of the sequestered content by hydrolases [1]. Autophagy is essential for survival, development, and homeostasis and may protect against pathologies, including neurodegeneration and aging [2, 3].

Autophagic vesicles are commonly monitored using fluorescently tagged Atg8/LC3. During autophagy induction, Atg8 is cleaved, conjugated to phosphatidylethanolamine, and inserted into the autophagosomal membrane [4]. GFP-tagged Atg8 visualizes phagophores, autophagosomes and amphisomes (collectively referred to below as autophagosomal vesicles) as fluorescent punctae. The *C. elegans* homolog of Atg8 [5], LGG-1, is expressed in various tissues of the adult animal, including neurons [6]. A GFP-tagged LGG-1/Atg8 reporter under the control of its

Sean P. Curran (ed.), *Aging: Methods and Protocols*, Methods in Molecular Biology, vol. 2144,
https://doi.org/10.1007/978-1-0716-0592-9_17,

endogenous promoter visualizes autophagosomal structures in hypodermal seam cells, intestinal cells, body-wall muscle and pharynx [6, 7], whereas a GFP-tagged LGG-1/Atg8 reporter under the control of a neuronal promoter (*rgef-1p*) specifically visualizes pan-neuronal autophagosomal structures [8]. However, quantifying the number of autophagosomes does not conclusively inform on the status of autophagy, which is a dynamic, multistep process [4]. An increase in the number of GFP::LGG-1/Atg8 punctae could result from increased formation of autophagosomes (i.e., increased autophagic activity), or a block of downstream steps of the autophagy process (i.e., decreased autophagic activity), respectively [9–11]. To distinguish between these two scenarios, acute inhibition of autophagy is performed using "autophagy flux" assays [4, 11]. In such assays, autophagy is inhibited by using chemical inhibitors such as bafilomycin A_1 (BafA), which blocks autophagosomal turnover by inhibiting V-ATPase activity and preventing lysosomal acidification [9, 11]. Autophagosome numbers are compared between BafA inhibition and the control conditions. A change in the number of autophagosomes upon BafA addition indicates that autophagy is active, whereas no change indicates that the cell/tissue is experiencing a block in autophagy (Fig. 1). Using this assay, we recently assessed autophagic activity in a tissue-specific manner of animals of different ages and found that autophagic activity declines with age in the intestine, pharynx, body-wall muscle, and nerve-ring neurons of wild-type *C. elegans*, albeit with tissue-specific differences [9, 10]. Furthermore, our analyses of long-lived animals revealed that they were capable of maintaining autophagic activity in distinct tissues with age [9, 10]. The tissue-specific analysis of autophagic activity with age is an important step in understanding the role of autophagy in lifespan and healthspan determination.

Here we describe our autophagy flux assay that can be used to assess autophagic activity in distinct tissues of adult *C. elegans* of different ages [9, 11–13].

2 Materials

2.1 C. elegans Strains

Strains expressing GFP-tagged LGG-1 (*see* **Note 1**).

1. *adIs2122[lgg-1p::gfp::lgg-1 + rol-6]* (DA2123) [6, 7] to assess autophagic flux in hypodermal seam cells, intestine, pharynx, and body-wall muscle.
2. *sqIs24[rgef-1p::gfp::lgg-1 + unc-122p::rfp]* (MAH242) [8] to assess autophagic flux in nerve-ring neurons.

Both *C. elegans* strains can be obtained from the Caenorhabditis Genetic Center (CGC).

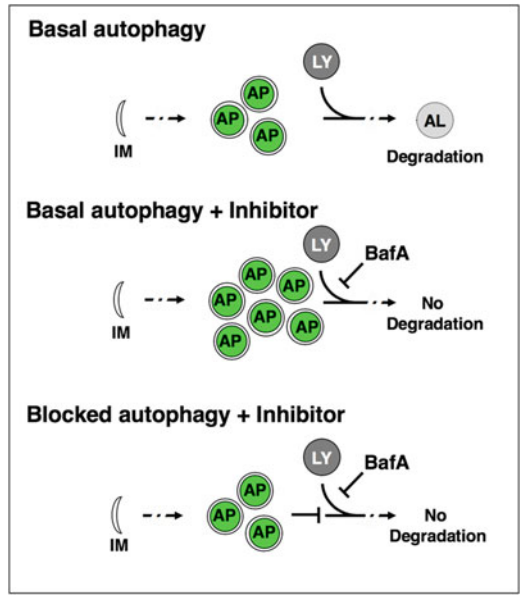

Fig. 1 Autophagy flux assay. Basal autophagy is initiated with the nucleation of a double membrane (isolation membrane, IM), which forms the phagofore. The phagofore expands into an autophagosome (AP) that sequesters cytosolic material (also referred to as cargo) destined for degradation. Autophagosomes fuse with acidic lysosomes (LY) to form autolysosomes (AL), in which the cargo is subsequently degraded. In autophagy flux assays, the chemical autophagy inhibitor Bafilomycin A (BafA) can be used to block autophagic turnover. In situations where autophagy is active, the addition of BafA will change the apparent number of autophagosomes. If autophagy is blocked, BafA addition will not change the number of autophagosomes compared to control conditions

2.2 C. elegans *Maintenance*

1. Worm pick: Cut ~3 cm of platinum wire (90% platinum, 10% iridium wire, 30 G, e.g., Genesee Scientific). Break off the thin part of a glass Pasteur pipette (5¾ in., e.g., Fisherbrand). Melt the glass at the site of breakage on a Bunsen burner and attach the platinum wire. Flatten the end of the platinum wire using small forceps or bend the platinum wire to create a small loop. The platinum wire pick should be sterilized over a flame while using.
2. Normal Growth Media (NGM) agar plates: Mix 2.5 g Bacto peptone, 3 g NaCl, and 20 g agar in 975 ml H_2O. After autoclaving, allow to cool down to ~55 °C, and add 1 ml of 1 M $CaCl_2$, 1 ml of 1 M $MgSO_4$, 1 ml of 5 mg/ml cholesterol in ethanol, and 25 ml of 1 M KPO_4 buffer (pH 6.0). Dispense into 6 cm dishes.
3. *E. coli* OP50 is used as a food source and can be obtained from the CGC. Culture OP50 in LB medium. Apply about 80–100 µl of OP50 culture to NGM plates and allow a lawn to grow before transferring animals.

C. elegans strains can be maintained and cultured under standard conditions at 20 °C [14]. For aging experiments, animals are synchronized by transferring eggs manually using a platinum wire worm pick (*see* **Note 2**). Eggs are allowed to hatch on NGM plates seeded with OP50 bacteria. Once reproductive (3 days of incubation at 20 °C), adult animals need to be transferred away from progeny daily until they reach the desired day of adulthood. Preferably, animals of all ages should be imaged on the same day, in which case eggs are picked on different days to achieve appropriate staging on the day of the experiment. (We note that a large number of experimental conditions may make it impossible to image all animals on the same day. Best practices should be used to ensure reproducibility.) Animals should always be well-fed, since autophagy activity is sensitive to the nutritional status of the animals.

2.3 Reagents for Injections

1. Dimethyl sulfoxide (DMSO, e.g., Sigma).
2. Water.
3. 1 mg of Bafilomycin A1 (BafA) (from BioViotica Rare Active Natural Products, Product number BVT-0252). Prepare a 25 mM BafA stock solution by dissolving 1 mg of BafA in 64 μl of DMSO. The stock concentration needs to be this high to keep the final DMSO concentration of 0.2% (w/v). Make aliquots of 5 μl and store BafA stock solution at −20 °C.
4. Dextran, Texas Red, 3000 MW Lysine Fixable (Thermo Fisher Scientific, Product number D3328). To control for successful injection into the tissue of interest, a dye like Dextran Texas Red that is visible under a fluorescent microscope and of a molecular weight larger than BafA is mixed with the BafA and DMSO. Prepare a 25 mg/ml stock solution by resuspending the coinjection dye in water. Make aliquots of 10–20 μl and store at −20 °C.
5. M9 buffer: 6 g Na_2HPO_4, 3 g KH_2PO_4, 5 g NaCl, and 0.25 g $MgSO_4{\cdot}7H_2O$ in 1 L H_2O. Sterilize by autoclaving.
6. Halocarbon oil 700 (e.g., Sigma) for mounting of the animals to be injected.

2.4 Injections

1. Needle puller (e.g., Flaming/Brown Micropipette Puller Model P-94, Sutter Instruments).
2. Injection needles: Injection needles are produced from thin glass capillaries, such as Kwik-Fil Borosilicate Glass Capillaries (1.0 mm, 4 in., e.g., World Precision Instruments, Inc.).
3. Pipette tips for loading needles (e.g., *Microloader* tips (e.g., Eppendorf) 0.5–20 μl, 100 mm) (*see* **Note 3**).
4. Injection scope (e.g., Zeiss Axio) with needle micromanipulator (e.g., Eppendorf) and joystick (e.g., Transferman NK2 (Eppendorf)).

5. Electronic microinjector that provides the pressure for injecting small volumes via the attached needle (e.g., Femtojet (Eppendorf)).
6. Microscope slide coverslips 22 × 50 mm with Thickness #1.5 (e.g., Slip-rite coverslip (Thermo)).
7. Injection pads are used to immobilize animals for the injection procedure. An injection pad is a glass coverslip (22 × 50 mm) (e.g., Slip-rite coverslip (Thermo)) with a dried layer of 2% (w/v) agarose (in water) on the center of it. Prepare boiling 2% agarose in water (usually 10 ml of water with 0.2 g of agarose), use a glass Pasteur pipette (5¾ in., e.g., Fisherbrand) to place 1–4 drops (~50 μl) onto the center of a 22 × 50 mm glass coverslip, immediately flatten the drop with another 22 × 50 mm coverslip. Let the pads dry for a few minutes and then slide the coverslip off. Let the slides dry for at least 1 day before use. Label the right side of the upward-facing coverslip with an "R" (optional).

2.5 Fluorescence Microscopy

1. Confocal microscope (e.g., Zeiss LSM 710) or Zeiss Imager Z1 including apotome.2.
2. Sodium azide is used to anesthetize live animals for imaging. Prepare M9 buffer containing 150 mM NaN_3 (add 1.5 ml of 1 M NaN_3 (dissolved in M9) to 8.5 ml of M9 buffer) (*see* **Note 4**).
3. Microscope slides (25 × 75 × 1 mm, e.g., Premium Microscope Slides Superfrost (Fisher Scientific)) and coverslips (22 × 50 mm, Thickness #1.5, e.g. Slip-rite coverslip (Thermo)).
4. Imaging slides are used to immobilize worms for imaging. Prepare boiling 2% agarose in M9 buffer and add NaN_3 to a final concentration of 150 mM (usually 8.5 ml of water with 0.2 g of agarose and 1.5 ml of 1 M NaN_3 in M9). This solution can be kept at 65 °C for repeated use. Using a glass Pasteur pipette (5¾ in. e.g., Fisherbrand), place 1–4 drops (~50 μl) of this solution to the center of a microscope slide (25 × 75 × 1 mm) and immediately flatten the drop with another microscope slide. Let the pads dry for a few minutes and then separate the microscope slides. Imaging pads should be made fresh and should not be allowed to dry out.

3 Methods

3.1 Preparing Solutions for Injection

The solutions for injections should be prepared fresh before the injections.

1. BafA solution: Make a 100 μM BafA working solution by adding 1 μl of the 25 mM BafA stock solution to 249 μl of

water. The working solution should not be reused. Make the BafA injection solution by mixing 5 μl of 100 μM BafA with 1 μl of the 25 mg/ml injection dye stock with 4 μl of water. The BafA concentration in the injection solution is 50 μM.

2. DMSO solution: Make a 0.4% DMSO (w/v) working solution by adding 1 μl of DMSO (e.g., Sigma) to 249 μl of water. Make the DMSO injection solution by mixing 5 μl of 0.4% DMSO with 1 μl of the 25 mg/ml injection dye stock with 4 μl of water. The DMSO concentration in the injection solution is 0.2%.

3.2 Preparing Injection Needles

The individual settings for the needle-pulling program have to be established individually and depend on the filament, the capillaries, and the needle-pulling machine. The parameters that determine the needle shape are typically heat, pull, velocity and time. The pulled needles should be sealed at the tip and have a taper of about 6 mm but will need to be adjusted depending on injection set-up. Pre-pulled injection needles can also be purchased from several companies (e.g., Femtotips II (Eppendorf)). *See* **Note 5** for needle-pulling protocol using Micropipette Puller model P-94 from Sutter Instruments.

3.3 Injections

Animals should be injected with BafA at least 2 h before imaging to achieve steady-state levels of autophagosomes after the treatment with the inhibitor; these levels do not appear to change over the next 24 h [9].

3.3.1 Loading the Needles

Use a 20 μl pipette with a 0.5–20 μl, 100 mm *Microloader* pipette tip (Eppendorf) to load 2–4 μl of the BafA or DMSO solution into the needle (*see* **Note 3**).

3.3.2 Breaking the Needle Tip

After placing the needle in the micromanipulator, it is necessary to physically break its tip to open the capillary and allow the flow of the solution. The needle can be broken on the side of a small coverslip (18 × 18 mm, e.g., micro cover glass (e.g., VWR)) attached to a larger cover slide (22 × 50 mm, e.g., Slip-rite coverslip (Thermo)). Place a drop of microinjection oil (Halocarbon oil 700) on a 22 × 50 mm coverslip and place the smaller 18 × 18 mm cover glass on top, so that the edge of the smaller cover glass is in the oil. Place this coverslip on the microscope and bring into focus using the 10× objective. Move the needle so that the needle tip is illuminated. Dip the needle tip into the oil and position it at the same level of the side of the small coverslip and then change to 40 or 100× objective. Using the needle manipulator joystick (e.g., Transferman NK2 (Eppendorf)), move the needle into the side of the coverslip to break off the tip. The tip needs to be small and sharp enough to penetrate the animal without injury. If the needle has been successfully broken, you should be able to see the solution

coming out of the needle by pressing the inject button (tip: the best needles have a beveled tip, which helps piercing the animal's cuticle).

3.3.3 Injection Settings for FemtoJet (Eppendorf)

The injection pressure (Pi) should be set to 1500–2000 hPa for *C. elegans* injections. The compensation pressure (Pc), which prevents anything from being sucked into the needle, should be set to ~125 hPa.

3.3.4 Injection Procedure

1. Mounting animals for injections: Take an injection pad and put a drop of microinjection oil on the dried agarose drop on the injection pad. Dip the worm pick into the Halocarbon oil and pick an animal of the desired age from its plate (should be well-fed). Avoid transferring large amounts of bacteria to the injection pad. Transfer the animal into the oil on the injection pad and gently press the animal onto the agarose to aid in immobilization of the animal. Make sure that the animal is submerged in enough oil to slow down desiccation, without preventing the animals from adhering to the agarose.
2. With the needle well above the slide, bring the animal into focus using the 10× objective. Bring the needle into the same level as the animal by gently lowering the needle until it comes into focus (tip: the needle should be *next* to the animal as it is lowered and not *on top* of it). Change to the 40× or 100× objective and focus on the anterior region of the animal.
3. To assess autophagic flux in intestine, pharynx, and muscle, DA2123 (*adIs2122[lgg-1p::gfp::lgg-1 + rol-6]*) (Fig. 2a) [6, 7] animals are injected into the anterior area of the animal. The injection dye should penetrate all desired tissues if injected into anterior intestinal cells, the extracellular space near posterior pharyngeal bulb, or into the intestinal lumen.

   To assess autophagic flux in nerve-ring neurons, MAH242 (*sqIs24[rgef-1p::gfp::lgg-1 + unc-122p::rfp]*) (Fig. 2e) [8] animals are injected in the space surrounding the pharynx but be careful not to damage the nerve-ring.

   Move the needle into the animal and press either the left mouse button or the foot pedal.
4. Once the animal has been injected, move the needle first out of the animal and then way above the injection pad (tip: once the needle is out of the animals, it is easiest to just move the needle up, then it will already be in the right position for the next animal and will only have to be lowered).
5. Recover the injected animal by placing a drop of M9 buffer on top of the animal to make it float and use the worm pick to lift it up and place it on an NGM plate with *E. coli* OP50. The animals should be incubated for at least 2 h at the cultivation temperature.

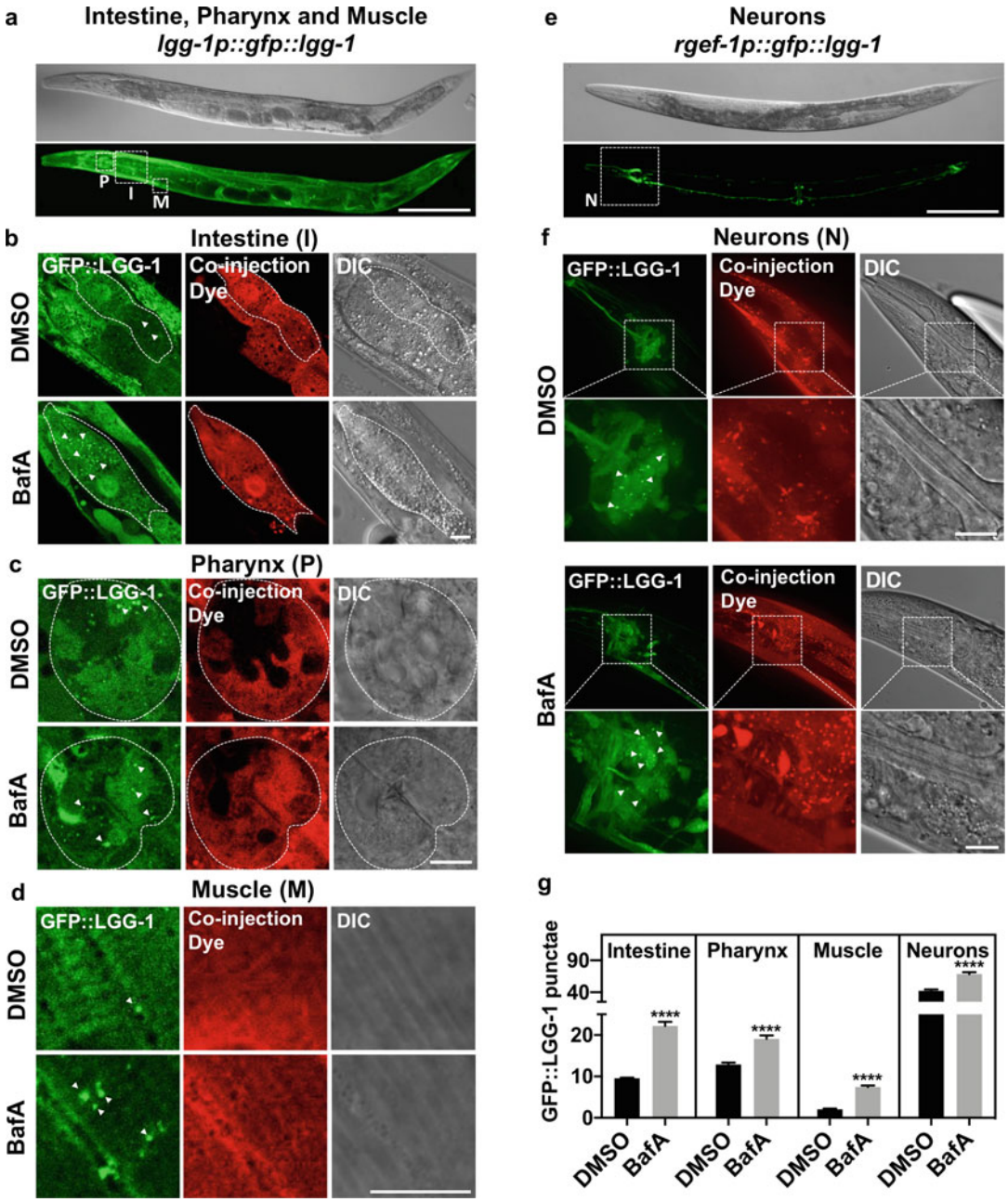

Fig. 2 Autophagic flux analysis in select tissues of adult *C. elegans*. (**a**) Representative image of strain DA2123 (*adIs2122[lgg-1p::gfp::lgg-1 + rol-6]*) used to assess autophagic flux in intestine (I), pharynx (P), and muscle (M), outlined by dashed boxes. Scale bar 200 μm. (**b**–**d**) Representative images of GFP::LGG-1-positive punctae (green, some indicated by arrowheads) in *lgg-1p::gfp::lgg-1*-expressing animals (DA2123) injected with DMSO (DMSO) or Bafilomycin A (BafA) with coinjection dye (Dextran, Texas Red) and differential interference contrast (DIC) images are shown. Scale bar 10 μm. Animals shown were injected on day 1 of adulthood. Tissues examined included the intestine (**b**), pharynx (**c**), and body-wall muscle (**d**). (**e**) Representative image of strain MAH242 (*sqIs24[rgef-1p::gfp::lgg-1 + unc-122p::rfp]*) used to assess autophagic flux in

3.4 Imaging

3.4.1 Mounting Animals for Imaging

Prepare a fresh imaging slide (*see* Subheading 2.5) and place a drop (~10 μl) of M9 buffer containing 150 mM NaN_3 onto the flattened agarose. Manually transfer the living and injected worms onto the pad. Cover the slide with a 22 × 50 mm coverslip (Thickness #1.5, e.g., Slip-rite coverslip (Thermo)) and image immediately. Imaging pads should be made fresh and should not be allowed to dry out.

3.4.2 Imaging

Imaging can be performed using a confocal microscope (e.g., Zeiss LSM 710) or Zeiss Imager Z1 including apotome.2.

1. Using the 10× objective determine whether the animals have been properly injected by monitoring the coinjected dye using the red channel. The tissue of interest should be positive for the dye as well as the GFP signal.
2. To assess autophagic flux in the anterior intestine, use the 100× objective and position the animal ideally with the terminal pharyngeal bulb in one of the corners and the rest of the animal positioned along the diagonal. Images can be acquired as a Z-stack or as a single snap of the anterior intestinal cells (for analysis the best slices of the Z-stack are chosen). When focusing on the intestinal cells, ideally, the nuclei should be visible. Note that the intestine is much dimmer than the pharynx and the gain or exposure time will have to be adjusted accordingly (Fig. 2b).
3. To assess autophagic flux in the terminal pharyngeal bulb, use the 100× objective and position the animals with the terminal pharyngeal bulb in the center of the view field, or in one of the corners and the animal positioned along the diagonal, if the anterior intestine will be imaged as well. Make sure that the coinjection dye has penetrated the pharyngeal bulb; as we found that the pharynx is more resistant to dye-filling than other tissues [9]. Focus on the terminal pharyngeal bulb so that the pharyngeal opening is visible and acquire an image (Fig. 2c).
4. To assess autophagic flux in the body-wall muscle, two separate regions can be chosen. Use the 100× objective and focus either on the body-wall muscle in the head region, or on the body-wall muscle region above the germ line arm, rather than above

Fig. 2 (continued) nerve-ring neurons (N), outlined by a dashed box. Scale bar 200 μm. (**f**) Representative images of GFP::LGG-1-positive punctae (green) in *regf-1p::gfp::lgg-1*-expressing animals (MAH242) injected with DMSO (DMSO) or Bafilomycin A (BafA) with coinjection dye (Dextran, Texas Red) and differential interference contrast (DIC) images are shown. Scale bar 10 μm. Animals shown were injected on day 1 of adulthood. (**g**) Quantification of GFP::LGG-1 punctae in animals injected with DMSO (DMSO) or Bafilomycin A (BafA) on day 1 of adulthood. Data are the mean ± SEM of ≥25 animals combined from at least three experiments. $^{****}P < 0.0001$ by Student's *t*-test. The data in this figure were published in Fig. 3, Supplement 3 of [9]

the intestine (in contrast to the intestine, the germ line does not have *gfp::lgg-1* expression making focusing on the body-wall muscle easier). Body-wall muscle striation should be visible when acquiring this image (Fig. 2d).

5. To assess autophagic flux in the nerve-ring neurons use the 100× objective and focus on the area between the pharyngeal bulbs. For imaging of the nerve-ring neurons, images should be acquired as a Z-stack (~20–25 slices with 1 μm intervals). Collapse the images to a stack using maximal orthogonal projection (this step can also be performed during image analysis using Image J (National Institute of Health) (Fig. 2f).
6. Differential interference contrast (DIC) images can be acquired if desired or if unsure about the tissues.
7. Collect and save the acquired images.

3.4.3 Image Analysis and Statistical Analysis

1. Open images in Image J (National Institute of Health).
2. Use the cell counter function to count the GFP::LGG-1-positive punctae.
3. To assess autophagic flux in the terminal pharyngeal bulb, count the green GFP::LGG-1-positive punctae in the terminal pharyngeal bulb.
4. To assess autophagy flux in the anterior intestinal cell, count the green GFP::LGG-1-positive punctae in the individual cells that are visible in the image.
5. To assess autophagic flux in the body-wall muscle, draw a box that is 1000 μm^2 using the polygon tool. The size of the area can be determined using the measure tool and can be saved as an ROI. Count the green GFP::LGG-1-positive punctae in the 1000 μm^2 area.
6. To assess autophagic flux in the nerve-ring neurons, collapse the images to a stack using maximal projection (this can be done either with the microscope software or using Image J). The nerve-ring will be clearly visible, count the green GFP::LGG-1-positive punctae therein (i.e., between the two pharyngeal bulbs).
7. Document the obtained data for each tissue for DMSO-injected animals and BafA-injected animals (Fig. 2g).

3.4.4 Statistical Analysis

Statistical analysis of the number of GFP::LGG-1-positive punctae can be done using Student's *t*-test if DMSO and BafA conditions are compared at a single timepoint (as in Fig. 2g). If more than one condition or strain is analyzed at a single timepoint, two-way ANOVA should be performed. Analysis of multiple timepoints need to be compared using extended statistical analysis, that is, Poisson regression [9].

4 Notes

1. Strains expressing dual-tagged LGG-1, that is, mCherry::GFP::LGG-1, can also be used for BafA injections [9]:

   qIs11[lgg-1p::mcherry::GFP::lgg-1 + rol-6] (MAH215) to assess autophagy flux in intestine, pharynx, and body-wall muscle.

   sqEx67[rgef-1p::mcherry::GFP::lgg-1 + rol-6] (MAH508) (pick animals with Rol phenotype to maintain) to assess autophagy flux in nerve-ring neurons.

   Both strains can be obtained from the Caenorhabditis Genetic Center (CGC).

   These reporters inform on the pool size of autophagosomes (punctae positive for green and red fluorescence) as well as the pool size of autolysosomes (punctae positive for red fluorescence, since the fluorescence of pH-sensitive GFP will be quenched in the acidic environment of the lysosomes [15]). If autophagy is active, BafA injection may cause changes in the pools of either autophagosomes (punctae positive for green and red fluorescence) or autolysosomes (punctae positive for red fluorescence), or both. If autophagy is blocked, BafA injections should not change the pool sizes of autophagosomes or autolysosomes [9]. We note that the intensity of the red fluorescence compared to green is stronger and in order to see mCherry-positive punctae clearly, the gain of the red channel needs to be set lower than for the green channel. If the intensity of the red channel is increased to effectively overexpose red punctae, the cytoplasmic mCherry::GFP::LGG-1 signal will appear yellow [9]. The number of autolysosomes is calculated as the total number of punctae positive in the red channel subtracted by the number of punctae positive in the green channel, with the latter number of punctae representing the number of autophagosomes. We acknowledge that red punctae can also represent amphisomes, resulting from the fusion of autophagosomes with acidic endosomes [4].

   The coinjection dye to use for BafA injection of animals carrying the tandem LGG-1 reporter is Dextran, Cascade Blue 3000 MW, Anionic Lysine Fixable (Thermo Fisher Scientific, Product number D7132).

2. Animals can be synchronized by hypochlorous acid treatment. Hypochlorous acid solution is made by mixing 150 ml of 5% (v/v) NaOCl (sodium hypochlorite, bleach) with 75 ml 5 N KOH and 275 ml H_2O to a final volume of 500 ml. The solution is mixed and sterile filtered. The bleach is light sensitive, and the solution should be stored covered in aluminum

foil at 4 °C. For hypochlorous acid treatment, gravid animals are washed off NGM plates using a 5–10 ml M9 solution and collected in a 15 ml conical tube. Centrifuge the 15 ml conical tube at low speed 1500–2000 × *g* for 30 s to gently pellet the animals. Aspirate the M9 medium leaving 200–500 μl of M9, depending on the size of the worm pellet. Add 10 ml of hypochlorous acid solution. Mix by inverting or rocking. Monitor under a stereoscope until worms release the eggs and dissolve. Centrifuge at 1500–2000 × *g* for 30 s. A white or clear egg pellet should be visible. Aspirate as much of the hypochlorous acid solution as possible without disturbing the egg pellet. Quickly add 10 ml of M9 medium and mix to remove the hypochlorous acid solution. Centrifuge at 1500–2000 × *g* for 30 s and aspirate most of the solution. Repeat the washing step one more time. Transfer the eggs onto an NGM media plate with OP50 bacteria immediately after bleaching or transfer eggs into a fresh 15 ml conical tube containing 3-5 ml M9 medium for overnight hatching. Transfer the hatched L1 larvae onto NGM plates with OP50 bacteria the next day.

3. Injection needles can be loaded with injection solution by capillary forces. Pipet 2–4 μl of the injection solution on the unpulled end of the injection needle and allow 5–7 min for collection of the solution in the needle tip. The disadvantage of this method is that air bubbles can be trapped in the needle tip, which will prevent injection.
4. The *gfp::lgg-1* reporter is sensitive to the type of anesthetics used to mount the transgenic animals for imaging. In contrast to 150 mM sodium azide, 0.2–2 mM of Levamisole or Tetramisole hydrochloride leads to the formation of different sized GFP-positive punctae 5–10 min after mounting [11].
5. Needle pulling using Micropipette Puller model P-94 from Sutter Instruments:
   (a) Turn on the needle puller. Place the capillary on the ridge on the left side and slide toward and past the filament without touching the filament. Once the capillary has passed through the filament, tighten the screw.
   (b) Push both levers toward the filament.
   (c) Loosen the left screw just enough so that the capillary is still is held in the ridge but can slide along the ridge. Push the capillary further through the filament so that the middle of the capillary is right in the filament and the two pulled needles will have the same length.
   (d) Tighten both screws and close the lid.

(e) Initiate needle pulling and the filament will heat up and melt the capillary. Once the glass is molten, the levers will snap back, resulting in two needles.

(f) Take out the needles without touching the tips and place them into a needle holder box (an empty 15 cm petri dish with a strip of modeling clay or wax to hold the needles).

(g) Check the needles under a dissecting scope to see whether they look correct.

Acknowledgments

The nematode strains used in this work can be obtained by the Caenorhabditis Genetics Center (University of Minnesota), which is supported by the NIH—Office of Research Infrastructure Programs (P40 OD010440). This work was funded by the Julie Martin Mid-Career Award in Aging Research from The Ellison Medical Foundation/AFAR (to M.H.), and by NIH grants AG058038 (to C.K.) and AG028664 (to M.H.).

References

1. Mizushima N, Levine B, Cuervo AM, Klionsky DJ (2008) Autophagy fights disease through cellular self-digestion. Nature 451 (7182):1069–1075. https://doi.org/10.1038/nature06639. nature06639 [pii]
2. Rubinsztein DC, Marino G, Kroemer G (2011) Autophagy and aging. Cell 146 (5):682–695. https://doi.org/10.1016/j.cell.2011.07.030
3. Hansen M, Rubinsztein DC, Walker DW (2018) Autophagy as a promoter of longevity: insights from model organisms Nat Rev Mol Cell Biol 19:579–593
4. Klionsky DJ et al (2016) Guidelines for the use and interpretation of assays for monitoring autophagy (3rd edition). Autophagy 12 (1):1–222. https://doi.org/10.1080/15548627.2015.1100356
5. Manil-Segalen M, Lefebvre C, Jenzer C, Trichet M, Boulogne C, Satiat-Jeunemaitre B, Legouis R (2014) The *C. elegans* LC3 acts downstream of GABARAP to degrade autophagosomes by interacting with the HOPS subunit VPS39. Dev Cell 28(1):43–55. https://doi.org/10.1016/j.devcel.2013.11.022
6. Melendez A, Talloczy Z, Seaman M, Eskelinen EL, Hall DH, Levine B (2003) Autophagy genes are essential for dauer development and life-span extension in *C. elegans*. Science 301 (5638):1387–1391
7. Kang C, You YJ, Avery L (2007) Dual roles of autophagy in the survival of *Caenorhabditis elegans* during starvation. Genes Dev 21 (17):2161–2171. https://doi.org/10.1101/gad.1573107
8. Gelino S, Chang JT, Kumsta C, She X, Davis A, Nguyen C, Panowski S, Hansen M (2016) Intestinal autophagy improves healthspan and longevity in *C. elegans* during dietary restriction. PLoS Genet 12(7):e1006135. https://doi.org/10.1371/journal.pgen.1006135
9. Chang JT, Kumsta C, Hellman AB, Adams LM, Hansen M (2017) Spatiotemporal regulation of autophagy during *Caenorhabditis elegans* aging. Elife 6. https://doi.org/10.7554/eLife.18459
10. Chang JT, Hansen M (2018) Age-associated and tissue-specific decline in autophagic activity in the nematode *C. elegans*. Autophagy 14 (7):1276–1277. https://doi.org/10.1080/15548627.2018.1445914
11. Zhang H, Chang JT, Guo B, Hansen M, Jia K, Kovacs AL, Kumsta C, Lapierre LR, Legouis R, Lin L, Lu Q, Melendez A, O'Rourke EJ, Sato K, Sato M, Wang X, Wu F (2015) Guidelines for monitoring autophagy in

Caenorhabditis elegans. Autophagy 11 (1):9–27. https://doi.org/10.1080/15548627.2014.1003478

12. Kumsta CCJ, Schmalz J, Hansen M (2017) Hormetic heat stress and HSF-1 induce autophagy to improve survival and proteostasis in *C. elegans*. Nat Commun 8:14337
13. Wilkinson DS, Jariwala JS, Anderson E, Mitra K, Meisenhelder J, Chang JT, Ideker T, Hunter T, Nizet V, Dillin A, Hansen M (2015) Phosphorylation of LC3 by the Hippo kinases STK3/STK4 is essential for autophagy. Mol Cell 57(1):55–68. https://doi.org/10.1016/j.molcel.2014.11.019
14. Brenner S (1974) The genetics of *Caenorhabditis elegans*. Genetics 77(1):71–94
15. Kimura S, Noda T, Yoshimori T (2007) Dissection of the autophagosome maturation process by a novel reporter protein, tandem fluorescent-tagged LC3. Autophagy 3 (5):452–460. 4451 [pii]

Chapter 18

Assay Development and Measurement of the Aging Biomarker Humanin

Brendan Miller and Junxiang Wan

Abstract

Biomarkers that reflect aging could be used to target age-related diseases with precision and monitor treatment efficacy. One such biomarker is humanin, a 24-amino acid mitochondrial-derived peptide encoded within the mitochondrial *16S rRNA* gene. Humanin is measured in biological fluids, associates with many aging phenotypes, and attenuates aging in several animal models. In this chapter, we highlight the development and protocol of an enzyme-linked immunosorbent assay that quantifies humanin levels in biological fluid.

Key words Humanin, Mitochondria-derived peptides, Aging

1 Introduction

Developing novel biomarkers that reflect the aging process in humans will undoubtedly increase healthlifespan. The National Institute of Health defined a biomarker as "a characteristic that is objectively measured and evaluated as an indicator of normal biological processes, pathogenic processes, or pharmacological responses to a therapeutic intervention [1]." Biomarkers that capture aging could be used by clinicians and researchers to monitor disease progression and examine responses to therapies for age-related diseases.

Several unique biomarkers at the genomic and mitochondriomic levels reflect aspects of the aging process. For example, Levine et al. developed a unique biomarker of aging by implementing epigenetic features of human genome. Using data from blood, the Levine lab found that certain epigenetic features predicted differences in DNA damage response, inflammation, mitochondrial function, and age [2]. In addition, since metabolic outcomes have been correlated to aging, some researchers have focused on mitochondrial outcomes. This mitochondriomic approach led to the development of tissue-specific measurements that capture

Sean P. Curran (ed.), *Aging: Methods and Protocols*, Methods in Molecular Biology, vol. 2144,
https://doi.org/10.1007/978-1-0716-0592-9_18,

respiration and molecules related to mitochondrial function, such as mitochondrial-derived peptides [3, 4].

Mitochondrial-derived peptides (MDPs) are a novel class of bioactive molecules encoded by mitochondrial DNA and perhaps nuclear mitochondrial DNA segments (NUMTs) [5]. The first MDP, named humanin, was discovered by Hashimoto et al. during a screen for novel genes that protect neurons from amyloid beta toxicity [6, 7]. Since the discovery of humanin, its biological effects have been comprehensively characterized. Humanin mitigates pathology in several AD models, signals through the GP130/IL6ST complex, and modifies lipid metabolism [8–10]. There are hundreds of additional peer-reviewed science papers that have shown not just the cytoprotective effects of humanin but also additional, newly discovered MDPs [11–13].

The potent biological effects of humanin led to the development of an enzyme-linked immunosorbent assay (ELISA) that captures the MDP in various biological tissues and fluid. Developed by Cohen et al., the humanin ELISA has been used to monitor aging progression and reflect age-related disease pathology. In humans, Yen et al. showed that circulating plasma levels of humanin associate with cognitive age and differ by ethnicity [14]. In mice, humanin levels are higher in growth hormone and IGF-1 deficient, long lived mice than short-lived mice [15].

In this chapter, the development of the humanin ELISA is outlined.

2 Materials

2.1 Capture Antibody Materials

1. Rabbit anti-humanin antiserum (custom from Yenzym Antibodies).
2. NAb™ protein A/G spin kit (product #89980, Thermo Scientific).
3. 15 mL centrifuge tubes.
4. Borosilicate glass tube 12 × 75 mm.
5. Amicon Ultra-4 50K MW cut off centrifugal filters (product #UFC805008, Millipore).

2.2 Detection Antibody Materials

1. CarboxyLink Immobilization Kit with UltraLink Support (product #53154, Thermo Scientific).
2. Binding/Wash buffer: BupH Phosphate Buffered Saline Packs (product #28372, Thermo Scientific).
3. EZ-Link Sulfo-NHS-LC-Biotin (product #21335, Thermo Scientific).
4. Neutralization Buffer: 1 M Tris, pH 8.5.

2.3 Sample Preparation Materials

1. EDTA-treated lavender top tubes.
2. Extraction buffer: 90% acetonitrile, 10% 1 N HCl.
3. SpeedVac.
4. Sample diluent: 50 mM PBS, 150 mM NaCl, 0.5% Tween 20, 0.01% thimerosal.

2.4 ELISA Materials

1. Capture antibody (from Subheading 2.1).
2. Detection antibody (from Subheading 2.2).
3. Coating buffer: 50 mM sodium bicarbonate buffer, pH 9.5.
4. Normal rabbit serum.
5. Sample diluent: 50 mM PBS, 150 mM NaCl, 0.5% Tween 20, 0.01% thimerosal.
6. tPBS: 137 mM NaCl, 2.7 mM KCl, 10 mM Na_2HPO_4, 1.8 mM KH_2PO_4, 405 mM thimerosal, pH 7.4.
7. sPBS: 50 mM PBS, 0.5% Tween 20, 1% normal rabbit serum.
8. Wash buffer: 0.1% Tween 20 in tPBS.
9. Assay buffer: 10% normal rabbit serum in sample diluent.
10. Blocking buffer: SuperBlock T20 (product #37516, Thermo Scientific).
11. Streptavidin-HRP (product #DY998, R&D systems): working concentration 1:200.
12. 1-Step™ Ultra TMB-ELISA (product #34028, Thermo Scientific).
13. Stop solution: 2 N H_2SO_4.
14. Humanin peptide (Bachem, Torrance, CA).
15. Trifluoroacetic acid (TFA).

3 Methods

The humanin ELISA development includes capture antibody preparation (Subheading 3.1), detection antibody preparation (Subheading 3.2), sample preparation (Subheading 3.3), ELISA procedures (Subheading 3.4).

3.1 Capture Antibody Preparation

1. Equilibrate NAb™ protein A/G spin kit column and buffers 20–30 min to room temperature.
2. Dilute 1 mL rabbit anti-humanin antiserum with 1 mL binding buffer (from NAbTM protein A/G spin kit).
3. Gently snap off bottom closure and remove the top cap. Place column in a 15 mL collection tube and allow storage solution to drain.

4. Equilibrate column by adding 5 mL of binding buffer and allow the solution to drain (*see* **Notes 1–3**).
5. Cap the bottom of the column tightly. Apply the diluted sample to the column. Cap the top of the column tightly.
6. End-to-end rotating the column for 15 min at room temperature.
7. Remove the caps of the bottom and top. Place column in a 15 mL collection tube. Allow the nonbound antibodies flow-through.
8. Wash column with 15 mL of binding buffer.
9. Add 100 μL neutralization buffers (from NAbTM protein A/G spin kit) into borosilicate glass tubes as collection tubes.
10. Elute antibodies with 5 mL elution buffer (from NAb^{TM} protein A/G spin kit). Collect five seperate1 mL fractions in each of the buffer-containing tubes.
11. Measure the absorbance of each fraction at 280 nm. Observer the peak fraction (usually in second fractions).
12. Transfer the peak fraction into a column with Amicon 50K MWCF centrifugal filter.
13. Centrifuge at 1800 × *g* for 15 min at room temperature with swing-bucket rotor. Discard the flow-through.
14. Wash the column with 1 mL binding buffer.
15. Repeat **steps 13** and **14** once.
16. Insert a pipettor into the bottom of the filter and withdraw the sample (*see* **Note 4**). Add the appropriate volume of binding buffer. Measure the absorbance at 280 nm. Calculate the concentration of total IgG: (A_{280} of each fraction − A_{280} of binding buffer)/1.4. Note that 1.4 is the rabbit extinction coefficient.
17. Aliquot 50 μg total IgG to each 0.5 mL centrifuge tube as capture antibody. Store the antibodies at −80 °C.

3.2 Detection Antibody Preparation

1. Dissolve contents of the BupH MES Buffered Saline Pack in 500 mL distilled water (*see* **Note 5**).
2. Equilibrate a column of DADPA UltraLink Support, a vial of EDC and the bottle of wash buffer to temperature — all from the CarboxyLink Immobilization Kit with UltraLink Support.
3. Dissolve 5 mg of humanin peptide in 2 mL of coupling buffer (from the CarboxyLink Immobilization Kit). For later estimation of coupling efficiency, measure the absorbance of this sample at 280 nm.
4. Remove the top cap and twist off the bottom tab from the column. Use supplied white tips to recap column bottom.

5. Allow the storage buffer to drain from the column.
6. Equilibrate resin by adding 10 mL of Coupling Buffer to the column and allowing it to drain through (*see* **Notes 1–3**).
7. Replace the bottom cap and add the 2 mL peptide sample to the column.
8. Place the top cap on the column and mix the sample–resin slurry gently end-over-end for 15 min.
9. Add 0.5 mL of the coupling buffer to the vial of EDC.
10. Immediately after the EDC is dissolved, add the 0.5 mL of reagent to the sample–resin slurry from **step 8**.
11. Place the top cap on the column and mix the reaction slurry gently end-over-end for 3 h at room temperature.
12. Stand the column upright. Allow several minutes for the resin to settle, then remove the top and bottom caps and drain the reaction solution into a clean collection tube.
13. Pass more wash buffer (5–10 mL) through the column to wash the column more thoroughly.
14. Equilibrate the column in an appropriate storage buffer or binding buffer by passing 6 mL through the column.
15. Equilibrate the prepared humanin peptide immobilized column to room temperature.
16. Remove top and bottom caps and allow excess storage solution to drain from column.
17. Wash column with 6 mL of Binding/Wash Buffer and allowing it to drain from column.
18. Replace the bottom cap. Add 3–5 mg rabbit anti-humanin IgG to column. Recap the top of the column (*see* **Note 6**).
19. Gently end-to-end rotating overnight in cold room.
20. Remove top cap and bottom caps from column, place column in new collection tube, and wash the column with 12 mL of Binding/Wash Buffer.
21. Elute the bound protein by applying 8 mL of Elution Buffer. Collect eight seperate 1 mL fractions. The pH of each fraction can be adjusted to neutral by adding 50 μL of Neutralization Buffer per 1 mL of collected eluate.
22. Monitor elution by absorbance at 280 nm.
23. Determine the peak, and pool fractions of interest.
24. Exchange the elution buffer with binding/wash buffer using Amicon 50K MWCF centrifugal filter.
25. Prepare ~200 μg ligand affinity purified IgG in 0.5 mL binding/wash buffer.
26. Prepare 10 mM Sulfo-NHS-LC-Biotin solution by adding 180 μL dH_2O into 10 mg vial, freshly made just before use.

27. Add 60–80 μL of 10 mM biotin reagent solution to the IgG solution, gently mix well.
28. Incubation the mixture for 1 h at room temperature.
29. Transfer the mixture to the column of Amicon 50K MWCF filter tube.
30. Centrifuge at 1800 × *g* for 15 min at room temperature with swing-bucket rotor.
31. Discard the flow-through. Add 1 mL binding buffer to the column.
32. Repeat **steps 30** and **31** three more times.
33. Insert a pipettor into the bottom of the filter and withdraw the sample. Add the appropriate volume binding buffer. Measure the absorbance at 280 nm. Calculate the concentration of protein: (A_{280} of each fraction − A_{280} of binding buffer)/1.4. Note that 1.4 is the rabbit extinction coefficient.
34. Aliquot 5 μg biotinylated ligand affinity purified IgG (Detection antibodies) to each 0.5 mL centrifuge tube. Store the antibodies at −80 °C.

3.3 Sample Preparation

1. Collect whole blood into EDTA-treated tubes.
2. Centrifuge for 15 min at 2000 × *g* at 4 °C.
3. Following centrifugation, immediately transfer the supernatant (plasma) into a clean polypropylene tube.
4. Assay immediately or aliquot and store, transport at −20 °C or lower. Avoid repeated freeze–thaw cycles.
5. Add 200 μL extraction buffer into 100 μL plasma sample and mix well.
6. Incubate for 30 min at room temperature. Vortex once during incubation.
7. Centrifuge at 11,000 × *g* for 15 min at 4 °C.
8. Transfer 250 μL supernatant to a new 1.5 mL Eppendorf centrifuge tube without lid.
9. Place the tube containing supernatant samples in the SpeedVac, dry down 2–3 h (*see* **Note 7**).
10. Reconstitute the dried samples with 250 μL sample diluent (*see* **Note 8**).
11. Incubate for 30 min at room temperature. Vortex once during incubation.
12. Centrifuge at 11,000 × *g* for 10 min at 4 °C.
13. Transfer supernatant to a clean 1.5 mL Eppendorf centrifuge tube without disturbing the pellets and is ready to use for Humanin ELISA.

3.4 ELISA Procedures

1. Prepare standard stock solution. Add 0.5 mL 0.1% trifluoroacetic acid (TFA) in dH_2O to humanin for a concentration 0.5 mg/mL. Dilute with sPBS to 1.0 μg/mL. Aliquot 50 μL per vial and store −80 °C. Pipette 990 μL assay buffer into the 1.5 mL tube, add 10 μL standard stock solution into it to produce the concentration 10,000 pg/mL (S9) as the highest standard.
2. Pipette 300 μL assay buffer into each (S0–S8). Transfer 300 μL from S9 to S8 to produce twofold dilution (5000 pg/mL). Then make twofold dilution series to S1 (19.5 pg/mL). Mix each tube thoroughly before the next transfer. Assay buffer serves as the zero standard (0 pg/mL).

Tube	S9	S8	S7	S6	S4	S5	S4	S3	S2	S1	S0
pg/mL	10,000	5000	2500	1250	625	312.5	156.25	78.13	39.06	19.5	0

3. Coating the 96-well plate: add 50 μg coating antibody into 20 mL coating buffer, apply 200 μL into each well.
4. Incubate the plate for 3–4 h at room temperature on shaker at 500–1000 rpm.
5. Wash the plate twice with 300 μL wash buffer.
6. Wash the plate twice with 300 μL blocking buffer.
7. Add 100 μL standards, controls and samples into each well.
8. Add 5 μg detection antibody into 10 mL assay buffer, mix well. Apply 100 μL detection solution on the top of standards, controls and samples.
9. Incubate the plate overnight on shaker at 300–400 rpm.
10. Wash the plate three times with 300 μL wash buffer.
11. Add 200 μL Streptavidin-HRP solutions to each well.
12. Incubate the plate on shaker at 500 rpm for 30 min at room temperature.
13. Wash the plate three times with 300 μL wash buffer.
14. Add 200 μL 1-Step™ Ultra TMB-ELISA solutions to each well.
15. Incubate the plate on shaker at 500 rpm for 10–20 min.
16. Add 50 μL stop solution to each well and incubate on shaker for 2 min.
17. Determine the absorbance on a plate spectrophotometer at 450 nm.

4 Notes

1. For columns used in IgG purification and affinity purification (Subheadings 3.1 and 3.2), degas all buffers to avoid introducing air bubbles into the column.
2. Throughout the procedure of IgG and affinity purification (Subheadings 3.1 and 3.2), do not allow the resin bed to become dry; replace bottom cap as soon as buffer drains down to the top of resin bed.
3. For best results, add a sample volume that is less than 80% of the column's antibody-binding capacity (Subheading 3.2) (*See* **Note 3**). Collect the flow-through. If the sample contains more IgG than can bind to the column, the flow-through will contain the excess antibody. By saving the flow-through, non-bound antibody can be recovered and analyzed.
4. In the process of buffer exchange (Subheading 3.1 and 3.2), to recover the concentrated solute, insert a pipettor into the bottom of the filter device and withdraw the sample using a side-to-side sweeping motion to ensure total recovery.
5. After using coupling buffer for first immobilization reaction (Subheading 3.2), add thimerosal to a final concentration of 0.02% to the remainder and store at 4 °C.
6. All the columns need regeneration after each use and equilibration with binding/wash buffer with 0.01% thimerosal, and are stored at 4 °C (Subheading 3.1 and 3.2) (*See* **Note 6**).
7. Extracted plasmas need to be dried down completely by Speed-Vac (Subheading 3.3).
8. When reconstitute the dried samples, test the pH of the samples by pH paper and make sure the pH of sample is neutral (Subheading 3.3).

References

1. Crimmins E, Vasunilashorn S, Kim JK, Alley D (2008) Biomarkers related to aging in human populations. Adv Clin Chem 46:161–216
2. Levine ME, Lu AT, Quach A, Chen BH, Assimes TL, Bandinelli S, Hou L, Baccarelli AA, Stewart JD, Li Y et al (2018) An epigenetic biomarker of aging for lifespan and healthspan. Aging (Albany NY) 10:573–591. https://doi.org/10.18632/aging.101414
3. Xiao J, Howard L, Wan J, Wiggins E, Vidal A, Cohen P, Freedland SJ (2017) Low circulating levels of the mitochondrial-peptide hormone SHLP2: novel biomarker for prostate cancer risk. Oncotarget 8:94900–94909. https://doi.org/10.18632/oncotarget.20134
4. Chin YP, Keni J, Wan J, Mehta H, Anene F, Jia Y, Lue YH, Swerdloff R, Cobb LJ, Wang C et al (2013) Pharmacokinetics and tissue distribution of humanin and its analogues in male rodents. Endocrinology 154:3739–3744. https://doi.org/10.1210/en.2012-2004
5. Yen K, Lee C, Mehta H, Cohen P (2013) The emerging role of the mitochondrial-derived peptide humanin in stress resistance. J Mol Endocrinol 50:R11–R19. https://doi.org/10.1530/JME-12-0203

6. Hashimoto Y, Ito Y, Niikura T, Shao Z, Hata M, Oyama F, Nishimoto I (2001) Mechanisms of neuroprotection by a novel rescue factor humanin from Swedish mutant amyloid precursor protein. Biochem Biophys Res Commun 283:460–468. https://doi.org/10.1006/bbrc.2001.4765
7. Hashimoto Y, Niikura T, Tajima H, Yasukawa T, Sudo H, Ito Y, Kita Y, Kawasumi M, Kouyama K, Doyu M et al (2001) A rescue factor abolishing neuronal cell death by a wide spectrum of familial Alzheimer's disease genes and Abeta. Proc Natl Acad Sci U S A 98:6336–6341. https://doi.org/10.1073/pnas.101133498
8. Mehta HH, Xiao J, Ramirez R, Miller B, Kim SJ, Cohen P, Yen K (2019) Metabolomic profile of diet-induced obesity mice in response to humanin and small humanin-like peptide 2 treatment. Metabolomics 15:88. https://doi.org/10.1007/s11306-019-1549-7
9. Kim SJ, Xiao J, Cohen P, Yen K (2017) Subcellular fractionation for ERK activation upon mitochondrial-derived peptide treatment. J Vis Exp (127). https://doi.org/10.3791/56496
10. Kim SJ, Guerrero N, Wassef G, Xiao J, Mehta HH, Cohen P, Yen K (2016) The mitochondrial-derived peptide humanin activates the ERK1/2, AKT, and STAT3 signaling pathways and has age-dependent signaling differences in the hippocampus. Oncotarget 7:46899–46912. https://doi.org/10.18632/oncotarget.10380
11. Lu H, Wei M, Zhai Y, Li Q, Ye Z, Wang L, Luo W, Chen J, Lu Z (2019) MOTS-c peptide regulates adipose homeostasis to prevent ovariectomy-induced metabolic dysfunction. J Mol Med (Berl) 97(4):473–485. https://doi.org/10.1007/s00109-018-01738-w
12. Lee C, Kim KH, Cohen P (2016) MOTS-c: a novel mitochondrial-derived peptide regulating muscle and fat metabolism. Free Radic Biol Med 100:182–187. https://doi.org/10.1016/j.freeradbiomed.2016.05.015
13. Lee C, Zeng J, Drew BG, Sallam T, Martin-Montalvo A, Wan J, Kim SJ, Mehta H, Hevener AL, de Cabo R et al (2015) The mitochondrial-derived peptide MOTS-c promotes metabolic homeostasis and reduces obesity and insulin resistance. Cell Metab 21:443–454. https://doi.org/10.1016/j.cmet.2015.02.009
14. Yen K, Wan J, Mehta HH, Miller B, Christensen A, Levine ME, Salomon MP, Brandhorst S, Xiao J, Kim SJ et al (2018) Humanin prevents age-related cognitive decline in mice and is associated with improved cognitive age in humans. Sci Rep 8:14212. https://doi.org/10.1038/s41598-018-32616-7
15. Lee C, Wan J, Miyazaki B, Fang Y, Guevara-Aguirre J, Yen K, Longo V, Bartke A, Cohen P (2014) IGF-I regulates the age-dependent signaling peptide humanin. Aging Cell 13:958–961. https://doi.org/10.1111/acel.12243

Chapter 19

Staining and Quantification of β-Amyloid Pathology in Transgenic Mouse Models of Alzheimer's Disease

Amy Christensen and Christian J. Pike

Abstract

Studies of Alzheimer's disease (AD) using experimental systems most often involve transgenic mouse models that are characterized by neural accumulation of β-amyloid protein (Aβ), which is widely hypothesized to have a key role in AD pathogenesis. Quantification of Aβ in transgenic mice typically is accomplished through both biochemical and histochemical approaches. In this chapter, we describe two techniques for the histological detection of Aβ, immunostaining with Aβ antibodies and staining with the amyloid dye thioflavin S, and its quantification using digital imaging.

Key words β-Amyloid, Immunohistochemistry, Quantitative imaging, Thioflavin S, Transgenic mice

1 Introduction

AD neuropathology is characterized by multiple components but is typically defined by two primary lesions. The first is termed neurofibrillary tangles and are composed of insoluble, hyperphosphorylated forms of the microtubule associated protein tau [1]. The second is plaques, which are extracellular deposits of aggregated Aβ protein [1]. There is compelling evidence that both lesions prominently contribute to the initiation and/or progression of the disease [2], although Aβ has long been hypothesized to have the key pathogenic role [3] and has been the primary target for therapeutic intervention strategies [4].Consequently, quantitative assessments of Aβ will continue to be important outcome measures for preclinical studies in transgenic mouse models of AD.

There are two widely used approaches for measurement of Aβ. First, brain levels of Aβ are effectively measured by ELISA following a sequential series of fractionation steps, as previously described [5]. This technique has the advantage of determining Aβ amounts in different states of peptide solubility but is limited spatially in terms of brain region specificity. The second approach is histological assessment. Extracellular and, in some cases, intracellular

Sean P. Curran (ed.), *Aging: Methods and Protocols*, Methods in Molecular Biology, vol. 2144,
https://doi.org/10.1007/978-1-0716-0592-9_19,

accumulations of aggregated Aβ deposits are detected by immunochemistry using antibodies directed against Aβ. In addition, fibrils of Aβ that have acquired β-sheet conformation characteristic of amyloids can be detected by several amyloid dyes, including thioflavin S. These two staining approaches yield subtle but important differences in that all Aβ deposits will be detected with Aβ immunochemistry, and a subset of these with thioflavin S. Histological approaches have the strength of precise regional quantification of Aβ burden but the disadvantage of assessing only larger accumulations of aggregated Aβ (i.e., not detecting various soluble forms of Aβ). We describe histological protocols for the detection and quantification of Aβ from mouse brain, including tissue preparation, Aβ immunochemistry with antigen unmasking, thioflavin S staining, and digital image acquisition and analysis of stained tissue.

2 Materials

1. Phosphate-buffered saline (PBS), pH 7.4 (137 mM NaCl, 10 mM phosphate, 2.7 mM KCl).
2. Sorenson's phosphate buffer, pH 7.0–7.5 (80.4 ml 133 mM Na_2HPO_4; 19.6 ml 133 mM KH_2PO_4).
3. PBS with 0.03% sodium azide, pH 7.4.
4. Tris-buffered saline (TBS), pH 7.4 (0.137 M sodium chloride, 0.0027 M potassium chloride, and 0.025 M Tris/Tris–HCl).
5. 95% formic acid.
6. Quench buffer: TBS with 10% methanol, 3% H_2O_2 (freshly prepared).
7. TBS with 0.1% Triton-X (TBS-TX).
8. Blocking buffer: TBS with 2% bovine serum albumin.
9. Primary antibody: rabbit anti-amyloid β (Thermo Fisher, Cat #71-5800) diluted 1:300 in blocking buffer.
10. Secondary antibody: biotinylated goat anti-rabbit antibody (Vector Laboratories, Cat #BA-1000) diluted 1:1000 in blocking buffer.
11. Avidin-biotin solution: prepare 30 min prior to use using ABC reagents from VECTASTAIN Elite Standard ABC kit (Vector Laboratories, Cat #PK-6100) diluted into TBS.
12. 3′3′ Diaminobenzidine (DAB) solution: prepare fresh using Vector DAB kit.
13. Ethanol solutions: 50%, 70%, 95%, 100%.
14. Xylene.
15. Permanent mounting solution (e.g., Krystalon, Millipore, Cat #64969).

16. 1% thioflavin-S (Sigma, Cat #T-1892).
17. Anti-fade mounting medium (e.g., VECTASHIELD™ Hard-set, Vector Laboratories, Cat #H-1400; or ProLong™ Gold, Thermo Fisher, Cat #P36930).
18. ImageJ software (imagej.nih.gov/ij/).
19. Sorenson's phosphate buffer with 4% paraformaldehyde, pH 7.0–7.5.

3 Methods

3.1 Tissue Preparation

1. Collect mouse brains after perfusion with ice-cold PBS alone or PBS followed by perfusion with 4% paraformaldehyde in Sorenson's phosphate buffer (*see* **Note 1**). If perfused with only PBS, brains are immediately placed into 4% paraformaldehyde and immersion fixed at 4 °C for 48–72 h. Store fixed brains at 4 °C in PBS/0.03% sodium azide until sectioning.
2. Section brains exhaustively in the horizontal plane at a thickness of 30–40 μm on a vibratome. Tissue should be collected and stored in a manner that maintains spatial ordering. This is readily accomplished by collecting sections singly into sterile 48-well plates, which can be sealed with Parafilm™ and stored at 4 °C in PBS/0.03% sodium azide; staining should be completed in a timely manner. Every eighth section containing the hippocampus is used for Aβ or thioflavin staining (*see* **Note 2**). The remaining sections can be used for other stains, as needed.

3.2 Amyloid β Immunohistochemistry

All procedures can be performed at room temperature, unless otherwise stated. All solutions should be thoroughly mixed prior to use. Sections should be placed on an orbital shaker during incubation and rinse periods.

1. Transfer brain sections into wells from a 24-well plate containing TBS (*see* **Note 3**). Each well should contain 1–5 sections. Use every eighth section per brain (8–10 sections per brain) (*see* **Note 4**).
2. Incubate sections in 95% formic acid for 5 min (*see* **Note 5**).
3. Rinse sections 3× in TBS for 5 min.
4. Incubate sections for 10 min in quench buffer (*see* **Note 6**).
5. Rinse sections 3× for 5 min in TBS-TX.
6. Incubate sections for 30 min in blocking buffer (*see* **Note 7**).
7. Incubate sections overnight in the primary antibody (*see* **Note 8**). This step should be performed at 4 °C and, if possible, on an orbital shaker set to low speed (*see***Note 9**).
8. Rinse sections 3× for 5 min in TBS-TX.

9. Incubate sections for 15 min in blocking buffer.
10. Incubate sections for 60 min in secondary antibody.
11. Rinse sections 3× for 5 min in TBS-TX.
12. Incubate sections for 15 min in blocking buffer.
13. Incubate sections for 60 min in avidin-biotin solution.
14. Rinse sections 3× for 5 min in TBS.
15. Transfer sections into the staining solution of 3′3’ diaminobenzidine (DAB) (*see* **Note 10**) and incubate 5 min (*see* **Note 11**).
16. Rinse sections 3× for 5 min in TBS.
17. Mount stained sections on glass microscope slides (*see* **Note 12**).
18. Dry slides with mounted sections overnight at room temperature or on a slide warmer.
19. Dehydrate air-dried sections by rinsing in a series of increasing alcohol solutions (*see* **Note 13**). All times are minimums.
    (a) 1× in 70% alcohol for 3 min.
    (b) 1× in 95% alcohol for 3 min.
    (c) 2× in 100% alcohol for 3 min.
    (d) Dip in xylene.
    (e) 1× in xylene for 15 min (*see* **Note 14**).
20. Coverslip the slides one at a time (leaving remaining slides in xylene rinse) using a permanent mounting solution and allow to cure overnight (*see* **Note 15**).

3.3 Thioflavin-S Staining

1. Mount tissue sections on subbed glass slides and air dry overnight at room temperature.
2. Wash dried slides 3× for 3 min each in 50% alcohol.
3. Dip slides in water then wash in purified water 1× for 3 min.
4. Incubate slides for 10 min in 1% thioflavin S solution (*see* **Note 16**).
5. Wash slides 5× times for 3 min each in 70% alcohol.
6. Wash slides 3× for 3 min each in 50% alcohol (*see* **Note 17**).
7. Wash slides 2× for 15 min each in purified water.
8. Air dry slides for 15–30 min.
9. Coverslip slides using an antifade mounting medium and store in darkness.

3.4 Imaging and Quantification of Amyloid β Immunohistochemical Load

1. Confirm optimized settings on light microscope with attached digital camera imaging system (*see* **Note 18**).
2. Place stained slide on microscope stage and locate hippocampal formation on amyloid β immunostained section. Capture non-overlapping digital images using the 20× objective (*see* **Note 19**) (Fig. 1).

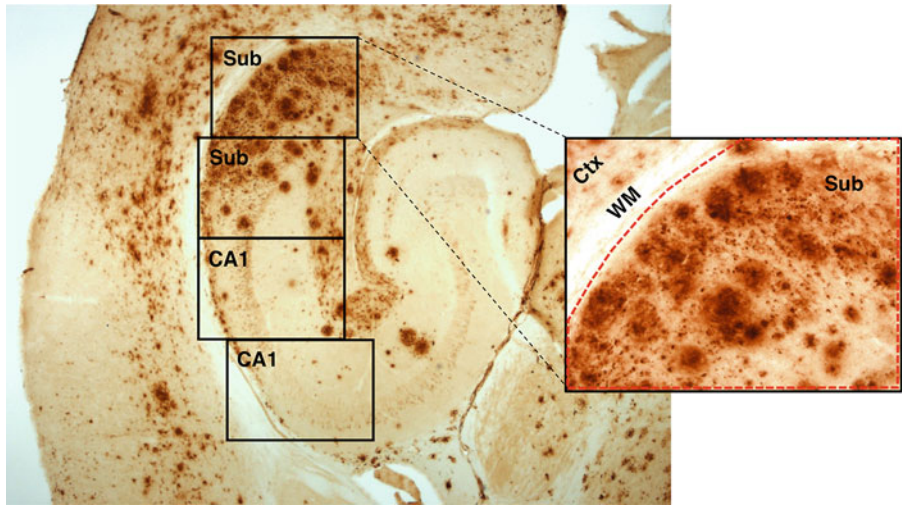

Fig. 1 Illustration of image collection and region of interest determination. Horizontal section of EFAD transgenic mouse showing extensive pathology by amyloid β immunoreactivity using protocol described in Subheading 3.1. Boxes show pattern of image collection using 20× objective for subiculum (Sub) and CA1 hippocampus (CA1). Inset shows larger view of first subiculum image. Using the polygon function, the region of interest (ROI) is defined (dotted red line) to include subiculum but not adjacent cortex (Ctx) and white matter (WM) (as described in Subheading 3.4)

3. For image analysis, begin by opening Image J (NIH) software. Next, under the Analyze tab, choose Set Measurements and confirm that the Area, Area Fraction, and Limit to Threshold options are selected.
4. Open saved files and define the region of interest (ROI) by outlining with the polygon function located on the toolbar (*see* **Note 20**).
5. Convert images with defined ROI into 8-bit grayscale by selecting the following tabs in Image J: Image > Type > 8-bit.
6. Prior to quantification, grayscale images need to be converted to binary images in which each pixel is either black or white (Fig. 2). To perform this threshold function, select the tabs: Image > Adjust > Threshold. Select the predetermined threshold value (*see* **Note 21**).
7. To quantify the amount of positive immunolabeling (i.e., black pixels) within the ROI, select Analyze > Measure and record both "Area" (represents the total number of stained pixels within the ROI) and "Percent area" (represents the proportion of the ROI with positive labeling). For example, if you collect two images of subiculum, there will be Area1 and Area2 as well as Percent area1 and Percent area2 corresponding to the values for each image.

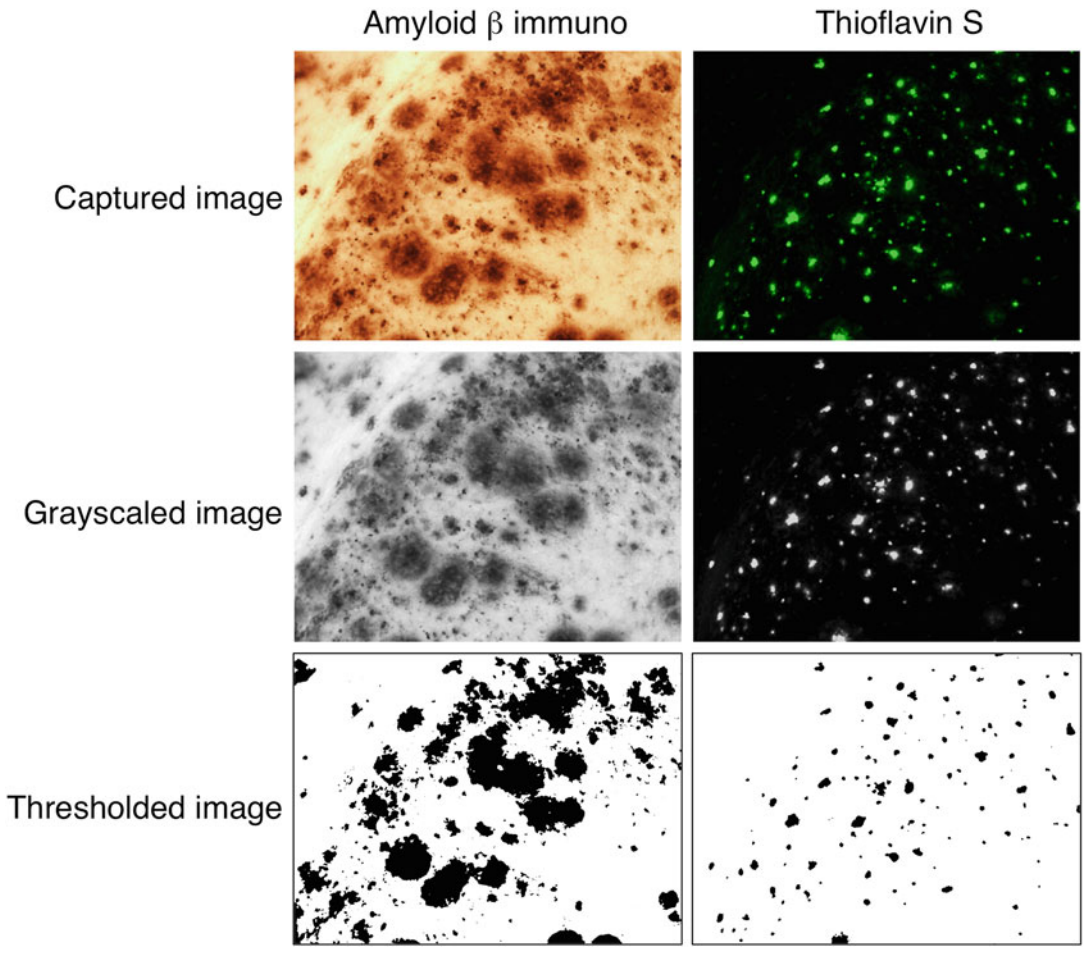

Fig. 2 Examples of image transformation prior to quantification. Panels show a single microscopic field from subiculum in an EFAD transgenic mouse of either amyloid β immunoreactivity (left column) or thioflavin S staining (right column) at initial image collection of labeling (Captured image), following conversion to grayscale (Grayscaled image), and after the threshold step (Thresholded image). The thresholded images are suitable for quantification (described in Subheadings 3.4 and 3.5). Note that the ROI is not shown

8. Calculate the ROI area, which will be the total number of pixels within the outlined area, for each image as: (100/percent area) ∗ area. For example, from subiculum image 1 this will be calculated as follows:

$$(100/\text{Percent area1}) * \text{Area1} = \text{Total area1}$$

9. Calculate the percent staining for the combined ROI of the subregion of the hippocampus for each section by adding the stained areas (given by Image J) divided by the sum of the total areas (calculated by the experimenter). This allows the

experimenter to account for differences in sizes of ROIs. For example, the total percent staining in the subiculum will be calculated as:

$$(\text{Area1} + \text{Area2})/(\text{Total area1} + \text{Total area2}) * 100 = \text{amyloid } \beta \text{ load of the subiculum of section 1}$$

10. When all images for a specific animal have been quantified, average the total percent staining across all sections, yielding the amyloid β load (also referred to as immunohistochemical burden) for the subiculum and CA1 regions of the hippocampus. These values are suitable for statistical analyses.

3.5 Imaging and Quantification of Thioflavin Staining

1. Visualize thioflavin-stained sections using an epifluorescence microscope with a 20× objective (*see* **Note 22**).
2. Capture images of the hippocampus as described for amyloid β immunoreactivity (Subheading 3.5, **step 2**) and save as TIFF files.
3. Calibrate Image J to measure plaque size in μm rather than pixels (*see* **Note 23**).
4. Next, under the Analyze tab, select Set Measurements and make sure Area and Limit to Threshold are selected.
5. Open images of thioflavin-stained sections in Image J and convert to 8-bit grayscale images by selecting the following tabs: Image > Type > 8-bit.
6. Convert grayscale to binary images by selecting the tabs: Image > Adjust > Threshold using a predetermined threshold value (*see* **Note 24**).
7. In the Threshold menu, select the box that says "Dark background." This will invert the image so that the plaques will appear black against a white background.
8. To quantify plaque size, use the Ellipse tool to place circles around individual plaques. Under the Analyze tab, select Measure (*see* **Note 25**).
9. Record all plaque sizes (listed as area in μm^2) in a separate file (e.g., Excel) (*see* **Note 26**).

4 Notes

1. Tissue can also be collected and stored using cryopreservation techniques.
2. Sectioning in the horizontal plane allows excellent visualization of hippocampal subfields across the hippocampus. Approximately 90 sections of 40 μm that contain hippocampus are generated by exhaustive sectioning of mouse brain. Sectioning

in other planes and/or at other tissue thicknesses may require modifications in microscope settings, and image collection and processing (Subheading 3.4).

3. A fine paintbrush is used to gently move the sections from well to well. However, several other methods of tissue movement or solution change can be used, including glass probes, net wells, and light suction. It is recommended to transfer sections down to adjacent wells for each step, moving left to right across a 24-well plate oriented to yield four rows and six columns.
4. Ideally, immunostaining runs should be balanced across experimental groups to control for inter-experiment variability.
5. This is an antigen-unmasking step that is essential for robust Aβ immunostaining [6]. Formic acid is flammable and toxic. Appropriate PPE including lab coats, gloves, and eye protection should be worn, and formic acid should be manipulated in a chemical fume hood.
6. This solution must be prepared immediately prior to use due to the labile nature of hydrogen peroxide. This step serves to quench endogenous peroxidases that can interfere with visualization.
7. Solution should be freshly prepared. This step is used to block nonspecific labeling. Depending upon the primary antibody, the level of blocking component in the buffer may need to be increased up to 5% BSA, 1–5% normal serum, or a combination of BSA and serum.
8. In addition to the described primary antibody (Thermo Fisher, Cat #71-5800), other anti-amyloid β antibodies (e.g., MOAB2) can be substituted but the dilution will need to be optimized. The inclusion of 0.1% TX may be useful with some antibodies to minimize nonspecific binding.
9. If a refrigerated shaker is not available, sections can be stored without shaking in at 4 °C overnight. In this case, sections should remain on the room temperature shaker for a few hours before storage, if possible.
10. DAB is a suspected carcinogen and should be handled carefully including use of appropriate PPE and engineering controls. We use DAB kits from Vector Laboratories (Cat #SK-4100), preparing the solution immediately prior to use according to manufacturer's instructions. This kit and others that use soluble DAB reduce the risk of contamination, but DAB solutions are still toxic. Disposal of DAB requires decontamination, which is best achieved by adding to an equal volume of a 1:1 0.2 M potassium permanganate and 2 M sulfuric acid solution. The final solution is then two parts DAB, one part potassium permanganate, and one part sulfuric acid. Although this

solution is thought to completely decontaminate DAB, we collect it and dispose of it as a hazardous chemical.

11. Optimal incubation times in DAB solution are affected by various parameters (primary and secondary antibodies, temperature, rodent strain, etc.) but are usually between 4 and 8 min. Incubation time in DAB may need to be optimized and should remain constant within an experiment.
12. Slides should be either subbed (precoated with gelatin solution) or commercially prepared tissue slides (e.g., Superfrost® Plus slides), both of which facilitate tissue adhesion. Mounting sections in sequential order (4–10 per slide) is preferred and is easily accomplished by transferring sections onto a slide partially submerged in a small dish filled with TBS.
13. Alcohol solutions should be replaced regularly. We use histological grade reagent alcohol (Thermo Fisher, Cat #A962-P4).
14. All dehydration rinses should be performed in a chemical fume hood. Xylene is toxic and should be used with appropriate PPE including lab coat, nitrile gloves, and goggles.
15. We use Krystalon (Millipore, Cat #64969) as a mounting medium, but other similar media are suitable including Permount (Thermo Fisher, Cat #SP15) and DPX (Sigma, Cat #06522). All listed mounting media are toxic and flammable and should be used only in a chemical fume hood with appropriate PPE. After curing overnight, excess mounting media can be removed from coverslipped slides by scraping with a razor.
16. One percent thioflavin-S (Sigma, Cat #T-1892) should be made by adding thioflavin powder slowly to rapidly stirring purified water. When the powder is fully dissolved, filter the solution through #1 Whatman filter paper. Thioflavin solution should be made fresh but can be stored in foil-wrapped bottle in a dark cupboard for up to 2 weeks.
17. **Steps 6–9** describe the process for storing stained sections in a fluorescent antifade solution. Another option is to dehydrate and coverslip without antifade. In this case, replace **steps 6–9** with **steps 19** and **20** described in Subheading 3.1.
18. The optical settings on the microscope (e.g., centering and intensity of light, condenser focus) should be optimized prior to image collection. The depth of field should be adjusted to a relatively collapsed setting such that most of the staining is in focus. We generally use a setting between 0.4 and 0.6, depending upon the transgenic mouse line. The exposure time should also be optimized. For our system, one-third overexposure generally yields images with the highest signal–noise relationship. Optimized settings should be held constant across all image collections for a given study.

19. Typically, we collect two images of subiculum and three of cornu Ammonis 1 (CA1) per section. Additional hippocampal subfields can be imaged similarly as can entorhinal cortex, which is located superior to hippocampal formation. It may be most practical to limit image collection to the sections with well-defined hippocampal subfields. We find it best to save images as TIFF files.
20. Images usually include areas in addition to the specific brain regions that should be excluded from the ROI. Subiculum images often contain cortex, a portion of CA1 and/or adjacent white matter. In some CA1 images, the hippocampal fissure will be visible. *See* Fig. 1 for an example.
21. Properly adjusting the threshold will maximize the amount of specific immunoreactivity and minimize nonspecific staining. The proper threshold setting can be affected by several variables including optical (e.g., depth of field), tissue-related (e.g., tissue thickness, transgenic strain), and immunochemistry quality. The optimal threshold setting must be empirically determined by comparing regions of specific and nonspecific immunostaining on grayscale images with corresponding regions on binary images. We find that within specific strains of Alzheimer's transgenic mice, an optimal threshold setting can be applied to all animals. For example, with EFAD mice sectioned at 40 μm and stained as described under Subheading 3.2, we use a threshold setting of 95. There are instances in which, even within the same immunostaining run, different animals exhibit somewhat lower or higher levels of background immunoreactivity. In these cases, all sections from a lightly stained animal would be thresholded using a predetermined increment (e.g., 5–10 U) above the standard. Conversely, sections from a darkly stained animal would be thresholded at a slightly lower setting. Generally, such animals comprise <10% of all animals. The threshold value should be the same for all sections from each animal.
22. Thioflavin can be viewed using both blue (green light, used for FITC) and ultraviolet (blue light, used for DAPI) filters. The user will need to determine which has the best contrast for their use.
23. We calibrate using a stage micrometer, which is imaged using the same final magnification as the images to be analyzed. Open the image of the stage micrometer in Image J and select Calibration tab. Using the computer mouse, trace a defined length and enter the corresponding value (e.g., 100 μm). The program will now convert pixels to microns.

24. As with amyloid β immunoreactivity, the threshold value must be optimized. However, because thioflavin S staining typically shows low background in mouse brain and is not subject to the variability inherent to immunochemistry, determining the thioflavin threshold is straightforward and does not require correction.
25. You do not need to closely trace the plaque when using the Ellipse tool. The software will measure only the labeled pixels. However, make sure to include only one plaque in each ellipse.
26. In addition to quantifying plaque areas, you can simply sum the number of measured plaques to generate plaque number. These data can be further refined into plaque density by expressing as a function of area. In addition, the thioflavin load or burden can be determined as described for amyloid β immunoreactivity (Subheading 3.4) using thioflavin-labeled sections.

Acknowledgments

This work was supported by NIH grant AG058068 to C.J.P.

References

1. Vinters HV (2015) Emerging concepts in Alzheimer's disease. Annu Rev Pathol 10:291–319
2. Bloom GS (2014) Amyloid-β and tau: the trigger and bullet in Alzheimer disease pathogenesis. JAMA Neurol 71:505–508
3. Selkoe DJ, Hardy J (2016) The amyloid hypothesis of Alzheimer's disease at 25 years. EMBO Mol Med 8:595–608
4. Sala Frigerio C, De Strooper B (2016) Alzheimer's disease mechanisms and emerging roads to novel therapeutics. Annu Rev Neurosci 39:57–79
5. Schmidt SD, Mazzella MJ, Nixon RA, Mathews PM (2012) Aβ measurement by enzyme-linked immunosorbent assay. Methods Mol Biol 849:507–527
6. Cummings BJ, Mason AJL, Kim RC, Sheu PC-Y, Anderson AJ (2002) Optimization of techniques for the maximal detection and quantification of Alzheimer's-related neuropathology with digital imaging. Neurobiol Aging 23:161–170

Chapter 20

Multimodal Imaging of Cerebral Microhemorrhages and White Matter Degradation in Geriatric Patients with Mild Traumatic Brain Injury

Maria Calvillo, Di Fan, and Andrei Irimia

Abstract

Traditionally, neurobiologists have utilized *microscale* techniques of scientific investigation to uncover the fundamental organization and function of brain cells and neuronal ensembles. In recent decades, however, *macroscale* brain imaging methods like magnetic resonance imaging (MRI) and computed tomography (CT) have facilitated a wider scope of understanding neural structure and function across the lifespan. Thanks to such methods, a broader picture of the relationship between microscale processes—studied by neurobiologists—and macroscale observations—made by clinicians—has emerged. More recently, the vascular component of neurodegeneration has come under renewed scrutiny partly due to increased appreciation of the relationship between neurovascular injury, cardiovascular disease, and senescence. Cerebral microbleeds (CMBs) are among the smallest lesions of the cerebrum which can be visualized using MRI to indicate blood–brain barrier (BBB) impairment; as such, this class of hemorrhages are important for the evaluation and macroscale detection of geriatric patients' microscale pathologies associated with neurovascular disease and/or neurodegeneration. This chapter details a streamlined protocol for MRI/CT multimodal imaging data acquisition, archiving and digital processing, including methods tailored for the analysis of susceptibility-weighted imaging (SWI) and diffusion-weighted imaging (DWI) scans to reveal CMB-related alterations of the human connectome. Efficient and effective MRI/CT methods like ours, when tailored for CMB and connectome analysis, are essential for future progress in this important field of scientific inquiry.

Key words Magnetic resonance imaging, Computed tomography, Diffusion tensor imaging, Susceptibility-weighted imaging, Cerebral microbleed, Aging, Geriatrics, Image processing, Traumatic brain injury, Cognitive impairment

1 Introduction

Microscale alterations effected upon the brain by neurological and metabolic disease are typically studied by cell biologists at the level of cells and neuronal assemblies using *microscale* imaging techniques. Nevertheless, *macroscale* imaging methods like magnetic resonance imaging (MRI) and computed tomography (CT) may complement such efforts by enabling scientists to relate microscale

Sean P. Curran (ed.), *Aging: Methods and Protocols*, Methods in Molecular Biology, vol. 2144,
https://doi.org/10.1007/978-1-0716-0592-9_20,

pathology to macroscale findings, thereby offering a broader picture of aging and neurodegeneration. Throughout the past two decades, multisite brain imaging studies have become increasingly common, such that it is vital for imaging data to be acquired, processed and analyzed using streamlined workflows which minimize site-related differences in acquisition and analysis procedures. The adequate management of imaging data acquired from older adult populations has special significance, given geriatric patients' higher rates of overall morbidity, neurologic disease and neuropathology incidence. For example, persons aged 65 and older are more vulnerable to traumatic brain injury (TBI)—particularly mild TBI (mTBI)—and mild cognitive impairment (MCI) than any other group of adults; this can lead to substantially lower quality of life compared to younger individuals, often in tandem with cardiovascular, neurovascular, neurological, and metabolic diseases, including dementia [1].

Improving the validity and reliability of procedures for the analysis of brain imaging data acquired from vulnerable populations—like the elderly—is of high priority in geriatrics and gerontology research. To achieve such improvement, research procedures and protocols must be described in detail, recorded thoroughly and published. Openly available protocol descriptions can improve the reproducibility of neuroimaging studies, define reference workflows for the implementation of multisite studies, and clarify methodological imprecisions to both scientists and clinicians.

In recent years, the vascular component of neurodegeneration has received increased attention due to mounting evidence on the relationship between neurovascular injury, cardiovasculardisease and aging. Cerebral microbleeds (CMBs) are parenchymal lesions of the cerebrum which can indicate impairment of the blood–brain barrier (BBB). They may be small as ~1 mm^3 on certain types of MRI [1], and are diagnostically important in geriatric patients because they represent macroscale manifestations of microscale pathological processes associated with neurovascular disease and neurodegeneration. This chapter describes a set of standardized, streamlined methods for the acquisition, processing and comprehensive analysis of CMB-positive MRI/CT scans of the aging brain, including the specification of suitable inclusion and exclusion criteria for older participants, MRI and CT scanner specifications, MRI imaging sequence parameters, data archiving strategies and processing methods for both CT and MRI, including T_1- and T_2-weighted anatomic MRI, diffusion-weighted imaging (DWI), and susceptibility-weighted imaging (SWI, which can assist in identifying CMBs) [1].

2 Methods

The first part of this section outlines procedures to recruit volunteers for imaging studies like those previously undertaken by our laboratory. This is followed by a description of our data acquisition protocol and then by a detailed narrative of data archiving and processing steps to prepare data for subsequent CMB analysis and connectomics.

2.1 Inclusion and Exclusion Criteria

The following are inclusion and exclusion criteria for older healthy control (HC) participants, for individuals with MCI and for TBI survivors.

2.1.1 Inclusion Criteria for All Groups

1. Be at least 40 years of age.
2. Speak English fluently.
3. Be competent to provide informed consent.

2.1.2 Exclusion Criteria for All Groups

1. A diagnosis of comorbid neurological or psychiatric disease.
2. Being currently nursing or pregnant, or intending to become pregnant.
3. Not speaking English fluently.
4. Suffering from AIDS.
5. Suffering from claustrophobia.
6. Having any metal objects in the body which are affected by strong magnetic fields.

2.1.3 Additional, Group-Specific Inclusion Criteria

1. For TBI participants, the volunteer must have experienced one or more TBIs.
2. For MCI participants, the volunteer must have reported memory concerns.

2.2 Data Acquisition and Archiving

2.2.1 MRI Acquisition

MRIs are acquired using a whole-body, MAGNETOM Prisma^{FIT} 3T scanner (Siemens Corporation, Erlagen, Germany) with a 60 cm bore diameter. All head scans are acquired using a 20-channel head–neck matrix coil. The following are the technical specifications of the Prisma^{FIT} scanner:

1. Magnetic homogeneity of 0.103 parts per million (ppm) within the 40 cm diameter spherical volume of the bore.
2. 64 parallel radiofrequency (RF) receiver channels and up to 204 coil elements.
3. Dual-channel parallel transmit and slice-accelerated "multiband" acquisition.
4. A total imaging matrix (TIM) of 204 × 64.
5. A 2× Tesla C2075 graphics processing unit (GPU).

6. A XR 80/200 gradient system with a maximum amplitude of 80 mT/m per axis and a maximum slew rate of 200 T/m/s per axis.
7. Active shimming using three linear and five second-order channels.
8. A field of view (FOV) of at most 500 mm and at least 5 mm.
9. A maximum matrix size of 1024 × 1024.
10. A maximum in-plane resolution of 7 μm.
11. Integrated Tx/Rx solid-state DirectRF technology.
12. Syngo MR VD13D software.

A total of ten sequences are included in this protocol for acquiring MRI scans. The sequence names and their parameters are listed in Table 1.

Table 1
MRI acquisition parameters

Parameter	Unit	MPRAGE T1	FSE T1	T2	FLAIR	FLASH	fMRI	GRE SWI	DWI
Repetition time (TR)	ms	30	3.15	3.15	3.15	800	10,000	1950	8300
Echo time (TE)	ms	20	1.37	1.37	1.37	20	88	2.98	72
Inversion time (TI)	ms	–	–	–	–	–	–	900	–
Pixel width	mm	0.5	1.625	1.6	1.6	1	0.82	1	2
Pixel height	mm	0.5	1.625	1.6	1.6	1	0.82	1	2
Slice thickness	mm	2	1.6	1.6	1.6	4	3.5	1	2
Interslice gap	mm	0	0	0	0	5.2	3.5	0	2
Sampling	%	50	100	100	100	100	100	100	100
Phase FOV	%	75	100	100	100	75	100	100	100
Pixel bandwidth	Hz	100	540	540	540	180	200	240	1345
Flip angle	°	15	8	8	8	20	120	9	90
Echo train length (ETL)	–	1	1	1	1	1	17	1	47
Acquisition matrix width	–	384	160	162	162	192	256	256	128
Acquisition matrix height	–	512	160	162	162	256	256	256	128
Acquisition type	–	3D	3D	3D	3D	2D	2D	3D	2D
Number of averages	–	1	1	1	1	1	1	1	1
Echo number	–	1	1	1	1	1	1	1	1
Phase encoding steps	–	191	118	118	118	269	333	255	95
Phase encoding direction	–	ROW	ROW	ROW	ROW	ROW	ROW	ROW	COL

Listed here are selected parameters for eight MRI sequences, as utilized with the acquisition protocol described. Importantly, (A) the TR, TE and TI are fundamental temporal parameters which determine the properties of the MRI signal, whereas (B) pixel width, height, slice thickness, and interslice gap determine the spatial resolution of a scan

2.2.2 CT Acquisition

CT scans are acquired using a 16-slice General Electric (GE) BrightSpeed™ scanner. Images are acquired using the following parameters:

1. Width: 512 pixels.
2. Height: 512 pixels.
3. Mode: helical.
4. Slice thickness: 0.6250 mm.
5. Slice spacing: 0.6250 mm.
6. Kilovoltage peak (kVp): 120 kV.
7. Data collection diameter: 250 mm.
8. Reconstruction diameter: 223 mm.
9. Gantry detector tilt: 0°.
10. Rotation direction: clockwise.
11. Exposure time: 1397 ms.
12. X-ray tube current: 140 mA.
13. Filter type: head filter.
14. Generator power: 16,800 kW.
15. Focal spot: 0.7 mm.
16. Convolution kernel type: soft.
17. Revolution time: 1 s.
18. Single collimation width: 0.625 mm.
19. Total collimation width: 10 mm.
20. Table speed: 9.3750 mm/s.
21. Table feed per rotation: 9.375 mm.
22. Spiral pitch factor: 0.9375.
23. Pixel spacing: 0.435547 mm.

2.2.3 MRI/CT Archiving

After acquisition, data are stored in DICOM (digital imaging and communications in medicine) format. They are then deidentified and delinked to preserve privacy and confidentiality. This is achieved by removing identifying information from the DICOM file headers. Next, data are transferred to a secure online database managed by the scanning facility (*see* **Note 1**). Following this transfer, data are transferred to a depository maintained by the laboratory, where they can be accessed and processed at ease (*see* **Note 2**).

2.3 Neuroimage Data Processing

All data processing steps are based upon protocols used in past studies conducted in our laboratory [2–7]. This section describes preprocessing steps for both MRI and CT scans. A set of universal MRI processing steps are applied to all MRI volumes, whereas DWI

and SWI data undergo additional processing steps which are specific only to these two types of data. All steps for universal MRI processing and DTI are undertaken using the fMRI Standard Library (FSL) image processing toolbox (fsl.fmrib.ox.ac.uk/fsl).

2.3.1 MRI Preprocessing Steps

The following set of preprocessing steps is applied to all MRI volumes, including those acquired using DWI and SWI sequences.

1. DICOM files are converted into NIFTI format using dcm2niix (https://www.nitrc.org/plugins/mwiki/index.php/dcm2nii:MainPage).
2. Motion correction is performed.
3. Voxels beyond the area of the brain are excluded (i.e., imaging volumes are skull-stripped).
4. Image intensities within the brain mask are identified.
5. The intensities of voxels within the brain are normalized across subjects by dividing their intensities by their median intensity (*see* **Note 3**).
6. Bias field correction is applied to each volume using a fourth-order polynomial [8].

2.3.2 DWI Processing Steps

The following steps are applied to DWI data in addition to those previously described.

1. B_0 volumes are identified as those volumes acquired while no diffusion gradient is being applied.
2. Skull removal is implemented and the brain mask is computed.
3. Susceptibility artifact correction is implemented.
4. Motion correction is applied.
5. Eddy-current artifact correction is performed.
6. A suitable rotation of the B matrix is applied to alleviate orientation artifacts (*see* **Note 4**).
7. B_0 images are coregistered to their corresponding T_1-weighted volumes using a rigid, affine (six-parameter) registration.
8. Diffusion tensors are fitted to DWI images.
9. Fractional anisotropy (FA) calculations are performed.
10. Deterministic tractography via fixed step-length streamline propagation is used to reconstruct white matter (WM) streamlines using the following parameters:
    - Seed spacing: 0.5 mm.
    - Linear measure start threshold: 0.3.
    - Stopping value: 0.17.
    - Minimum streamline length: 20 mm.

- Maximum streamline length: 110 mm.
- Stopping criterion: fa value.
- Stopping criterion value: 0.17.
- Stopping track curvature: 0.96 mm^{-1}.
- Integration step length: 0.5 mm.

11. Streamlines are visualized in TrackVis (trackvis.org) and 3D Slicer (www.slicer.org).

If longitudinal MRI/DWI data are available, one can estimate and reduce the extent to which diffusion tractography measures can be influenced by confounding factors, such as subject motion, scanner noise, MRI inhomogeneity differences and other computational errors and inaccuracies. Such estimation is completed through the following technique:

1. At each WM voxel, the uncertainty ellipsoid is defined as a volume around a voxel where any DTI-derived WM measures require detailed analysis, since they may be influenced by confounding factors to a greater extent (*see* **Note 5**).
2. If quantification of WM changes over time is required, the following steps are taken:
   (a) Streamlines are assumed to be piecewise-differentiable 3D space curves with an invariant curvature and torsion.
   (b) Any two curves are determined to have equal curvature and torsion if they lie within the same transformation of each other and if there is a curve index correspondence between parametrizations.
   (c) Within each subject, curve index correspondence is established [9] by generating arc length parametrizations for each curve, time point, and perilesional streamline bundle.
   (d) Point-to-point coregistration is performed by implementing a local transformation using Schönemann's solution to the orthogonal Procrustes problem [10].
   (e) The global residue of squared intercurve distances within the local transformations is minimized to approximate a global transformation which matches source and target curves.
   (f) FA values and pointwise descriptive statistics of each measure are calculated for the arc-length coordinates of each streamline [9, 11].
   (g) The range of arc-length coordinates shared between most streamlines within each bundle of interest is identified.

(h) To compare mean FA differences over time within perilesional streamline bundles and then evaluate whether or not they may be due to artifacts, two empirical reference mean FA distributions are established (one for younger subjects and one for older subjects).

(i) The mean and variance of the reference distributions are calculated over the streamlines.

(j) Distribution parameter values are pooled within each age group.

(k) The null hypothesis of no difference in FA across time points is tested for each perilesional streamline bundle of interest.

3. WM streamline prototyping is implemented as follows:

(a) An anatomical clustering atlas is used to annotate and categorize WM streamline clusters (*see* **Note 6**) as deep WM bundles (such as major association and projection bundles, commissural bundles, cerebellar and brainstem connection bundles), short bundles and medium-range superficial bundles, which are organized by the brain lobes that they connect.

(b) Connections identified as potential false positives are annotated for exclusion.

(c) Following WM parcellation, WM prototyping is implementing by identifying the most representative WM streamline in each cluster, that is, the streamline whose trajectory is most similar to the average trajectory of the streamline in the bundle (*see* **Note 7**).

2.3.3 SWI Processing Steps

The following steps are implemented to process SWI volumes and identify CMBs:

1. SWI volumes are skull-stripped and coregistered rigidly to their respective T_1-weighted volumes.
2. CMB identification is accomplished using the following algorithms.
   - The image intensity gradient of the skull-stripped SWI volume is computed at each brain voxel using MATLAB.
   - Binary erosion of the gradient magnitude volume is performed using a spherical morphological structuring element (radius = 11 pixels) to remove areas exhibiting sharp gradient changes at the edges of the brain.
   - A gradient magnitude histogram is calculated over all brain voxels.

- The eroded volume is thresholded to exclude values belonging to the tails of its intensity distribution.
- Within the thresholded volume, the volume of each connected component consisting of contiguous nonzero voxels is computed.
- The largest component—associated with voxels on the borders between cerebrospinal fluid (CSF) and WM—is removed.
- Components associated with voxels within the sulcal banks of the neocortex and on the boundaries between brain and blood vessels are eliminated by removing voxels which were identified as isointense (i.e., within $\mu \pm 2\sigma$ of the image intensity distribution of the SWI image).
- Remaining nonzero voxel components are assigned CMB labels.

The sensitivity and precision of the CMB identification method can be evaluated against a manual CMB labeling method conducted by a neuroanatomy and neuroradiology expert. Specifically, to calculate the sensitivity and precision of the approach, a manual detection algorithm is used, as follows.

1. Potential CMBs are identified in images using a voxel classifier based on Microbleed Anatomic Rating Scale (MARS) guidelines [12].
2. Identified CMBs are classified as either certain (represented by small, clearly delineated circular shapes) or doubtful (represented as components which are not well-delineated and which do not conform to strictly circular shapes).
3. Hypointensities on the boundary of the brain are disregarded, as CMBs are not associated with the meninges.
4. An object-based classifier which assesses CMB shape is applied to eliminate false positives CMB assignments.
5. CMB sphericity violations are determined by calculating CMB object curvature and identifying values which exceed the curvature of a sphere by a substantial amount [13].
6. If CMB etiology must be classified as either traumatic or nontraumatic (e.g., related to cerebral amyloid angiopathy or hypertensive vasculopathy), a CMB is assumed to be TBI-related if (A) at the acute stage of TBI, the CMB is partially or fully surrounded by one or more focal FLAIR hyperintensities, and (B) at the chronic stage of TBI, the FLAIR hyperintensities are no longer detectable.

2.3.4 CT Processing Steps

CT segmentation is performed using an approach whose results are presented elsewhere [14–19]. The steps of the algorithm are as follows.

1. The parameters of Gaussian intensity distributions are computed for three tissue classes [WM, gray matter (GM), and cerebrospinal fluid (CSF)].
2. Using the following steps, probabilities are assigned to voxels to reflect their likelihood of belonging to a specific tissue class in the Gaussian mixture model:
   (a) An objective function is derived from several Gaussian random variable models and its value is minimized using a nonlinear optimization procedure of the user's choice.
   (b) To complete the classification process, a priori tissue probability maps available in a modified MINI_{152} probabilistic atlas [20] are identified for each tissue class.
   (c) To accommodate the intensity profile of CT scans—where CSF is hypointense—the atlas is modified to assign low intensities to CSF voxels in the atlas.
   (d) The objective function is used to weigh the probability maps using Bayesian inference principles.
   (e) The probability maps are deformed to match each subject's brain CT volumes to be segmented.
   (f) The volumes are segmented by assigning probabilities to each voxels, which specify the likelihood that the voxel belongs to a certain tissue class.
   (g) Posterior probabilities are computed according to each subject's voxel intensity values.
   (h) The interface between the resulting GM and WM volumes is smoothed using a nonlinear Wiener filter, subject to the topological constraints of the brain's intensity profile.
   (i) Topology-constrained probabilistic classification refinement is performed [16] in three steps:
      - The plane which crosses the WM/GM boundary and is intersected by voxels with minimal intensity variance is identified.
      - Voxels in the identified plane are assigned according to whether most of them have an unclear intensity classification, or whether they are close to voxels with varying class memberships.
      - A voxel's class assignment is changed to the more appropriate one if this reduces the in-plane density variance.

Figure 1 shows the output produced by the preprocessing of DWI and SWI scans acquired from a sample geriatric mTBI patient.

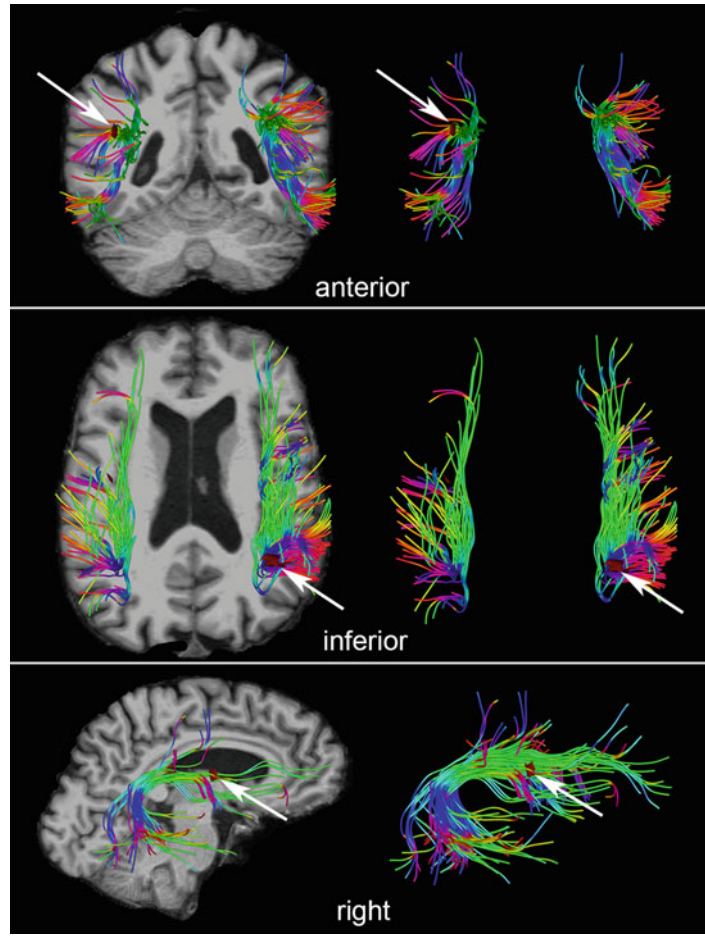

Fig. 1 Example output of a DWI/SWI analysis revealing the colocalization of two CMBs (arrows) relative to the arcuate fasciculus (AF) of the two cerebral hemispheres. The AF is a WM structure with substantial involvement in speech production. Two CMBs are depicted as small, red, ovoidal objects located in the spatial vicinity of the AF. Shown are anterior (top row), inferior (middle row), and right (bottom row) views of the cerebral cortex, cerebellum, lateral ventricles and brain stem. Because of their locations, only one CMB is visible in any of the three views. Specifically, one (smaller) CMB is visible in the anterior and lateral views (top and bottom rows), and one (larger) CMB is visible in the inferior view (middle row). T_1-weighted images of the cortex are overlaid to indicate the location of the CMBs and AF relative to the anatomy of the brain. WM streamline orientation is color-coded (red: left to right; green: anterior to posterior; blue: inferior to superior). The left column localizes the AF relative to the brain, whereas the right column isolates this WM structure for easier visualization

3 Notes

1. Interaction with the secure database to which the MRI scans were uploaded is facilitated by Flywheel software (flywheel.io).
2. MRI data transfer is made to a HIPAA-compliant Amazon Web Services (AWS) online cloud environment.
3. Intensity normalization is implemented to account for the potentially confounding effect of inter-subject intensity brain differences.
4. The additional rotation of the B matrix in DWI image processing is necessary because resulting orientational information may be affected by the increased head motion which is often associated with DWI, given this modality's relatively long acquisition times [21].
5. In the estimation of confounding factors, the use of the ellipsoid—rather than that of a sphere—is advantageous because it facilitates the evaluation of the local water-diffusion WM anisotropy.
6. The anatomically curated streamline clustering atlas used is described in reference [6]. This atlas is suitable because it allows the whole-brain WM to be parceled into 800 streamline clusters.
7. The approach to WM prototyping was based upon methods described elsewhere [3, 6, 7, 9, 22]. Streamline prototyping is important in diffusion MRI tractography, as the latter technique may generate false streamlines which are not representative of real WM connections. Establishing a streamline prototype for an entire cluster allows for a more accurate detection of underlying WM structure and of its trajectory.

Acknowledgments

This work was supported by NIH grant R01 NS 100973, by DoD contract W81-XWH-1810413 and by the Undergraduate Research Associate Program (URAP) at the University of Southern California. The authors wish to thank Nikhil N. Chaudhari, Nahian F. Chowdhury, and Kenneth A. Rostowsky for their comments and suggestions, as well as Drs. Lauren J. O'Donnell and Fan Zhang (Harvard Medical School) for their advice on DWI preprocessing. AI would like to thank the Department of Electrical Engineering and Computer Science at the Massachusetts Institute of Technology, where part of this research was carried out.

References

1. Irimia A, Van Horn JD, Vespa PM (2018) Cerebral microhemorrhages due to traumatic brain injury and their effects on the aging human brain. Neurobiol Aging 66:158–164. https://doi.org/10.1016/j.neurobiolaging.2018.02.026
2. Fan D, Chaudhari NN, Rostowsky KA, Calvillo M, Lee SK, Chowdhury NF, Zhang F, O'Donnell LJ, Irimia A (2019) Post-traumatic cerebral microhemorrhages and their effects upon white matter connectivity in the aging human brain. Conf Proc IEEE Eng Med Biol Soc 2019:198–203
3. Rostowsky KA, Maher AS, Irimia A (2018) Macroscale white matter alterations due to traumatic cerebral microhemorrhages are revealed by diffusion tensor imaging. Front Neurol 9:948. https://doi.org/10.3389/fneur.2018.00948
4. Irimia A, Maher AS, Rostowsky KA, Chowdhury NF, Hwang DH, Law EM (2019) Brain segmentation from computed tomography of healthy aging and geriatric concussion at variable spatial resolutions. Front Neuroinform 13:9–9. https://doi.org/10.3389/fninf.2019.00009
5. Maher AS, Rostowsky KA, Chouwdhury NF, Irimia A (2018) Neuroinformatics and analysis of connectomic alterations due to cerebral microhemorrhages in geriatric mild neurotrauma: microhemorrhages in geriatric neurotrauma. Paper presented at the Proceedings of the 2018 ACM international conference on bioinformatics, computational biology, and health informatics, Washington, DC, USA
6. Zhang F, Wu Y, Norton I, Rigolo L, Rathi Y, Makris N, O'Donnell LJ (2018) An anatomically curated fiber clustering white matter atlas for consistent white matter tract parcellation across the lifespan. Neuroimage 179:429–447. https://doi.org/10.1016/j.neuroimage.2018.06.027
7. Norton I, Essayed WI, Zhang F, Pujol S, Yarmarkovich A, Golby AJ, Kindlmann G, Wassermann D, Estepar RSJ, Rathi Y, Pieper S, Kikinis R, Johnson HJ, Westin C-F, O'Donnell LJ (2017) SlicerDMRI: open source diffusion MRI software for brain cancer research. Cancer Res 77(21):e101–e103. https://doi.org/10.1158/0008-5472.CAN-17-0332%J
8. Sled JG, Zijdenbos AP, Evans AC (1998) A nonparametric method for automatic correction of intensity nonuniformity in MRI data. IEEE Trans Med Imaging 17(1):87–97. https://doi.org/10.1109/42.668698
9. Donnell LJO, Westin C (2007) Automatic tractography segmentation using a high-dimensional white matter atlas. IEEE Trans Med Imaging 26(11):1562–1575. https://doi.org/10.1109/TMI.2007.906785
10. Leemans A, Sijbers J, De Backer S, Vandervliet E, Parizel P (2006) Multiscale white matter fiber tract coregistration: a new feature-based approach to align diffusion tensor data. Magn Reson Med 55(6):1414–1423. https://doi.org/10.1002/mrm.20898
11. Maddah M, Grimson WEL, Warfield SK, Wells WM (2008) A unified framework for clustering and quantitative analysis of white matter fiber tracts. Med Image Anal 12(2):191–202. https://doi.org/10.1016/j.media.2007.10.003
12. Gregoire SM, Chaudhary UJ, Brown MM, Yousry TA, Kallis C, Jäger HR, Werring DJ (2009) The Microbleed Anatomical Rating Scale (MARS). Reliability of a tool to map brain microbleeds. Neurology 73(21):1759–1766. https://doi.org/10.1212/WNL.0b013e3181c34a7d
13. Romeny BMT (2011) Multi-scale and multi-orientation medical image analysis. In: Deserno T (ed) Biomedical image processing. Springer Berlin, Heidelberg, pp 177–196. https://doi.org/10.1007/978-3-642-15816-2_7
14. Ashburner J, Friston K (1997) Multimodal image coregistration and partitioning—a unified framework. Neuroimage 6(3):209–217. https://doi.org/10.1006/nimg.1997.0290
15. Ashburner J, Friston KJ (2000) Voxel-based morphometry—the methods. Neuroimage 11(6):805–821. https://doi.org/10.1006/nimg.2000.0582
16. Ashburner J, Friston KJ (2005) Unified segmentation. Neuroimage 26(3):839–851. https://doi.org/10.1016/j.neuroimage.2005.02.018
17. Ashburner J, Friston K (2007) Segmentation. In: Friston K, Ashburner J, Kiebel S, Nichols T, Penny W (eds) Statistical parametric mapping. Academic Press, London, pp 81–91. https://doi.org/10.1016/B978-012372560-8/50006-1
18. Dale AM, Fischl B, Sereno MI (1999) Cortical surface-based analysis: I. Segmentation and surface reconstruction. Neuroimage 9(2):179–194. https://doi.org/10.1006/nimg.1998.0395
19. Fischl B, Sereno MI, Dale AM (1999) Cortical surface-based analysis: II. Inflation, flattening, and a surface-based coordinate system.

Neuroimage 9(2):195–207. https://doi.org/10.1006/nimg.1998.0396

20. Grabner G, Janke AL, Budge MM, Smith D, Pruessner J, Collins DL (2006) Symmetric atlasing and model based segmentation: an application to the hippocampus in older adults. In: Larsen R, Nielsen M, Sporring J (eds) Medical image computing and computer-assisted intervention – MICCAI 2006. Springer Berlin Heidelberg, Berlin, Heidelberg, pp 58–66
21. Leemans A, Jones DK (2009) The B-matrix must be rotated when correcting for subject motion in DTI data. Magn Reson Med 61 (6):1336–1349. https://doi.org/10.1002/mrm.21890
22. O'Donnell LJ, Westin C-F, Golby AJ (2009) Tract-based morphometry for white matter group analysis. Neuroimage 45(3):832–844. https://doi.org/10.1016/j.neuroimage.2008.12.023

Chapter 21

Detection of HNE Modification of Proteins in Aging Mouse Tissues: A Western Blot-Based Approach

Hongqiao Zhang, Natalie Lyn, Amin Haghani, and Henry Jay Forman

Abstract

4-Hydroxenonenal (HNE) is one of the major α,β-unsaturated aldehyde products of lipid peroxidation. HNE can form conjugates with macromolecules, including protein, and thereby alter their function. HNE and its conjugation with proteins are increased in aging and age-related diseases. To elucidate how HNE is involved in these aging-related pathophysiological changes, it is necessary to assess HNE modification of proteins. Here a simple and convenient Western-blot based method is presented to detect HNE modification of proteins in tissues of aging mice.

Key words HNE, HNE–protein adduct, Aging, Oxidative stress, Western blot

1 Introduction

Aerobic organisms including human beings are constantly exposed to oxidants produced endogenously as products of biological processes or exogenously from the environment. These oxidants are often referred to as reactive oxygen species (abbreviated as ROS), which includes the free radicals superoxide ($O_2^{\cdot -}$) and hydroxyl ($^{\cdot}OH$) as well as the nonradical hydrogen peroxide (H_2O_2), singlet oxygen (which is uncharged but has greater oxidizing potential than ground state triplet O_2), and ozone (O_3). These species are markedly different chemically and in their biological effects. But each may contribute to producing oxidative stress, which occurs when antioxidant defenses fail to prevent injury. Oxidants can damage macromolecules, including lipids, proteins, and nucleic acids, and thereby cause cellular dysfunction or cell death. Oxidative stress has been implicated in various pathologies, including atherosclerosis, chronic obstructive pulmonary disease, cancers, diabetes, cataract, and neurodegenerative diseases [1–4].

The aging process is accompanied by increased oxidative stress, probably due to a combined effect of both an increased generation of $O_2^{\cdot -}$ and H_2O_2 from dysfunctional mitochondria [5–8] and

Sean P. Curran (ed.), *Aging: Methods and Protocols*, Methods in Molecular Biology, vol. 2144,
https://doi.org/10.1007/978-1-0716-0592-9_21,

increased expression/activity of oxidant-producing enzymes [9–17], and a decreased capacity of antioxidant defenses including the Nrf2-mediated antioxidant response [18, 19]. Several biomarkers have been used to evaluate the age-related increase in oxidative damage, including H_2O_2 level [16], ratio of GSH/GSSG [20, 21], F2-isoprostane [22] and 4-hydroxynonenal (HNE) [23] (lipid peroxidation), protein carbonyl [24, 25] (protein oxidation), and 8-hydroxy-2-deoxyguanosine (8-OHdG, DNA oxidation) [26, 27].

HNE is a major α,β-unsaturated aldehyde derived from the decomposition of peroxidation products of omega-6 polyunsaturated fatty acids, such as arachidonic acid and linoleic acid in plasma membranes. The combined effect of the two conjugated functional groups of HNE, the carbonyl (–HC=O) and the double bond (C2/C3, –C=C–) groups, enables HNE to react readily with biomolecules including lipids, nucleic acids, and proteins. Since most HNE in cells is present in the form of HNE–protein adducts and proteins are the key players of redox signaling and phenotypic changes, the study of HNE modification of proteins has drawn the most attention. HNE mainly forms Michael adducts with its C=C to cysteine, histidine, and/or lysine residues or Schiff base adducts with its aldehyde function to lysine. These adducts are relatively stable and can be retained for several hours before being degraded [28, 29]. HNE–protein adducts are increased upon oxidative stress, with aging, and in various age-related diseases [23]. Therefore, HNE modification of proteins has been well accepted as a marker of oxidative stress, lipid peroxidation, and protein oxidation.

HNE–protein adducts can be detected with several methods, such as enzyme-linked immunosorbent assay (ELISA) [30], Western blot, and mass spectrometry [31], depending on the research purpose. Here we describe a Western blot-based method used in our laboratory to detect the overall change of HNE–protein adducts in tissues of aging mouse.

2 Materials

All chemicals are obtained from Sigma-Aldrich (St. Louis, MO, USA), unless noted otherwise.

2.1 Mouse Tissues and Protein Extraction

All animal procedures are approved by the University of Southern California (USC) Institutional Animal Care and Use Committee (IACUC). Tissues are dissected from euthanized mice and immediately frozen in dry ice, then stored in −80 °C for future assays.

1. 1× RIPA lysis buffer, 50 mM Tris, pH 7.4, 150 mM NaCl, 1 mM EDTA, 1% NP-40.
2. 0.25% deoxycholic acid.

3. Protein inhibitor cocktail.
4. Mechanical stirrer.
5. Benchtop refrigerated centrifuge.

2.2 SDS–Polyacrylamide Gel Electrophoresis (SDS-PAGE) (See Note 1)

1. Tris–glycine gel, 4–20% (Thermal Fisher Scientific, Rockford, IL, USA).
2. SDS-PAGE running buffer: 0.025 M Tris–HCl, pH 8.3, 0.192 M glycine, 0.1% SDS.
3. 2× laemmli sample buffer (Bio-Rad, Hercules, CA, USA).
4. Protein marker.
5. Vertical Mini Gel Electrophoresis System.

2.3 Immunoblotting (See Note 2)

1. PVDF membrane.
2. Western blot transfer buffer: 0.025 M Tris–HCl, 0.192 M glycine, 20% methanol.
3. Tris-buffered saline (TBS; 1×): 150 mM NaCl, 10 mM Tris–HCl, pH 7.4.
4. Washing buffer, TBS containing 0.05% Tween 20 (TBST).
5. Blocking buffer, 5% fat-free milk in TBST.
6. Fat-free milk powder.
7. 4-Hydroxynonenol antibody, mouse (B&D Systems, Minneapolis, MN, USA).
8. Anti-β-actin horseradish peroxidase (Abcam, Cambridge, MA, USA).

2.4 Image Capture

1. SuperSignal West Femto Maximum Sensitivity Substrate (Thermal Fisher Scientific, Rockford, IL, USA).
2. Syngene PXi6 imaging system (Syngene, Cambridge, UK).

2.5 Stripping Membrane and Reblot

1. Reblot Plus-mild (10×) stripping buffer (Millipore Sigma, Burlington, MA, USA).

3 Methods

3.1 Protein Extraction

1. Cut about 5 mg of lung tissues on dry ice and put in 1.5 ml Eppendorf tube in ice.
2. Add 200 μl of ice-cold 1× RIPA lysis buffer with protease inhibitor (*see* **Note 3**).
3. Lyse tissues using an overhead stirrer for 30–120 s.
4. Incubate the lysed tissues on ice for 60 min.
5. Centrifuge at 15,000 × *g*, 4 °C, for 10 min.

6. Transfer the supernatant to a new tube.
7. Measure the protein concentration.
8. Continue or store the extracted protein at −80 °C.

3.2 Gel Electrophoresis

1. Using 10–15 μg of protein. Prepare the mixture of protein and sample buffer in a 1.5-ml tube (the total volume is dependent on the maximal amount that the well can hold). Heat the mixture at 95 °C for 10 min.
2. Centrifuge the samples at 2000 × *g* for 1 min to bring down the condensate.
3. Set up the gel for electrophoresis. Insert the gel in gel box, tighten the inner chamber, fill the inner chamber with running buffer completely, and make sure the inner chamber is not leaky. Then add running buffer in the outer chamber. For mini electrophoresis gel box, a total of 600 ml of running buffer is needed.
4. Load the samples and protein marker in the wells with fine gel loading tips.
5. Electrophorese at 120 V for 2 h or until the blue dye front reached the bottom of the gel.
6. Following electrophoresis, pry the gel plate open with a spatula, trim the gel, and place the gel in transfer buffer.

3.3 Gel Transfer (See Note 2)

1. Pretreat the PVDF membrane as following: immerse in methanol for 45 s, rinse with deionized H_2O once, and then immerse the membrane in transfer buffer for use. Wet the pads and filter papers with transfer buffer.
2. Set up the transfer sandwich in a plate. Open cassette with dark side down and place the following layers in order: pad–filter paper–gel–membrane–filter paper–pad. Using a roller (or 15-ml tube) to roll over each layer to remove bubbles. Lock the sandwich cassette.
3. Put the cassette in the holder of the transfer tank with dark side of the cassette facing the black side of the chamber (so the membrane is positioned at the cathode side of the gel).
4. Turn on the power and run the transfer at 80 V for 2 h.
5. Take out the membrane and rinse with TBST for blotting.

3.4 Blotting with Antibodies (See Note 4)

1. Block the membrane by incubating the membrane with 10 ml of 5% fat-free milk and shaking for 40 min. Prepare 10 ml of primary HNE Ab with 1:2500 dilution.
2. Discard the blocking milk and add diluted HNE Ab.
3. Incubate overnight at 4 °C with mild shaking.

4. Wash the membrane with 1× TBST buffer for 3 × 10 min with shaking. During this time, prepare 10 ml of 2rd Ab.
5. Incubate the membrane with 2rd Ab at room temperature for 2 h with shaking.
6. Wash the membrane with 1× TBST buffer 6 × 10 min with shaking.

3.5 Image Capture (See Note 5)

1. Prepare West Femto mixture by mixing equal volume of Luminol/Enhancer solution and stable peroxide solution in a 2 ml tube (1:1 ratio).
2. Place the membrane on a transparent plastic film at flat surface.
3. Drop the West Femto mixture evenly on the membrane.
4. Incubate at room temperature for 5 min.
5. Cover the membrane with a smaller transparent plastic film and capture the image with Imager.

3.6 Strip Membrane and Reblotting for Internal Loading Control (See Note 6)

1. Prepare 10 ml of 1× stripping buffer.
2. Incubate the membrane with stripping buffer with shaking for 10–15 min.
3. Rinse the membrane with TBST once.
4. The membrane is ready for reblotting (Fig. 1).

4 Notes

1. 10% SDS-PAGE gel and 5× sample buffer can be used. 5× sample buffer can be prepared using the following recipe: 0.25 M Tris–HCl, pH 6.8, 10% SDS, 0.5 M DTT, 10% 2-mercaptoethanol, 1% Triton X-100, 50% glycerol, 0.5% bromophenol blue.
2. Dry transfer with iBlot Transfer System (Thermal Fisher Scientific, Rockford, IL, USA) is faster compared to the conventional wet-transfer method as described here.
3. During the storage, lipid peroxidation and HNE production occurs. To prevent oxidative modification of proteins, reducing agents such as DTT and 2-mercaptoethanol should be added into the lysis buffer for long time storage.
4. Commercial blocking buffer or BSA can be used for blocking membrane and diluting antibodies. Antibody dilution should be optimized based on information recommended by the manufacturers. Incubation with primary antibody can also be performed at room temperature with shaking for 3 h.
5. If fluorescence based secondary antibodies are used, specific buffers and membrane may be required.

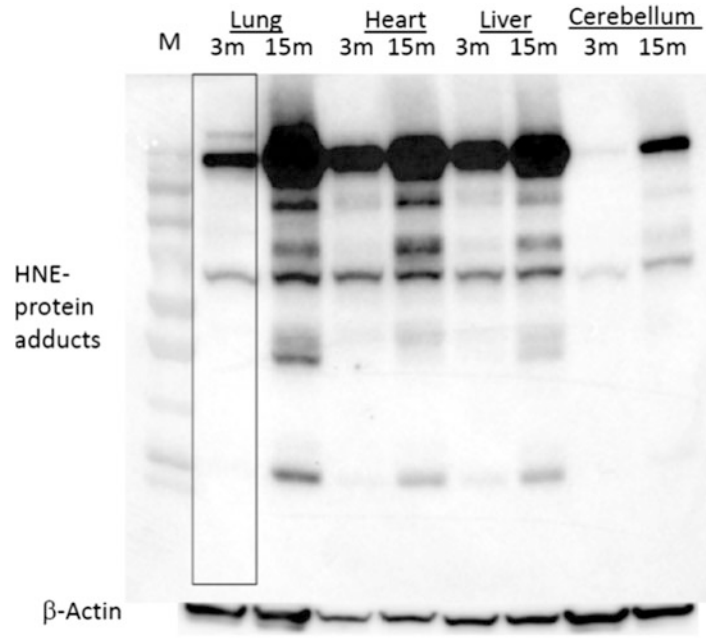

Fig. 1 A representative Western blot image HNE–protein adducts in aging mouse tissues. Tissues were from 2- and 15-month-old male mice, and Western blot was performed as described. Anti-HNE antibody, 1:2500 dilution in 5% milk; anti-actin, 1:4000 dilution in 5% milk. The boxed lane was shown as an example of selected area for quantification of signal intensity. *M* marker of molecular weight

6. Normalization with internal loading control is critical for data quality. Usually total protein staining and housekeeping protein such as β-actin are used as internal loading controls. Importantly, signals of target protein and loading control should be from the same membrane.

Acknowledgments

This work was supported by NIH grants R01 ES023864 and P01 AG055367.

References

1. Butterfield DA, Howard BJ, LaFontaine MA (2001) Brain oxidative stress in animal models of accelerated aging and the age-related neurodegenerative disorders, Alzheimer's disease and Huntington's disease. Curr Med Chem 8 (7):815–828
2. Beal MF (2002) Oxidatively modified proteins in aging and disease. Free Radic Biol Med 32 (9):797–803
3. Emerit J, Edeas M, Bricaire F (2004) Neurodegenerative diseases and oxidative stress. Biomed Pharmacother 58(1):39–46
4. Jacob KD, Noren Hooten N, Trzeciak AR, Evans MK (2013) Markers of oxidant stress that are clinically relevant in aging and age-related disease. Mech Ageing Dev 134 (3–4):139–157. https://doi.org/10.1016/j.

mad.2013.02.008. S0047-6374(13)00028-6 [pii]
5. Benzi G, Moretti A (1995) Age- and peroxidative stress-related modifications of the cerebral enzymatic activities linked to mitochondria and the glutathione system. Free Radic Biol Med 19(1):77–101
6. Cadenas E, Davies KJ (2000) Mitochondrial free radical generation, oxidative stress, and aging. Free Radic Biol Med 29(3–4):222–230
7. Sastre J, Pallardo FV, Vina J (2003) The role of mitochondrial oxidative stress in aging. Free Radic Biol Med 35(1):1–8
8. Sohal RS, Orr WC (2012) The redox stress hypothesis of aging. Free Radic Biol Med 52 (3):539–555. https://doi.org/10.1016/j.freeradbiomed.2011.10.445. S0891-5849(11) 01109-9 [pii]
9. Newaz MA, Yousefipour Z, Oyekan A (2006) Oxidative stress-associated vascular aging is xanthine oxidase-dependent but not NAD(P) H oxidase-dependent. J Cardiovasc Pharmacol 48(3):88–94. https://doi.org/10.1097/01.fjc.0000245402.62864.0a
10. Chung HY, Song SH, Kim HJ, Ikeno Y, Yu BP (1999) Modulation of renal xanthine oxidoreductase in aging: gene expression and reactive oxygen species generation. J Nutr Health Aging 3(1):19–23
11. Vida C, Corpas I, De la Fuente M, Gonzalez EM (2011) Age-related changes in xanthine oxidase activity and lipid peroxidation, as well as in the correlation between both parameters, in plasma and several organs from female mice. J Physiol Biochem 67(4):551–558. https://doi.org/10.1007/s13105-011-0100-8
12. Law A, Dore S, Blackshaw S, Gauthier S, Quirion R (2000) Alteration of expression levels of neuronal nitric oxide synthase and haem oxygenase-2 messenger RNA in the hippocampi and cortices of young adult and aged cognitively unimpaired and impaired Long-Evans rats. Neuroscience 100(4):769–775
13. Kang MJ, Kim HJ, Kim HK, Lee JY, Kim DH, Jung KJ, Kim KW, Baik HS, Yoo MA, Yu BP, Chung HY (2005) The effect of age and calorie restriction on HIF-1-responsive genes in aged liver. Biogerontology 6(1):27–37. https://doi.org/10.1007/s10522-004-7381-z
14. Kireev RA, Tresguerres AC, Garcia C, Borras C, Ariznavarreta C, Vara E, Vina J, Tresguerres JA (2010) Hormonal regulation of pro-inflammatory and lipid peroxidation processes in liver of old ovariectomized female rats. Biogerontology 11(2):229–243. https://doi.org/10.1007/s10522-009-9242-2
15. Zuo Z, Lei H, Wang X, Wang Y, Sonntag W, Sun Z (2011) Aging-related kidney damage is associated with a decrease in klotho expression and an increase in superoxide production. Age (Dordr) 33(3):261–274. https://doi.org/10.1007/s11357-010-9176-2
16. Sullivan-Gunn MJ, Lewandowski PA (2013) Elevated hydrogen peroxide and decreased catalase and glutathione peroxidase protection are associated with aging sarcopenia. BMC Geriatr 13:104. https://doi.org/10.1186/1471-2318-13-104
17. Hamilton CA, Brosnan MJ, McIntyre M, Graham D, Dominiczak AF (2001) Superoxide excess in hypertension and aging: a common cause of endothelial dysfunction. Hypertension 37(2 Pt 2):529–534
18. Zhang H, Davies KJ, Forman HJ (2015) Oxidative stress response and Nrf2 signaling in aging. Free Radic Biol Med 88 (Pt B):314–336. https://doi.org/10.1016/j.freeradbiomed.2015.05.036
19. Pomatto LCD, Davies KJA (2017) The role of declining adaptive homeostasis in ageing. J Physiol 595(24):7275–7309. https://doi.org/10.1113/JP275072
20. Zhu Y, Carvey PM, Ling Z (2006) Age-related changes in glutathione and glutathione-related enzymes in rat brain. Brain Res 1090 (1):35–44. https://doi.org/10.1016/j.brainres.2006.03.063
21. Rebrin I, Sohal RS (2008) Pro-oxidant shift in glutathione redox state during aging. Adv Drug Deliv Rev 60(13–14):1545–1552. https://doi.org/10.1016/j.addr.2008.06.001. S0169-409X(08)00167-1 [pii]
22. Ward WF, Qi W, Van Remmen H, Zackert WE, Roberts LJ 2nd, Richardson A (2005) Effects of age and caloric restriction on lipid peroxidation: measurement of oxidative stress by F2-isoprostane levels. J Gerontol A Biol Sci Med Sci 60(7):847–851. https://doi.org/10.1093/gerona/60.7.847
23. Zhang H, Forman HJ (2017) 4-Hydroxynonenal-mediated signaling and aging. Free Radic Biol Med 111:219–225. https://doi.org/10.1016/j.freeradbiomed.2016.11.032
24. Starke-Reed PE, Oliver CN (1989) Protein oxidation and proteolysis during aging and oxidative stress. Arch Biochem Biophys 275 (2):559–567
25. Gonos ES, Kapetanou M, Sereikaite J, Bartosz G, Naparlo K, Grzesik M, Sadowska-Bartosz I (2018) Origin and pathophysiology of protein carbonylation, nitration and chlorination in age-related brain diseases and aging.

Aging (Albany NY) 10(5):868–901. https://doi.org/10.18632/aging.101450

26. Kaneko T, Tahara S, Matsuo M (1996) Non-linear accumulation of 8-hydroxy-2-′-deoxyguanosine, a marker of oxidized DNA damage, during aging. Mutat Res 316 (5–6):277–285
27. Hamilton ML, Van Remmen H, Drake JA, Yang H, Guo ZM, Kewitt K, Walter CA, Richardson A (2001) Does oxidative damage to DNA increase with age? Proc Natl Acad Sci U S A 98(18):10469–10474. https://doi.org/10.1073/pnas.171202698
28. Marques C, Pereira P, Taylor A, Liang JN, Reddy VN, Szweda LI, Shang F (2004) Ubiquitin-dependent lysosomal degradation of the HNE-modified proteins in lens epithelial cells. FASEB J 18(12):1424–1426. https://doi.org/10.1096/fj.04-1743fje
29. Liu W, Akhand AA, Kato M, Yokoyama I, Miyata T, Kurokawa K, Uchida K, Nakashima I (1999) 4-Hydroxynonenal triggers an epidermal growth factor receptor-linked signal pathway for growth inhibition. J Cell Sci 112 (Pt 14):2409–2417
30. Weber D, Milkovic L, Bennett SJ, Griffiths HR, Zarkovic N, Grune T (2013) Measurement of HNE-protein adducts in human plasma and serum by ELISA—comparison of two primary antibodies. Redox Biol 1:226–233. https://doi.org/10.1016/j.redox.2013.01.012. REDOX32 [pii]
31. Carini M, Aldini G, Facino RM (2004) Mass spectrometry for detection of 4-hydroxy-trans-2-nonenal (HNE) adducts with peptides and proteins. Mass Spectrom Rev 23(4):281–305. https://doi.org/10.1002/mas.10076

Chapter 22

Measurements of Hydrogen Peroxide and Oxidative DNA Damage in a Cell Model of Premature Aging

Juan Manuel Iglesias-Pedraz and Lucio Comai

Abstract

Reactive oxygen species (ROS) represent a number of highly reactive oxygen-derived by-products generated by the normal mitochondrial respiration and other cellular metabolic reactions. ROS can oxidize macromolecules including lipids, proteins, and nucleic acids. Under physiological condition, the cellular levels of ROS are controlled by several antioxidant enzymes. However, an imbalance between ROS production and detoxification results in oxidative stress, which leads to the accumulation of macromolecular damage and progressive decline in normal physiological functions.

Oxidative deterioration of DNA can result in lesion that are mutagenic and contribute to aging and age-related diseases. Therefore, methods for the detection of ROS and oxidative deterioration of macromolecules such as DNA in cells provide important tool in aging research. Here, we described protocols for the detection of cytoplasmic and mitochondria pools of hydrogen peroxide, and the DNA modification 8-oxoguanine, a biomarker of oxidative damage, that are applicable to cell-based studies on aging and other related areas.

Key words Oxidative stress, Hydrogen peroxide, PF6-AM, MitoPY-1, DNA damage, 8-Oxoguanine, Senescence, Cancer, Flow cytometry, Immunofluorescence

1 Introduction

ROS are oxygen-derived by-products that include hydroxyl radical (HO•), superoxide radical (O_2^-) and hydrogen peroxide (H_2O_2). Superoxide radicals are very reactive and short-lived molecule [1] that are rapidly converted to more stable hydrogen peroxide by mitochondrial dismutase (MnSOD) or cytoplasmic dismutase (CuSOD) [2]. At low to moderate levels, H_2O_2 is an important molecule that plays a critical role as a second messenger serving as a signal for cell proliferation, differentiation, and migration [3], and many other cellular process [4–9]. Under physiological conditions the cellular levels of ROS generated by mitochondria as by-products of respiration or other sites in the cell such as plasma membrane-associated enzymes as nicotinamide adenine

Sean P. Curran (ed.), *Aging: Methods and Protocols*, Methods in Molecular Biology, vol. 2144,
https://doi.org/10.1007/978-1-0716-0592-9_22,

dinucleotide phosphate (NADPH) oxidases are neutralized by antioxidant defense enzymes including superoxide dismutase, catalase, glutathione peroxidase, and thioredoxin peroxidase [7–10]. Nonetheless, pathophysiological conditions that alter the delicate balance between ROS production and clearance raise the levels of ROS within a cell attacking DNA and other macromolecules, resulting in the accumulation of oxidative lesions [11]. It is well established that damage to macromolecules including DNA is associated with the initiation and progression of many diseases, including aging (review in [12, 13]). Due to its lowest oxidation potential, guanine is one of the most oxidizable natural DNA base [14], generating the mutagenic product 8-oxo-7,8-dihydroguanine (8-oxoG), which is a major biomarker of DNA damage caused by oxidative stress [12, 15].

We reported that depletion of the Werner syndrome helicase (WRN), a protein whose loss of function mutations result in the premature aging disease Werner Syndrome, results in oxidative stress, as determined by accumulation of hydrogen peroxide and oxidative-damaged DNA, in rapidly proliferating cells. We imaged cellular and mitochondria hydrogen peroxide in living cells with the fluorescent indicators peroxyfluor-6 acetoxymethyl ester (PF6-AM) and 4-[4-[3-oxo-6′-(4,4,5,5-tetramethyl-1,3,2-dioxaborolan-2-yl) spiro[isobenzofuran-1(3H),9′-[9H]xanthen]-3′-yl]-1-piperazinyl] butyl-triphenyl-phosphonium iodide (MitoPY-1), respectively. PF6-AM is a fluorescent marker with improved sensitivity and selectivity for detecting cellular H_2O_2, while the fluorescent probe MitoPY-1 is highly selective for detecting H_2O_2 over superoxide, nitric oxide, and hydroxyl radical in the mitochondria. An antibody that specifically recognized 8-oxoG lesions was used to assess levels of oxidative DNA damage in cells after fixation. In this chapter, we describe protocols that utilize these tools to quantify biomarkers of oxidative stress in living cells under many experimental settings.

2 Materials

2.1 Cell Lines

1. HeLa cells transduced with lentivirus expressing shRNA for conditional WRN depletion (shWRN) or a scrambled shRNA (shCTR) [16].

2.2 General Reagents and Solutions

1. Complete Dulbecco's modified Eagle's medium (DMEM) is modified to contain 4.5 mg/mL glucose, 4 mM L-glutamine, 10% heat-inactivated fetal bovine serum (HI-FBS), and 1× penicillin–streptomycin solution.
2. Fetal bovine serum (FBS) is heated for 30 min at 56 °C with mixing to inactivate complement proteins (*see* **Note 1**).

3. Penicillin–streptomycin (Pen-Strep) solution: a 100× solution containing 10,000 U/mL of penicillin and 10,000 μg/mL of streptomycin is purchased from ThermoFisher and stored at −20 °C.
4. 1.0 mg/mL doxycycline (dox) in DMSO stored in the dark at −20 °C (*see* **Note 2**).
5. 20× PBS: To 800 mL of milliQ water add, in the following order, 160 g NaCl, 4 g KCl; 14.4 g Na_2HPO_4 (dibasic anhydrous), and 2.4 g KH_2PO_4 (monobasic anhydrous). Stir with magnetic stirrer until the salts are completed dissolved and adjust pH to 7.4 with 1 N HCl. Bring volume up to 1 L with milliQ and continue stirring overnight. Next day, autoclave the solution and store at room temperate.
6. 1× PBS and 1× PBS plus 0.1% TX-100 working solutions are prepared from 20× PBS in water (*see* **Note 3**).
7. 1× DPBS (containing chloride and magnesium): sold by different vendors.
8. Trypan blue staining solution for counting cells: sold by different vendors.

2.3 Flow Cytometry

1. Trypsin–EDTA: a 100× stock solution containing 0.025% trypsin and 00.1% EDTA in PBS (100× stock) is purchased from ThermoFisher and stored at −20 °C.
2. 1× trypsin–EDTA working solution: under sterile conditions mix one part of 100× stock solution with nine parts of sterile 1× PBS. Store at −20 °C.
3. FACS buffer: Add FBS to sterile 1× DPBS at 2% final concentration and use the same day.
4. 5 mM Peroxyfluor-6-acetoxymethyl ester (PF6-AM) (Cat# A14086 AdooQ Bioscience) stock solution in DMSO (*see* **Note 4**).
5. 5 mM Mitochondria Peroxy Yellow-1 (MitoPY-1) (Cat# 4428, Tocris Bioscience) stock solution in DMSO (*see* **Note 4**).
6. 5 μM PF6-AM and 5 μM MitoPY-1 working solutions in FACS buffer.

2.4 Immunofluorescence

1. 100% methanol, stored at −20 °C (*see* **Note 5**).
2. Prepare 1.5 N HCl solution in autoclaved milliQ water (*see* **Note 6**).
3. Prepare 0.1 M NaOH solution in autoclaved milliQ water.
4. 5% BSA solution in 1× PBS (*see* **Note 7**).
5. 10 mg/mL RNase A DNase-free stock solution stored at −20 °C (*see* **Note 8**).

6. 2000 U DNase I RNase-free stock solution stored at −20 °C (*see* **Note 8**).
7. 5% Normal Donkey Serum (NDS), or serum of the same species where the secondary antibody was made, prepared in BSA Blocking solution, store at 4 °C (*see* **Note 9**).
8. 200 μg/mL 8-oxoG DNA Lesion mouse monoclonal IgM (in this work we use the antibody SC-130914 from Santa Cruz Biotechnology) prepared in Isotype Blocking solution.
9. 200 μg/mL Normal Mouse IgM prepared in Isotype Blocking solution.
10. 2 mg/mL Alexa Fluor 594 donkey anti-mouse antibody (in our study we used Cat# A21203 from Molecular Probes) prepared in BSA Blocking solution.
11. Antifade mounting medium with DAPI (Vector Labs).

2.5 Materials and Equipment

1. 100 mm tissue culture treated dishes.
2. 8-Well chamber slide (we use Lab-Tek chamber slides).
3. 24 × 50 mm No. 1.5 thickness glass coverslips.
4. 5 mL round bottom polystyrene fluorescence-activated cell sorting (FACS) tubes.
5. 50 mL sterile conical tubes.
6. 10 mL serological pipettes.
7. 5 mL serological pipettes.
8. 0.22 μm nylon or PTFE syringe filters.
9. Refrigerated centrifuge.
10. 5% CO_2 incubator.
11. Hemocytometer.
12. Flow Cytometry FACSCanto II, BD Biosciences or equivalent instrument.
13. Confocal microscope with 60× magnification oil immersion objective.

2.6 Analysis Software

1. FlowJo software (Tree Star Inc., Ashland, OR).
2. ImageJ software (National Institute of Health, Bethesda, MD, USA).
3. GraphPad Prism software (GraphPad Software, LLC, San Diego, CA, USA).

3 Methods

3.1 Cell Culture and Conditional WRN Depletion

1. HeLa cells carrying the conditional silencing system for WRN (shWRN) and parental cells carrying a scrambled shRNA as a control (shCTR) are maintained in Complete DMEM in a 95% humidity incubator with 5% CO_2 under atmospheric (21%) oxygen.
2. Culture the cells in 100 mm tissue culture dishes until they reach 60% confluence.
3. Add doxycycline to a final concentration of 1.0 μg/mL to each of the plates and incubate for 5 days under the same conditions specified as above.
4. On the third day of dox incubation detach cells from the plate by incubating cells in 0.8–1 mL of 1× trypsin–EDTA working solution at 37 °C for 5 min (*see* **Note 10**).
5. Add 5 mL of Complete DMEM media (*see* **Note 11**) and recover the cells in a 50 mL conical tube.
6. Spin down at 1500 × *g* for 5 min at 4 °C.
7. Decant supernatant and resuspend cells in Complete DMEM containing 1 μg/mL of dox (*see* **Note 12**).
8. Count cells using the hemocytometer by the Trypan Blue exclusion method.
9. Bring the cells to a density of 1×10^6 cell/mL.
10. Seed 3×10^5 cells in each well of an eight-well chamber slide in a final volume of 500 μL (*see* **Note 13**).
11. The remaining cells are seeded on 100 mm tissue culture dishes. They will be used for Flow Cytometry and Western Blot (WB) analysis after 5 days of dox treatment. WB is performed to measure the levels of WRN depletion using antibodies against WRN. To confirm that protein loading is the same across the gel use a constitutive expression protein such as tubulin, actin or GAPDH (*see* Fig. 1) (*see* **Note 14**).
12. Continue culturing the cells for 2 additional days to complete 5 days of dox treatment before any analysis.

3.2 Flow Cytometry for Intracellular ROS Detection in WRN Depleted and Control HeLa Cells

1. On the fifth day of incubation, wash the cells with 1× PBS, twice.
2. Add 1× trypsin–EDTA working solution and incubate at 37 °C for 5 min.
3. Add 5 mL of Complete media (*see* **Note 11**) and recover the cells in a 50 mL conical tube.
4. Spin down at 1500 × *g* for 5 min at 4 °C.

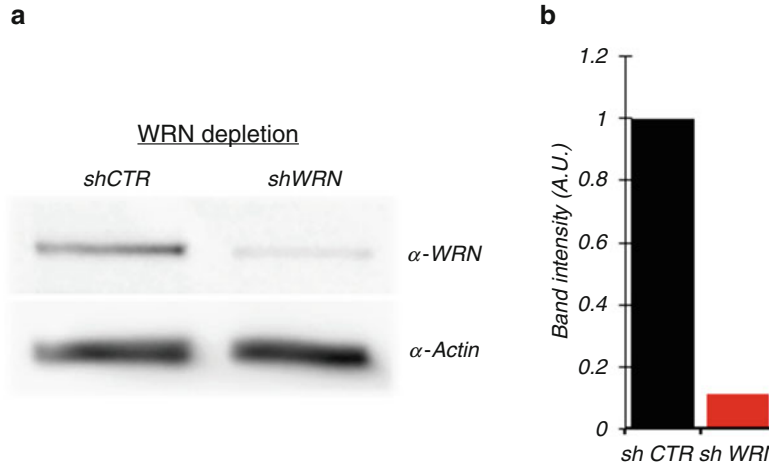

Fig. 1 Western blot analysis to assess WRN protein levels after knockdown. (**a**) Whole cell extracts prepared from HeLa cells transduced with lentiviral vectors (shWRN or shCTR) after 5 days of doxycycline treatment. The extracts were resolved in an 8% polyacrylamide gel and electrotransferred to nitrocellulose membrane. Anti-WRN (1/5000 dilution) and anti-actin (1/10,000 dilution) antibodies were used to probe the membrane. (**b**) Quantification of chemiluminescent signals from western blots was performed from images obtained by the Image Analyzer LAS-4000 (Fujifilm Life Science, Stamford, CT, USA) using ImageJ software. The graph shows the band intensity of WRN normalized against actin (shCTR was set at 1 in arbitrary units (A.U.))

5. Resuspend the cells in Complete DMEM at room temperature (RT).
6. Count cells using the hemocytometer by trypan blue exclusion method (*see* **Note 15**).
7. Aliquot the cells in several 1.5 mL chilled tubes, each at a final density of 2×10^6 cells (*see* **Note 16**).
8. Spin down the cells in each aliquot at 1500 × *g* for 5 min at 4 °C.
9. Wash the cell twice in 1× PBS at RT. Centrifuge as above.
10. Wash the cells twice in 1 mL of FACS buffer (*see* **Note 17**).
11. Resuspended the cells in 1 mL of FACS buffer containing 5 μM PF6-AM or 5 μM MitoPY-1.
12. Incubate the samples for 1 h at 37 °C in the CO_2 incubator.
13. Wash off excess of dye using 1 mL of FACS buffer equilibrated at 37 °C once, then transfer samples to a 5 mL FACS tube. Keep the samples on ice until ready for flow cytometry (*see* **Note 18**).
14. Analyze the cells by flow cytometry, with the excitation wavelength set at 488 nm and the emission wavelength at 525 nm.

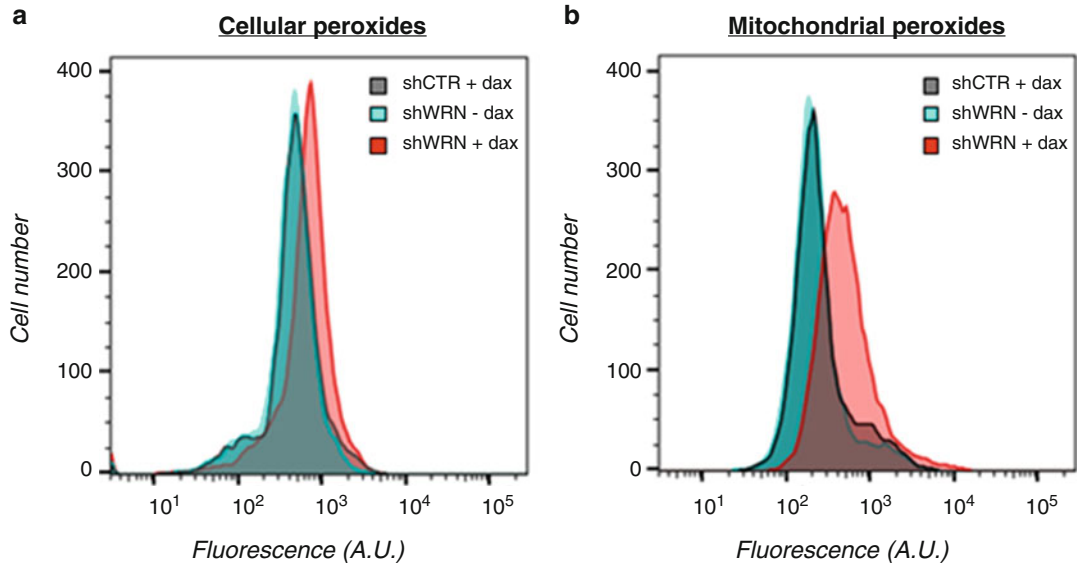

Fig. 2 Measurements of cellular and mitochondrial hydrogen peroxide in Werner syndrome protein (WRN)-knockdown HeLa cells. For each cell line, 10,000 events (cells) were analyzed by flow cytometry. (**a**) The cells were grown in the absence (−) or presence (+) of doxycycline (dox) for 5 days and cellular hydrogen peroxide was detected using the fluorescent indicator peroxyfluor-6 acetoxymethyl ester-6 (PF6-AM). (**b**) Same as in (**a**) the cells were grown in the absence (−) or presence (+) of doxycycline (dox) for 5 days and hydrogen peroxide in the mitochondrial compartment were detected using the mitochondrial Peroxy Yellow-1 (MitoPY-1) dye. (**a**) and (**b**) show histograms from representative experiments and mean fluorescence emission for each sample

15. Use untreated cells as control for auto fluorescence background.
16. Use at least 10,000 events (cells) for each experimental point of the analysis.
17. The data are processed using FlowJo software (*see* Fig. 2).

3.3 Detection of 7,8-Dihydro-8-Oxoguanine (8-OxoG) by Immunofluorescence

All the procedures are conducted at RT, unless indicated otherwise.

The most critical step in the preparation of the samples for microscopy is the fixation–permeabilization steps [17]. There are several methods to achieve proper fixation of cells which depends of the specific target to be analyzed. Most common methods include cross-linking with aldehydes such as paraformaldehyde or glutaraldehyde and organic solvents such as methanol, ethanol, acetone, or a combination of them (for a more detailed list of fixative agents *see* ref. 18). Since each of the different fixation protocols has its advantages and disadvantages over the sample, and there isn't a standard method for preserving the entire whole-cell structures, it is strongly recommended to perform trial experiments to optimize the desired detection. In many cases, denaturation of DNA is a necessary step for the detection of DNA modifications. The use of acid treatment followed by alkali neutralization is generally a good choice for the

detection of 8-oxoG [19]. In our experiments, a fixation with 100% methanol at −20 °C followed by a 30 min incubation with HCl resulted in the best detection of 8-oxoG lesions in HeLa cells [16, 20–24].

1. Remove the eight-well slide chamber from the incubator once completed 5 days of incubation.
2. Gently wash each well three to four times with ice-cold 1× PBS thoroughly but carefully (*see* **Note 19**).
3. Add ice-cold methanol to each well and transfer slide chamber to −20 °C freezer.
4. Incubate for 20–30 min at −20 °C (*see* **Note 20**).
5. Remove the sample from the −20 °C freezer and rehydrate in 1× PBS for 20 min (*see* **Note 21**).
6. Add 1.5 N HCl to each well and incubate the samples for 30 min at RT in a rocker (*see* **Note 22**).
7. Add 0.1 M NaOH to neutralize the HCl and incubate for 5 min at RT on a rocker.
8. Wash five times in 1× PBS at RT to remove the excess of alkali (*see* **Note 23**).
9. Treat the cells with RNase A at final concentration of 10 μg/mL and, for the control cell samples, add DNase I at final concentration of 10 U/mL (*see* **Notes 8** and **24**).
10. Incubate samples for 1 h at 37 °C.
11. Wash the samples thoroughly in 1× PPBS (*see* **Note 19**).
12. Incubate the cells in Isotype Blocking solution at RT for 1 h (*see* **Note 9**).
13. Prepare the primary antibody against 8-oxoG in Isotype Blocking solution (*see* **Note 25**).
14. Add primary antibody solution to the samples and incubate at 4 °C overnight.
15. The next day wash the samples with 1× PBS containing 0.1% TX-100 three times, 5 min each.
16. Incubate the samples with the secondary Alexa Fluor 594–conjugated antibody at RT for 1 h, in the dark (*see* **Note 26**).
17. Wash cells three times as before.
18. Disassemble the chamber slide following the manufacturer's instructions and drain the excess of buffer as much as possible, without drying the samples, using an absorbent paper or other methods.
19. Add 30 μL of Antifade Mounting Medium with DAPI to each well of the chamber slide (*see* **Note 27**).
20. Analyze the samples by confocal microscopy (*see* Fig. 3) (*see* **Note 28**).

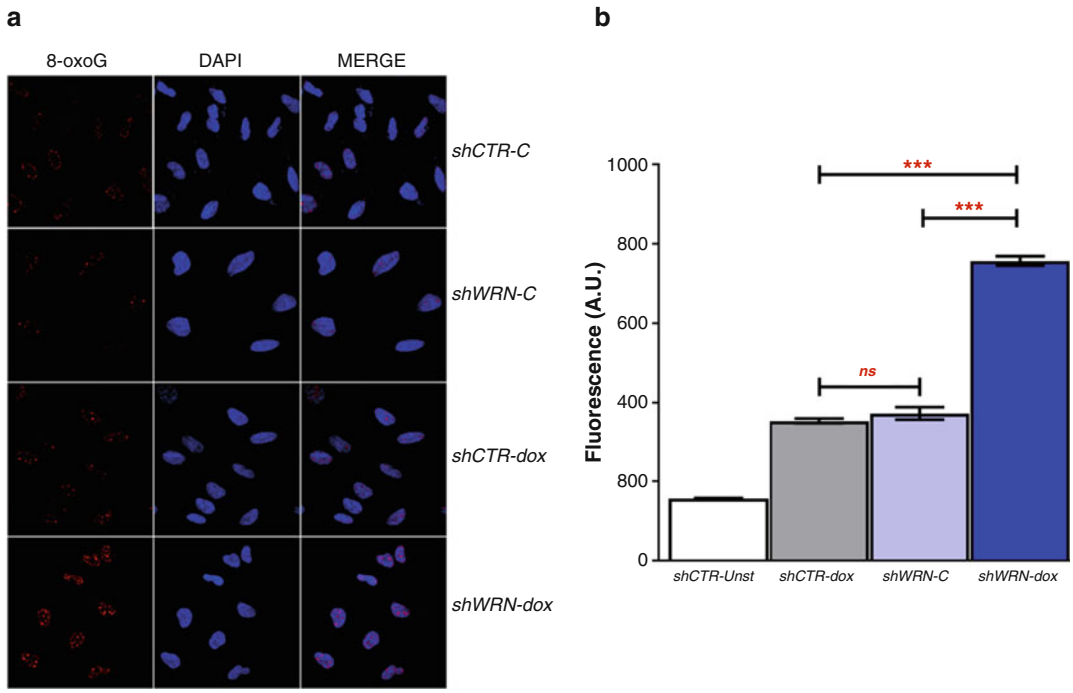

Fig. 3 Confocal microscopy of cells stained by indirect immunofluorescence. (**a**) WRN-depleted HeLa (shWRN) and parental (shCTR) cells were grown in eight-well chamber slides in the absence (−dox) or presence of doxycycline (+dox) for 5 days and the oxidized nucleoside 8-oxo-7,8-dihydroguanine (8-oxoG) was detected by immunofluorescence microscopy. DAPI, is used to visualize the nuclear compartment. (**b**) Corrected nuclear intensities were generated using ImageJ software. At least 100 cells per experiment were counted and the results were tabulated ±SEM using GraphPad Prism software. *ns* not significant; ∗∗∗ denotes a *p* value ≤0.0001 calculated by two-tailed Student's *t*-test

4 Notes

1. Check each reagent for the expiration date. Thaw FBS in a water bath at 37 °C and make 50 mL aliquots under sterile conditions. Keep aliquots at −20 °C until ready to use.
2. Use sterile cell culture grade or molecular biology grade DMSO. Nonsterile DMSO should be filtered through a disposable syringe with a 0.2 μm Nylon or PTFE filter.
3. The 1× PBS solution that is used for cultured cells is sterilized by autoclaving.
4. Peroxyfluor-6-acetoxymethyl ester (PF6-AM) and mitochondrial Peroxy Yellow-1 (MitoPY-1) fluorescent probes used on our experiments were kindly provided as a powder by Dr. Christopher J. Chang, University of California, Berkeley. The powder was resuspended in DMSO at a concentration of 5 mM and kept at −80 °C. These probes are now available from commercial vendors.

5. In our hands, cold methanol fixation at −20 °C gives better results than other fixative methods for detection and analysis of 8-oxoG. Nonetheless, other methods can be considered if the integrity of specific internal structures must be preserved.
6. Concentrated hydrochloric acid releases toxic vapors that cause severe irritations to mucous membranes if inhaled. Prepare diluted solution in chemical hoods.
7. BSA is prepared at final concentration of 5% in 1× PBS and small (500-μL) aliquots are kept at −20 °C for several months.
8. The treatment of samples with nucleases assures of the specificity of the antibody for IF. Thus, while RNase A treatment serves to prevent the detection of 8-oxoguanine in RNA molecules, the treatment with DNase I is used to validate the specificity of the antibody against DNA.
9. It is recommended to use normal serum from the same species where the secondary antibody was raised as a blocking reagent. This step will minimize the background fluorescence caused by unspecific binding of the Alexa Fluor–conjugated secondary antibody.
10. HeLa cells carrying shWRN but not control cells (shCTR) display reduced proliferation 2 days after doxycycline treatment. Therefore, we routinely transfer both cell lines on the third day of doxycycline treatment to maintain uniform the cell densities in both cell cultures and continue culture until reach the fifth day of dox treatment.
11. After 5 min of trypsinization, add 5 mL of complete media to inactivate trypsin. Gently pipet up and down several times to detach cells from the plate and to make a homogeneous cell suspension.
12. Add doxycycline to the resuspension media to ensure having the correct concentration of doxycycline in each plate or chamber slide.
13. We find that the optimal density for HeLa cells in an eight-well chamber slide is 3×10^5 cells/well. Optimal density for other cell lines may need optimization.
14. We used an antibody against actin as a loading control for western blotting but depending on the experimental system or antibody availability, other proteins can be used as well. Refer to protocols on western blots for suggested loading controls in other systems.
15. Keep cells on ice during counting.
16. Make sure that each tube is correctly labelled to avoid mixing of samples, which can lead to potential problems in the interpretation of the results.

17. Prepare the FACS buffer in advance and keep it at 37 °C in the CO_2 incubator.
18. If the samples are not processed immediately on the FACS analyzer, keep them on ice until ready to use, preferably within 2 h or less after staining.
19. The washes with PBS are critical for removing nonadherent cells and debris from the slide. Impurities present in the sample can give rise to autofluorescence and interfere with the desired signal. However, care must be taken during the washes steps to avoid loss of adherent cells.
20. The length of time for fixation/permeabilization depends on the type of cells and the molecular target. Generally, 20 min of incubation in 100% methanol at −20 °C is sufficient for many cell types. Once the samples are fixed, they can be preserved for several days or weeks in 100% methanol at −20 °C.
21. Do this by incubating the samples in 1× PBS and change the media every 5 min during 20 min.
22. The length of incubation time for DNA denaturation depends on the cell type and the method of fixation. To achieve the best results, time course experiments are strongly recommended.
23. To assure that neutralisation step is performed correctly, measure the pH of each wash solution using a pH-indicator strip.
24. The nuclease treatment, which is used as a control for antibody specificity, is carried out in 1× DPBS with 2 mM magnesium.
25. In our experiments, a 1:500 dilutions of 8-oxoG antibody yields the best results. However, we suggest to test several antibody dilutions to determine the best working condition for other experimental setting.
26. The secondary antibody is a donkey anti-mouse antibody, which is diluted in 1× PBS plus 5% BSA at the final dilution of 1/200. In general, testing different dilutions is necessary to determine the best signal-to-noise ratio. From here to the end of the experiment, avoid exposure the samples to any direct light source since it will bleach the Alexa Flour–conjugated antibody.
27. After placing the coverslip on the slide, the excess of mounting medium is gently removed by laying an absorbent paper at the border of the coverslip.
28. For the best results, the sample should be kept in the dark at RT at least one night to allow the mounting medium to cure.

Funding

This work was supported by grant Nº 150-2017-FONDECYT from Consejo Nacional de Ciencia, Tecnología e Innovación Tecnológica (CONCYTEC) to JMI-P, and grant R01AG034156 form the National Institute of Aging, NIH, USA to LC.

References

1. Forkink M, Smeitink JA, Brock R, Willems PH, Koopman WJ (2010) Detection and manipulation of mitochondrial reactive oxygen species in mammalian cells. Biochim Biophys Acta 1797(6–7):1034–1044. https://doi.org/10.1016/j.bbabio.2010.01.022
2. Miller AF (2012) Superoxide dismutases: ancient enzymes and new insights. FEBS Lett 586(5):585–595. https://doi.org/10.1016/j.febslet.2011.10.048
3. Rhee SG (2006) Cell signaling. H_2O_2, a necessary evil for cell signaling. Science 312 (5782):1882–1883. https://doi.org/10.1126/science.1130481
4. Schieber M, Chandel NS (2014) ROS function in redox signaling and oxidative stress. Curr Biol 24(10):R453–R462. https://doi.org/10.1016/j.cub.2014.03.034
5. Bolisetty S, Jaimes EA (2013) Mitochondria and reactive oxygen species: physiology and pathophysiology. Int J Mol Sci 14 (3):6306–6344. https://doi.org/10.3390/ijms14036306
6. Gorrini C, Harris IS, Mak TW (2013) Modulation of oxidative stress as an anticancer strategy. Nat Rev Drug Discov 12(12):931–947. https://doi.org/10.1038/nrd4002
7. Circu ML, Aw TY (2010) Reactive oxygen species, cellular redox systems, and apoptosis. Free Radic Biol Med 48(6):749–762. https://doi.org/10.1016/j.freeradbiomed.2009.12.022
8. Kotiadis VN, Duchen MR, Osellame LD (2014) Mitochondrial quality control and communications with the nucleus are important in maintaining mitochondrial function and cell health. Biochim Biophys Acta 1840 (4):1254–1265. https://doi.org/10.1016/j.bbagen.2013.10.041
9. Nogueira V, Hay N (2013) Molecular pathways: reactive oxygen species homeostasis in cancer cells and implications for cancer therapy. Clin Cancer Res 19(16):4309–4314. https://doi.org/10.1158/1078-0432.CCR-12-1424
10. Phaniendra A, Jestadi DB, Periyasamy L (2015) Free radicals: properties, sources, targets, and their implication in various diseases. Indian J Clin Biochem 30(1):11–26. https://doi.org/10.1007/s12291-014-0446-0
11. Avery SV (2011) Molecular targets of oxidative stress. Biochem J 434(2):201–210. https://doi.org/10.1042/BJ20101695
12. Sedelnikova OA, Redon CE, Dickey JS, Nakamura AJ, Georgakilas AG, Bonner WM (2010) Role of oxidatively induced DNA lesions in human pathogenesis. Mutat Res 704 (1–3):152–159. https://doi.org/10.1016/j.mrrev.2009.12.005
13. Lopez-Otin C, Blasco MA, Partridge L, Serrano M, Kroemer G (2013) The hallmarks of aging. Cell 153(6):1194–1217. https://doi.org/10.1016/j.cell.2013.05.039
14. Thapa B, Schlegel HB (2015) Calculations of pKa's and redox potentials of nucleobases with explicit waters and polarizable continuum solvation. J Phys Chem A 119(21):5134–5144. https://doi.org/10.1021/jp5088866
15. Guo C, Ding P, Xie C, Ye C, Ye M, Pan C, Cao X, Zhang S, Zheng S (2017) Potential application of the oxidative nucleic acid damage biomarkers in detection of diseases. Oncotarget 8(43):75767–75777. https://doi.org/10.18632/oncotarget.20801
16. Li B, Iglesias-Pedraz JM, Chen LY, Yin F, Cadenas E, Reddy S, Comai L (2014) Down-regulation of the Werner syndrome protein induces a metabolic shift that compromises redox homeostasis and limits proliferation of cancer cells. Aging Cell 13(2):367–378. https://doi.org/10.1111/acel.12181
17. Donaldson JG (2001) Immunofluorescence staining. Curr Protoc Cell Biol. Chapter 4: Unit 4.3. https://doi.org/10.1002/0471143030.cb0403s00
18. Howat WJ, Wilson BA (2014) Tissue fixation and the effect of molecular fixatives on downstream staining procedures. Methods 70 (1):12–19. https://doi.org/10.1016/j.ymeth.2014.01.022
19. Campalans A, Kortulewski T, Amouroux R, Menoni H, Vermeulen W, Radicella JP (2013)

Distinct spatiotemporal patterns and PARP dependence of XRCC1 recruitment to single-strand break and base excision repair. Nucleic Acids Res 41(5):3115–3129. https://doi.org/10.1093/nar/gkt025

20. Amouroux R, Campalans A, Epe B, Radicella JP (2010) Oxidative stress triggers the preferential assembly of base excision repair complexes on open chromatin regions. Nucleic Acids Res 38(9):2878–2890. https://doi.org/10.1093/nar/gkp1247
21. Bennett BT, Bewersdorf J, Knight KL (2009) Immunofluorescence imaging of DNA damage response proteins: optimizing protocols for super-resolution microscopy. Methods 48 (1):63–71. https://doi.org/10.1016/j.ymeth.2009.02.009
22. Bhattacharyya D, Hammond AT, Glick BS (2010) High-quality immunofluorescence of cultured cells. Methods Mol Biol 619:403–410. https://doi.org/10.1007/978-1-60327-412-8_24
23. Melan MA, Sluder G (1992) Redistribution and differential extraction of soluble proteins in permeabilized cultured cells. Implications for immunofluorescence microscopy. J Cell Sci 101(Pt 4):731–743
24. Soultanakis RP, Melamede RJ, Bespalov IA, Wallace SS, Beckman KB, Ames BN, Taatjes DJ, Janssen-Heininger YM (2000) Fluorescence detection of 8-oxoguanine in nuclear and mitochondrial DNA of cultured cells using a recombinant Fab and confocal scanning laser microscopy. Free Radic Biol Med 28 (6):987–998

Chapter 23

Integrating Longitudinal Population Studies of Aging in Biological Research

Amin Haghani, Brendan Miller, T. Em Arpawong, and Jennifer Ailshire

Abstract

Aging is a complicated biological process defined by a combination of species-specific phenotypes. Understating this complex system in humans requires collaboration across a wide range of scientists including molecular biologists, biochemists, biophysicists, biostatisticians, geneticists, demographers, and epidemiologists. Longitudinal data on humans is an essential tool for both discovery and hypothesis testing for validation. Several longitudinal studies of aging exist that have collected both social and biological data in humans that can be used to understand the human aging processes. This chapter aims to introduce aging biologists to these valuable resources and also explain some of the essential skills necessary to work with these large population-based datasets.

Key words Human subject research, Longitudinal data, Longitudinal statistics, R

1 Introduction

Translating experimental data derived from model organisms into a therapy for humans is an enormous challenge. Aging is a complex biological process that is defined by a combination of traits rather than a simple passage of time. Human aging starts from initial developmental stages in the womb, infancy through adolescence, reproductive years through later adulthood, followed by gradual deterioration with varying degrees of more resilient or frail processes that occur until death. This complicated and long developmental path cannot practically be studied in real-time for experimental purposes. Thus, biologists are compelled to use nonhuman organisms with shorter life spans as models of aging. Experimental biologists who try to study human aging processes face a variety of challenges relating findings from nonhuman organisms to human aging.

1. The initial challenge of the biologist is to select an appropriate organism that has similar parameters to human aging. Rodents,

Sean P. Curran (ed.), *Aging: Methods and Protocols*, Methods in Molecular Biology, vol. 2144,
https://doi.org/10.1007/978-1-0716-0592-9_23,

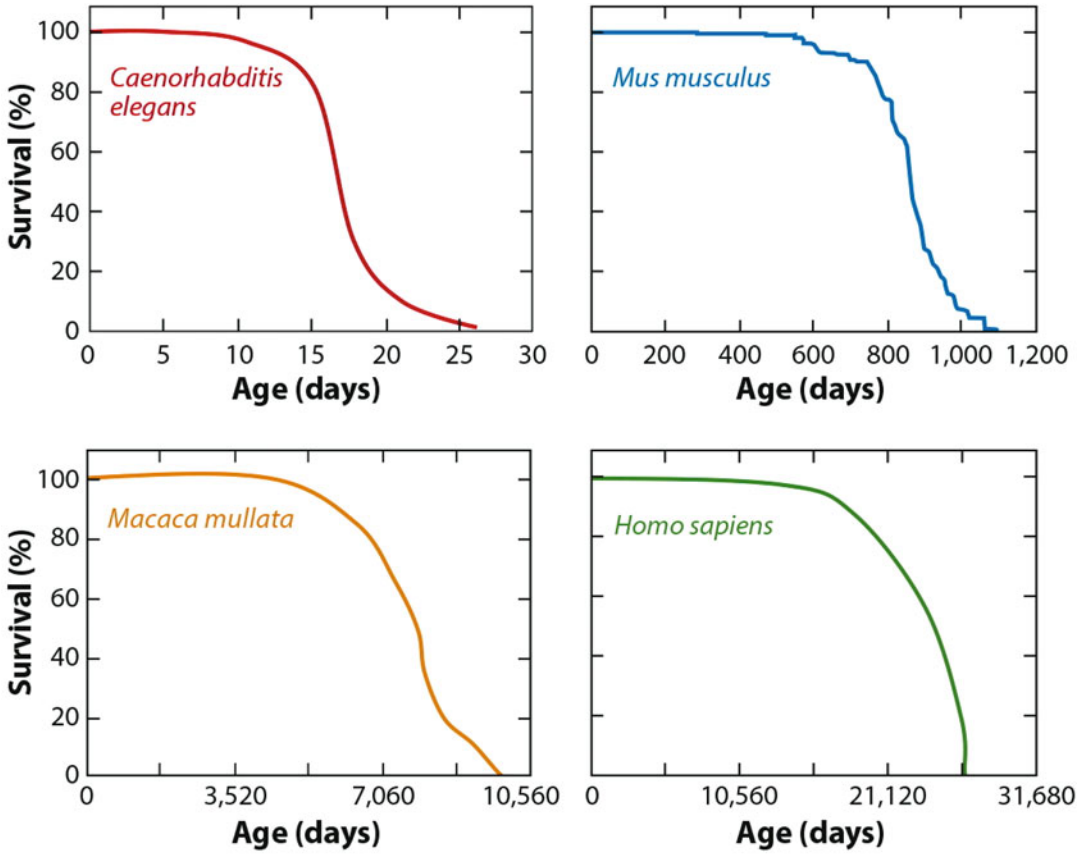

Fig. 1 Comparison of human life span curve with some of the animal models used in aging research [1]

chimpanzee, *Drosophila melanogaster, Caenorhabditis elegans*, yeast, zebrafish, and killifish are some of the models that biologists developed over the years to achieve this. While all these models share some aspects of aging biology with humans, different programming mechanisms lead to a wide range of life spans across model organisms. This raises a key question about how to relate age ranges between animal models and humans. As shown in Fig. 1, while the maximum age of the animals differs, the life span curve of animals used in biological research has a similar pattern to that of humans. Using this similarity in the life span curve, we can estimate different age ranges of animals matched with humans.

2. The other challenge is that some phenotypes that mark aging parameters are specific to humans and not common to other species. Therefore, biologists use genome engineering techniques to produce a model that manifests a phenotype that resembles the one in humans. The results of these models are just suggestive unless it is validated in human populations.

3. Another issue in using animal models is the difference between "natural living" and "laboratory living" environments. Animal models are moved from their natural habitats and domesticated to laboratory environments. While wild mice live around 1.5 years, laboratory mice can live for around 3 years. In their natural habitat, *C. elegans* live in soil, whereas in the laboratory, they live in agar plates. In general, the laboratory environment is constrained and controlled.

Therefore, it is not easy to translate findings from model systems into humans. It is essential that biologists who conduct research on aging constantly validate and translate their findings from these models into research with humans to understand the implications for human health and longevity. Longitudinal population data thus becomes an essential validation tool that aids in confirming experimental findings, and complements research with experimental systems into successful therapeutics for age-related diseases.

It is common to observe an imbalance in aging research between experimental biology and human epidemiological analyses. A common first step in aging research is to utilize population data for initial discovery and hypotheses building. Formulated hypotheses based on human data can then be applied to a controlled experimental paradigm in molecular biology labs. Undoubtedly, implementing a coordinated epidemiological and molecular approach in aging research requires harmonized work across both population-level analysis of human data and experimental biology. Such integration allows us to answer complex biological questions and, ultimately, make greater strides toward improving health span in humans.

2 Longitudinal Data, an Essential Tool in Aging Research

Human studies are distinct from experimental biology in many aspects. Humans live longer than all mentioned models; therefore, it is not feasible to observe individuals throughout their life span. Instead, human data rely on observational studies of populations followed over varying number of years or for whom data have been collected at only one point in time (i.e., cross-sectional data). A key point for experimental biologists who want to integrate human data into their research is to understand that the nature of population data is different from examinations of the causal relationship of a variable and an outcome in a controlled experiment. Human data is a representation of the real world, which is inherently confounded with several unknown variables. For example, experimental modeling of Alzheimer disease cannot include many important factors such as race/ethnicity, socioeconomic status, educational

difference (long-term brain training vs. genetic ability), injuries, chronic diseases, medications for conditions, adherence to medications, behaviors (physical activity, diet, sleep), other substance abuse, wide ranges of ages, cultural differences, environmental toxins, access to food, access to healthcare, social networks, different genetic structures, and many other unknown factors. Therefore, many of the findings in a controlled experiment cannot be validated in the population data due to an unrealistic experimental design or animal model selection. This problem originates from the complexity of the scientific question or lack of inclusion of prior knowledge of the field in designing an experiment.

Working with longitudinal population data requires unique skills that are different from a typical experimental biology training program. Ideally, data include numerous variables relevant to a specific question such as aging-associated diseases that should be explored. Inference of these relationships requires a deep knowledge of multivariate statistics that is usually missing in biological training. In reality, statistical analysis is the last step of the study. The main challenge of the population data is preprocessing of the data which includes selection and cleaning up the variables relevant to the question, managing the missing data, and identification of the eligible or censored individuals for the study. Other difficulties in working with population data include data storage and management with command line programming languages. The current chapter aims to introduce some of the essential tools and handling techniques of longitudinal population data for an experimental biologist who tends to integrate human association analysis in his research.

2.1 Finding and Accessing Longitudinal Population-Based Data

There are several publicly available databases that are well-suited for conducting aging-related analysis. Some of these databases are listed in National Institute of Aging website (https://www.nia.nih.gov/research/dbsr/publicly-available-databases-aging-related-secondary-analyses-behavioral-and-social) and also the National Archives of Computerized Data on Aging (https://www.icpsr.umich.edu/icpsrweb/NACDA/). The target database should be selected based on the research question as well as the availability of the required data.

Accessing public data typically only requires that users register an account with the study. Accessing more sensitive and/or restricted data may require more than a simple registration. Sensitive and/or restricted data typically include variables that could identify study participants such as genetic or geolocation data. These data are typically made available to users through a proposal submission process. It is important to keep in mind that it may take some time to get access to restricted data. Users should therefore anticipate that their projects will be delayed by several months while they apply for and await approval for accessing restricted data.

2.2 Training and Certificates

A requirement to work with human data, particularly restricted data, is institutional training on human subject research. This training consists of a set of courses that introduce researchers to key concepts related to conducting research involving humans such as, ethical issues in working with human subjects, the purpose and functions of institutional review boards, and definitions and legal consequences of research misconducts. Researchers can choose among several modules related to human subjects, such as Social and Behavioral Research and the Health Insurance Portability and Accountability Act compliance. Learning about human subject research and obtaining certification of completion of the training is an institutional requirement for any researchers who want to work with human data. Additional details about human subjects research can be found on the National Institute of Health's website: https://grants.nih.gov/policy/humansubjects/training-and-resources.htm.

2.3 Data Use Agreements

Another issue to consider in research on human subjects is appropriate practices related to data security, storage, access, and sharing of protected health information. The main concern is minimizing the extent to which data can be used to identify a study participant, which would violate the rights of study subjects to confidentiality.

3 Statistical Training

Working with population data requires a moderate to advance statistical knowledge to manage and analyze the data. These skill sets are usually not a part of experimental biology training. The main statistical models that are used in population data analysis are multivariate linear regression, survival analysis, Cox proportional hazards, mixed effects models, and multivariate logistic regression models. It is recommended that biologists who want to incorporate human data in their research register in applied multivariate statists courses to learn about these statistical tools and interpretation of results.

3.1 Data Management and Analysis

Longitudinal data on humans is considered high-dimensional data, with potentially tens of thousands of variables and hundreds of thousands of observations. Handling such large data requires command line statistical programs that might not be common in experimental biology. Some of the most popular software programs for the management and analysis of large data sets include the following:

- R; www.r-project.org
- Stata; www.stata.com

- SAS; www.sas.com
- Python; www.python.org

Here we show an example in R to introduce readers to longitudinal data analysis. Other programming languages have different syntax but similar capabilities to manage and analyze the data. To install R or Rstudio go to websites "www.r-project.org" or "www.rstudio.com" and download the version recommended for your system. R is an open source statistical language that is widely used in science, education, and industry. Rstudio is the most popular integrated development environment (IDE) for R that includes a console and syntax-highlighting editor, as well as a variety of tools for plotting, history tracking and workspace management. Some other alternative IDEs for R includes RIDE, Radiant, R tools for Visual Studio, Architect, displayr, and Rbox.

3.2 Structure of Longitudinal Data

This kind of data consists of repeated measures of several variables from the same individuals over time. At each interval, several new participants might be added to the data and also many people might exit the study for a variety of reasons such as institutionalization (e.g., in a hospital or nursing home), loss to follow-up (i.e., the participant could not be found at the next data collection period), or death. These are some of the challenges for human population statistical analysis. Statistical analysis of these data constitutes both intra- and interindividual variations. The results of longitudinal data are generalized across the population from which the sample of subjects was drawn. In addition, longitudinal data can differentiate between aging effect (changes over time within the individuals) and the cohort effects (baseline differences between subjects). An example of publicly available longitudinal data is "The Health and Retirement Study," a nationally representative sample of more than 26,000 Americans age over 50 years that were followed for every 2 years since 1992.

Here, we constructed a random repeated measured data to walk you through some of the steps in data preprocessing and statistical analysis. The data contains the height of the 400 males and females that were measured over three 2 year intervals for each individual. Population data usually refer to male and females in terms of gender, and less commonly use the terminology of "sex" that is used in biology. Gender usually refers to culturally and socially constructed roles and behaviors, and is self-reported. Sex refers to the biological difference between males and females, which includes sex-linked chromosomes, sex organs, and hormonal differences, characteristics that are rarely collected in human data. The NIH expects funded-projects to include sex (or gender) as a biological variable in experimental and human population research. Biological differences between males and females are sometimes

overlooked in many research questions such as drug development and clinical trials.

Code to construct the random data:

```
# install required packages
list.of.packages <-
c("MASS", "ggplot2", "gridExtra", "lattice", "nlme")
new.packages <- list.of.packages[!(list.of.packages
                 %in%installed.packages()[,"Package"]
)]
if(length(new.packages)) install.packages(new.packages)

# Simulating a longitudinal data
library (MASS)
# Height for males
set.seed (2019)
data.gender.M <- mvrnorm(n=200, mu=c(50, 54, 69),
                    Sigma=matrix(c(25.0, 17.5, 12.3,
                                   17.5, 25.0, 17.5,
                                   12.3,17.5, 25.0), nrow=3,
byrow=TRUE))
# Height for females
set.seed(2019)
data.gender.F <- mvrnorm(n=200, mu=c(48, 55, 63),
                 Sigma=matrix(c(25.0, 17.5, 12.3,
                             17.5, 25.0, 17.5,
                             12.3, 17.5, 25.0), nrow=3,
byrow=TRUE))
# Combining male and female data
data <- data.frame(rbind(data.gender.M, data.gender.F))
names(data) = c('height.1', 'height.2', 'height.3')

data <- data.frame(id=factor(1:400), gender=rep(c('M', 'F'),
each=200), data)

# Removing unwanted variables
rm(list=c("data.gender.M", "data.gender.F"))
head(data)
## id gender height.1 height.2 height.3
## 1 1 M 53.61231 59.77618 68.97937
## 2 2 M 47.11489 51.12956 68.10377
## 3 3 M 47.88078 42.26972 61.92831
## 4 4 M 50.25227 58.33672 76.32973
## 5 5 M 44.38648 52.31223 59.35358
## 6 6 M 51.17846 57.46781 73.96208
```

3.3 Preprocessing of the Data

Data manipulation is an essential skill in working with large data. This often includes merging data from multiple sources using common identifiers, creating a subset of the data intended for analysis, creating variables, and other aspects of data management necessary to facilitate statistical analysis. In this example, we divided the constructed data into three separate datasets with random orders. Using a few command lines, we could remerge these data sets into its original format.

```
data1 <- data[,c(1:3)]
head(data1)
## id gender height.1
## 1 1 M 53.61231
## 2 2 M 47.11489
## 3 3 M 47.88078
## 4 4 M 50.25227
## 5 5 M 44.38648
## 6 6 M 51.17846
data2 <- data[sample(1:nrow(data)), c(1,2,4)]
head(data2)
## id gender height.2
## 198 198 M 52.76421
## 227 227 F 45.04731
## 195 195 M 53.57419
## 43 43 M 55.43935
## 233 233 F 57.94240
## 337 337 F 53.50021
data3 <- data[sample(1:nrow(data)), c(1,2,5)]
head(data3)
## id gender height.3
## 273 273 F 63.18088
## 12 12 M 77.32946
## 342 342 F 62.16001
## 90 90 M 74.52722
## 59 59 M 65.39955
## 231 231 F 59.86785
data.merged <- merge(data1, data2, by=c("id", "gender"), all =
TRUE)
data.merged <- merge(data.merged, data3, by=c("id", "gender"),
all = TRUE)

# Sort the data based on original ID
data.merged <- data.merged[order(match(data.merged$id, data
$id)), ]
identical(data.merged$id, data$id)
## [1] TRUE
head(data.merged)
## id gender height.1 height.2 height.3
```

```
## 1 1 M 53.61231 59.77618 68.97937
## 112 2 M 47.11489 51.12956 68.10377
## 223 3 M 47.88078 42.26972 61.92831
## 334 4 M 50.25227 58.33672 76.32973
## 346 5 M 44.38648 52.31223 59.35358
## 357 6 M 51.17846 57.46781 73.96208
```

The constructed data is an example of a cleaned-up repeated measured longitudinal data. Reaching this step usually requires multiple steps of preprocessing and data clean up. In the next steps, we can use this data for statistical analysis. In this example, our question is if there is any height difference between males and females. Since height was measured on several occasions for each individual, the statistical model should include a statistical adjustment to account for the repeated measurements for each individual. First, let us visualize the data to see the changes in height over time in males and females.

3.4 Reshaping the Data

The current data is in wide format, which means each row represents a person. For statistical analysis, the data should be converted to long format, which means each row represents a person-period, which is to say that rows represent observations of individuals at multiple times and columns represent variables. An additional variable should be constructed that identifies the time of each measurement.

```
# For statistical analysis, repeated measures of height should be considered as one variable. The time of the measures is another variable. Here we reshaped the data to have a variable for time and a variable for height.
data <- reshape(data, varying=c('height.1', 'height.2', 'height.3'), idvar='id', direction='long')
# rescaling the time for statistical analysis
data $time <- data $time-min(data $time)
head(data[order(data $id),])
## id gender time height
## 1.1 1 M 0 53.61231
## 1.2 1 M 1 59.77618
## 1.3 1 M 2 68.97937
## 2.1 2 M 0 47.11489
## 2.2 2 M 1 51.12956
## 2.3 2 M 2 68.10377
```

3.5 Statistical Analysis

As we can see in Figs. 2 and 3, the data suggest differences in height for males and females. Next, we will fit a mixed effect model (https://en.wikipedia.org/wiki/Mixed_model) to test if the

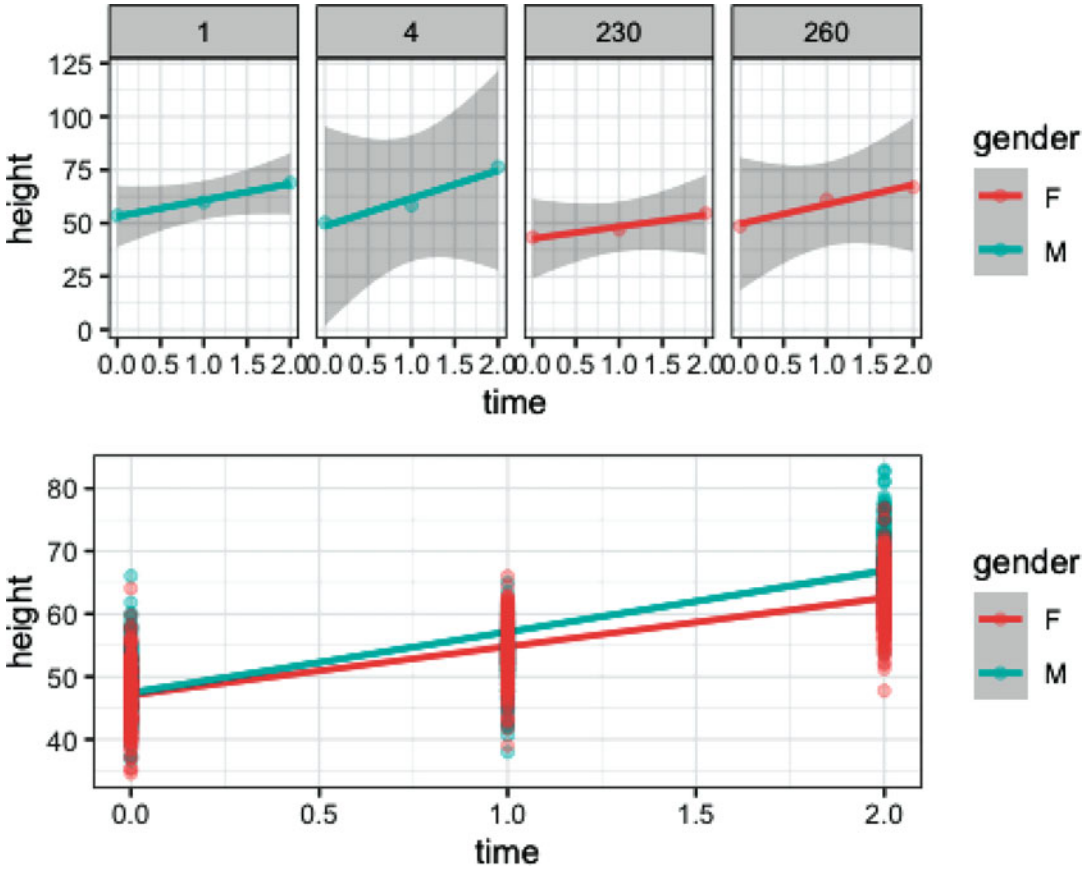

Fig. 2 The figures shown are possible when transforming data into the long format. The top figure shows the change in height over time for selected individuals in the sample, for two males (blue) and two females (orange). The bottom figure shows the mean change in height over time for the full sample, with males and females plotted separately

difference between males and females are statistically significant. Selection of the best statistical model for the data and also the interpretation of the findings requires advanced statistical knowledge. As mentioned before, it is essential that any biologists who want to analyze longitudinal data to register for an applied multivariate statistics course.

```
library(ggplot2)
library(gridExtra)
p1 <- ggplot(data[data$id %in% c(1, 4,260, 230), ],
aes(time, height, colour=gender))+
facet_grid(~id)+
geom_smooth(method = "lm")+
geom_point(alpha = 0.3)+
theme_bw()
p2 <- ggplot(data,aes(time, height, colour=gender))+
```

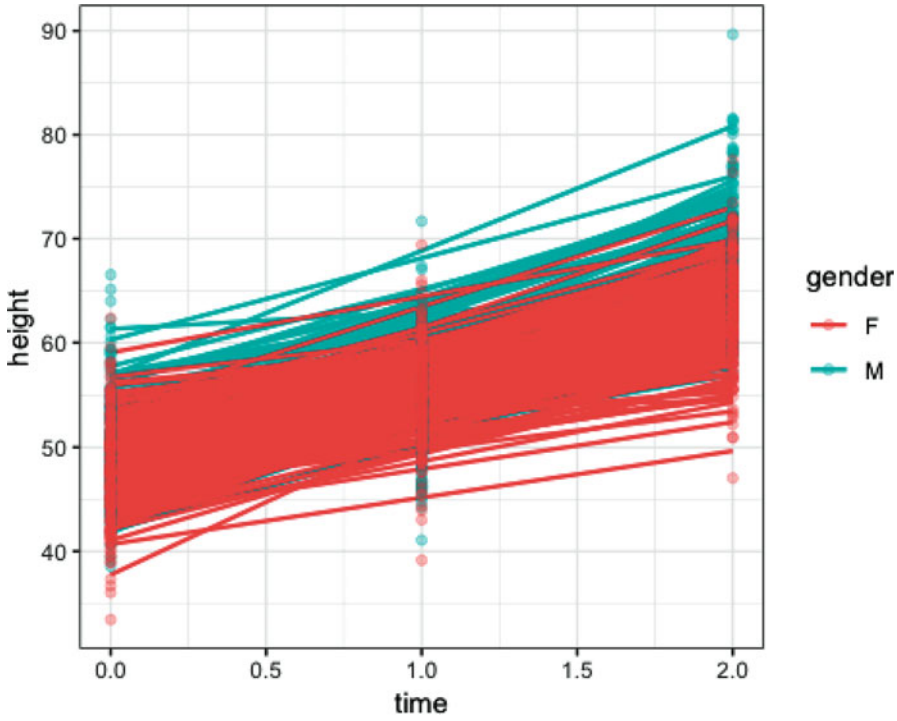

Fig. 3 Changes in height over time are shown for individual respondents, with males (blue) and females (orange)

```
geom_smooth(method = "lm")+
geom_point(alpha = 0.3)+
theme_bw()
grid.arrange(p1,p2, ncol=1)

library(nlme)model <- lme(height~gender, random = ~1+time|id,
method = "ML", data = data)
summary(model)
## Linear mixed-effects model fit by maximum likelihood
## Data: data
## AIC BIC logLik
## 8152.056 8182.597 -4070.028
##
## Random effects:
## Formula: ~1 + time | id
## Structure: General positive-definite, Log-Cholesky parame-
trization
## StdDev Corr
## (Intercept) 8.901431 (Intr)
## time 8.659395 -0.925
## Residual 4.049322
##
```

```
## Fixed effects: height ~ gender
## Value Std.Error DF t-value p-value
## (Intercept) 54.46168 0.2908277 800 187.26440 0
## genderM 2.24517 0.4112925 398 5.45882 0
## Correlation:
## (Intr)
## genderM -0.707
##
## Standardized Within-Group Residuals:
## Min Q1 Med Q3 Max
## -2.94654779 -0.40353890 0.05874286 0.45304723 2.11515763
##
## Number of Observations: 1200
## Number of Groups: 400
intervals(model)
## Approximate 95% confidence intervals
##
## Fixed effects:
## lower est. upper
## (Intercept) 53.891284 54.461684 55.032083
## genderM 1.437269 2.245172 3.053075
## attr(,"label")
## [1] "Fixed effects:"
##
## Random Effects:
## Level: id
## lower est. upper
## sd((Intercept)) 7.4469612 8.9014309 10.6399738
## sd(time) 8.0155789 8.6593947 9.3549222
## cor((Intercept),time) -0.9502548 -0.9252388 -0.8883627
##
## Within-group standard error:
## lower est. upper
## 3.778190 4.049322 4.339911

# plotting individual changes
data$fit <- predict(model)
ggplot(data,aes(time, height, colour=gender))+
geom_line(aes(y=fit, group=id), size=0.8)+
geom_point(alpha = 0.3)+
theme_bw()
```

As shown in summary statistics, the mixed model confirmed that there is a significant difference between the height of the males and females in this example dataset ($\beta = 2.24$, Confidence interval: 1.43–3.05, standard error: 0.41, p-value $< 10^{-7}$). This is an example model and is not the best model to fit this data. Model selection

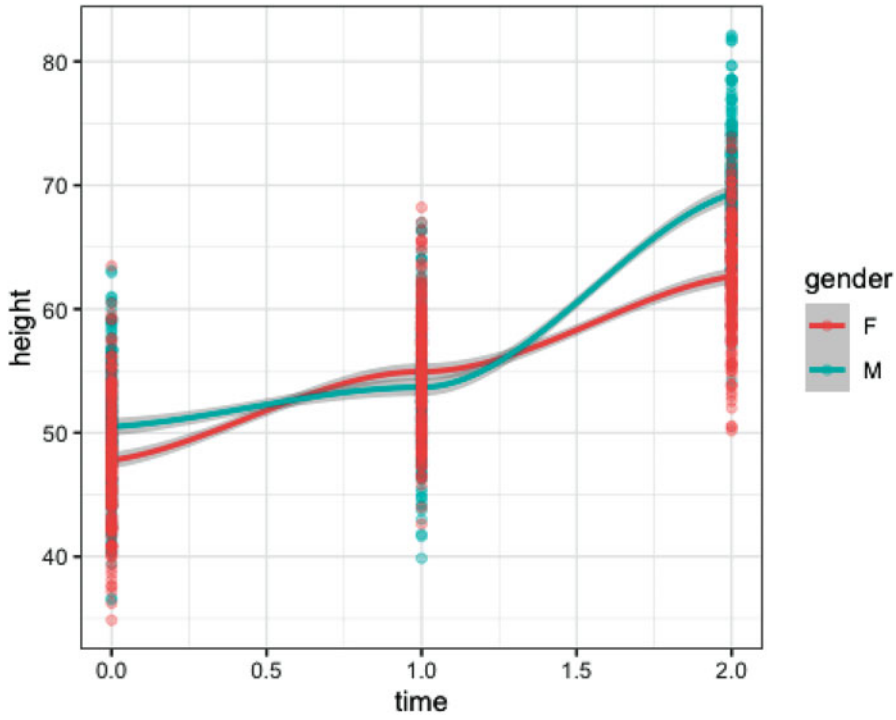

Fig. 4 A nonlinear relationship between height and time are shown for males (blue) and females (orange)

depends on the data and questions of the study. The relationship between predictors and the outcome are often nonlinear. Therefore, many researchers use polynomial or spline models to explain the data. In our example, while a linear model could show the gender difference over time, the association of the height and time is nonlinear, which means the trajectories of height changes with time. This is depicted in Fig. 4. Selection of the best model for data inference or prediction depends on the research question.

```
ggplot(data,aes(time, height, colour=gender))+
geom_smooth(method = "auto")+
geom_point(alpha = 0.3)+
theme_bw()
```

4 Examples of Multidisciplinary Aging Research

Over the years, many scientists working in the field of biology of aging have combined experimental and epidemiological data to build, examine and validate a hypothesis. For instance, one research group (PI: Dr. Caleb Finch) that was among the first to implement

such an approach published a hallmark paper highlighting similarities in synaptic loss between rodents and human during normal aging, even in the absence of neurological disorders [2]. Building on this research, they then combined human data and mouse experiments to investigate the underlying mechanism of Alzheimer disease, sex differences in neurodegeneration, inflammation contribution to aging, and neurodegenerative effects of environmental toxicants during aging process. Another research group (PI: Dr. Pinchas Cohen) has also implemented several multidisciplinary approaches in order to study the effect of mitochondrial genetic variation on micropeptides derived from mitochondrial DNA. Major findings include identifying a mitochondrial SNP in the micropeptide humanin-encoding sequence associated with cognitive age and lower circulating humanin levels. To demonstrate causality, humanin was injected into aging mice and circumvented brain inflammation and improved cognition [3]. Utilizing both large-scale human data and experimental data is a powerful approach that will lead to rapid translation of therapeutics.

Intervention development is another field of research that requires a combination of experimental model and human data. An example of this kind of research is translation of caloric restriction diets from yeasts, to worms, rodents and then into humans. One research group (PI: Dr. Valter Longo) working on the frontier of caloric restriction diets has translated findings from research in yeast into clinical trials for cancer patients in human. This work is summarized in a review paper that also explains the similarities of caloric restriction effects between animal models and human [4].

Another field of research that requires the integration of human and experimental data is genetics. Human genetics is often used for both discovery and validation of experimental findings. In the next chapter, we will describe the implications of population genetics in aging research and the required skills to integrate this kind of data in your research.

Acknowledgments

Contributions to this work were partially supported by funding from the National Institutes of Health, with support for B. Miller from a National Institute on Aging training grant (T32 AG00037; PI: Eileen Crimmins), for A. Haghani from a National Institute on Aging training grant (T32 AG052374: PI: Kelvin Davies), and for T.E. Arpawong through a pilot award from the National Institute on Aging (parent award P30 AG017265; PI: Eileen Crimmins).

References

1. Mitchell SJ et al (2015) Animal models of aging research: implications for human aging and age-related diseases. Annu Rev Anim Biosci **3**:283–303
2. Morgan DG, May PC, Finch CE (1987) Dopamine and serotonin systems in human and rodent brain: effects of age and neurodegenerative disease. J Am Geriatr Soc **35**(4):334–345
3. Yen K et al (2018) Humanin prevents age-related cognitive decline in mice and is associated with improved cognitive age in humans. Sci Rep 8(1):14212
4. Fontana L, Partridge L, Longo VD (2010) Extending healthy life span--from yeast to humans. Science 328(5976):321–326

INDEX

Sean P. Curran (ed.), *Aging: Methods and Protocols*, Methods in Molecular Biology, vol. 2144,
https://doi.org/10.1007/978-1-0716-0592-9,

H

I

L

M

N

O

P

Q

R

S

T

U

V

W